

# Application of Electrospray Ionization Mass Spectrometry Towards the Elucidation of Free Radical Polymerization Mechanisms

Zur Erlangung des akademischen Grades eines

DOKTORS DER NATURWISSENSCHAFTEN

(Dr. rer. nat.)

Fakultät für Chemie und Biowissenschaften

Karlsruher Institut für Technologie (KIT) – Universitätsbereich

Genehmigte

DISSERTATION

von

Sandy Pin Siong Koo

aus

Moka, Mauritius

Dekan: Prof. Dr. S. Bräse

Referent: Prof. Dr. C. Barner-Kowollik

Korreferent: Prof. Dr. M. Wilhelm

Tag der mündlichen Prüfung: 13. Juli 2010



Die vorliegende Arbeit wurde von Februar 2007 bis Juni 2010 unter Anleitung von Prof. Dr. Christopher Barner-Kowollik an der University of New South Wales, Sydney, Australia (Februar 2007 - Juni 2008) und am Karlsruher Institut für Technologie (KIT) (Juli 2008 - Juni 2010) – Universitätsbereich angefertigt.



*For my Family*

*Ruth, Shin, and Shane*

This is not a manuscript to be tossed aside lightly; it should be thrown with great force.

*Non Sum Qualis Eram*

*Education is an admirable thing, but it is well to remember from time to time that nothing that is worth knowing can be taught – Oscar Wilde (1854-1900)*



## Abstract

Free radical polymerization (FRP) has been extensively used for over 70 years in the industrial production of polymers. Poly(acrylates) synthesized *via* FRP span the entire range from high volume, low cost commodity polymers to low volume, high added value specialty polymers, and are thus industrially very significant. However, many details of the mechanism and the underlying kinetics of acrylate FRP, remain to be determined, including information related to transfer processes, as well as secondary reactions such as  $\beta$ -scission, the propagation of midchain radicals and their effects on the final polymer structure. Meanwhile, electro-spray ionization mass spectrometry (ESI-MS) has played an integral role in polymer characterization and understanding of polymerization mechanisms in recent years. The strength of ESI as a soft ionization technique is its ability to provide accurate macromolecular masses without fragment ions, which allows for the determination of polymer structure and end groups, in addition to number- and weight-average molecular masses.

The present thesis contributes to fundamental knowledge of acrylate polymerizations, particularly with respect to midchain radicals and the subsequent reactions they can undergo, through an in-depth investigation of the mediating ability of 1-octanethiol on *n*-butyl acrylate FRP, followed by the synthesis of high purity macromonomer obtained in an optimized reaction. This macromonomer is employed in the attempt to form star polymers *via* radical catalyst-free thiol-ene coupling, which leads to an exploration of the limitations of the thiol-ene reaction for polymer-polymer conjugation, dispelling the current notion that radical thiol-ene coupling of polymers can be considered a *click* reaction. In addition, Arrhenius parameters for the propagation rate coefficient of methyl acrylate and 2-ethyl hexyl acrylate in bulk are determined *via* high frequency PLP-SEC and reported for temperatures up to 80 °C, which has previously been unreported. A branching study is also conducted utilizing the concept of local dispersity to compare branching characteristics of poly(methyl acrylate) and poly(2-ethyl hexyl acrylate). Last but not least, photo-initiation is employed to quantify the relative initiation ability of benzoyl and mesitoyl radicals in methyl methacrylate polymerization, providing important information on the reactivities of these radicals.

## Contents

Abstract.....	9
1 Introduction.....	15
1.1 Motivation.....	15
1.2 Thesis Overview .....	19
1.3 References.....	21
2 Theory and Background .....	25
2.1 Free Radical Polymerization.....	25
2.2 Ideal Free Radical Reaction Kinetics.....	26
2.2.1 Mechanism of Free Radical Polymerization.....	27
2.2.2 Chain Transfer Reactions .....	28
2.2.3 The Gel Effect.....	31
2.2.4 The Mayo Method .....	31
2.2.5 The Chain Length Distribution Method .....	32
2.2.6 Thiols as Chain Transfer Agents.....	34
2.3 Size Exclusion Chromatography (SEC).....	35
2.3.1 Triple Detection SEC.....	37
2.3.2 Concentration Sensitive Detectors .....	37
2.3.3 Static Light Scattering Detection .....	38
2.3.4 Viscometric Detection.....	40
2.3.5 SEC Calibration .....	41
2.4 The Arrhenius equation.....	44
2.5 Acrylate Free Radical Polymerization.....	45
2.6 A Closer Look at Midchain Radicals.....	46
2.6.1 Intramolecular Transfer .....	48
2.6.2 Backbiting.....	49
2.6.3 Intermolecular Transfer .....	50
2.6.4 Midchain Radical Reactions .....	51
2.7 Photo-Initiation .....	57
2.7.1 Some Important Photo-Initiators.....	60
2.8 Mass Spectrometry of Polymers .....	61
2.8.1 Ionization Methods.....	63
2.8.2 Mass Analyzers.....	65
2.8.3 Detectors.....	68
2.9 References.....	71
3 Methods and Materials .....	77

3.1	In-depth Probing of the Product Spectrum of High Conversion <i>n</i> -Butyl Acrylate Free Radical Polymerization Mediated by 1-Octanethiol .....	77
3.1.1	General Polymerization Procedures .....	77
3.1.2	Size Exclusion Chromatography .....	78
3.1.3	Electrospray Ionization Mass Spectrometry .....	78
3.1.4	<sup>13</sup> C Nuclear Magnetic Resonance .....	78
3.2	Macromonomer Synthesis and the Limitations of Thiol-ene Chemistry for Polymer-Polymer Conjugation .....	79
3.2.1	Materials: Macromonomer Formation .....	80
3.2.2	Macromonomer Synthesis Method .....	80
3.2.3	Materials: Thiol-ene experiments .....	80
3.2.4	General Procedure for Thiol-ene Reactions for the Formation of Star Polymers from Poly( <i>n</i> -Butyl Acrylate) Macromonomer .....	81
3.2.5	Size Exclusion Chromatography .....	81
3.2.6	Electrospray Ionization Mass Spectrometry .....	81
3.3	Pulsed Laser Polymerization (PLP) for the Quantification of the Efficiency of Photo-Initiation Processes in Methyl Methacrylate Free Radical Polymerization .....	82
3.3.1	Materials for polymerizations .....	82
3.3.2	Polymerizations .....	82
3.3.3	Synthesis of 1,2-dimesitylethane-1,2-dione (Mesityl) .....	83
3.3.4	UV Spectra .....	84
3.3.5	Electrospray Ionization Mass Spectrometry .....	84
3.4	Pulsed Laser Polymerization (PLP) for the Determination of $k_p$ of 2-Ethyl Hexyl Acrylate and MA beyond Ambient Temperature .....	84
3.4.1	General PLP procedure .....	84
3.4.2	Size Exclusion Chromatography .....	85
3.4.3	Mark-Houwink-Kuhn-Sakurada Parameter Determination for 2-Ethyl Hexyl Acrylate .....	85
3.5	PREDICI® .....	86
3.6	References .....	86
4	In-depth Probing of the Product Spectrum of High Conversion <i>n</i> -Butyl Acrylate Free Radical Polymerization Mediated by 1-Octanethiol .....	87
4.1	Introduction .....	87
4.2	Integration of Mass Spectra – Some considerations .....	91
4.2.1	Integration .....	92
4.3	Experimental Results – Thiol Mediated <i>n</i> -BA Polymerizations .....	95
4.4	Intermezzo – <sup>13</sup> C-Nuclear Magnetic Resonance for Quantitative Determination of Branching .....	100

4.5	Determination of the Transfer Constant of 1-Octanethiol Towards <i>n</i> -BA.....	111
4.6	Quantitative Evaluation of the Poly( <i>n</i> -BA) Product Spectrum <i>via</i> ESI-MS.....	112
4.6.1	Survey of Data and Consideration of Less Abundant Side Products .....	120
4.7	Summary of Results.....	121
4.8	References.....	123
5	Butyl Acrylate Macromonomer Synthesis & Its Application in Radical Catalyst-Free Polymer-Polymer Conjugation <i>via</i> Thiol-ene Coupling .....	127
5.1	Self-Directed Formation of Uniform Unsaturated <i>n</i> -Butyl Acrylate Macromonomers at High Temperatures .....	128
5.1.1	Macromonomer Synthesis.....	130
5.1.2	Summary – Synthesis of Butyl Acrylate Macromonomer.....	137
5.2	Limitations of the Thiol-ene Coupling Reaction for Polymer-Polymer Conjugation ...	137
5.2.1	Implications of the <i>Click</i> concept for Polymer Conjugation Reactions.....	141
5.2.2	Star polymers <i>via</i> Thiol-ene Chemistry .....	143
5.2.3	Comparison – Functional and Block Copolymers, and Star Polymers <i>via</i> Radical Thiol-ene Chemistry .....	160
5.2.4	Summary – Radical Thiol-ene Coupling as a <i>Click</i> Reaction.....	162
5.3	Conclusions.....	164
5.4	References.....	166
6	Quantifying the Efficiency of Photo-Initiation Processes in Methyl Methacrylate <i>via</i> Pulsed Laser Polymerization and the Determination of $k_p$ for Methyl Acrylate and 2-Ethyl Hexyl Acrylate beyond Ambient Temperature.....	169
6.1	Photo-polymerizations.....	169
6.2	Quantifying the Efficiency of Radicals Generated from Benzoin (2-hydroxy-1,2-diphenylethanone) and Mesitol (1,2-dimesitylethane-1,2-dione) .....	171
6.3	Data Analysis and Evaluation of the ESI-MS Spectra .....	177
6.4	Summary - Quantifying the Efficiency of Radicals Generated from Benzoin (2-hydroxy-1,2-diphenylethanone) and Mesitol (1,2-dimesitylethane-1,2-dione) .....	183
6.5	Pulsed Laser Polymerization for the Determination of Propagation Coefficients for MA and 2-EHA above Ambient Temperature .....	184
6.6	Problems Encountered in PLP of Acrylates and their Causes .....	188
6.7	Pulsed Laser Polymerization of Methyl Acrylate beyond 40 °C.....	190
6.8	Mark-Houwink-Kuhn-Sakurada Parameter Measurements .....	190
6.9	Results and Discussion – PLP of MA beyond 40 °C .....	194
6.10	Pulsed Laser Polymerization of 2-Ethyl Hexyl Acrylate beyond 25 °C .....	202
6.11	The Concept of Local Dispersity .....	210
6.12	2-Ethyl Hexyl Acrylate and Methyl Acrylate Local Dispersities.....	211
6.13	Summary of Results.....	218

6.14	References.....	220
7	Concluding Remarks and Outlook .....	225
7.1	Concluding Remarks.....	225
7.2	Outlook & Future Work.....	228
7.3	References.....	231
8	Appendix: Proposed PREDICI <sup>®</sup> Model for Evaluating Acrylate FRP in the presence of a Chain Transfer Agent.....	232
9	List of Abbreviations.....	239
10	Curriculum Vitae.....	242
11	Publications .....	243
12	Conference Contributions .....	244
13	Acknowledgments .....	246



# 1 Introduction

## 1.1 Motivation

Free radical polymerization (FRP) has been extensively used for over 70 years in the industrial production of polymers. The first 'synthetic' polymers of the 19th century were made by modifying natural polymers, for example, nitrocellulose was manufactured by reacting cellulose with nitric acid. The first entirely man-made polymer, the phenol-formaldehyde resin bakelite, was synthesized in 1907 by Leo Hendrik Baekeland. Since the development of synthetic polymers, they have been widely incorporated into vast numbers of products found in daily life and are therefore industrially very significant.

Many FRP processes have been developed and refined over the years for a variety of monomer and polymer types. Poly(styrene), poly(vinyl acetate) and poly(methyl methacrylate) are examples of mass produced polymers made *via* free radical polymerization. Materials synthesized *via* FRP include block copolymers and graft copolymers which find use in many common industrial and household applications such as adhesives, paints and coatings, textiles, non-woven fabrics, personal care products, wallpaper, construction materials, specialty additives, and many other areas.

The main acrylate monomers synthesized in bulk are methyl acrylate, ethyl acrylate, *n*-butyl acrylate and 2-ethyl hexyl acrylate. They are obtained by the esterification of acrylic acid, or by the transesterification of ethyl acrylate. Some other acrylate monomers used industrially include *tert*-butyl acrylate, *iso*-butyl acrylate and dodecyl acrylate. Polyacrylates are mostly obtained *via* FRP by thermal initiation, photo-initiation, or with ionizing radiation. Acrylates are commonly used in copolymerization reactions, often with styrene, acrylonitrile, vinyl acetate and methyl methacrylate. Copolymers of butyl acrylate can be prepared with acrylic acid and its salts, amides and esters, and with methacrylates, acrylonitrile, maleic acid esters, vinyl acetate, vinyl chloride, vinylidene chloride, styrene, butadiene and unsaturated polyesters and drying oils.<sup>1</sup> Butyl acrylate is also a very useful feedstock for chemical syntheses, because it readily undergoes addition reactions with a wide variety of organic and inorganic compounds.

Polymers synthesized *via* FRP span the entire range from high volume, low cost commodity polymers to low volume, high added value specialty polymers. There have been significant developments in polymer synthetic methods with the aim of producing highly specialized architectures using FRP in the last two decades however, many details of the mechanism and the underlying kinetics of FRP, especially in the case of acrylates, remain to be determined. When the polymerization process is scaled up to commercial proportions, a detailed understanding of the chemistry behind the kinetic processes is essential even before the plans for a reactor are drawn. For example, it is highly advantageous to know about the thermal effects taking place while the reaction occurs, such as whether the reaction is exothermic. In reactor design this may involve incorporation of heat exchangers and may allow the recovery and recycling of energy in the form of heat which thus lowers production costs.<sup>2</sup> As another example, having information at hand relating to the temperature dependence of reaction rates is useful in calculations to determine the required reaction time and is essential for the optimization of the manufacturing process. Knowledge of the fundamental kinetics involved is critical in production plant optimization to maximize the efficiency and cost benefits of mass production, and results in high quality, tailored polymers manufactured with minimal operating problems and at market competitive prices. Accurate knowledge of kinetic parameters in FRP processes also improves control of final polymer properties.

Acrylate monomers form very reactive propagating radicals which explains their high propagation rate coefficients. Furthermore, terminal secondary propagating radicals are highly susceptible to hydrogen transfer reactions, both *intermolecularly* and *intramolecularly*, resulting in the formation of a tertiary midchain radical (MCR). Propagation of the MCR creates branched polymer which can be of exceedingly high microstructural heterogeneity depending on the synthetic conditions.<sup>3-5</sup> In addition, a consequence of the tertiary nature of the MCR is that it has very different kinetics compared to a secondary propagating radical. Indeed, studies have been conducted to estimate the propagation rate coefficients of MCRs employing acrylate dimers as model compounds.<sup>6</sup> As electron spin resonance (EPR) studies have indicated that at 60 °C, 80 % of all radicals present are in the form of MCRs,<sup>7</sup> it can be envisaged that MCRs exert a considerable influence on the overall polymerization kinetics. MCRs and their subsequent reactions are

now generally accepted to be the source of many anomalies observed in acrylate polymerizations<sup>3,8-14</sup> and are the reason for the difficulties in obtaining well structured molecular weight distributions in Pulsed Laser Polymerization-Size Exclusion Chromatography (PLP-SEC) experiments on acrylates above ambient temperature,<sup>15-20</sup> until very recently.<sup>21</sup>

The full kinetic spectrum of a polymerization reaction includes initiation, propagation, termination and chain transfer reactions. The chain transfer class of reactions is itself highly complex, and may involve any combination of transfer to monomer, initiator, solvent, or to impurities.<sup>22</sup> As a result, the number of species participating in a polymerization reaction is potentially infinite. To add to the complexity, transfer agents are often used, for example to manipulate the molecular weight, which bring into play even more reactions. When the reactions that take place in the polymerization have been established, the rate coefficients for each reaction would ideally be known as this would enable a complete description of the final product *via* modeling and simulation of the reaction. The propagation rate coefficient is accessible *via* such methods as PLP-SEC,<sup>14,23-31</sup> and the termination rate coefficient by single pulse pulsed laser polymerization experiments<sup>32-34</sup> but unfortunately not all rate coefficients may be determined *via* rate measurements or by examination of the final product. Rate coefficients related to MCR reactions, for example  $\beta$ -scission and backbiting, and some transfer reactions are such that different methodologies must be developed to enable the extraction of these coefficients and for the moment, only estimates exist or values which have not yet been confirmed by alternate methods.<sup>35</sup>

Mass spectrometry (MS) of polymers may at first glance seem to be an oxymoron as gas phase ions are involved and polymers are by definition of high molecular weight and are difficult to elevate into the gas phase, but nevertheless, technological developments in the last two decades have enabled the analysis of polymers by the extremely useful technique of MS. MS techniques now enable the characterization of many aspects of bulk polymers, such as the chemical composition of the repeat units, the end groups and the molecular weight distributions of the polymer. One major strength of MS is the ability to observe individual polymer chains and their absolute molecular weights, and only require trace amounts of sample.

Gas chromatography-mass spectrometry (GC-MS) has been used to characterize very low molecular weight oligomeric material,<sup>36</sup> as well as the pyrolysis degradation products of polymers<sup>37-38</sup> and the combined technique of pyrolysis GC-MS has been employed to monitor the thermal curing of polymers.<sup>39</sup>

Field desorption (FD)<sup>40</sup> and fast atom bombardment (FAB)<sup>41</sup> MS were early techniques that enabled the analysis of polymer samples up to a few thousand  $\text{g}\cdot\text{mol}^{-1}$  which are difficult to volatilize,<sup>42-47</sup> but today, with the advent of Matrix Assisted Laser Desorption Ionization (MALDI) and Electrospray Ionization (ESI), both discussed shortly, FD and FAB are declining in use.

MALDI-MS is an important technique by which a large variety of polymers are still characterized today,<sup>48-54</sup> including poly(ethylene glycol) (PEG),<sup>55-56</sup> poly(methylmethacrylate) (pMMA),<sup>57-60</sup> polyesters,<sup>61-62</sup> and poly(styrene) (PS).<sup>63-64</sup> The difficulty in carrying out MALDI-MS arises in the appropriate choice of solvent<sup>65-66</sup> and matrix composition<sup>67-69</sup> which are crucial for a successful analysis as well as optimization of the laser to maximize ablation while retaining as much structural integrity as possible of the polymer chains to obtain reasonable spectra. MALDI-MS has the advantage of being able to measure relatively high molecular weight molecules, up to about  $100\,000\text{ g}\cdot\text{mol}^{-1}$ .<sup>70</sup>

Electrospray Ionization (ESI) MS has made a large impact on mass spectrometry particularly in the field of polymer characterization since the first reported instance of electrospraying of poly(styrene) macroions into an evaporation chamber to create negative macroions, and subsequent sampling of the gaseous mixture with a Faraday cage by Dole *et al.* in 1968.<sup>71</sup> ESI-MS experienced a resurgence in the late 1980s<sup>72-74</sup> and since then ESI-MS has been used to characterize a variety of polymers including PEG,<sup>75</sup> pMMA<sup>76-77</sup> and more recently, PS.<sup>78-79</sup> ESI-MS has been extensively used in mechanistic studies<sup>70</sup> and comprehensive reviews have been published<sup>80-83</sup> therefore no reiteration will be made here. It is sufficient to note that ESI-MS is a technique which affords information with accuracy and precision unparalleled by any other technique and is therefore increasingly being used, and in light of recent developments regarding the extraction of accurate molecular weight distributions *via* SEC-ESI-MS,<sup>84</sup> is showing itself to be a very promising instrumental analysis technique.

Given the far reaching consequences of MCR formation and subsequent reactions, any work which is concerned with providing more information on the behavior of MCRs under various conditions and explores methods of controlling the fate of MCRs once they form, would provide valuable information of high interest in both academia and in industry. The development and refining of ESI-MS makes available an invaluable tool for the investigations carried out herein, and allows the evaluation of product obtained to afford new insights into the formation processes in acrylate FRP.

## 1.2 Thesis Overview

The present thesis investigates many facets of the mechanism of acrylate (and methacrylate) FRP, from the behavior of radical initiation processes induced by UV-radiation, to the efficient tuning of the product spectrum of thermally initiated *n*-butyl acrylate polymerization to high conversions *via* the addition of a transfer agent, to an investigation into the thiol-ene coupling reaction to synthesize star polymers and an exploration of the branching characteristics of acrylate FRP polymers. The theme central to this thesis is the formation of MCRs as an inevitable side reaction in the FRP reaction mechanism, followed by the reaction pathways which the MCR can subsequently undergo.

The work undertaken herein aims to control the fate of MCRs once they form, either by exploiting the side reactions which MCRs undergo under certain conditions, or by effectively repairing and eliminating the MCR once it has formed. Both avenues lead to highly uniform product which requires no purification before further reactions are possible. The macromonomer product formed in one case is subsequently employed in a critical evaluation of the thiol-ene coupling reaction, with the aim of polymer-polymer conjugation to construct star polymer structures. An in-depth analysis of the product spectrum formed is conducted *via* ESI-MS in the thermally initiated FRP of *n*-butyl acrylate under various conditions of temperature and thiol concentration, demonstrating the versatile tunability of the product spectrum only by controlling temperature and added thiol concentration. A method for quantitative evaluation of the MS spectra obtained is also introduced.

In another section of work, PLP is used as a tool to investigate the nature and chemical reactivity of radicals produced under UV irradiation by clear unambiguous identification of the end groups of the resulting polymers. While the bulk of the mass in a typical polymer is

composed of the monomer repeat units, the chemical structure of the end groups can be extremely important to the performance properties of any polymer material. Conventional PLP-SEC experiments are also performed, with the aim of providing heretofore inaccessible propagation rate coefficients above ambient temperature for 2-ethyl hexyl acrylate and methyl acrylate. A study of the branching characteristics of poly(2-ethyl hexyl acrylate) in comparison to that of poly(methyl acrylate) is undertaken, utilizing the concept of local dispersity.

An integral characterization technique employed throughout is electro-spray ionization (ESI) coupled to a quadrupole mass analyzer – to give the technique of ESI-MS. ESI-MS has been identified as an extremely useful and increasingly powerful technique for polymer endgroup characterization.<sup>85</sup> As the polymer chains are not fragmented in the ionization process, intact polymer chains can be observed *via* mass spectrometry and the end groups of the polymer under study can therefore be determined. The observation of unfragmented polymer chains is seminal in the analysis of the product spectra formed in the work presented.

In summary, the current thesis contributes to the field of photo-initiated free radical polymerization by providing new information on the reactivity of selected photo-initiators, as well as to the field of acrylate kinetics by extending the fundamental understanding of FRP mechanism processes, in particular with respect to side reactions arising from the formation of MCRs during the polymerization reaction.

### 1.3 References

- 1 BASF; Corporation,  
<http://www2.basf.us/businesses/chemicals/acrylates/pdfs/butacry.pdf>, Ed.;  
Charlotte Technical Center: Accessed 11/05/2010, 2003.
- 2 Anxionnaz, Z.; Cabassud, M.; Gourdon, C.; Tochon, P. *Chemical Engineering and Processing: Process Intensification* 2008, 47, 2029-2050.
- 3 Castignolles, P. *Macromol. Rapid Commun.* 2009, 30, 1995-2001.
- 4 Plessis, C.; Arzamendi, G.; Alberdi, J. M.; van Herk, A. M.; Leiza, J. R.; Asua, J. M. *Macromol. Rapid Commun.* 2003, 24, 173-177.
- 5 Saunders, G.; Cormack, P. A. G.; Graham, S.; Sherrington, D. C. *Macromolecules* 2005, 38, 6418-6422.
- 6 Tanaka, K.; Yamada, B.; Fellows, C. M.; Gilbert, R. G.; Davis, T. P.; Yee, L. H.; Smith, G. B.; Rees, M. T. L.; Russell, G. T. J. *Polym. Sci., Part A: Polym. Chem.* 2001, 39, 3902-3915.
- 7 Willemse, R. X. E.; Herk, A. M. v.; Panchenko, E.; Junkers, T.; Buback, M. *Macromolecules* 2005, 38, 5098-5103.
- 8 Ahmad, N. M.; Heatley, F.; Lovell, P. A. *Macromolecules* 1998, 31, 2822-2827.
- 9 Arzamendi, G.; Plessis, C.; Leiza, J. R.; Asua, J. M. *Macromol. Theory Simul.* 2003, 12, 315-324.
- 10 Busch, M.; Wahl, A. *Macromol. Theory Simul.* 1998, 7, 217-224.
- 11 Lím, D.; Wichterle, O. *Journal of Polymer Science* 1958, 29, 579-584.
- 12 Nikitin, A. N.; Hutchinson, R. A. *Macromolecules* 2005, 38, 1581-1590.
- 13 Nikitin, A. N.; Hutchinson, R. A. *Macromol. Theory Simul.* 2006, 15, 128-136.
- 14 O'Shaughnessy, B.; Vavylonis, D. *Macromol. Theory Simul.* 2003, 12, 401-412.
- 15 van Herk, A. M. *Macromol. Rapid Commun.* 2001, 22, 687-689.
- 16 Plessis, C.; Arzamendi, G.; Alberdi, J. M.; Agnely, M.; Leiza, J. R.; Asua, J. M. *Macromolecules* 2001, 34, 6138-6143.
- 17 Plessis, C.; Arzamendi, G.; Leiza, J. R.; Schoonbrood, H. A. S.; Charmot, D.; Asua, J. M. *Macromolecules* 2000, 33, 4-7.
- 18 Quan, C.; Soroush, M.; Grady, M. C.; Hansen, J. E.; Simonsick, W. J. *Macromolecules* 2005, 38, 7619-7628.
- 19 Sato, E.; Emoto, T.; Zetterlund, P. B.; Yamada, B. *Macromol. Chem. Phys.* 2004, 205, 1829-1839.
- 20 Theis, A.; Feldermann, A.; Charton, N.; Davis, T. P.; Stenzel, M. H.; Barner-Kowollik, C. *Polymer* 2005, 46, 6797-6809.
- 21 Barner-Kowollik, C.; Günzler, F.; Junkers, T. *Macromolecules* 2008, 41, 8971-8973.
- 22 Odian, G. *Principles of Polymerization*; Wiley Interscience: Hoboken, New Jersey, 2004.
- 23 Asua, J. M.; Beuermann, S.; Buback, M.; Castignolles, P.; Charleux, B.; Gilbert, R. G.; Hutchinson, R. A.; Leiza, J. R.; Nikitin, A. N.; Vairon, J.-P.; van Herk, A. M. *Macromol. Chem. Phys.* 2004, 205, 2151-2160.
- 24 Bergert, U.; Beuermann, S.; Buback, M.; Kurz, C. H.; Russell, G. T.; Schmaltz, C. *Macromol. Rapid Commun.* 1995, 16, 425-434.
- 25 Beuermann, S.; Buback, M. *Prog. Polym. Sci.* 2002, 27, 191-254.
- 26 Beuermann, S.; Buback, M.; Schmaltz, C. *Macromolecules* 1998, 31, 8069-8074.
- 27 Buback, M.; Feldermann, A.; Barner-Kowollik, C.; Lacik, I. *Macromolecules* 2001, 34, 5439-5448.

- 
- 28 Hutchinson, R. A.; Richards, J. R.; Aronson, M. T. *Macromolecules* 1994, 27, 4530-4537.
- 29 Junkers, T.; Voll, D.; Barner-Kowollik, C. *e-polymers* 2009, 076.
- 30 Lacik, I.; Beuermann, S.; Buback, M. *Macromolecules* 2003, 36, 9355-9363.
- 31 Nikitin, A. N.; Hutchinson, R. A.; Buback, M.; Hesse, P. *Macromolecules* 2007, 40, 8631-8641.
- 32 Barner-Kowollik, C.; Buback, M.; Egorov, M.; Fukuda, T.; Goto, A.; Olaj, O. F.; Russell, G. T.; Vana, P.; Yamada, B.; Zetterlund, P. B. *Prog. Polym. Sci.* 2005, 30, 605-643.
- 33 Buback, M.; Egorov, M.; Feldermann, A. *Macromolecules* 2004, 37, 1768-1776.
- 34 Buback, M.; Kuelpmann, A.; Kurz, C. *Macromol. Chem. Phys.* 2002, 203, 1065-1070.
- 35 Junkers, T.; Barner-Kowollik, C. *J. Polym. Sci., Part A: Polym. Chem.* 2008, 46, 7585-7605.
- 36 Parees, D. M.; Hanton, S. D.; Cornelio Clark, P. A.; Willcox, D. A. *J. Am. Soc. Mass Spectrom.* 1998, 9, 282.
- 37 Minard, R. D.; Hatcher, P. G.; Gourley, R. C.; Matthews, C. N. *Origins Life Evol. Biosphere* 1998, 28, 461.
- 38 Richter, F.; Schneider, S.; Distler, F.; Schubert, R. *Polym. Degrad. Stab.* 1999, 65, 315.
- 39 Galipo, R. C.; Egan, W. J.; Aust, J. F.; Myrick, M. L.; Morgan, S. L. *J. Anal. Appl. Pyrolysis* 1998, 45, 23.
- 40 Lattimer, R. P.; Harmon, D. J.; Welch, K. R. *Anal. Chem.* 1979, 51, 1293.
- 41 Barber, M.; Bordoli, R.; Sedgwick, R. D.; Tyler, A. N. *J. Chem. Soc., Chem. Commun.* 1981, 325.
- 42 Montaudo, G.; Scamporrino, E.; Vitalini, D. *Macromolecules* 1991, 24, 376-382.
- 43 Rollins, K.; Scrivens, J. H.; Taylor, M. J.; Major, H. *Rapid Commun. Mass Spectrom.* 1990, 4, 355.
- 44 Jackson, A. T.; Jennings, K. R.; Scrivens, J. H. *Rapid Commun. Mass Spectrom.* 1996, 10, 1449.
- 45 Klee, J. E.; Haegele, K.; Przybylski, M. *J. Polym. Sci.: Part A: Polym. Chem.* 1996, 34, 2791.
- 46 Ganesh, K.; Paramasivam, S.; Kishore, K. *Polym. Bull.* 1996, 37, 785.
- 47 Montaudo, M.; Puglisi, C.; Samperi, F.; Montaudo, G. *Macromolecules* 1998, 31, 8666.
- 48 Madkour, A. E.; Koch, A. H. R.; Lienkamp, K.; Tew, G. N. *Macromolecules* 2010, 10.1021/ma100330u.
- 49 Gu, Y.; He, J.; Li, C.; Zhou, C.; Song, S.; Yang, Y. *Macromolecules* 2010, doi: 10.1021/ma1000139.
- 50 Lonsdale, D. E.; Bell, C. A.; Monteiro, M. J. *Macromolecules* 2010, 43, 3331-3339.
- 51 Plamper, F. A.; Schmalz, A.; Penott-Chang, E.; Drechsler, M.; Jusufi, A.; Ballauff, M.; Müller, A. H. E. *Macromolecules* 2007, 40, 5689-5697.
- 52 Colombani, O.; Ruppel, M.; Schubert, F.; Zettl, H.; Pergushov, D. V.; Müller, A. H. E. *Macromolecules* 2007, 40, 4338-4350.
- 53 Goodwin, A. P.; Lam, S. S.; Fréchet, J. M. J. *J. Am. Chem. Soc.* 2007, 129, 6994-6995.
- 54 Liu, J.; Tanaka, T.; Sivula, K.; Alivisatos, A. P.; Fréchet, J. M. J. *J. Am. Chem. Soc.* 2004, 126, 6550-6551.
- 55 Dey, M.; Castoro, J. A.; Wilkins, C. L. *Anal. Chem.* 1995, 67, 1575.

- 
- 56 Hofmann, A. M.; Wurm, F.; Hühn, E.; Nawroth, T.; Langguth, P.; Frey, H. *Biomacromolecules* 2010, 11, 568-574.
- 57 Larsen, B. S.; Simonsick, W. J.; McEwen, C. N. *J. Am. Soc. Mass Spectrom.* 1996, 7, 287.
- 58 Kapfenstein, H. M.; Davis, T. P. *Macromol. Chem. Phys.* 1998, 199, 2403.
- 59 Rashidzadeh, H.; Guo, B. *Analytical Chemistry* 1998, 70, 131-135.
- 60 Hanton, S. D.; Liu, X. M. *Analytical Chemistry* 2000, 72, 4550-4554.
- 61 Sahota, H. S.; Lloyd, P. M.; Yeates, S. G.; Derrick, P. J.; Taylor, P. C.; Haddleton, D. M. *J. Chem. Soc., Chem. Commun.* 1994, 2445.
- 62 Montaudo, M. S.; Puglisi, C.; Samperi, F.; Montaudo, G. *Macromolecules* 1998, 31, 8666.
- 63 Schreimer, D. C.; Li, L. *Anal. Chem.* 1997, 69, 4176.
- 64 Nielen, M. W. F.; Malucha, S. *Rapid Commun. Mass Spectrom.* 1997, 11, 1194.
- 65 Yalcin, T.; Dai, Y.; Li, L. *J. Am. Soc. Mass Spectrom.* 1998, 9, 1303.
- 66 Yalcin, T.; Schreimer, D. C.; Li, L. *J. Am. Soc. Mass Spectrom.* 1997, 8, 1220.
- 67 Lehrle, R. S.; Sarson, D. S. *Rapid Commun. Mass Spectrom.* 1995, 9, 91.
- 68 Lehrle, R. S.; Sarson, D. S. *Polym. Degrad. Stab.* 1996, 51, 197.
- 69 Linnemayr, K.; Vana, P.; Allmaier, G. *Rapid Commun. Mass Spectrom.* 1998, 12, 1344.
- 70 Barner-Kowollik, C.; Davis, T. P.; Stenzel, M. H. *Polymer* 2004, 45, 7791-7805.
- 71 Dole, M.; Mack, L. L.; Hines, R. L.; Mobley, R. C.; Ferguson, L. D.; Alice, M. B. *The Journal of Chemical Physics* 1968, 49, 2240-2249.
- 72 Fenn, J. B.; Mann, M.; Meng, C. K.; Wong, S. F.; Whitehouse, C. M. *Mass Spectrom. Rev.* 1990, 9, 37-70.
- 73 Fenn, J. B.; Mann, M.; Meng, K.; Wong, S. F.; Whitehouse, C. M. *Science* 1989, 64, 64.
- 74 Yamashita, M.; Fenn, J. B. *J. Phys. Chem.* 1984, 88, 451.
- 75 Maziarz, E. P.; Baker, G. A.; Wood, T. D. *Macromolecules* 1999, 32, 4411.
- 76 Haddleton, D. M.; Feeney, E.; Buzy, A.; Jasieczek, C. B.; Jennings, K. R. *Chem. Commun.* 1996 1157-1158.
- 77 McEwen, C. N.; Simonsick, W. J. J.; Larsen, B. S.; Ute, K.; Hatada, K. *Journal of the American Chemical Society Mass Spectrometry* 1995, 6, 906-911.
- 78 Gruending, T.; Hart-Smith, G.; Davis, T. P.; Stenzel, M. H.; Barner-Kowollik, C. *Macromolecules* 2008, 41, 1966-1971.
- 79 Ladavière, C.; Lacroix-Desmazes, P.; Delolme, F. *Macromolecules* 2008, 42, 70-84.
- 80 Saf, R.; Mirtl, C.; Hummel, K. *Acta polymer.* 1997, 48, 513-526.
- 81 Gruending, T.; Weidner, S.; Falkenhagen, J.; Barner-Kowollik, C. *Polymer Chemistry* 2010, DOI: 10.1039/b9py00347a.
- 82 Santos, L. S. *European Journal of Organic Chemistry* 2008, 235-253.
- 83 He, M. Y.; Chen, H. *Curr. Org. Chem.* 2007, 11, 909-923.
- 84 Gruending, T.; Guilhaus, M.; Barner-Kowollik, C. *Analytical Chemistry* 2008, 80, 6915-6927.
- 85 Hanton, S. D. *Chem. Rev.* 2001, 101, 527-569.



## 2 Theory and Background

### 2.1 Free Radical Polymerization

The background section will provide an introduction to ideal and non-ideal free radical polymerization kinetics, with a focus on acrylate monomers, the class of monomers to which most attention was devoted to in the present thesis. This thesis investigates the kinetic and mechanistic aspects of butyl acrylate free radical polymerization (FRP) under various synthetic conditions, including thermal and UV initiation, in the presence of thiol transfer agents as molecular weight mediator as well as microstructure mediator. Initial work is undertaken to attempt to model butyl acrylate FRP at high conversion to extract kinetic coefficients related to side product formation which are otherwise inaccessible *via* analysis of the final product. Acrylate polymerization kinetics deviate strongly from ideal polymerization kinetics, and a discussion of the non-ideality of acrylate kinetics is paramount in the context of this thesis. The work is primarily concerned with exploring the acrylate side reactions that have now been accepted to give rise to the particular characteristics of acrylate polymerizations.

Branch formation is one peculiarity of acrylate polymerization, specifically the observation that branching occurs to different extents throughout the analogous series. Branching is investigated in a comparative study of methyl acrylate and 2-ethyl hexyl acrylate *via* pulsed laser polymerization (PLP). The background therefore contains a short discussion of photo-initiation, in the context of PLP experiments, and the behavior of 2,2-dimethoxy-2-phenylacetophenone (DMPA) under UV radiation, as it is employed as an initiator. For a description of the PLP-SEC technique and the underlying theory please refer to Chapter 6. SEC is used to determine the maximum inflection point in the first derivative of the MWD,  $L_{0,i}$ , from which  $k_p$  is calculated, in the work detailed in Chapter 6. A consensus has emerged that the best estimate of  $L_{0,i}$  is the point of inflection on the low molar mass side of the peak of the Molar Weight Distribution (MWD) usually determined by searching for a maximum on a differential plot of the MWD.<sup>1</sup>

Also present are the background and basic principles of size exclusion chromatography (SEC) and electrospray ionization mass spectrometry (ESI-MS) which are ubiquitous

characterization methods employed throughout the work conducted, and therefore warrant detailed discussion. A comprehensive kinetic literature review pertaining to midchain radicals is presented in Chapter 4 rather than in the background section due to its highly specific nature. The software package PREDICI has been employed in preliminary simulation work as a framework towards the determination of heretofore inaccessible kinetic coefficients, and a general discussion of the methodology involved is presented in the outlook.

## 2.2 Ideal Free Radical Reaction Kinetics

Ideal free radical polymerizations are underpinned by four assumptions:

- Monomeric species are only consumed in propagation and transfer reactions
- All reactions are irreversible
- Termination only takes place by bimolecular termination or by disproportionation
- All radicals, irrespective of chain length, exhibit the same reactivity

In practice however, ideal polymerization kinetics are the exception rather than the norm.

There are innumerable factors which can contribute to make a polymerization non ideal.

Some of these complicating factors include:

- Transfer reactions
- Chain length dependent termination and propagation,
- Non-ideal initiation conditions,
- Solvent effects influencing the propagation rate coefficient,
- The cage effect, where newly created radicals are trapped for some short period before they diffuse apart. The radicals in the solvent cage may undergo recombination, or may react with each other or with monomer, or they may diffuse out of the solvent cage. Once outside the solvent cage, the radicals may react with any other radical in close proximity.
- Influence of the initiation rate by additives or solvents,
- Change in the termination rate dependent on medium viscosity.

Furthermore, many side reactions also readily occur, such as transfer reactions, which are discussed shortly.

The polymerization of acrylates in particular is interesting in its non-ideality. Much of the work in this thesis is concerned with investigating the non-ideality of acrylate polymerizations and increasing current understanding of the complex interplay of the kinetic interactions which occur in acrylate free radical polymerizations.

### 2.2.1 Mechanism of Free Radical Polymerization

Polymerizations consist of several steps, from the initial radical generation which starts the polymerization to the various termination reactions which produce the final end polymer. In general a polymerization will have the following steps: initiation, propagation, and termination, either by combination or by disproportionation. Chain transfer can also occur in the presence of a suitable chain transfer agent.

During initiation, the initiator molecule, represented by I, decomposes by a first order reaction with a rate coefficient  $k_d$  to give two free radicals.



The radical subsequently adds to a monomer by taking an electron from the electron-rich double bond, forming a single bond with the monomer but leaving an unpaired electron at the other end.



$P_1$  represents a growing polymer radical with one repeating unit. The product of the addition is still a free radical, and it proceeds to propagate the chain by adding another monomer unit to itself.



The unpaired electron is maintained at the chain end, and this enables addition of more monomer units.

The propagation reaction is typically written as:



An assumption here is that reactivity is independent of chain length by using the same  $k_p$  for each propagation step.

A growing chain can be terminated in one of two ways, by combination or by disproportionation.



The relative proportion of each termination mode depends on the particular polymer and the reaction temperature, but in most cases one or the other predominates.<sup>2</sup> The termination rate coefficient is diffusion controlled and therefore dependent upon the following reaction parameters:<sup>3</sup>

- The temperature
- The chain length of the terminating free macroradicals
- The system viscosity
- The pressure
- The polymer concentration

The concept of Chain-Length-Dependent termination (CLDT) emerged with the realization that if the termination rate is diffusion controlled, and large radicals move more slowly than small radicals, then it is to be expected that large radicals terminate more slowly than small radicals. The advent of pulsed laser polymerization (see Chapter 6) has allowed  $k_p$  to be determined independently of termination and has paved the way for the development of methods of deducing  $k_t$ . A thorough review was recently published by Barner-Kowollik and Russell<sup>4</sup> covering the fundamentals of CLDT, the experimental methods by which  $k_t$  is accessible as well as case studies of published literature.

### 2.2.2 Chain Transfer Reactions

Free radicals are generally very reactive and can participate in many different side reactions in a given polymerization system. One type of reaction often observed is chain transfer. Chain transfer reactions terminate a growing chain radical and generate a new radical which

can reinitiate polymerization if transfer occurs onto a dead polymer chain. Subsequent propagation reactions from such a radical creates branched polymers.



Thus chain transfer results in shorter chains, and if reinitiation is as fast as the propagation reaction then chain transfer will not change the overall rate of polymerization appreciably. R'-H is known as a chain transfer agent. Under appropriate conditions any compound or impurity in the reaction mixture may act as a chain transfer agent, including initiator, monomer, solvent, impurities and terminated polymer.<sup>2</sup> Chain transfer reactions occur as an intrinsic reaction in the mechanism of acrylate polymerizations, but certain chain transfer reactions may also be deliberately induced, for example by the addition of a chain transfer agent. The chain transfer constant is defined as the ratio of the transfer rate coefficient to the propagation rate coefficient, see Equation 2-13. For methyl acrylate, transfer constants to polymer ranging from  $0.5 \cdot 10^{-4}$  to  $1.0 \cdot 10^{-4}$  have been published which are reasonably low at temperatures below 0 °C.<sup>5</sup> However at high temperatures, i.e. > 60 °C, backbiting and  $\beta$ -scission become important and are the cause of many of the irregularities observed in acrylate polymerizations. This is discussed in more detail in section 2.6.

The effects of chain transfer on the rate of polymerization and on number-average molecular weight ( $\overline{M}_n$ ) is summarized in Table 2-1. The effect of chain transfer on the polymerization rate depends on how comparable the rate of reinitiation is to the rate of propagation of the original radical. When reinitiation is rapid, as in the first two situations

outlined in the table, then no change in polymerization rate is observed. The relative decrease of  $\overline{M}_n$  depends on the magnitude of the transfer constant. When the transfer constant is close to or larger than unity, a small polymer is produced, also known as a telomer or an oligomer, depending on the concentration of monomer and transfer agent.

The residual degree of polymerization,  $\overline{DP}_n$ , can be calculated according to the Mayo equation:

$$\overline{DP}_n^{-1} = \overline{DP}_n^{\infty} - \frac{k_{tr}[CTA]}{k_p[M]} \quad \text{Equation 2-13}$$

The Mayo equation describes the effect of various transfer reactions on the number-average degree of polymerization. Equation 2-13 describes a particular case of the Mayo equation where transfer to transfer agent is the most significant transfer reaction, often in the case where a transfer agent is added to the polymerization mixture.

Table 2-1: Effect of Chain Transfer on  $R_p$  and  $\overline{M}_n$  <sup>3</sup>

Relative rate constants of Transfer, Propagation and Reinitiation	Type of Effect	Effect on $R_p$	Effect on $\overline{M}_n$
$k_p \gg k_{tr}$ and $k_a \approx k_p$	Normal chain transfer	None	Decrease
$k_p \ll k_{tr}$ and $k_a \approx k_p$	Telomerization	None	Large decrease
$k_p \gg k_{tr}$ and $k_a < k_p$	Retardation	Decrease	Decrease
$k_p \ll k_{tr}$ and $k_a < k_p$	Degradative chain transfer	Large decrease	Large decrease
$k_p \ll k_{tr}$ and $k_a > k_p$	RAFT*	None	Decrease

\*Reversible Addition-Fragmentation Chain Transfer

A chain transfer constant  $C$  for a substance is defined to be the ratio of the rate coefficient  $k_{tr}$  for the chain transfer of a propagating radical with that substance to the rate coefficient  $k_p$  for propagation of the radical. The chain transfer constants for monomer and chain transfer agent are respectively given by:

$$C_M = \frac{k_{tr,M}}{k_p} \quad \text{and} \quad C_{CTA} = \frac{k_{tr,CTA}}{k_p} \quad \text{Equation 2-14: Chain transfer constants}$$

Current methods do not allow a direct evaluation of the chain transfer coefficient  $k_{tr}$ , rather they allow the determination of the chain transfer constant as related to  $k_p$ , in the form of  $C_M$  and  $C_{CTA}$  as seen in Equation 2-13.

If polymerization is carried out under conditions which minimize the contribution of bimolecular termination as a termination reaction, as in the case of a transfer polymerization where by definition the bimolecular termination reaction is diminished, the highly uniform end group that is introduced may be used for further reaction including chain extension and block copolymer formation. One example of very efficient transfer agents are thiols, which are successfully employed in the work presented in this thesis.

### 2.2.3 The Gel Effect

Radical chain polymerizations exhibit an auto-acceleration of the polymerization rate as the reaction proceeds.<sup>6</sup> Normally, it is expected that the reaction rate would decrease with time as the monomer and initiator concentrations decrease with time. However, the opposite behavior is observed in many polymerizations, where the reaction rate is seen to increase with conversion. This behavior is referred to as the gel effect, as is also known as the Trommsdorff effect or the Norrish–Smith effect (or the Norrish-Trommsdorff effect). Similar behavior has been observed for a variety of monomers, including styrene, vinyl acetate, and methyl methacrylate.<sup>7-9</sup> The gel effect occurs as a result of a series of changes which occur during the polymerization reaction. As monomer is converted to polymer, the viscosity of the solution increases. This causes a reduction in  $k_t$ , which has the effect of increasing the rate of polymerization. Since polymerization is an exothermic reaction, the temperature of the solution increases, further increasing the rate of polymerization. The viscosity also increases as a result of the increased rate of polymerization, and the cycle starts over again, leading to the gel effect. The gel effect is the normal behavior for most polymerizations, unless the polymerization is carried out in dilute solution or in telomerization reactions.

### 2.2.4 The Mayo Method

The Mayo method of chain transfer constant determination is based on polymer chain length, which is represented by the average degree of polymerization  $\overline{DP}_n$ :

$$\overline{DP}_n = \frac{r_p}{r_{t,com} + r_{t,dis} + \sum_{i=0}^n r_{tr,i}} \quad \text{Equation 2-15}$$

Where  $r_{t,com}$  is the rate of termination by combination,  $r_{t,dis}$  is the rate of termination by disproportionation, and  $r_{tr}$ ,  $r_{td}$  and  $r_{tr,i}$  are the rates of termination by transfer to other species, denoted by  $i$ .

From this equation, one can obtain:

$$\overline{DP}_n^{-1} = \frac{(k_{t,com} + 2k_{t,dis})[R]}{k_p[M]} + \sum_{CTA} \frac{k_{tr,i}[CTA]}{k_p[M]} \quad \text{Equation 2-16}$$

Now,  $r_p = k_p[M][R]$  and  $C_{tr,CTA} = \frac{k_{tr,CTA}}{k_p}$ . Introducing these two equations into Equation 2-16, and extracting the transfer to monomer, the equation can be re-arranged to give the Mayo equation:

$$\overline{DP}_n^{-1} = \frac{(k_{t,com} + 2k_{t,dis})r_p}{(k_p[M])^2} + C_{tr,M} + \sum_{CTA} C_{tr,CTA} \frac{[CTA]}{[M]} \quad \text{Equation 2-17}$$

The value of the sought after transfer constant is determined from the slope of the plot of  $\overline{DP}_n^{-1}$  vs the concentration of transfer agent employed. Drawbacks of this methods arise due to the fact that the transfer constant is determined based on  $\overline{DP}_n$ .  $\overline{DP}_n$  is most commonly determined by size exclusion chromatography and average molar masses evaluated by SEC have potentially high errors of around 20 % associated with them.  $\overline{DP}_n$  values obtained by several laboratories on the basis of identical polystyrene standards were at best within 16 %<sup>66</sup> of each other and at worst discrepancies of up to 800 %<sup>67</sup> were observed. Furthermore, this method relies on two conditions which are difficult to practically satisfy: (i) that no impurities be present in case of transfer reactions to these impurities, (ii) that no transfer to polymer exists as any transfer reactions limiting the chain length must be considered. However, to date this is still the method most commonly used to determine transfer coefficients. A plot of  $\frac{1}{\overline{DP}_n}$  vs [CTA] gives a straight line with slope  $\frac{[CTA]}{[M]}$  and intercept  $(\overline{DP}_n^\infty)^{-1}$ .

### 2.2.5 The Chain Length Distribution Method

An alternative method of determining  $C_{CTA}$  is the chain length distribution (CLD) method. The CLD method is based on the molecular weight distributions resulting from size exclusion

chromatography analysis.<sup>10-11</sup> The theory concerning the CLD method has to do with the statistical probability of the reactions which a propagating radical can participate in, namely propagation, termination, or chain transfer. At any given point in the polymerization, the probability that a radical undergoes propagation is given by:

$$S = \frac{R_p}{R_p + R_{tr} + R_t} \quad \text{Equation 2-18}$$

Where  $R_p$  is the rate of polymerization,  $R_{tr}$  is the rate of transfer and  $R_t$  is the rate of termination. Furthermore,  $R_p$ ,  $R_{tr}$ , and  $R_t$  can each be expressed as follows:

$$R_p = k_p[M][P \cdot] \quad \text{Equation 2-19}$$

$$R_{tr} = k_{tr,CTA}[CTA][P \cdot] + k_{tr,I}[I][P \cdot] + k_{tr,M}[M][P \cdot] \quad \text{Equation 2-20}$$

$$R_t = k_t[P \cdot]^2 \quad \text{Equation 2-21}$$

Where  $k_t = k_{t,com} + k_{t,dis}$

Substituting Equation 2-19, Equation 2-20 and Equation 2-21 into Equation 2-18 and rearranging gives:

$$\frac{1}{S} = 1 + C_{CTA} \frac{[CTA]}{[M]} + C_I \frac{[I]}{[M]} + C_M + \frac{k_t[P \cdot]}{k_p[M]} \quad \text{Equation 2-22}$$

where  $C_{CTA}$ ,  $C_I$  and  $C_M$  are the transfer constants for transfer to chain transfer agent, transfer to initiator and transfer to monomer respectively.

The probability that a chain will propagate and terminate to give a final polymer of length  $i$  is given by:

$$P_i = (1 - S)S^{i-1} \quad \text{Equation 2-23}$$

Equation 2-23 is the Schulz-Flory most probable distribution, where:

$$\overline{DP}_n = \frac{1}{1-S} \quad \text{Equation 2-24}$$

and

$$S = 1 - \frac{1}{\overline{DP}_n} \quad \text{Equation 2-25}$$

Substituting Equation 2-24 and Equation 2-25 into Equation 2-22 gives the Mayo equation, see Equation 2-17.

A plot of the ln chain length distribution ( $\ln P_i$ ) vs  $i$  is known as the ln CLD plot, and affords a straight line with slope  $\ln S$ . The determination of the chain transfer constant can then be made similarly to the conventional Mayo analysis. When negligible transfer to initiator and termination by combination apply, Equation 2-22 is reduced to:

$$\frac{1}{S} = 1 + \frac{1}{DP_n^\infty} + C_{CTA} \frac{[CTA]}{[M]} \quad \text{Equation 2-26}$$

The transfer constant is then obtained from a plot of  $\frac{1}{S} - 1$  vs  $\frac{[CTA]}{[M]}$ , where the resulting intercept is  $\frac{1}{DP_n^\infty}$ . However, as  $\frac{1}{S} - 1 = -(1 - \frac{1}{S}) \approx \ln S$ , the ln CLD plot may be plotted against  $\frac{[CTA]}{[M]}$  instead of  $i$  with similar results. Heuts *et al.*<sup>12</sup> established that the results obtained *via* the Mayo method and the CLD method are comparable and produce essentially identical results provided each method is applied following the prescribed conditions.

### 2.2.6 Thiols as Chain Transfer Agents

Thiols have long been used as transfer agents, patents dating back to the 1930s<sup>13</sup> can be found on the use of thiols as molecular weight control agents and new discoveries involving the use of thiols are still being made to this day.<sup>14</sup> A recent review exhaustively describes the reasons for which thiols are extensively used and will not be re-iterated here.<sup>15</sup>

The processes behind chain transfer reactions are investigated to this day. Most of the studies on the behavior of thiols as chain transfer agents deal with aliphatic thiols.<sup>12,16-19</sup> Encinas and coworkers<sup>17</sup> systematically studied the behavior of 4-substituted thiophenols as chain transfer agents in the free-radical photopolymerization of vinyl monomers both in aqueous solution and organic media. Functional polymers have been successfully prepared by using functional thiols. For example, carboxylic acid<sup>20</sup> and hydroxyl<sup>21</sup> functionalities were introduced to the polymer chain ends by using 3-mercaptopropionic acid and 2-mercaptoethanol as functional chain transfer agents, respectively. Karasu *et al.*<sup>22</sup> used a polymeric photo-initiator having a thiol endgroup in the free-radical polymerization of styrene and methyl methacrylate, and as a consequence of the chain transfer reactions,

they synthesized polymers with endgroups capable of acting as a photo-sensitizer in a subsequent free-radical polymerization. Yamaguchi *et al.*<sup>23</sup> have synthesized polymers containing thiol at the terminal position by radical polymerization using bis(2,4-dinitrophenyl) disulfide as chain transfer agent.

### 2.3 Size Exclusion Chromatography (SEC)

Size exclusion chromatography (SEC) is the standard technique for the determination of molar mass averages and molecular weight distributions of polymers. SEC makes use of a column or series of columns packed with particles of a porous substrate for separation on the basis of hydrodynamic volume.

The term gel permeation chromatography more specifically refers to a separation column filled with cross-linked polymer that is swollen by the employed solvent. This is the most common type of substrate, but other substrates, such as glass beads, are also used.

The column is maintained at a constant temperature, and solvent is passed through it at a constant rate. At the start of a run a small amount of polymer solution is injected into the start of the column and the solvent flow carries the polymer through the column. The smaller molecules have easy access to the substrate pores and diffuse in and out of them. The large molecules cannot fit into the pores and are carried more or less directly through the interstices in the packing. Thus a separation is achieved, where the larger molecules are washed out of the column first, followed by successively smaller ones. SEC is a relative method. To provide quantitative results the relation between molecular weight and volume of solvent that has passed through the detector since sample injection (also known as the elution volume) must be established by calibration with monodisperse polymer standards.<sup>2</sup>

A concentration sensitive detector is placed at the outlet of the column. Common detectors are differential refractometers, which measure the difference in refractive index between pure solvent and the polymer solution leaving the column, and ultraviolet or infrared detectors, which can be used if the polymer contains some group that absorbs the radiation.<sup>2</sup> Since separation in SEC is governed by the size of solute molecules in solution, solutes of similar hydrodynamic volume but different molecular weight will elute at the same retention volume. Thus a linear molecule may elute at the same time as a branched

molecule. A more spherical molecule having the same molecular weight as a linear molecule will be of more compact size and will elute later.

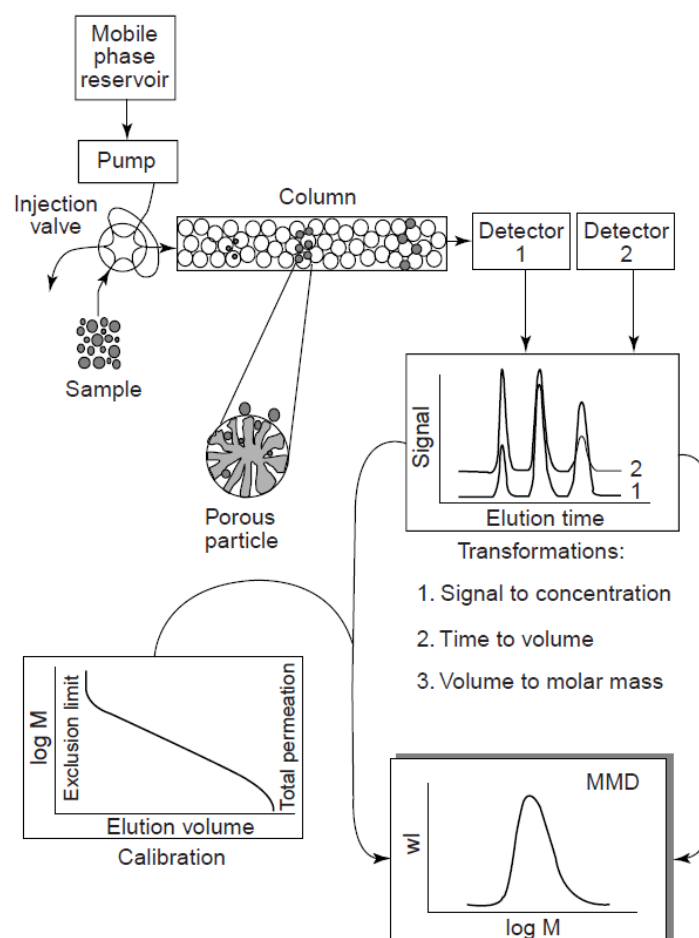


Figure 2-1: Schematic representation of SEC. Reproduced from Trathnigg, B., in *Encyclopedia of Analytical Chemistry*, R.A. Meyers (Ed.), John Wiley & Sons, 2000

Molecular size must be defined in terms of solvent and temperature conditions as the size of a polymer coil in solution can be extended or contracted by varying solvent and/or temperature.

To relate molecular size to molecular weight, as ultimately the goal of SEC analysis is to provide a molecular weight measurement of the polymer being analyzed, the concept of intrinsic viscosity,  $[\eta]$ , is employed. It can be computed and is related to the size, shape and molecular weight of the polymer in solution. When a polymer is dissolved in solution, the

solution viscosity increases because of the presence of solvated polymer chains and the relationship between  $[\eta]$  and MW is quantified in the Flory-Fox equation as follows:

$$[\eta] = \Phi_0 \frac{(r^2)^{3/2}}{M} \quad \text{Equation 2-27: Flory-Fox equation}$$

Where  $(r^2)^{1/2}$  is the unperturbed root-mean-square end-to-end distance of the polymer chain, and  $\Phi_0$  is the Flory constant, equal to  $2.1 \times 10^{23} \text{ mol}^{-1}$ . The Flory constant is theoretically the same for all linear, flexible chains in an unperturbed state. By substituting the radius of gyration for the root-mean-square, where  $r^2 = 6(R_g^2)$  and the molecular hydrodynamic volume  $V_h = (R_g^2)^{3/2}$  and rearranging, an equation is obtained which relates  $[\eta]M$  to the molecular hydrodynamic volume  $V_h$  of a polymer:

$$[\eta]M = \Phi_0 6^{3/2} V_h \quad \text{Equation 2-28}$$

### 2.3.1 Triple Detection SEC

For the accurate characterization of polymers, often several detectors are used in tandem. Triple detection SEC allows the determination of exact molecular weight *via* a combination of chemical and/or physical detectors. Some chemical detectors include infrared (IR), mass spectrometry (MS), nuclear magnetic resonance (NMR), while some physical detectors include the viscometer and the light-scattering photometer. There are many ways in which the various detectors can be coupled and an exhaustive description of all the available detectors and analytical set-ups is beyond the scope of this thesis and there is abundant literature on the topic.<sup>24-25</sup> The discussion here will focus on the description of the detectors used in the system employed in the work contained in this thesis, namely the deflection-type differential refractometer, coupled with the ultraviolet (UV)/visible detector as a concentration sensitive detector, and the multi-angle light scattering photometer.

### 2.3.2 Concentration Sensitive Detectors

This type of detector measures the concentration of analyte at each elution volume, and is by far the most widely used, as they meet the minimum detection requirements for the determination of average molecular weights and in combination with Mark-Houwink calibration curves.

### 2.3.2.1 Differential Refractometers

The commonly used differential refractive index (DRI) detector is a type of concentration sensitive detector which measures a bulk property of the eluent. DRI detectors operate on a deflection-type system, and use the principle of refraction. A tungsten lamp or pulsed light-emitting diode produces light which is passed through a flow cell containing the sample and reference solvent, reflected off a mirror back through the sample and reference, and onto a detector. If the sample and reference have the same refractive index, the detector, usually a set of photodiodes, produces equal signals. When a difference in refractive index exists, a voltage difference is created between the photodiodes, which is displayed as a signal in volts or refractive index units, and is proportional to the concentration of the analyte in that particular elution volume.

### 2.3.2.2 UV/Visible Detectors

The UV/Visible detector is a solute property detector and can be applied to polymers containing light active groups such as carbonyl bonds or double bonds. The underlying principle governing UV/Visible detection is given by Beer's Law:

$$A = \log \frac{I_0}{I} = \epsilon bc \quad \text{Equation 2-29}$$

Where  $A$  is absorbance,  $I_0$  is the intensity of incident radiation,  $I$  is the intensity of transmitted radiation,  $b$  is the path length of the cell, and  $\epsilon$  is the molar absorptivity. Values of  $\epsilon$  are specific for a given polymer in a given solvent at a given temperature and at a given wavelength. UV and light visible detectors are very versatile because many solvents have high transmittance and can be used for the detection of numerous solutes.

### 2.3.3 Static Light Scattering Detection

Static light scattering is one of the most powerful methods of detection in SEC, being able to provide information pertaining to molar mass of a polymer, information about long chain branching, conformation, dilute solution dynamics, and size of the polymer.<sup>26</sup> Light scattering detectors are molar mass sensitive detectors and therefore affords the molar mass of each elution volume. The response of such a detector is dependent upon the concentration and the molar mass of the polymer, so a light scattering detector must be used in conjunction with a concentration sensitive detector.

### 2.3.3.1 Multi Angle Light Scattering (MALS)

The Rayleigh-Gans-Debye approximation is the equation which describes the operational basis of light scattering, and is given by:

$$\frac{K*c}{R(\theta)} = \frac{1}{P(\theta)} \left( \frac{1}{M_w} + 2A_2c + 3A_3c^2 + \dots \right) \quad \text{Equation 2-30}$$

where 
$$K * = \frac{4\pi^2 n_0^2 \left( \frac{\delta n}{\delta c} \right)^2}{\lambda_0^4 N_A} \quad \text{Equation 2-31}$$

$$R(\theta) = \frac{I_\theta r^2}{I_0} \quad \text{Equation 2-32}$$

and 
$$\frac{1}{P(\theta)} = 1 + \frac{16\pi^2}{3\lambda^2} \langle r^2 \rangle_2 \sin^2 \frac{\theta}{2} + \dots \quad \text{Equation 2-33}$$

Where  $N_A$  is Avogadro's number,  $n_0$  is the refractive index of the solvent,  $\lambda_0$  is the vacuum wavelength of the incident radiation,  $c$  the concentration of polymer in solution, and  $M_w$  the weight-average molecular mass. The second virial coefficient  $A_2$  provides a measure of the excess chemical potential between polymer and solvent molecules in solution, and typically higher terms tend to zero and are not required. The particle scattering factor  $P(\theta)$  describes the angular dependence of the scattered light. The root-mean-square radius,  $\langle r^2 \rangle^{1/2}$ , also referred to as the radius of gyration, is defined as the root-mean-square distance of an array or group of atoms from their common centre of mass.

$$\frac{\delta n}{\delta c} = \lim_{c \rightarrow 0} \frac{n - n_0}{c} \quad \text{Equation 2-34}$$

Equation 2-34 is a factor known as the specific refractive index increment of the solution, where  $n$  and  $n_0$  are the refractive indices of the solution and solvent respectively, and  $c$  is the concentration of the analyte in solution. The value of the specific refractive index depends on the temperature of the experiment, the vacuum wavelength of the incident radiation and the chemistry of the analyte.

In an SEC-MALS experiment the scattered light is detected, at multiple angles, for each elution volume from the SEC column.  $M_w$  is measured at each elution volume, and is independent of experimental conditions such as temperature and solvent, and is therefore called the absolute  $M_w$ . SEC-MALS is an excellent method for detecting high molecular weight material, as even small amounts of high molecular weight polymer will scatter substantial amounts of light. MALS detectors are available in two-, three-, seven and

eighteen-angle configurations, all employing linearly polarized lasers according to the same principle.

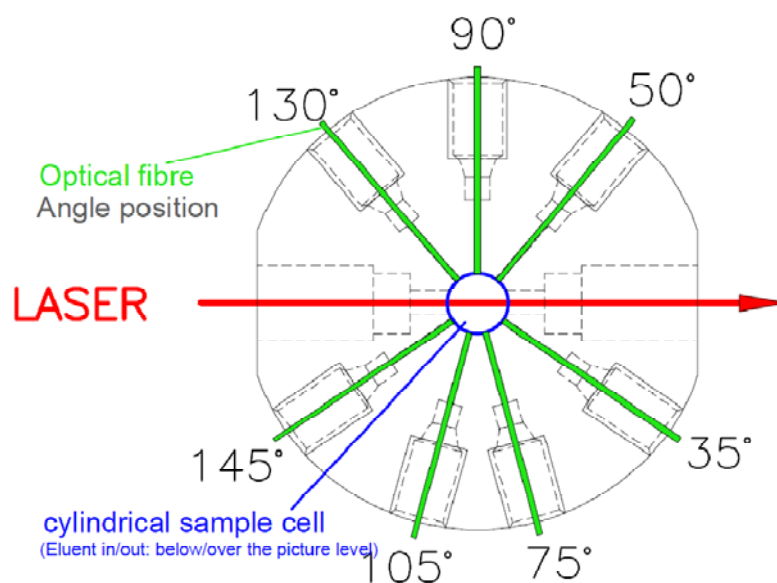


Figure 2-2: Multi angle light scattering detector. Reproduced from PSS Polymer Standards Service USA.

### 2.3.4 Viscometric Detection

#### 2.3.4.1 Differential Viscometers

In differential viscometry the polymer solution is channeled through one part of the viscometric detector and the neat solvent through another part, and a pressure imbalance is created as a result. The typical Viscotek detector is a fluid flow analog of the Wheatstone bridge electrical circuit where the electrical resistors have been replaced with capillaries which measure the flow impedance, i.e. the viscosity  $\eta$ , and the underlying theoretical basis follows the Hagen-Poiseuille equation:

$$\Delta P = \frac{8L\eta Q}{\pi r^4} \quad \text{Equation 2-35}$$

Where  $\Delta P$  is the pressure drop, with a capillary of length  $L$  and radius  $r$ , and  $\eta$  is the viscosity of the solution flowing through the tube and  $Q$  is the volumetric flow rate through the tube. When  $L$ ,  $r$  and  $Q$  are known,  $\eta$  can be directly related to  $\Delta P$ . Most experimental set-ups are built around this principle, with carefully controlled flow rates and capillaries of known dimensions.

### 2.3.5 SEC Calibration

As SEC is a relative method for the determination of molecular weight, such instrumentation needs to be calibrated. Separation in SEC occurs on the basis of hydrodynamic volume, so to obtain the molar mass distribution information from the SEC chromatogram a calibration must be established relating the elution volume ( $V_e$ ) to the molar mass of the polymer sample. The molar mass calibration is valid only for the particular polymer and solvent system, as well as for the particular experimental set-up, since the retention time of molecules is determined by the relative sizes of the polymer molecules and the pore size of the column packing. If a different column is used, the different pore size or packing structure will affect the  $V_e$ . Therefore calibrations are only valid for specific polymer-solvent systems in specific column types and arrangements.

Calibrations can be made with either broad or narrow polydispersity standards, and again, the focus will be directed to the background pertinent to the work carried out in this thesis so as to not wax lyrical. Therefore only calibration with narrow polydispersity standards will be outlined. For information regarding calibration with broad polydispersity standards the reader is directed to ref.<sup>25</sup>

#### 2.3.5.1 Calibration with Narrow Molecular Weight Standards

If a series of standards with a narrow molar mass distribution is available, their elution volumes can be determined, and a calibration can be established in the form of a polynomial fit of the obtained data points. The molar mass for a given elution volume is obtained from the  $V_e$  of the sample and the calibration curve fit. Narrow molecular weight standards are available for some polymers such as poly(styrene), poly(ethylene), poly(methyl methacrylate), and poly(ethylene glycol)/poly(ethylene oxide), and range in molecular weights from oligomers to  $1 \cdot 10^6 \text{ g} \cdot \text{mol}^{-1}$ . However, this type of calibration is valid only when similar polymers to the calibration polymers are analyzed, i.e. poly(styrene) analyzed on a system calibrated with poly(styrene) standards. This is rather limiting in the scope for analysis, but is remedied by the application of the Mark Houwink Kuhn Sakurada calibration, discussed next.

### 2.3.5.1.1 Mark Houwink Kuhn Sakurada Calibration

In the late 1930s and early 1940s Mark, Houwink, Kuhn and Sakurada arrived at an empirical relationship between the molecular weight and the intrinsic viscosity,  $[\eta]$ , which has come to be known as the Mark-Houwink equation and is shown in Equation 2-36.

$$[\eta] = K \cdot M^\alpha \quad \text{Equation 2-36: The Mark-Houwink equation}$$

Where  $K$  and  $\alpha$  are related factors dependent on polymer type, solvent and temperature, and  $M$  is the molar mass.

$K$  and  $\alpha$  vary with polymer chemistry and architecture, solvent and temperature. The exponent  $\alpha$  provides an indication of the molecule conformation. A spherical conformation where there is no dependence of molecular weight on intrinsic viscosity would result in  $\alpha = 0$ , and varies up to a value of 2 for a rigid-rod conformation, while for flexible polymers  $0.5 < \alpha < 0.8$ . Values  $\alpha < 0.5$  indicate branched polymer structures, while values  $\alpha > 0.8$  indicate more extended conformations.

If the Mark-Houwink constants of both the calibration standards and the analyte are known, absolute values of molar mass can be determined *via* the relationship:

$$[\eta]_1 M_1 = [\eta]_2 M_2 \quad \text{Equation 2-37}$$

Following from Equation 2-37,

$$K_1 M_1^{1+a_1} = K_2 M_2^{1+a_2} \quad \text{Equation 2-38}$$

And solving for  $M_2$ :

$$\log M_2 = \frac{1}{1-a_2} \left( \frac{K_1}{K_2} \right) + \frac{1+a_1}{1+a_2} \log M_1 \quad \text{Equation 2-39}$$

In the literature, reported values of  $K$  and  $\alpha$  can exhibit high discrepancies, so the Mark-Houwink calibration is best used for qualitative and semi-quantitative analyses, and universal calibration, discussed in the next section, is better used when accuracy is critical. Although accurate  $K$  and  $\alpha$  values may be accurately known for a set of standards and an analyte with particular chemistry, the molecular conformation, i.e. the architecture, of the analyte at hand may be different to that from which  $K$  and  $\alpha$  values were determined, and will introduce error into the computed molecular weight averages obtained.

### 2.3.5.1.2 Universal Calibration

The method of universal calibration was introduced in 1967 by Grubisic *et al.*<sup>27</sup> Narrow polydispersity, anionically synthesized polystyrenes are most often used for the calibration. Other polymers used for calibration include poly(methyl methacrylate), polyisoprene, polybutadiene, poly(ethylene oxide), and the sodium salt of poly(methacrylic acid). Available molecular weight ranges start from oligomers of only a few hundred  $\text{g}\cdot\text{mol}^{-1}$ , up to polymers of 20 000 000  $\text{g}\cdot\text{mol}^{-1}$ . In all cases, the use of narrow molecular weight distribution standards is preferred. When a polymer sample is analyzed on an SEC system which has been calibrated using a polymer other than that being analyzed, there is the issue of whether the retention time of the analyzed polymer is the same as that of the polymer used for calibration. If indeed the retention times for the various molecular weights are identical, then the output of the SEC will provide the desired molecular weights. This problem could be avoided by calibrating the SEC system with the same polymer that is to be analyzed but for practical reasons this is often tedious. However, if the Mark-Houwink parameters of the polymer to be analyzed are known, then the molecular weights as determined from the calibration curve can be adjusted, according to the following equation:

$$K_1 \cdot M_1^{(\alpha_1+1)} = K_2 \cdot M_2^{(\alpha_2+1)} \quad \text{Equation 2-40: Universal Calibration}$$

A universal calibration curve is valid for a particular set of columns, in a particular solvent, at a particular temperature. A new calibration must be performed if any of the parameters are varied. The use of universal calibration curves for the analysis of homopolymers is decreasing now that online static light-scattering detectors are becoming more widespread, as absolute molecular weights are accessible without the need for calibration curves. However for analysis of polymers of unknown structure and chemical composition, and for copolymers, universal calibration curves are still a good option.

The main differences between universal calibration and Mark-Houwink calibration are:<sup>25</sup>

- No assumptions need to be made regarding macromolecular structure, whereas in the Mark-Houwink calibration this is not the case.

- Mark-Houwink calibration does not take into account the possibility of branching, whereas universal calibration affords the true molecular weight, irrespective of the degree and type of branching.
- No prior knowledge of Mark-Houwink parameters is required to apply or construct a universal calibration curve. In universal calibration  $[\eta]$  is obtained from the ratio of the signals of the viscosity detector and the concentration-sensitive detector, so prior knowledge of the Mark-Houwink parameters  $K$  and  $\alpha$  of either the calibration standards or the analyte are not required. In fact,  $K$  and  $\alpha$  are usually obtained by applying a universal calibration curve to a polymer analysis.
- Construction of a universal calibration curve requires an online viscometer, whereas in the case of the Mark-Houwink calibration a viscometer is not required. Hardware and software costs, as well as analysis time, data processing and training are thus reduced in the application of the Mark-Houwink calibration.

## 2.4 The Arrhenius equation

The Arrhenius equation is an empirical relation relating the propagation rate coefficient,  $k_p$ , to temperature.

$$k_p = A_p e^{-\frac{E_A^p}{RT}} \quad \text{Equation 2-41}$$

Where  $k_p$  is the rate of propagation,  $E_A^p$  is the activation energy,  $T$  is the temperature in Kelvin,  $R$  is the gas constant, and  $A_p$  is the pre-exponential factor. This relation can be expressed linearly in the form of:

$$\ln k_p = \ln A_p - \frac{E_A^p}{R} \left( \frac{1}{T} \right) \quad \text{Equation 2-42}$$

And from a plot of  $\ln k_p$  vs  $\frac{1}{T}$ , the activation energy and pre-exponential factor can be derived.

Despite being an empirical relation, the Arrhenius equation is useful and widely employed in the understanding of the link between the structure of the monomer and its reactivity, for example towards a propagating radical. The activation energy is the difference between the initial state and the transition state, as defined in transition state theory, and is related to

the stability of the radical and that of the monomer. The pre-exponential factor  $A_p$  is a measure of the number of collisions which lead to a reaction to form product, which is related to the steric hindrance of the monomer.

## 2.5 Acrylate Free Radical Polymerization

The polymerization kinetics of alkyl acrylates have been observed to deviate considerably from the behavior observed with other monomers.<sup>28-36</sup> Ideal polymerizations follow first order kinetics with the following rate law:

$$R_p = -\frac{d[M]}{dt} = \frac{k_p}{\sqrt{k_t}} [M] \sqrt{2k_d \cdot f \cdot [I]} \quad \text{Equation 2-43}$$

where  $R_p$  is the rate of polymerization,  $[M]$  is the monomer concentration,  $k_p$  is the rate of propagation,  $k_t$  is the rate of termination,  $k_d$  is the rate of initiator decomposition,  $f$  is the initiator efficiency, and  $[I]$  is the initiator concentration. It can be seen that

$$R_p \propto [M]^\omega \cdot [I]^{0.5} \quad \text{Equation 2-44}$$

Reaction orders  $\omega$  of 1 are not found in the case of many acrylates, rather,  $\omega$  is found to lie between 1.4 and 1.8 and to vary with monomer concentration.<sup>34,37-38</sup> The ratio  $\frac{k_p}{k_t^{0.5}}$  also apparently varies with  $[M]$ . For example, Madruga and Fernandez-Garcia<sup>36</sup> have shown that  $\frac{k_p}{k_t^{0.5}}$  for *n*-butyl acrylate decreases from 1.5 to 1.4 at 50 °C as the monomer concentration in benzene is decreased from 5 to 3 mol·L<sup>-1</sup>. The same experiment for methyl methacrylate did not show any change in the  $\frac{k_p}{k_t^{0.5}}$  ratio. The unexpected kinetic behavior of acrylates has been extensively studied and many hypotheses have been proposed for this deviation from ideality. Some of these hypotheses include the effect of primary radical termination and degradative chain transfer,<sup>34</sup> chain-length dependence of termination rate coefficients,<sup>29</sup> and the theory of hot radicals.<sup>35</sup> Scott and Senogles<sup>33</sup> also suggested the influence of intramolecular transfer to polymer, or monomer/solvent complexation as a possible cause. Since the work of Scott and Senogles, strong evidence has emerged to show that backbiting and slow reinitiation of the resulting midchain radical is indeed an important process during acrylate polymerization, even at low temperatures. Midchain radicals have been observed *via* ESR<sup>39-41</sup> and Ahmad *et al.*<sup>42</sup> have observed quaternary carbon atoms *via* <sup>13</sup>C NMR. The quaternary carbon atoms are an indication of branching on the polymer backbone that

result from addition to the midchain radical to produce a short-chain branch. Further work by the group concluded that the branches originate from inter- and intra-molecular transfer reactions<sup>43-45</sup> and supported the theory of backbiting initially proposed by Scott and Senogles.<sup>31-33</sup> The intramolecular chain transfer reaction, sometimes referred to as backbiting, is well-known in high-temperature ethylene homopolymerization.<sup>46</sup> It has also been observed in ethylene/BA copolymerizations that the methine hydrogens on BA units in the polymer chain are much more susceptible to abstraction than hydrogens from a -CH<sub>2</sub> unit in the backbone.<sup>47</sup> Quaternary carbons and midchain radicals are found under conditions of very low polymer concentration and low temperatures, for example, branching on poly(*n*-BA) samples resulting from backbiting has been detected at -16 °C,<sup>48-50</sup> indicating that the intramolecular/backbiting reaction must be thoroughly considered when evaluating the acrylate kinetic studies in the literature. Furthermore, this non-ideality of acrylate polymerization combined with the high propagating rate coefficients have also been the cause of failure to determine, until recently,<sup>51</sup>  $k_p$  values for many acrylates above ambient temperature. Pulsed-laser polymerization studies demonstrate that addition of monomer to a chain-end radical is very fast,<sup>52-53</sup> but the observed propagation rates of BA polymerization are significantly lower than would be expected from this estimate.<sup>49,54</sup> The result may be explained with evidence suggesting that monomer addition to the midchain radical proceeds at a much slower rate than addition to the secondary propagating end-chain radical. Evidence of the slow propagation of midchain radicals stems from an ESR study of methyl acrylate trimer polymerization,<sup>55</sup> a monomer which possesses a similar radical structure to that of the midchain radical. Experimental and modeling studies have also been carried out by Asua, Leiza and co-workers,<sup>49-50,56</sup> Nikitin *et al.*,<sup>57-58</sup> and Peck and Hutchinson,<sup>54</sup> suggesting that the intramolecular transfer event followed by slow reinitiation has a significant effect on acrylate polymerization rate, even at low temperatures. Thus, more knowledge of MCR formation and reaction behavior is an important step towards fundamental understanding of acrylate polymerization systems, and can assist in efficient tuning of product composition for targeted applications.

## 2.6 A Closer Look at Midchain Radicals

Midchain radicals (MCRs) are formed as part of the many side reactions which occur in radical polymerization, and have been accepted as an inevitable side effect. Some examples

of transfer reactions occurring in free radical polymerizations are transfer to monomer, transfer to solvent, or transfer to polymer. This is more generally discussed in section 2.2.2. MCRs originate from the transfer to polymer reaction and are named as such due to the nature of the propagating radical being transferred onto the backbone of the polymer, to a 'midchain' location. Most commonly MCRs form on a carbon atom on the backbone which also possesses an ester moiety in the case of poly(acrylates), because it creates a more stable tertiary radical compared to the terminal secondary propagating radical. A greater understanding of the formation pathways and subsequent reactions that MCRs participate in will provide important information to enable better control of the final product. While MCR formation is usually regarded as an inevitable reaction that complicates the reaction kinetics as well as the product spectrum, it may be utilized to generate very specific structures. Increasing activation energies of the rate coefficient for conventional propagation, propagation of MCRs, backbiting and  $\beta$ -scission may allow for backbiting and  $\beta$ -scission reactions to become dominant over the termination of radicals. The most recent rate data endorse such a kinetic scenario, provided that the monomer as well as overall radical concentrations are low enough.<sup>59-60</sup> While the kinetic situation explains the generation of macromonomers, questions remain as to what other endgroup/s may be found in the polymer product. As  $\beta$ -scission occurs equally to either side of the radical functionality, at least two products are expected in the product spectrum, as one side of the MCR contains an initiator fragment and the other side is capped by a proton due to the preceding hydrogen transfer reaction. A further complication arises from the difficulty of finding a suitable initiator as most initiators decompose quickly at elevated temperatures.

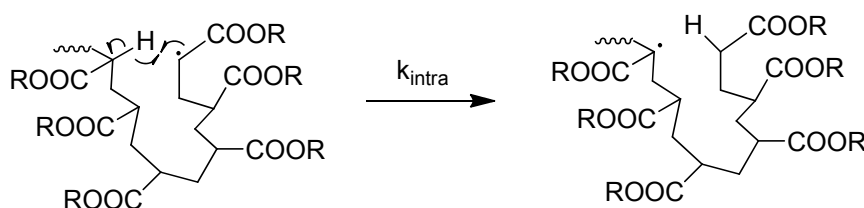
Researchers are now recognizing that MCRs are important to consider in the free radical polymerization kinetics of acrylate monomers. The detailed kinetic implications and equations related to MCRs is elaborated on in Chapters 4 and 5. For the current section it is sufficient to note the reaction pathways leading to the formation of MCRs and the ensuing reactions that MCRs and MCR side products can undergo, and to realize that MCRs have a marked effect on the reaction kinetics of acrylate free radical polymerizations. A significant impact on the final product spectrum is seen, but however, it is only in the last decade or so that studies of MCRs have been recognized as an important avenue of research. The rest of

the present discussion will focus on the formation pathways of MCRs, and the reactions that they can participate in once they form.

There are three ways in which MCRs can form, by intermolecular transfer, intramolecular transfer, or by backbiting. Each of these three cases will now be considered. It should be noted that although the MCRs are generated in different three ways, the resulting MCRs are chemically and electronically identical. The distinction of the means by which the MCR is formed is made because of the individual kinetics of the three reactions. Each of the three formation mechanisms is associated with particular reaction kinetics, and therefore when observing the end product of polymerization, the contribution of the individual pathways becomes significant as each contributes differently to the overall polymerization, and should be differentiated from one another.

### 2.6.1 Intramolecular Transfer

Random intramolecular transfer transfers a radical centre from a chain end onto a backbone position of the same polymer chain. Once a polymer has reached a certain chain length it is able to curl and fold back onto itself. The longer the polymer chain becomes, the more folding can occur and the higher the probability that the propagating radical is encircled by its own polymer tail. In some cases the propagating chain end encounters a hydrogen atom and transfer takes place, relocating the hydrogen atom onto the chain end and the radical onto a position on the backbone. Intramolecular transfer of this form results in long chain branching and produces polymer with a hydrogen as one end group.



Scheme 2-1: Intramolecular transfer to a random backbone position. Only one polymer chain is involved.

Scheme 2-1 depicts random intramolecular transfer. The radical centre is transferred from a secondary position to a tertiary position on the backbone. The increase in radical stability is

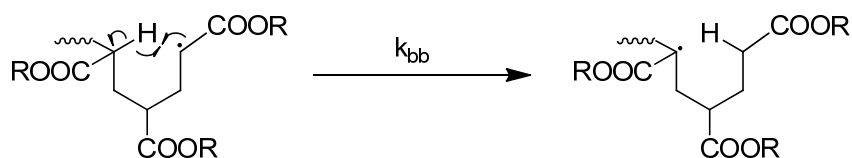
the driving force for this transfer reaction. As transfer occurs to a random position, either long chain branching or short chain branching can result. Intramolecular chain transfer to polymer becomes progressively more important at lower monomer concentrations.

### 2.6.2 Backbiting

The backbiting step is very important in the free-radical polymerization of acrylates, and leads to short-chain branching. It is comparable to the backbiting reaction in ethylene polymerizations which has been known for some time to occur.<sup>61</sup> In this work, backbiting is specifically defined as transfer, typically *via* a six-membered ring conformation, which results in the formation of an MCR with the radical being located on the third ester moiety from the chain end. In the literature very often the distinction between intramolecular transfer resulting in long chain branching and backbiting which predominantly forms short chain branching is not made and the two terms are used synonymously.

Backbiting results in well defined short chain branches rather than long chain branches of random length. The short chain branches are well defined in the sense that they are of similar length. While the 6-membered ring is favored, it is possible to envisage a backbiting step involving an 8- or even a 10-membered ring structure. An odd numbered ring however would produce an MCR with the radical centre on a methyl group of the backbone, which is another secondary radical, and therefore is unlikely to occur as the driving force of attaining higher radical stability does not exist in this case. Scheme 2-2 shows backbiting *via* the 6-membered ring transition structure, which results in short chain branching on the polymer backbone. The backbiting reaction is electronically favored and hence faster than inter- and random intra-molecular transfer.

A further important difference between backbiting and the random transfer is that the rate of backbiting only depends on the radical concentration whereas the transfer to a random position is a second order reaction, depending on radical concentration and concentration of monomer units polymerized, and hence becomes more important at later stages of the polymerization. Backbiting is known to take place from temperatures as low as  $-30\text{ }^{\circ}\text{C}$  and above.<sup>62</sup>



Scheme 2-2: Backbiting step *via* a 6-membered transition ring structure, resulting in short chain branching of the polymer.

The backbiting reaction is of critical importance in PLP-SEC experiments as it is the cause of the inability to measure, until recently, propagation rate coefficients at temperatures exceeding about 30 °C at 100 Hz pulsing frequency. With the technological advance of the present availability of lasers able to pulse at up to 500 Hz, this problem has been partially resolved with respect to  $k_p$  determination, however the issue of the presence of backbiting is still present. ESR studies have shown that up to 80 % of all radicals are present as MCRs in various acrylate polymerizations at temperatures of 60 °C,<sup>62-67</sup> and provides evidence supporting the theory that the backbiting reaction is the cause of failure of PLP at 100 Hz by disrupting the characteristic molecular weight distribution obtained by PLP.

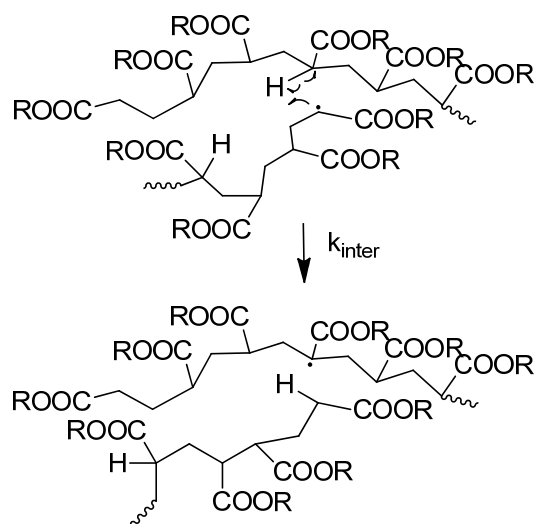
### 2.6.3 Intermolecular Transfer

Intermolecular transfer to polymer involves two separate polymer chains and results in the formation of a radical site on a different polymer chain than the one originally carrying the radical centre. If transfer occurs to a dead polymer chain, the result is a loss of a secondary propagating radical from one chain, and the introduction of a tertiary midchain radical on the other which is free to propagate.

The rate law for intermolecular transfer was derived by Junkers and Barner-Kowollik<sup>68</sup> and is reproduced here.

$$v = k_{tr,inter} \cdot [R] \cdot [U] \quad \text{Equation 2-45}$$

where  $k_{tr,inter}$  is the intermolecular transfer rate coefficient,  $[R]$  is the radical concentration of propagating radicals, and  $[U]$  is the number of backbone units available for transfer.



Scheme 2-3: Intermolecular transfer to polymer between a secondary propagating chain and a dead polymer chain, resulting in a tertiary propagating centre.

Thus, in the case of a system where no polymer is initially present,

$$[U] = ([M] - [M_0]) = (1 - X)[M_0] \quad \text{Equation 2-46}$$

where  $[M]$  is the monomer concentration and  $[M_0]$  is the initial monomer concentration.

One assumption made in this case is that the transfer reaction is not diffusion controlled by the translational motion of the polymer coils, and indeed, the reaction can be presumed to be chemically controlled in cases other than very high conversion where high viscosities are present.<sup>68</sup>

In some cases, for example in the synthesis of block copolymers where monomer is added to an already existing polymer, Equation 2-46 must be modified to account for the pre-existing polymer in the system, and the expression for the number of backbone units available for transfer becomes:

$$[U] = (1 - X)[M_0] + [P] \cdot \overline{DP}_n \quad \text{Equation 2-47}$$

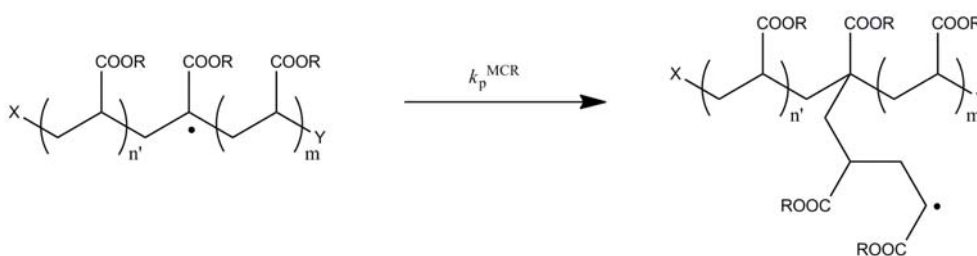
#### 2.6.4 Midchain Radical Reactions

Now that the source of MCRs has been established, the reactions that MCRs can subsequently participate in will be outlined. MCRs can propagate and terminate like any other radicals, forming either short or long-chain branches,<sup>69</sup> but they can also undergo

$\beta$ -scission. MCRs propagate noticeably slower than secondary propagating radicals,<sup>55,59</sup> and the slow propagation relative to secondary radicals is the cause of deviation from ideal polymer kinetics observed in acrylates, as previously discussed in section 2.5. Once an MCR has undergone a few propagation steps, it may transform back into a secondary propagating radical, which is then free to undergo more inter- or intra-molecular transfer reactions and results in a highly branched product.

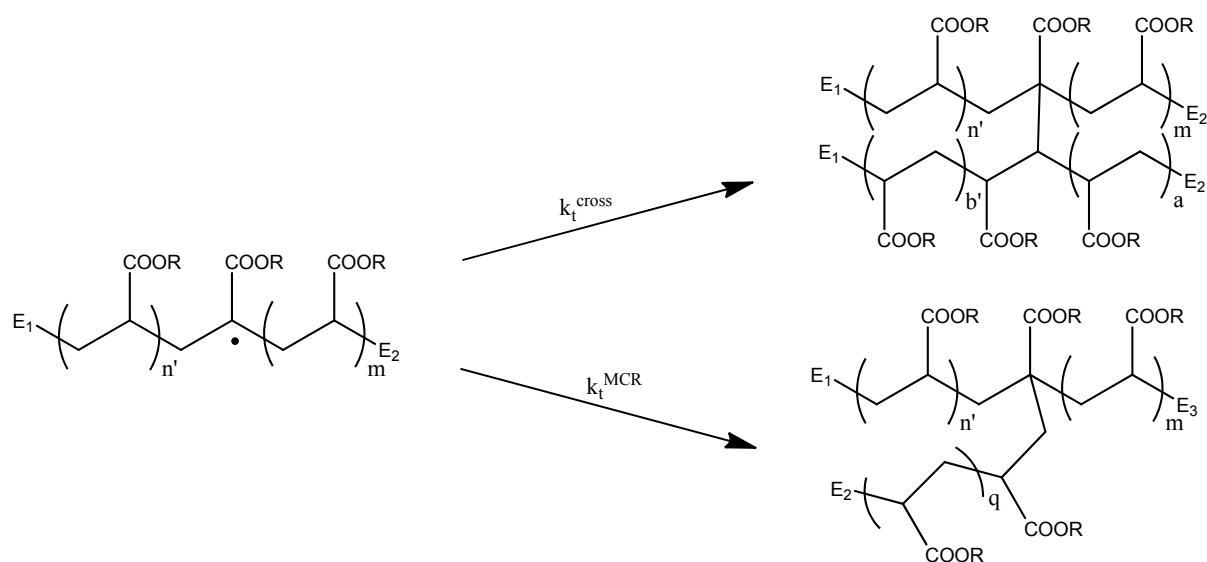
The levels of branching in acrylates have been studied by many methods,<sup>70-77</sup> in the context of final polymer properties with varying levels and type of branching, as well as in the context of obtaining accurate propagation rate coefficients by pulsed laser polymerization, and also from an analytical perspective, where the effect of branching on SEC separation was studied. The effect of branching on SEC analysis is an important area of study, as many synthesis methods rely on the knowledge of accurate molecular weights. Section 2.5 has more detail on the various methods by which the effects of MCRs on acrylate reactions have been observed.

Scheme 2-4 and Scheme 2-5 depict MCR propagation and MCR termination respectively. MCR propagation has the overall effect of lowering the rate of polymerization, because over time MCRs accumulate in the reaction mixture since the conversion of MCRs back into SPRs is much slower than the formation of MCRs as MCRs propagate much slower than SPRs.



Scheme 2-4: MCR propagation, leading to formation of a secondary propagating radical.

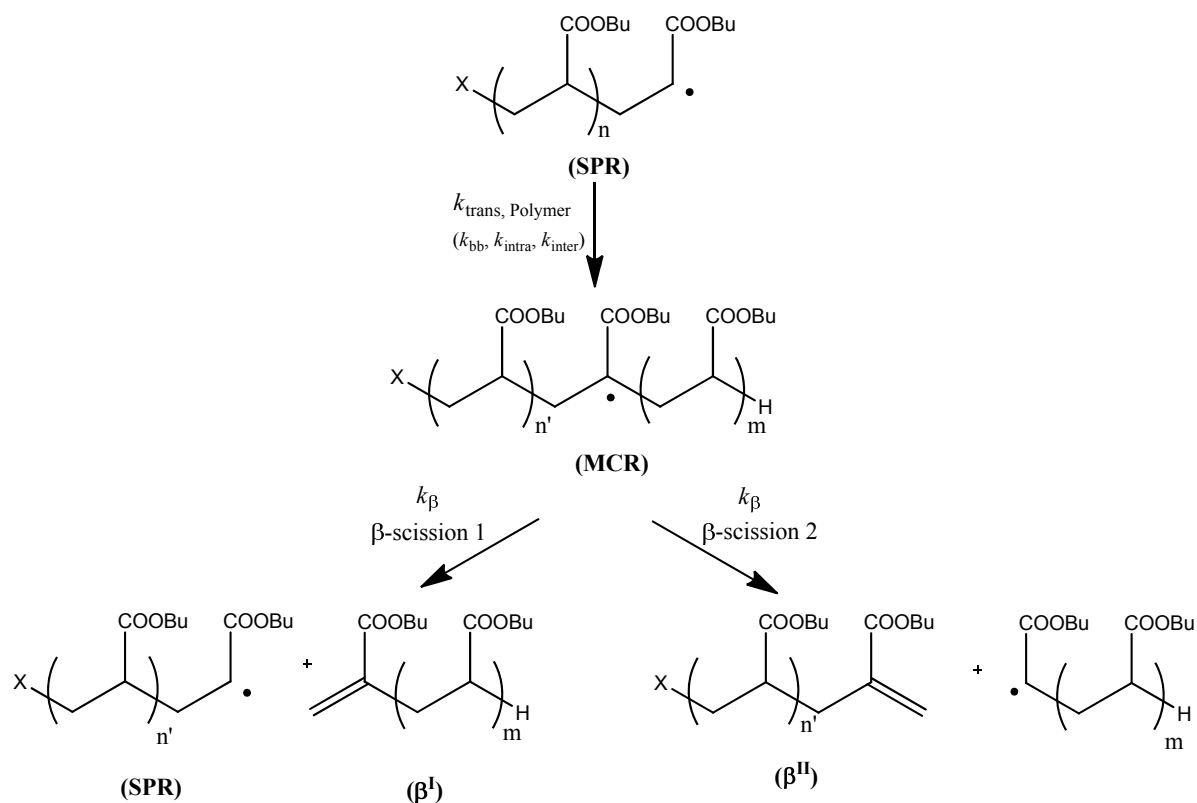
$\beta$ -Scission of a chain results in the formation of two smaller chains, one bearing an unsaturated end group, and the other a secondary radical which behaves like any other secondary radical in the polymerization system.



Scheme 2-5: MCR termination, giving two possible products. In the first case two MCRs combine, in the second case an MCR combines with a secondary propagating radical.  $E_1$ ,  $E_2$  and  $E_3$  are arbitrary endgroups.

The  $\beta$ -scission reaction itself can happen to either side of the radical center, resulting in different reaction products depending on the polymer endgroups. The unsaturated group is configured in a geminal conformation,<sup>78</sup> so it can be distinguished from the products of disproportionation which produce an unsaturated group in a vicinal conformation.

As a result,  $\beta$ -scission does not reduce the overall propagation rate but in fact increases the polymerization rate.<sup>79</sup> There is some evidence from the addition-fragmentation reaction employing MMA oligomers<sup>80</sup> which suggests that the scission reaction may have different rate coefficients depending on how close to the chain end the MCR is located. The unsaturated product of the  $\beta$ -scission reaction is effectively a macromonomer, and the macromonomer can react with a secondary propagating radical to form a midchain radical.<sup>81</sup> Junkers *et al.*<sup>82</sup> have fine-tuned the reaction conditions to exploit this equilibrium such that pure macromonomers are obtained. A complete synthesis and analysis of this effect can be found in Chapter 5.



Scheme 2-6: Possible  $\beta$ -scission products formed by cleavage to either side of the midchain radical.

Scheme 2-6 shows the pathway of a secondary propagating radical to form an MCR, and then subsequent  $\beta$ -scission to form 4 different species. As one of the endgroups is a hydrogen atom, it can be inferred that this particular MCR is the result of intramolecular transfer. A more detailed discussion of the kinetics of MCR formation can be found in Chapter 5.

Intramolecular transfer has been determined to be the predominant transfer process in PLP experiments.<sup>83</sup> Nikitin *et al.*<sup>74</sup> have derived an expression for the average propagation rate coefficient  $k_p^{av}$  in the presence of intramolecular transfer to polymer:

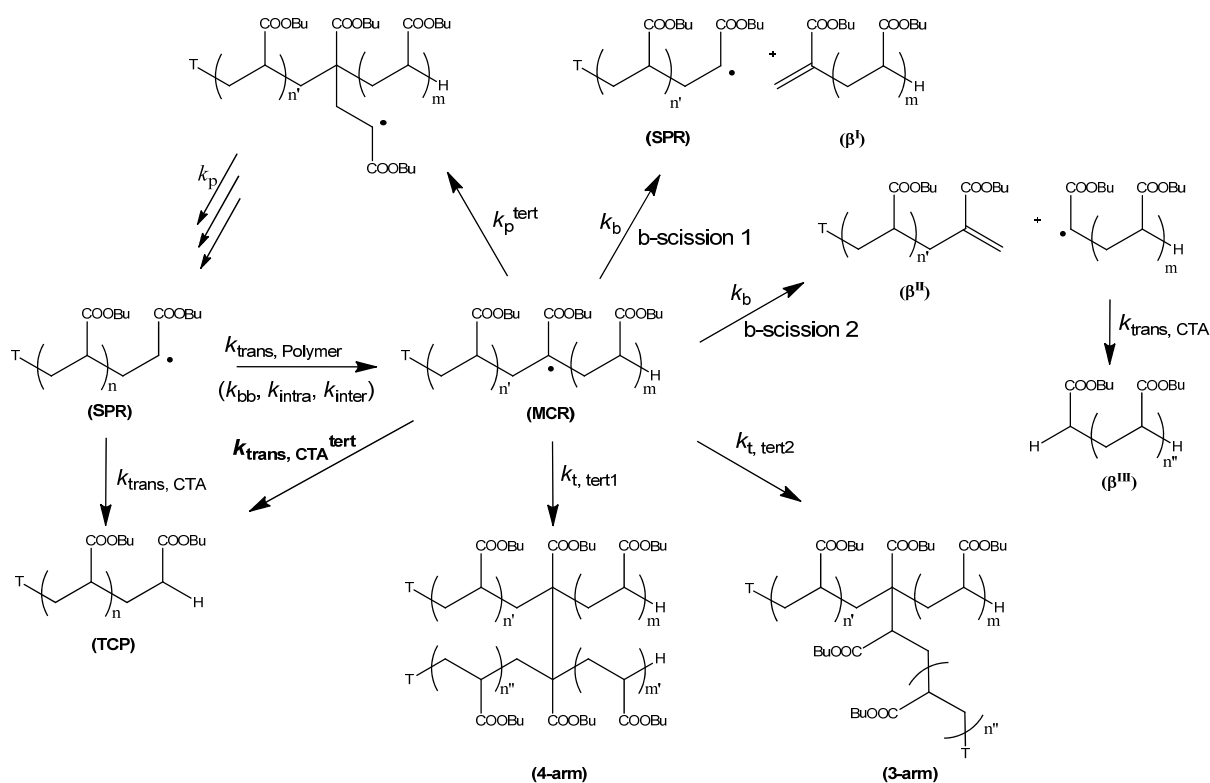
$$k_p^{av} = k_p - \frac{k_p - k_{p2}}{1 + \frac{k_{p2}[M]}{k_{bb}}} \quad \text{Equation 2-48}$$

Where  $k_p$  is the propagation rate coefficient on the terminal secondary radical,  $k_{p2}$  is the propagation rate coefficient of the MCRs, and  $k_{bb}$  is the rate coefficient of the backbiting reaction.

$k_{bb}$  is shown to be a very important parameter which exerts considerable influence on the final shape of the molecular weight distribution in PLP experiments. Another study by Nikitin *et al.*<sup>59</sup> have estimated that for *n*-butyl acrylate, the activation energy for  $k_{bb}$  is around 30 kJ·mol<sup>-1</sup>, while the activation energy of  $k_p$  is around 18 kJ·mol<sup>-151</sup> and that of  $\beta$ -scission, as determined by Hirano and Yamada<sup>55</sup> from MA trimer polymerization,  $E_A = 71.5$  kJ·mol<sup>-1</sup>. The large range of the various activation energies of  $k_{bb}$ ,  $k_p$  and  $k_\beta$  serve to highlight that polymerization at various temperatures will have a different major reaction. For example, at lower temperatures backbiting may predominate as the main reaction by which MCRs are formed, while at higher reaction temperatures  $\beta$ -scission is more prevalent once the MCR is formed. The effect of these different reaction pathways is a different product spectrum at each temperature. At lower temperatures, transfer reactions may not be so prominent because of their high activation energies.<sup>56</sup>

Scheme 2-7 depicts the reaction pathways available to midchain radicals once they are generated, *via* either inter- or intra-molecular transfer to polymer reactions from the SPR species. Midchain radicals can follow four major reaction pathways of which three are typical for any acrylate polymerization system.

MCRs can undergo chain propagation (associated with the reduced rate coefficient  $k_p^{\text{tert}}$ ), where the tertiary radical is transformed back into an SPR leading to an equilibration between both species and creating short-chain or long-chain branches. Alternatively, the MCR can undergo  $\beta$ -scission, resulting in up to 4 different products, one of which is again identical to the SPR. Two other fragments are dead polymer chains carrying an unsaturated endgroup (species  $\beta^I$  and  $\beta^{II}$ ). The fourth fragment is a radical that may undergo transfer to CTA (to give species  $\beta^{III}$ ) or chain extension until it is either terminated or its chain growth is ended by transfer which results in a polymer chain that is indistinguishable from  $\beta^{III}$  by spectrometric methods alone. In the presence of a CTA the transfer reaction is the most likely event to occur. The third reaction pathway for MCRs is termination to form either a 4-arm or a 3-arm star by combination. Considering the steric hindrance of an MCR, disproportionation may also take place, yielding unbranched dead chains that cannot be easily distinguished from conventional termination products. Transfer to polymer always results in radicals coinciding in mass with the corresponding SPR, so both termination products are fully indistinguishable from conventional termination products *via* MS.



Scheme 2-7: Possible reaction pathways of midchain radicals (MCR) formed upon intra- or intermolecular transfer to polymer reactions in presence of a potent chain-transfer agent (CTA)

The only exception would be stars that contain more than two endgroups other than a proton which are only produced by intermolecular transfer reactions. The fourth possible pathway of the MCR shown is the potential abstraction of a proton from the CTA, forming a dead, linear chain. This product is indistinguishable from that formed upon H-abstraction to an SPR.

The scheme shows a thiol-type transfer agent that transfers a proton to the radical site, leaving a radical fragment T that can reinitiate polymerization. As the majority of all chains will carry such a T end group, all structures in Scheme 2-7 originate from an SPR as depicted. *Intermolecular transfer* is a bimolecular reaction and requires dead polymer to be present which has not been included in the scheme in order not to overload the figure. The thiol group (denoted by a T) could alternatively be an AIBN or ACHN initiating fragment. In this case,  $\beta$ -scission would result in the formation of species  $\beta^I_{AIBN}$  or  $\beta^I_{ACHN}$ . In addition other reactions may occur, such as radical addition to the  $\beta^I$  and  $\beta^{II}$  species. Also, the radical

scission product that leads to the formation of  $\beta^{\text{III}}$  may undergo its specific scission and transfer reactions. However, in all these reactions, no further structurally different species are generated.

## 2.7 Photo-Initiation

UV radiation is best known for its deleterious effects on organic compounds, particularly upon prolonged sunlight exposure. By breaking chemical bonds, UV radiation causes severe changes in the mechanical and optical properties of polymer materials, thereby reducing their service life in outdoor applications. However, UV radiation can also have a beneficial effect and be used to initiate desired chemical reactions, like polymerization. By exposing a monomer for a brief time to intense UV radiation, in the presence of a photo-initiator, large amounts of free radicals are generated at once. The steady development of the UV-curing technology in the past 20 years has led the way to an ever-increasing number of end uses. The most important ones are to be found in the coating industry for the surface protection of all kinds of materials (metals, plastics, glass, paper, wood, etc.) by fast-drying varnishes, paints, or printing inks. A considerable amount of work has been devoted to UV-radiation curing, most of the research efforts being focused both on the kinetics and mechanism of such ultrafast cross-linking polymerization reactions, and on the design of new photo-initiators, monomers and telechelic oligomers best suited to producing high-performance polymer networks.

One of the prerequisite laws in photochemistry states that a photochemical reaction can only occur if light has been absorbed by the medium. As most monomers are essentially transparent to the radiation emitted by conventional UV sources, they do not produce initiating species in sufficiently high yields to start the polymerization reaction.<sup>84</sup> Therefore, it is necessary to introduce in the UV-curable formulation a photo-initiator which will effectively absorb the incident light and generate reactive free radicals or ions by cleavage of the electronically excited states. The Jablonksi diagram in Figure 2-3 demonstrates that there are several ways in which an excited molecule can return to the ground state, mostly by fluorescence or internal conversion. For the purposes of photo-initiation, the desired reaction is cleavage at the excited triplet state to generate initiating radicals.

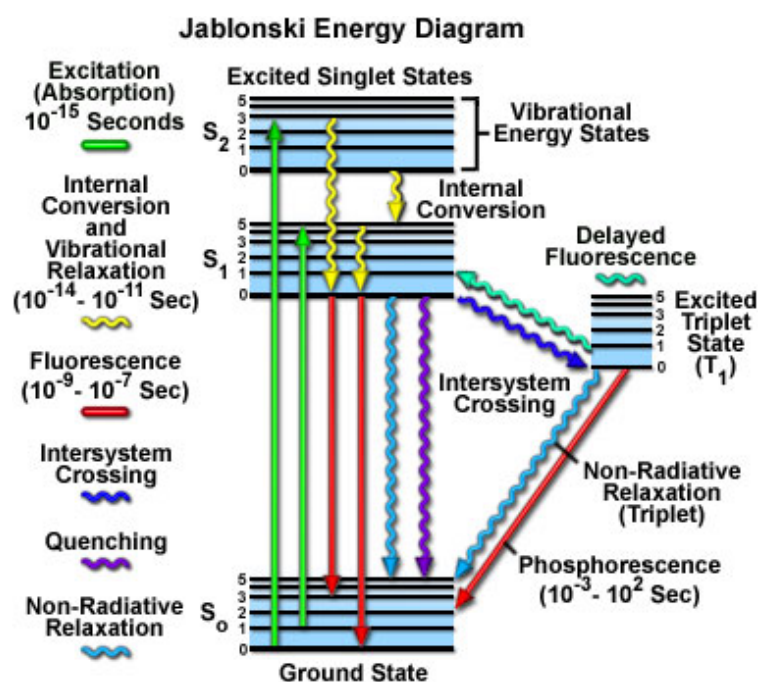
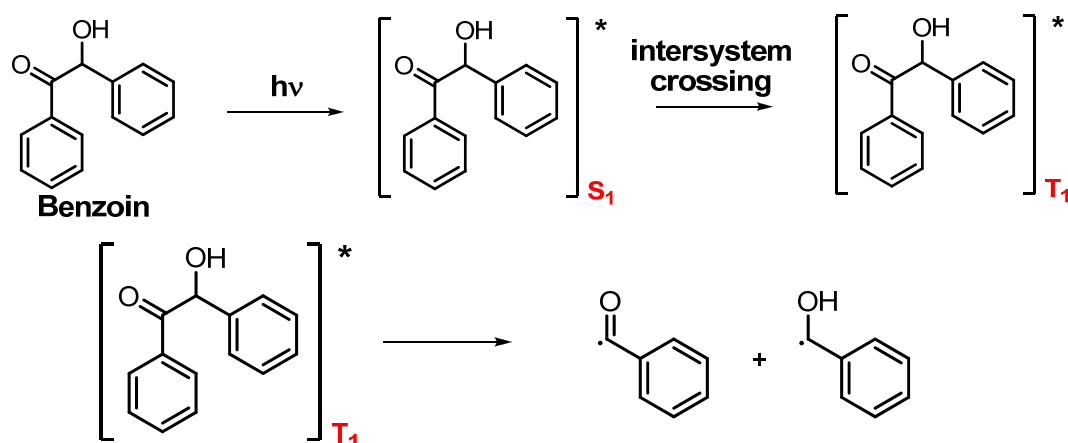


Figure 2-3: The Jablonski Diagram, which depicts the various pathways that a molecule can take from the ground state to the excited state, and back. Image reproduced from <http://www.olympusmicro.com/primer/java/jablonski/jabintro/index.html>, accessed 13/05/2010.

Scheme 2-8 shows the photo-excitation of benzoin, an  $\alpha$ -hydroxy ketone, used as a photo-initiator, followed by cleavage into radicals. The same principle applies to other commonly used photo-initiators.



Scheme 2-8: Photo-excitation of benzoin followed by cleavage to form initiating radicals.

The photo-initiator plays a key role in that it governs both the rate of initiation and the depth of cure through its absorbance. The decomposition of the photo-initiator upon irradiation should be fast compared to the polymerization that follows, and the photo-initiator should also have a high efficiency, which is a measure of how many of the generated radicals go on to start a growing chain. Ideally an efficiency of one would be present.

The rate of photochemical initiation  $r_{ini}$  is directly related to the intensity of absorbed light in moles of light quanta per liter-second ( $I_0$ ) and to the quantum yield of initiation ( $\Phi_i$ ):

$$r_{ini} = 2\Phi_i I_0 \quad \text{Equation 2-49}$$

The factor of 2 indicates that two radicals are produced per molecule undergoing photolysis. If only one radical is produced then the factor of 2 is omitted. The maximum value of  $\Phi_i$  is 1 for photo-initiated systems.

The expression for the rate of polymerization can then be expressed as follows:

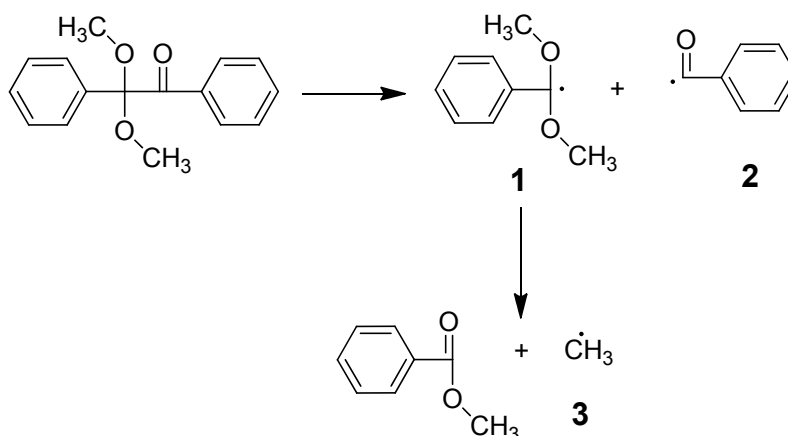
$$R_p = k_p [M] \left( \frac{\Phi_i I_0}{k_t} \right)^{1/2} \quad \text{Equation 2-50}$$

Photo-initiated radical chain polymerization begins with light irradiation of a sensitive compound which absorbs energy from the radiation. The activated compound typically fragments into two, or sometimes more, radicals that attack a monomer, converting it to a radical. The monomer radical attacks a second monomer and this process continues to add monomer units, thereby forming the polymer. The reaction is terminated either by the reaction with another radical (coupling) or by the transfer of a  $\beta$ -hydrogen from one radical to another, producing a saturated and an unsaturated compound (disproportionation). Essentially, once the polymerization has been initiated by the reaction of the initiating species with the monomer functional groups, the chain reaction proceeds very similarly to a conventional thermally initiated polymerization, except for the much larger rate of initiation that can be reached by intense illumination and for the lower temperature of the sample. Where multifunctional monomers and telechelic oligomers are employed, the polymerization will proceed in three dimensions to yield strongly cross-linked polymer networks.

One of the unique advantages of photo-induced reactions is the ability to precisely control the initiation step with respect to both the onset and the end of the period of initiation, as well as its magnitude, by variation of the light intensity. The initiation rate itself can be varied in the course of the reaction through an intensity modulator.<sup>85</sup>

### 2.7.1 Some Important Photo-Initiators

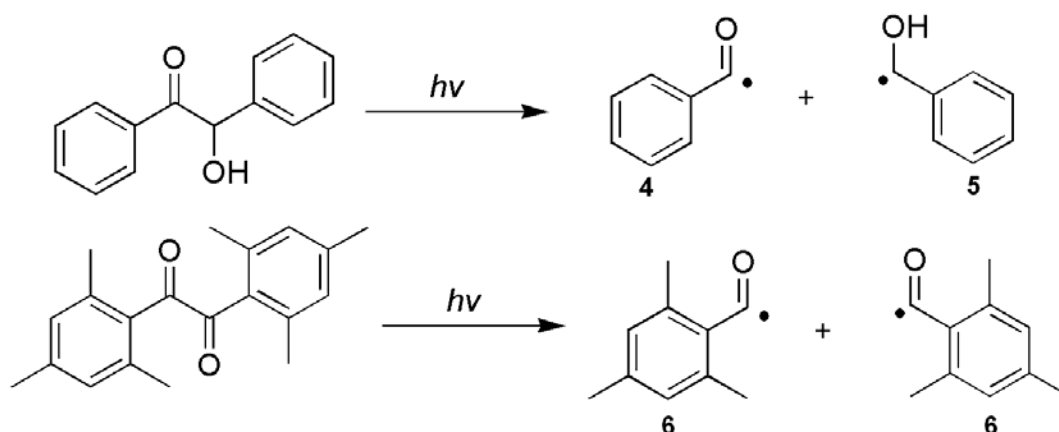
2,2-dimethoxy-2-phenylacetophenone (DMPA) is a common commercial photo-initiator which has been extensively studied with respect to its decomposition and excited states because of its high efficiency.<sup>86-89</sup> As a result it is also one of the most studied photo-initiators.<sup>87,89-94</sup> DMPA decomposes *via*  $\alpha$ -cleavage from the triplet state by a Norrish Type I mechanism,<sup>95</sup> characterized by a very short triplet lifetime, < 100 ps. Two radicals are obtained upon decomposition, a benzoyl type, see Scheme 2-9, **2**, and a dimethoxybenzoyl type radical, see Scheme 2-9, **1**. The benzoyl radical initiates polymerization at a rate  $k_{\text{ini}} \sim 10^5 - 10^6 \text{ L}\cdot\text{mol}^{-1}\cdot\text{s}^{-1}$  and termination with other radicals is diffusion controlled with rates of  $k_t \sim 1.3\cdot 10^9 \text{ L}\cdot\text{mol}^{-1}\cdot\text{s}^{-1}$ .<sup>90</sup> Photo-initiation employing DMPA is thus a very efficient process. In the case of the dimethoxybenzoyl radical,  $k_t$  is of the same value as that of the benzoyl radical, but  $k_{\text{ini}}$  is greatly reduced, in the order of  $\sim 10^4 \text{ L}\cdot\text{mol}^{-1}\cdot\text{s}^{-1}$ .<sup>90</sup> However, the dimethoxybenzoyl radical can further decompose to give methyl benzoate and a methyl radical. The methyl radical was shown to predominantly terminate polymerizations of methyl methacrylate, *n*-butylmethacrylate, and dimethyl itaconate.<sup>96</sup>



Scheme 2-9: Decomposition of 2,2-dimethoxy-2-phenylacetophenone under UV radiation.

The photochemical decomposition of the dimethoxybenzoyl radical has been studied using electron spin resonance (ESR)<sup>97</sup> and chemically induced electron polarization (CIDEP)<sup>98</sup> and optical techniques.<sup>90,97</sup>

With regards to pulsed laser polymerization, fast initiation is important to ensure minimal interference with the propagation reaction and therefore DMPA is a very good initiator for PLP type experiments.



Scheme 2-10: Photolytic decomposition of benzoin and 1,2-dimesitylethane-1,2-dione into their radical fragments.

Scheme 2-10 depicts the decomposition pattern of benzoin and 1,2-dimesitylethane-1,2-dione, which are comparatively evaluated as photo-initiators of MMA polymerization in Chapter 6. Benzoyl radicals (4) are usually effective starters of macromolecular growth, but the mesityl radical (6) was observed to react poorly after its generation from a phosphoryl-type photo-initiator, which inspired the study described in Chapter 6.

## 2.8 Mass Spectrometry of Polymers

Mass spectrometry involves the study of ions in the vapor phase. This analytical method has a number of features and advantages that make it an extremely valuable tool for the identification and structural elucidation of organic molecules, including synthetic polymers:<sup>99</sup> (i) The amount of sample needed is small; for direct analysis, a microgram or less of material is normally sufficient. (ii) The molar mass of the material can be obtained directly by measuring the mass of the molecular ion or a 'quasimolecular ion' containing the intact molecule. (iii) Molecular structures can be elucidated by examining molar masses, ion

fragmentation patterns, and atomic compositions determined by mass spectrometry. (iv) Mixtures can be analyzed by using ‘soft’ desorption/ionization methods and hyphenated techniques such as gas chromatography/mass spectrometry (GC/MS), liquid chromatography/mass spectrometry (LC/MS), and tandem mass spectrometry (MS/MS).<sup>99</sup>

Mass spectral analyses involve the formation of gaseous ions from an analyte and subsequent measurement of the mass-to-charge ratio ( $m/z$ ) of these ions. ‘Soft’ ionization methods such as matrix assisted laser desorption ionization (MALDI), electrospray ionization (ESI) and field desorption (FD)<sup>100</sup> generate predominantly molecular or quasi-molecular ions, whereas ‘hard’ ionization methods, such as fast atom bombardment (FAB), also yield fragment ions. The mass spectrometer separates the ions generated upon ionization according to their mass-to-charge ratio (or a related property) to give a graph of ion abundance vs  $m/z$ .<sup>101-102</sup> Mass spectrometric methods are routinely used to characterize a wide variety of biopolymers, such as proteins, polysaccharides, and nucleic acids, but the following discussion will focus on the mass spectrometry of polymers.

In recent years the interest in special techniques of mass spectrometry in determining molecular weights of oligomers and polymers has increased with the development of new ionization methods, and desorption/ionization techniques. It is now possible to eject large molecules into the gas phase directly from the sample surface, resulting in mass spectra of intact polymer molecules. This technology lies at the heart of this thesis work, as all analysis is based on mass spectra of intact polymer molecules. Mass spectrometers can provide absolute molecular weight. However, because polymers are mixtures of discrete compounds that differ in number and types of repeat units, end groups, architecture, and so forth, an accurate molecular weight analysis requires not only mass accuracy for each oligomer, but also the absence of fragmentation and a signal response that is independent of oligomer mass or at least a known function of mass.<sup>103</sup>

The basic aspects of the instrumentation of mass spectrometry will be covered in this section, in particular as they pertain to this work. Broadly the discussion will include ionization, mass analysis and detection with emphasis on the equipment employed in the course of this thesis.

### 2.8.1 Ionization Methods

In electrospray ionization (ESI) a strong electric field is applied to the capillary carrying the analyte solution and the spray is produced at atmospheric pressure. Typically, the potential difference between the capillary and the counter electrode placed 0.3-2 cm away from the capillary is 3-6 kV. Spraying under these conditions produces highly charged droplets whose charge is determined by the polarity of the field applied to the capillary.

ESI was performed in the 1960s by Dole and co-workers,<sup>104</sup> who electrosprayed a dilute polymer solution into an evaporation chamber to produce negative macroions. A 'molecular beam' could then be formed by sampling the gaseous mixture of macroions, solvent, and nitrogen molecules with a nozzle-skimmer system. In the 1980s Whitehouse *et al.*<sup>105</sup> refined ESI such that it was applicable as a soft ionization technique for large molecules.

ESI is extremely soft and can produce highly charged pseudomolecular ions and generally produces multiply charged quasimolecular ions except where the analytes have molecular weights < 1000 Da.<sup>99</sup> The first experiments in which ESI-MS was used for the investigation of polymers date back to the early 1990s<sup>106</sup> where Nohmi and Fenn analyzed poly(ethylene glycol) polymers up to weights of  $5 \cdot 10^6$  Da. ESI is based on the nebulization of a liquid into an aerosol of charged microdroplets due to strong electrical fields, a fundamental behavior of liquids that was first reported in 1917.<sup>107</sup> Electrospray interfaces are available from most mass spectrometer manufacturers nowadays, and the designs are somewhat different, but they all make use of the same principle.

A solution is injected at a constant flow into the system through a spraying capillary with a small diameter. The flow rate depends on the design of the interface. Typical values are from  $1 \mu\text{L} \cdot \text{min}^{-1}$  up to  $1 \text{mL} \cdot \text{min}^{-1}$ . The solution leaving the spraying capillary is sprayed into an aerosol of charged droplets (e.g., excess of protons) due to a potential difference between the needle and the metalized inlet of the capillary transfer tube. After the generally accepted formation of charged droplets, solvated multiply charged ions (macroions) are produced. A heated counter-current flow of nitrogen at temperatures of up to  $300 \text{ }^\circ\text{C}$  is used for the desolvation. Along with the temperature of the source this gas flow is essential for the evaporation of the solvent, both of the charged droplets and the solvated macroions.

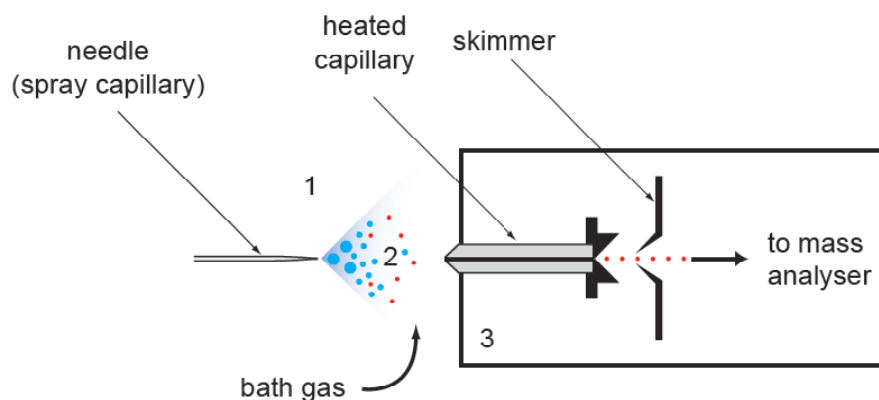


Figure 2-4: Schematic diagram depicting an ESI set-up. (1) nebulization of a sample solution into electrically charged droplets *via* a spray capillary, (2) the formation of analyte ions from the droplets with the aid of a bath gas and (3) sampling of the ions into a vacuum for mass analysis *via* a heated capillary and a skimmer. Reproduced with permission from the authors.<sup>108</sup>

Furthermore, the gas flow (gas curtain) prevents blockage or contamination of the inlet of the transfer capillary. Desolvation proceeds in the source, the desolvation capillary, and in the collision induced dissociation region, where cluster formation can also be prevented by applying suitable voltages. The complete process of ion formation is extremely soft and usually no or only little fragmentation occurs.

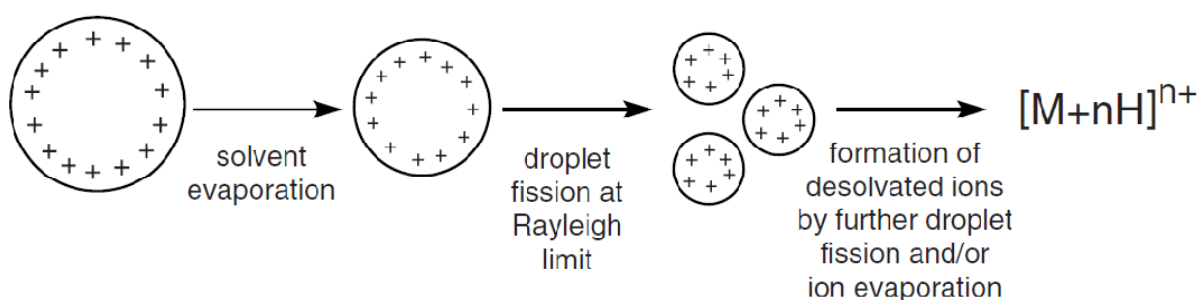


Figure 2-5: Schematic diagram for the formation of multiply charged species during ESI. Solvated macroions are generated from charged micro droplets. Multiply charged species are obtained after further desolvation. Reproduced from Montaudo, G.; Lattimer, R. P. *Mass Spectrometry of Polymers*; CRC Press, 2002.

The ions leaving the skimmer are transferred to the mass analyzer using electrostatic lenses, octapoles, further skimmer systems, etc. In principle, all important types of mass analyzers can be used. However, in recent years there has been a continuous development towards systems allowing MS-MS experiments due to the possibility of obtaining further structural information about multiply charged species by CID. Suitable mass analyzers are, for example, multiple-stage quadrupoles, ion traps, and Fourier transform mass spectrometers (FTMS). ESI-MS has proven to be an excellent method for the determination of end groups.<sup>69,82,96,109-116</sup>

### 2.8.2 Mass Analyzers

Mass analyzers disperse ions in space or time according to their mass to charge ratios ( $m/z$ ). Certain analyzers separate the ions simultaneously, while others are scanned to transmit to the detector a narrow  $m/z$  range at a given time. Important features of a mass analyzer are its upper mass limit, transmission, resolving power, mass accuracy, dynamic range and operating pressure. A polymeric ion can either be resolved into its individual isotopes or observed as an unresolved peak at the average  $m/z$  value of all isotopes. This depends on the resolution of the mass analyzer in the mass range of interest. Monoisotopic  $m/z$  ratios are preferred because they provide a higher mass accuracy. Also, resolved isotopic patterns clearly reveal the presence of elements with unique isotopic distributions such as bromine, silver or iron in the polymer.<sup>117</sup>

There are many types of mass analyzers. They are categorized into groups and then subgroups as follows. There are scanning mass analyzers and non-scanning mass analyzers. Scanning mass analyzers can further have a quadrupole mass filter, a quadrupole ion trap or magnetic and electric sensors. Non-scanning mass analyzers can be either Time-of-Flight (TOF) analyzers or Fourier transform ion cyclotron resonance (FT-ICR).<sup>2</sup> Some analyzers such as quadrupole or FT-ICR may be coupled to each other for facile tandem mass spectrometry (MS-MS) where an ion of particular mass may be selected for further fragmentation to obtain more information on its structure. For brevity only the quadrupole and quadrupole ion trap mass analyzers will be considered here but the various types of analyzers available should be noted.

## 2.8.2.1 Quadrupole Mass Analyzer

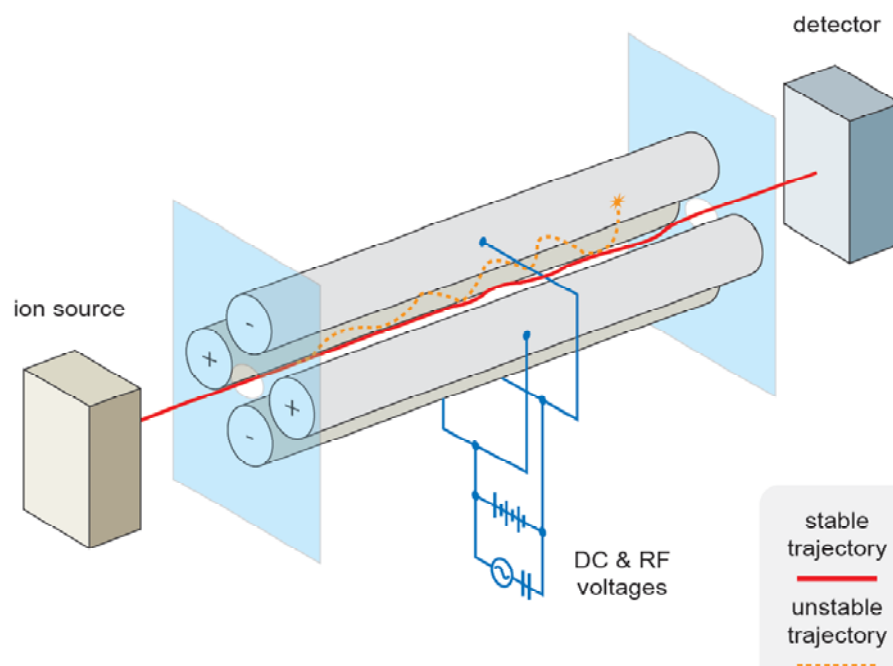


Figure 2-6: A simple quadrupole mass spectrometer consisting of an ion source, focusing lenses, a quadrupole mass filter, and an ion detector. Reproduced with permission from the authors.<sup>108</sup>

Figure 2-6 shows a simple quadrupole mass spectrometer. A quadrupole mass analyzer consists of four parallel, circular or hyperbolic, rods. Each pair of opposite rods are electrically connected and supplied voltages of the same magnitude but different polarity. The voltage applied to each pair consists of a direct current,  $U$ , and a radiofrequency (rf) component,  $V\cos(\omega t)$ .<sup>118</sup> Typical values are several hundred volts for  $U$ , several thousand volts for  $V$ , and megahertz for  $\omega$ . Ions are accelerated along the  $z$ -axis before entering the space between the quadrupole rods where they experience the combined field resulting from the rod potentials. A cation is attracted to the negative pole and vice versa. If the potential of the rod reverses sign before the ion discharges, the ion changes direction, and thus oscillates through the rods. Whether an ion is able to pass through the rods or discharges on them is determined by the  $U$  and rf voltages.

## 2.8.2.2 Quadrupole Ion Trap

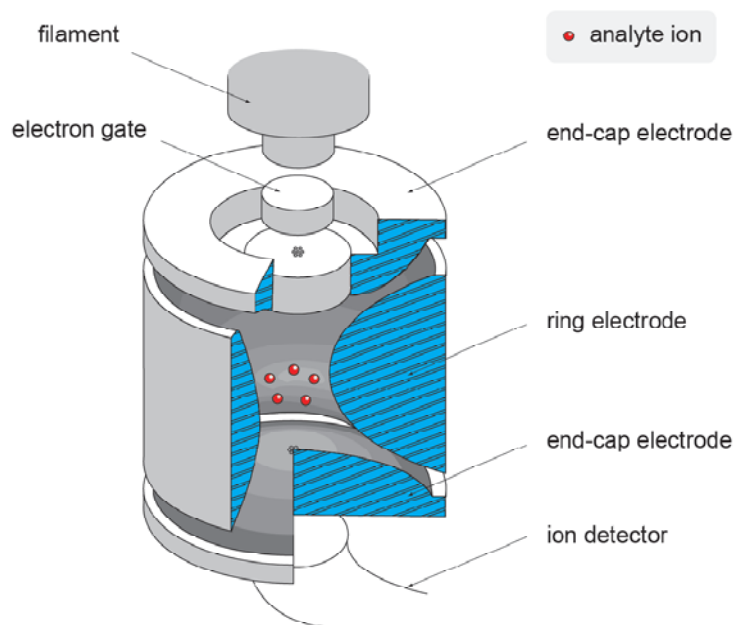


Figure 2-7: Schematic diagram of the quadrupole ion trap. Reproduced with permission from the authors.<sup>108</sup>

The quadrupole ion trap can be viewed as a three-dimensional quadrupole and consists of a ring electrode and two end caps.<sup>119</sup> Ions are stored inside the trap by means of the ring electrode with an rf voltage of low amplitude and grounding the end caps. Repulsive forces between the trapped ions increase the speed and amplitudes of their motion, which can lead to their expulsion from the trap. This is prevented by introducing helium gas into the trap ( $10^{-3}$  Torr), so that the ions are made to drift toward the trap center.<sup>120</sup> The ions may be created within the trap, for example by a short pulse of electrons, or injected into the trap from an external desorption or electrospray source.<sup>121</sup> A mass spectrum is subsequently obtained by scanning the rf potential, so that ions of increasing  $m/z$  successively develop unstable trajectories and escape the trap to strike an external ion detector. By applying a DC voltage to the ring electrode and ramping the rf voltage, it is possible to isolate a given ion in the trap for the acquisition of its tandem mass spectrum. MS/MS is then accomplished by fragmenting the isolated ion with a supplementary alternating voltage of appropriate frequency, applied to the end caps.<sup>120</sup> The newly formed fragment ions are finally detected by scanning the rf voltage.

### 2.8.3 Detectors

The detector converts ions of a given  $m/z$  value into a measurable electrical signal whose intensity is proportional to the corresponding ion current. With beam instruments (sectors, quadrupole or ToF analyzers) and the quadrupole ion trap, the ions are first separated according to their  $m/z$  value before detection, usually by an electron multiplier or a photon multiplier.<sup>2</sup>

#### 2.8.3.1 Electron Multipliers

The electron multiplier consists either of a series of discrete dynodes or of a continuous channel of dynodes.<sup>102,120,122-123</sup> Figure 2-8 depicts the continuous dynode type, also called a 'channeltron', which is the most widely used electron multiplier in modern instruments. A high negative potential is applied to the channeltron entrance, while the opposite end (anode) is usually grounded. Secondary electrons produced at the entrance by interfering ions or electrons experience a cascade of collisions with the walls, ejecting increasing numbers of electrons as they are accelerated down the channel.

Typically 10–20 stages of amplification take place until the anode is reached, where conventional amplifiers are connected in series before the signal readout is conducted. Mass-analyzed ions may strike the electron multiplier directly, ejecting secondary electrons that initiate the cascading emission of additional electrons down the channeltron, or alternatively, the ions may first collide with conversion dynodes, located in front of the channeltron, as shown in Figure 2-8. Positive ions hit the negative dynode, generating small negative ions and electrons; negative ions strike the positive dynode, generating small positive ions. These particles are then accelerated into the channeltron to start the amplification process described above. The gain, i.e., the number of secondary particles emitted per incoming ion, lies in the range of  $10^6$ – $10^7$ .

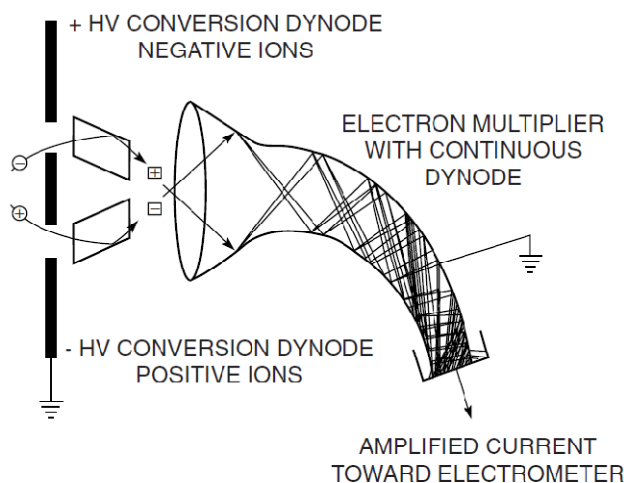


Figure 2-8: Channeltron electron multiplier with conversion dynodes for positive and negative ions.<sup>99</sup>

### 2.8.3.2 Photon Multipliers

Photon multiplier detectors consist of conversion dynodes, a scintillator, typically a phosphorescent screen, and a photomultiplier tube. Cations and anions are accelerated to the negative and positive conversion dynodes, respectively.

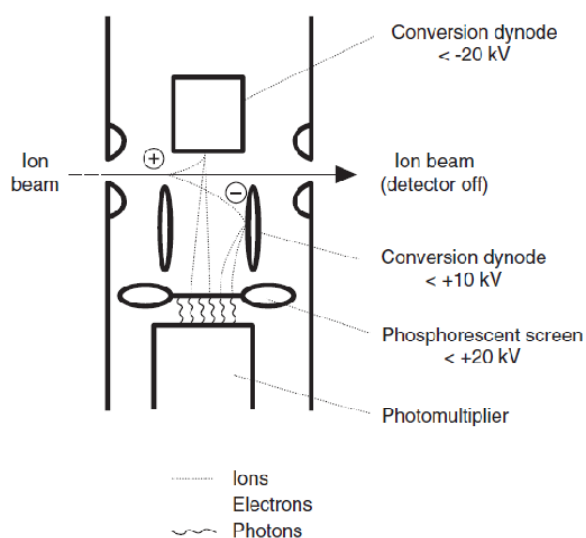


Figure 2-9: Photon multiplier detector.<sup>99</sup>

The following ion-surface collisions lead to the generation of secondary electrons which strike the phosphorescent screen where they are converted to photons. The latter are

detected by the photomultiplier. Overall, the ion beam reaching the detector is amplified  $10^4$ – $10^5$  times.<sup>99</sup> In contrast to electrons, photons can readily exit the vacuum system of the mass spectrometer through a glass window. For this reason, the photomultiplier is generally installed outside the vacuum system, which substantially increases its lifetime relative to that of the electron multiplier.

---

## 2.9 References

- 1 Hutchinson, R. A.; Beuermann, S.; Paquet, D. A.; McMinn, J. H. *Macromolecules* 1997, 30, 3490-3493.
- 2 Rosen, S. L. *Fundamental principles of polymeric materials*; Wiley-Interscience, 1982.
- 3 Odian, G. *Principles of Polymerization*; Wiley Interscience: Hoboken, New Jersey, 2004.
- 4 Barner-Kowollik, C.; Russell, G. T. *Prog. Polym. Sci.* 2009, 34, 1211-1259.
- 5 Busch, M.; Wahl, A. *Macromol. Theory Simul.* 1998, 7, 217-224.
- 6 North, A. M. *The Influence of Chain Structure on the Free Radical Termination Reaction*; Wiley-Interscience: New York, 1974.
- 7 Balke, S. T.; Hamielec, A. E. *J. Appl. Polym. Sci.* 1973, 17, 905-949.
- 8 Cardenas, J. N.; O'Driscoll, K. F. *J. Polym. Sci., Part A: Polym. Chem.* 1976, 14, 883-897.
- 9 Cardenas, J. N.; O'Driscoll, K. F. *J. Polym. Sci., Part A: Polym. Chem.* 1977, 15, 1883-1888.
- 10 Moad, G.; Moad, C. L. *Macromolecules* 1996, 29, 7727-7733.
- 11 Whang, B. C. Y.; Ballard, M. J.; Napper, D. H.; Gilbert, R. G. *Aust. J. Chem.* 1991, 44, 1133-1137.
- 12 Heuts, J. P. A.; Davis, T. P.; Russell, G. T. *Macromolecules* 1999, 32, 6019-6030.
- 13 Meisenburg, K.; Dennstedt, I.; Zaucker, E.; USPTO, Ed., 1943.
- 14 Roy, D.; Cambre, J. N.; Sumerlin, B. S. *Prog. Polym. Sci.* 2010, 35, 278-301.
- 15 Hoyle, C. E.; Lowe, A. B.; Bowman, C. N. *Chem. Soc. Rev.* 2010, 39, 1355 - 1387.
- 16 Valdebenito, A.; Encinas, M. V. *Polymer* 2005, 46, 10658-10662.
- 17 Henríquez, C.; Bueno, C.; Lissi, E. A.; Encinas, M. V. *Polymer* 2003, 44, 5559-5561.
- 18 Maxwell, I. A.; Morrison, B. R.; Napper, D. H.; Gilbert, R. G. *Die Makromolekulare Chemie* 1992, 193, 303-313.
- 19 Gower, M. D.; Shanks, R. A. *Macromol. Chem. Phys.* 2004, 205, 2139-2150.
- 20 Jiang, X.; Yin, J. *Macromolecules* 2004, 37, 7850-7853.
- 21 Jiang, X. S.; Xu, H. J.; Yin, J. *Polymer* 2005, 46, 11079-11084.
- 22 Karasu, F.; Arsu, N.; Yagci, Y. *J. Appl. Polym. Sci.* 2007, 103, 3766-3770.
- 23 Yamaguchi, K.; Taniguchi, R.; Kiyota, S.; Hamabe, T. *Polymer Preprints, Japan* 1999, 48, 162.
- 24 Trathnigg, B. In *Encyclopedia of Analytical Chemistry*; Meyers, R. A., Ed.; John Wiley & Sons: Chichester, 2000, p 8008-8034.
- 25 Striegel, A. M.; Yau, W. W.; Kirkland, J. J.; Bly, D. D. *Modern Size Exclusion Chromatography: Practice of Gel Permeation and Gel Filtration Chromatography*; John Wiley & Sons: Hoboken, New Jersey, 2009.
- 26 Wyatt, P. J. *Anal. Chim. Acta* 1993, 272, 1-40.
- 27 Grubisic-Gallot, Z.; Marais, L.; Benoit, H. *Journal of Polymer Science: Polymer Physics Edition* 1976, 14, 959-961.
- 28 McKenna, T. F.; Villanueva, A.; Santos, A. M. *J. Polym. Sci., Part A: Polym. Chem.* 1999, 37, 571.
- 29 Fernandez-Garcia, M.; Fernandez-Sanz, M.; Madruga, E. L. *Macromol. Chem. Phys.* 2000, 201, 1840.
- 30 Korolev, G. V.; Perepelitsina, E. O. *Polym. Sci., Ser. A* 2001, 43, 474.
- 31 Scott, G. E.; Senogles, E. J. *Macromol. Sci. Chem.* 1970, A4, 1105.
- 32 Scott, G. E.; Senogles, E. J. *Macromol. n. Rev. Macromol. Chem.* 1973, C9, 49.
- 33 Scott, G. E.; Senogles, E. J. *Macromol. Sci. Chem.* 1974, A8, 753.
- 34 Wunderlich, W. *Makromol. Chem.* 1976, 177, 973-989.

- 
- 35 Kaszas, G.; Foldes-Bereznich, T.; Tudos, F. *Eur. Polym. J.* 1983, 19, 469.
- 36 Madruga, E. L.; Fernandez-Garcia, M. *Macromol. Chem. Phys.* 1996, 197, 3743.
- 37 Kaszas, G.; Foldes-Bereznich, T.; Tudos, F. *Eur. Polym. J.* 1983, 19, 469-473.
- 38 Theis, A.; Feldermann, A.; Charton, N.; Davis, T. P.; Stenzel, M. H.; Barner-Kowollik, C. *Abstracts of Papers of the American Chemical Society* 2005, 230, 513-POLY.
- 39 Gilbert, B. C.; Lindsay Smith, J. R.; Milne, E. C.; Whitwood, A. C.; Taylor, P. J. *Chem. Soc., Perkin Trans.* 1994, 2, 1759.
- 40 Yamada, B.; Azukizawa, M.; Yamazoe, H.; Hill, D. J. T.; Pomery, P. J. *Polymer* 2000, 41, 5611.
- 41 Azukizawa, M.; Yamada, B.; Hill, D. J. T.; Pomery, P. J. *Macromol. Chem. Phys.* 2000, 201, 774.
- 42 Ahmad, N. M.; Heatley, F.; Lovell, P. A. *Macromolecules* 1998, 31, 2822-2827.
- 43 Britton, D.; Heatley, F.; Lovell, P. A. *Macromolecules* 1998, 31, 2828-2837.
- 44 Heatley, F.; Lovell, P. A.; Yamashita, T. *Macromolecules* 2001, 34, 7636-7641.
- 45 Britton, D.; Heatley, F.; Lovell, P. A. *Macromolecules* 2001, 34, 817-829.
- 46 Roedel, M. J. *J. Am. Chem. Soc.* 1953, 75, 6110-6112.
- 47 McCord, E. F.; Shaw, W. H.; Jr, n. *Macromolecules* 1997, 30, 246-256.
- 48 Ahmad, N. M.; Heatley, F.; Lovell, P. A. *Macromolecules* 1998, 31, 2822-2827.
- 49 Plessis, C.; Arzamendi, G.; Leiza, J. R.; Schoonbrood, H. A. S.; Charmot, D.; Asua, J. M. *Macromolecules* 2000, 33, 4-7.
- 50 Plessis, C.; Arzamendi, G.; Alberdi, J. M.; Herk, A. M. v.; Leiza, J. R.; Asua, J. M. *Macromol. Rapid Commun.* 2003, 24, 173-177.
- 51 Barner-Kowollik, C.; Günzler, F.; Junkers, T. *Macromolecules* 2008, 41, 8971-8973.
- 52 Beuermann, S.; Paquet, D. A.; McMinn, J. H.; Hutchinson, R. A. *Macromolecules* 1996, 29, 4206-4215.
- 53 Asua, J. M.; Beuermann, S.; Buback, M.; Castignolles, P.; Charleux, B.; Gilbert, R. G.; Hutchinson, R. A.; Leiza, J. R.; Nikitin, A. N.; Vairon, J. P.; van Herk, A. M. *Macromol. Chem. Phys.* 2004, 205, 2151-2160.
- 54 Peck, A. N. F.; Hutchinson, R. A. *Macromolecules* 2004, 37, 5944-5951.
- 55 Hirano, T.; Yamada, B. *Polymer* 2003, 44, 347-354.
- 56 Arzamendi, G.; Plessis, C.; Leiza, J. R.; Asua, J. M. *Macromol. Theory Simul.* 2003, 12, 315-324.
- 57 Nikitin, A. N.; Castignolles, P.; Charleux, B.; Vairon, J.-P. *Macromol. Theory Simul.* 2003, 12, 440-448.
- 58 Nikitin, A. N.; Castignolles, P.; Charleux, B.; Vairon, J. P. *Macromol. Rapid Commun.* 2003, 24, 778-782.
- 59 Nikitin, A. N.; Hutchinson, R. A.; Buback, M.; Hesse, P. *Macromolecules* 2007, 40, 8631-8641.
- 60 Beuermann, S.; Buback, M. *Prog. Polym. Sci.* 2002, 27, 191-254.
- 61 Toh, J. S. S.; Huang, D. M.; Lovell, P. A.; Gilbert, R. G. *Polymer* 2001, 42, 1915-1920.
- 62 Willemse, R. X. E.; Herk, A. M. v.; Panchenko, E.; Junkers, T.; Buback, M. *Macromolecules* 2005, 38, 5098-5103.
- 63 Azukizawa, M.; Yamada, B.; Hill, D. J. T.; Pomery, P. J. *Macromol. Chem. Phys.* 2000, 201, 774-781.
- 64 Yamada, B.; Azukizawa, M.; Yamazoe, H.; Hill, D. J. T.; Pomery, P. J. *Polymer* 2000, 41, 5611-5618.

- 
- 65 Yamada, B.; Westmoreland, D. G.; Kobatake, S.; Konosu, O. *Prog. Polym. Sci.* 1999, 24, 565-630.
  - 66 Barth, J.; Buback, M.; Hesse, P.; Sergeeva, T. *Macromol. Rapid Commun.* 2009, 30, 1969-1974.
  - 67 Buback, M.; Hesse, P.; Junkers, T.; Sergeeva, T.; Theist, T. *Macromolecules* 2008, 41, 288-291.
  - 68 Junkers, T.; Barner-Kowollik, C. *J. Polym. Sci., Part A: Polym. Chem.* 2008, 46, 7585-7605.
  - 69 Junkers, T.; Koo, S. P. S.; Davis, T. P.; Stenzel, M. H.; Barner-Kowollik, C. *Macromolecules* 2007, 40, 8906-8912.
  - 70 Castignolles, P. *Macromol. Rapid Commun.* 2009, 30, 1995-2001.
  - 71 Castignolles, P.; Graf, R.; Parkinson, M.; Wilhelm, M.; Gaborieau, M. *Polymer* 2009, 50, 2373-2383.
  - 72 Gaborieau, M.; Gilbert, R. G.; Gray-Weale, A.; Hernandez, J. M.; Castignolles, P. *Macromol. Theory Simul.* 2007, 16, 13-28.
  - 73 Gaborieau, M.; Nicolas, J.; Save, M.; Charleux, B.; Vairon, J.-P.; Gilbert, R. G.; Castignolles, P. *Journal of Chromatography A* 2008, 1190, 215-223.
  - 74 Nikitin, A. N.; Castignolles, P.; Charleux, B.; Vairon, J.-P. *Macromol. Rapid Commun.* 2003, 24, 778-782.
  - 75 Nikitin, A. N.; Hutchinson, R. A. *Macromolecules* 2005, 38, 1581-1590.
  - 76 Nikitin, A. N.; Hutchinson, R. A. *Macromol. Theory Simul.* 2006, 15, 128-136.
  - 77 Wang, W.; Nikitin, A. N.; Hutchinson, R. A. *Macromol. Rapid Commun.* 2009, 30, 2022-2027.
  - 78 Chiefari, J.; Jeffery, J.; Mayadunne, R. T. A.; Moad, G.; Rizzardo, E.; Thang, S. H. *Macromolecules* 1999, 32, 7700-7702.
  - 79 Junkers, T.; Barner-Kowollik, C. *Macromol. Theory Simul.* 2009, 18, 421-433.
  - 80 Moad, C. L.; Moad, G.; Rizzardo, E.; Thang, S. H. *Macromolecules* 1996, 29, 7717-7726.
  - 81 Sato, E.; Emoto, T.; Zetterlund, P. B.; Yamada, B. *Macromol. Chem. Phys.* 2004, 205, 1829-1839.
  - 82 Junkers, T.; Bennet, F.; Koo, S. P. S.; Barner-Kowollik, C. *J. Polym. Sci., Part A: Polym. Chem.* 2008, 46, 3433-3437.
  - 83 Plessis, C.; Arzamendi, G.; Alberdi, J. M.; van Herk, A. M.; Leiza, J. R.; Asua, J. M. *Macromol. Rapid Commun.* 2003, 24, 173-177.
  - 84 Decker, C. *Polymer International* 1998, 45, 133-141.
  - 85 Timpe, H.-J.; Strehmel, B. *Angew. Makromol. Chem.* 1990, 178, 131-142.
  - 86 Sandner, M. R.; Osborn, C. L. *Tetrahedron Lett.* 1974, 15, 415-418.
  - 87 Fouassier, J.-P.; Merlin, A. *Journal of Photochemistry* 1980, 12, 17-23.
  - 88 Merlin, A.; Lougnot, D. J.; Fouassier, J. P. *Polymer Bulletin* 1980, 3, 1-6.
  - 89 Merlin, A.; Lougnot, D.-J.; Fouassier, J.-P. *Polymer Bulletin* 1980, 2, 847-853.
  - 90 Fischer, H.; Baer, R.; Hany, R.; Verhoolen, I.; Walbiner, M. *J. Chem. Soc., Perkin Trans. 2* 1990, 787-798.
  - 91 Fouassier, J. P.; Jacques, P.; Lougnot, D. J.; Pilot, T. *Polymer Photochemistry* 1984, 5, 57-76.
  - 92 Banks, J. T.; Scaiano, J. C.; Adam, W.; Oestrich, R. S. *J. Am. Chem. Soc.* 1993, 115, 2473-2477.
  - 93 Kuhlmann, R.; Schnabel, W. *Polymer* 1977, 18, 1163-1168.
  - 94 Kuhlmann, R.; Schnabel, W. *Angew. Makromol. Chem.* 1978, 70, 145-157.

- 
- 95 Cowan, D. O.; Drisko, R. L. *Elements of Organic Photochemistry*; Plenum Press: New York, 1976.
  - 96 Szablan, Z.; Junkers, T.; Koo, S. P. S.; Lovestead, T. M.; Davis, T. P.; Stenzel, M. H.; Barner-Kowollik, C. *Macromolecules* 2007, 40, 6820-6833.
  - 97 Jent, F.; Paul, H.; Fischer, H. *Chem. Phys. Lett.* 1988, 146, 315-319.
  - 98 Blättler, C.; Jent, F.; Paul, H. *Chem. Phys. Lett.* 1990, 166, 375-380.
  - 99 Montaudo, G.; Lattimer, R. P. *Mass Spectrometry of Polymers*; CRC Press, 2002.
  - 100 Hanton, S. D. *Chem. Rev.* 2001, 101, 527-569.
  - 101 McLafferty, F. W.; Turecek, F. *Interpretation of Mass Spectra*; University Science Books: Mill Valley, CA, 1993.
  - 102 Hoffmann, E. d.; Charette, J.; Stroobant, V. *Mass Spectrometry: Principles and Applications*; Wiley: Chichester, 1996.
  - 103 McEwen, C. N.; Simonsick, W. J. J.; Larsen, B. S.; Ute, K.; Hatada, K. *Journal of the American Chemical Society Mass Spectrometry* 1995, 6, 906-911.
  - 104 Dole, M.; Mack, L. L.; Hines, R. L.; Mobley, R. C.; Ferguson, L. D.; Alice, M. B. *The Journal of Chemical Physics* 1968, 49, 2240-2249.
  - 105 Whitehouse, C. M.; Dreyer, R. N.; Yamashita, M.; Fenn, J. B. *Analytical Chemistry* 1985, 57, 675-679.
  - 106 Nohmi, T.; Fenn, J. B. *J. Am. Chem. Soc.* 1992, 114, 3241-3246.
  - 107 Zeleny, J. *J. Phys. Rev.* 1917, 10, 1.
  - 108 Hart-Smith, G.; Barner-Kowollik, C. Submitted 2010.
  - 109 Haddleton, D. M.; Feeney, E.; Buzy, A.; Jasieczek, C. B.; Jennings, K. R. *Chem. Commun.* 1996 1157-1158.
  - 110 Guittard, J.; Tessier, M.; Blais, J. C.; Bolbach, G.; Rozes, L.; Maréchal, E.; Tabet, J. C. *Journal of Mass Spectrometry* 1996, 31, 1409-1421.
  - 111 Saf, R.; Schitter, R.; Mirtl, C.; Stelzer, F.; Hummel, K. *Macromolecules* 1996, 29, 7651-7656.
  - 112 Mahon, A.; Kemp, T. J.; Buzy, A.; Jennings, K. R. *Polymer* 1997, 38, 2337-2349.
  - 113 Jasieczek, C. B.; Buzy, A.; Haddleton, D. M.; Jennings, K. R. *Rapid Commun. Mass Spectrom.* 1996, 10, 509-514.
  - 114 McEwen, C. N.; Simonsick, J. W. J.; Larsen, B. S.; Ute, K.; Hatada, K. *J. Am. Soc. Mass Spectrom.* 1995, 6, 906-911.
  - 115 Koo, S. P. S.; Junkers, T.; Barner-Kowollik, C. *Macromolecules* 2009, 42, 62-69.
  - 116 Gruending, T.; Weidner, S.; Falkenhagen, J.; Barner-Kowollik, C. *Polymer Chemistry* 2010, DOI: 10.1039/b9py00347a.
  - 117 F.W. McLafferty, F. T. *Interpretation of Mass Spectra*; University Science Books: Mill Valley, CA, 1993.
  - 118 Ferguson, R. E.; McCulloh, K. E.; Rosenstock, H. M. *The Journal of Chemical Physics* 1965, 42, 100-106.
  - 119 March, R. E.; Hughes, R. J. *Quadrupole Storage Mass Spectrometry*; John Wiley & Sons: New York, 1989.
  - 120 Chapman, J. R. *Practical Organic Mass Spectrometry*; John Wiley & Sons: New York, 1993.
  - 121 McLuckey, S. A.; Van Berkel, G. J.; Goeringer, D. E.; Glish, G. L. *Analytical Chemistry* 1994, 66, 689A-696A.
  - 122 Lambert, J. B.; Shurvell, H. F.; Lightner, D. A.; Cooks, R. G. *Organic Structural Spectroscopy*; Prentice Hall: Upper Saddle River, NJ, 1998.

---

123 Watson, J. T. Introduction to Mass Spectrometry; Lippincott-Raven: Philadelphia, PA, 1997.



### 3 Methods and Materials

This chapter is a collation of materials employed in the experiments conducted and the instrumentation conditions under which characterization and further analysis was performed. Some of the work was conducted at the University of New South Wales, New South Wales, Sydney, Australia, and at times multiple experimental and analytical set-ups may have been used. The sections are therefore organized chronologically according to the relevant chapter as they appear in this thesis, and all relevant materials and instrumentation related to the work conducted in each chapter is described in the associated subsections.

#### 3.1 In-depth Probing of the Product Spectrum of High Conversion *n*-Butyl Acrylate Free Radical Polymerization Mediated by 1-Octanethiol

This section contains materials and instrumentation conditions pertaining to Chapter 4, where the effect of 1-octanethiol as a transfer agent is qualitatively and quantitatively evaluated in the high conversion polymerization of *n*-butyl acrylate.

##### 3.1.1 General Polymerization Procedures

Bulk monomer solutions of BA, thiol and initiator, typically at  $C_{1\text{-octanethiol}} = 0.4 \text{ mol}\cdot\text{L}^{-1}$  and  $C_{\text{AIBN}} = 5\cdot 10^{-3} \text{ mol}\cdot\text{L}^{-1}$ , were combined, transferred into sample vials containing about 2 mL of reaction solution each and sealed with rubber septa, Parafilm and copper wire. Oxygen was removed by purging the samples with nitrogen for 15-20 min. After polymerization in a constant temperature oil bath (Julabo HD-4), the samples were rapidly cooled down in either a liquid nitrogen or an ice water bath to cease any further reaction. Monomer conversion was determined by gravimetry. To allow for polymerization to maximum monomer conversion, several samples were prepared for each reaction condition and the reaction was stopped after different time periods, ideally when all monomer had been consumed. The polymer that was obtained after the shortest time interval without showing significant further increase in conversion was subjected to ESI-MS analysis. Nevertheless, as prolonged heating of the polymer and initiator in the absence of monomer may lead to the formation of unwanted products, it was tested whether this may occur on the time scale of the experiment by analyzing polymer samples obtained at 60 °C where heating was continued for an extended time interval of 8 h instead of 4 h reaction time. No significant changes in the product spectrum were observed.

### 3.1.2 Size Exclusion Chromatography

For the determination of molecular weight distributions (MWD), a Shimadzu modular system, comprising an auto injector, a Polymer Laboratories 5.0  $\mu\text{m}$  bead-size guard column (50 x 7.5 mm), followed by three linear PL columns ( $10^5$ ,  $10^4$ , and  $10^3$  Å) and a differential refractive index detector using THF as the eluent at 40 °C with a flow rate of 1 mL·min<sup>-1</sup> was used. The SEC system was calibrated using narrow polystyrene standards ranging from 540 to  $2 \cdot 10^6$  g·mol<sup>-1</sup>. The resulting molecular weight distributions have been recalibrated using Mark Houwink parameters for poly(butyl acrylate),  $K = 12.2 \cdot 10^{-5}$  dL·g<sup>-1</sup>,  $\alpha = 0.70^1$  and for polystyrene,  $K = 14.1 \cdot 10^{-5}$  dL·g<sup>-1</sup> and  $\alpha = 0.70$ .<sup>2</sup>

### 3.1.3 Electrospray Ionization Mass Spectrometry

ESI-MS experiments were carried out using a Thermo Finnigan LCQ Deca quadrupole ion-trap mass spectrometer (Thermo Finnigan, San Jose, CA) in the positive ion mode. The ESI-MS is equipped with an atmospheric pressure ionization source which operates in the nebulizer assisted electrospray mode. The instrument was calibrated with caffeine, Met-Arg-Phe-Ala acetate (MRFA), and Ultramark 1621 (all from Aldrich) in the mass range 195-1822 amu. All spectra were acquired over the mass to charge range ( $m/z$ ) of 150-2000 Da with a spray voltage of 5 kV, a capillary voltage of 39 V and a capillary temperature of 275 °C. Nitrogen was used as sheath gas (flow: 40 % of maximum) while helium was used as auxiliary gas (flow: 5 % of maximum in all experiments). The eluent was a 3:2 v/v mixture of THF:methanol with the polymer concentration being  $\sim 0.4$  mg·mL<sup>-1</sup>. The instrumental resolution of the employed experimental setup is 0.1 amu.

### 3.1.4 <sup>13</sup>C Nuclear Magnetic Resonance

<sup>13</sup>C melt-state NMR experiments followed variations of a published method,<sup>3</sup> with single-pulse excitation under magic-angle spinning (SPE-MAS) at  $T_g+150$  °C and 75.47 MHz with 10 s relaxation delay. The poly(*n*-butyl acrylates) synthesized with thiol were packed in 7 mm rotors, while the poly(*n*-butyl acrylates) synthesized without thiol at 140 °C were packed in 4 mm rotors, yielding a somewhat lower sensitivity, but allowing faster spinning speeds (the homogeneity of sample packing being less of an issue). All samples could be spun at 9 kHz MAS at room temperature. Subsequent determination of the precision of the measurements showed that the observed differences were significant and the precision is thus sufficient.

The degree of branching (DB) was quantified in percents of the monomer units from the integrals  $I$  of the signals of the quaternary carbons at 49 ppm and of the OCH<sub>2</sub> moiety at 63 ppm, following the equation below:

$$DB (\%) = \frac{I(C_q) \cdot 100}{I(OCH_2)} \quad \text{Equation 3-1}$$

A signal from 1-octanethiol overlaps with the backbone signal of poly(*n*-BA), so therefore the latter could not be used for quantification. The relative standard deviation  $SD$  of  $DB$  was calculated from the signal-to-noise ratio of the quaternary carbon  $SNR$  using the equation below:<sup>3</sup>

$$SD (\%) = \frac{238}{SNR^{1.28}} \quad \text{Equation 3-2}$$

#### 3.1.4.1 Experimental Parameters

Measurements were undertaken on a Bruker Avance-II spectrometer (Bruker BioSpin, Germany) operating at a Larmor frequency of 75.47 MHz for <sup>13</sup>C (300 MHz for <sup>1</sup>H). Quantitative <sup>13</sup>C NMR spectra were recorded at  $T_g + 150$  °C with single-pulse excitation under magic-angle spinning (SPE-MAS) using a 4 or 5 μs 90° pulse, TPPM dipolar decoupling and a 10 s relaxation delay, accumulating 14000 to 17500 transients. Samples synthesized with thiol were measured in 7 mm zirconia rotors with boron nitride caps, at MAS rotational frequencies of 4.5, 3 and 1.8 kHz for increasing synthesis temperatures. Samples synthesized without thiol were measured in 4 mm zirconia rotors with Vespel caps at 9 kHz MAS, because extensive cross-linking prevented their proper spinning in 7 mm rotors.

### 3.2 Macromonomer Synthesis and the Limitations of Thiol-ene Chemistry for Polymer-Polymer Conjugation

This section pertains to work carried out in Chapter 6, where macromonomers are first synthesized and then subsequently used in a thiol-ene coupling reaction in an attempt at the easy formation of stars *via* MM attachment to a multi-arm core molecule.

### 3.2.1 Materials: Macromonomer Formation

Butyl acrylate (BA, Fluka, 99 %) and hexyl acetate (HAc, Aldrich, 99 %) were purified by percolating over a column of activated basic alumina twice. Butyl acetate (BuAc, Ajax Finechem, 99 %) was used as received.

### 3.2.2 Macromonomer Synthesis Method

Polymerizations were carried out in a two-neck flask equipped with a reflux condenser and a rubber septum. The reaction vessel containing only the solvent (200 ml) was heated up to reaction temperature and the liquid was de-oxygenated by purging with nitrogen gas. Butyl acrylate was similarly purged in a sealed glass vial separately and added *via* a cannula after stable temperature conditions were reached. To avoid contamination with air, purging of the reaction mixture was continued and a positive N<sub>2</sub> pressure was maintained throughout the whole polymerization. Samples of approximately 2 mL were taken using a syringe. Monomer-to-polymer conversion was determined gravimetrically and the molecular weight distributions were determined by size exclusion chromatography. It was found that the reaction rate varies significantly between different experimental runs, e.g. for the above described polymerization, full monomer-to-polymer conversion is observed at reaction times ranging from 3 to 24 hours.

### 3.2.3 Materials: Thiol-ene experiments

Butyl acrylate (BA, Fluka, 99 %) was freed from the inhibitor by passing over a column of activated basic alumina. 1-octanethiol (Aldrich, 98.5 %) was used as received as was the initiator 1,1-azobis(cyanocyclohexane) (VAZO 88, DuPont). 2,2'-Azobisisobutyronitrile (AIBN, DuPont) was recrystallized twice from methanol prior to use.

Thiols with varying degrees of thiol functionalities were purchased from Sigma-Aldrich and used as received: 1-octanethiol (> 98.5 %), 1,4-butanedithiol (97 %), trimethylolpropane tris(2-mercaptoacetate) (tech.), and pentaerythritol tetrakis(3-mercaptoacetate) (PTMP) (97 %). AIBN (Sigma-Aldrich) was recrystallized twice from methanol, 1,1 azobis(cyclohexanecarbonitrile) (ACHN) (98 %) (Sigma-Aldrich) was used as received, and hexyl acetate (97 %) and butyl acetate (CHROMASOLV® Plus, for HPLC, 99.7 %) were used as solvent. *n*-butyl acrylate (≥ 99 %) (Sigma-Aldrich) was de-inhibited over basic alumina before use.

### 3.2.4 General Procedure for Thiol-ene Reactions for the Formation of Star Polymers from Poly(*n*-Butyl Acrylate) Macromonomer

Butyl acrylate macromonomer, BA MM, was synthesized *via* the straight forward method described in section 3.2.2. No purification was necessary before the thiol-ene reaction could be performed. Samples were prepared as follows: AIBN ( $0.05 \text{ mol}\cdot\text{L}^{-1}$ , 0.5 eq.) were added to macromonomer (100 mg, 0.055 mmol) in 2 mL butyl acetate solvent, and varied amounts of thiol compound (1-10 eq.) were added. The mixture was degassed *via* the freeze-pump-thaw method, and then heated at  $60 \text{ }^\circ\text{C}$  for 16 h with stirring, after which time the samples were quenched in ice water. Excess unreacted thiol compound and solvent were removed by drying in a vacuum oven at  $30 \text{ }^\circ\text{C}$  for 24 h. BA MM with a number average molecular weight of  $1870 \text{ g}\cdot\text{mol}^{-1}$  and a polydispersity of 1.7 was employed in the thiol-ene reactions.

### 3.2.5 Size Exclusion Chromatography

#### 3.2.5.1 Macromonomer Formation and Thiol-ene coupling

For the determination of molecular weight distributions (MWD), a Shimadzu modular system, comprising an auto injector, a Polymer Laboratories  $5.0 \mu\text{m}$  bead-size guard column ( $50 \times 7.5 \text{ mm}$ ), followed by four linear PL columns ( $10^5$ ,  $10^4$  and  $10^3$  and  $500 \text{ \AA}$ ) and a differential refractive index detector using THF as the eluent at  $40 \text{ }^\circ\text{C}$  with a flow rate of  $1 \text{ mL}\cdot\text{min}^{-1}$  was used. The SEC system was calibrated using narrow polystyrene standards ranging from 560 to  $1.95\cdot 10^6 \text{ g}\cdot\text{mol}^{-1}$  (polystyrene ( $K = 14.1\cdot 10^{-5} \text{ dL}\cdot\text{g}^{-1}$  and  $\alpha = 0.70$ )).<sup>2</sup> The resulting molecular weight distributions have been universally recalibrated using Mark-Houwink parameters for poly(butyl acrylate), ( $K = 12.2\cdot 10^{-5} \text{ dL}\cdot\text{g}^{-1}$ ,  $\alpha = 0.70$ ).<sup>1</sup>

### 3.2.6 Electrospray Ionization Mass Spectrometry

#### 3.2.6.1 Macromonomer Formation

ESI-MS experiments were carried out on a Thermo Finnigan LCQ Deca quadrupole ion-trap mass spectrometer (Thermo Finnigan, San Jose, CA) in positive ion mode. The ESI-MS is equipped with an atmospheric pressure ionization source which operates in the nebulizer assisted electrospray mode. The instrument was calibrated with caffeine, MRFA, and Ultramark 1621 (all from Aldrich) in the mass range 195 – 1822 amu. All spectra were acquired over the mass to charge range ( $m/z$ ) of 150 – 2000 Da with a spray voltage of 5 kV, a capillary voltage of 39 V and a capillary temperature of  $275 \text{ }^\circ\text{C}$ . Nitrogen was used as

sheath gas (flow: 40 % of maximum) while helium was used as auxiliary gas (flow: 5 % of maximum in all experiments). The solvent was a 3:2 v/v mixture of THF:methanol with polymer concentration  $\sim 0.4 \text{ mg}\cdot\text{mL}^{-1}$ . The instrumental resolution of the employed experimental set-up is 0.1 amu.

### 3.2.6.2 Thiol-ene Coupling

Mass spectra were acquired on an LXQ mass spectrometer (ThermoFisher Scientific, San Jose, CA, USA) equipped with an atmospheric pressure ionization source operating in the nebulizer assisted electrospray mode. The instrument was calibrated in the  $m/z$  range 195-1822 Da using a standard containing caffeine, Met-Arg-Phe-Ala acetate (MRFA) and a mixture of fluorinated phosphazenes (Ultramark 1621) (all from Aldrich). A constant spray voltage of 3.5 kV and a dimensionless sheath gas of 10 and a sweep gas flow rate of 2 were applied. The capillary voltage, the tube lens offset voltage, and the capillary temperature were set to 60 V, 120 V and 275 °C respectively.

## 3.3 Pulsed Laser Polymerization (PLP) for the Quantification of the Efficiency of Photo-Initiation Processes in Methyl Methacrylate Free Radical Polymerization

The materials and conditions outlined in this section relate to work from Chapter 6, where PLP is employed as a tool to investigate the relative efficiency of 1,2-dimesitylethane-1,2-dione as a photo-initiator, in comparison to benzoin.

### 3.3.1 Materials for polymerizations

Methyl methacrylate (MMA, Fluka, 99 %) monomer was de-inhibited by percolating over a column of activated basic alumina. Benzoin (Aldrich) was recrystallized twice in ethanol prior to use. Tetrahydrofuran (THF, Aldrich, 99 %), *tert*-butyl lithium (*t*-BuLi, Aldrich), carbon monoxide (CO, BOC gases, 5.0) and  $\text{MgSO}_4$  (Aldrich, 99.5 %) were used as received without any further purification.

### 3.3.2 Polymerizations

All MMA samples consisted of monomer (sample volume  $\sim 1.0 \text{ mL}$ ) with a mixture of both photo-initiators with an overall concentration of  $c_{\text{PI}} = 5 \cdot 10^{-3} \text{ mol}\cdot\text{L}^{-1}$ . The samples were carefully freed of oxygen prior to laser irradiation *via* purging the reaction mixture with high purity nitrogen. Polymerization was performed at  $T = 5 \text{ }^\circ\text{C}$  by laser pulses generated from a

Lambda Physik COMPex Pro 110 XeF (351 nm, 20 ns pulse width) excimer laser system at constant frequency of 100 Hz for an overall polymerization time of  $\sim 15$  min. Single pulse energy ranged between 5 and 25 mJ. The laser beam was attenuated to  $1 \text{ cm}^2$  using Thor Labs optics. Laser energy measurements were carried out with an Ophir AN/2 power meter. Care was taken to ensure a homogeneous intensity profile over the whole optical cross section. The applied laser pulse patterns were controlled with a handheld keypad. The resulting polymers were isolated by evaporating off the residual monomer. Cell design limited the study to atmospheric pressure. No stirring was applied.

Isothermal reaction conditions were maintained (by first allowing the sample to equilibrate for 10 min) using a recirculating bath including a feedback loop through a thermocouple attached to the side of the reaction cell. The reaction cell is a copper cell (120 x 120 x 70 mm) designed to hold a soda glass vial (75 x 12 mm). The bath fluid used was a 50:50 v/v mix of ethylene glycol and water.

### 3.3.3 Synthesis of 1,2-dimesitylethane-1,2-dione (Mesityl)

The preparation procedure was adapted from a combination of refs.<sup>4-5</sup> 5 g (25 mmol) mesityl bromide is dissolved into 25 mL dry tetrahydrofuran (THF). 2 molar equivalents of *t*-BuLi solution (1.7 M) in hexane were added drop-wise under oxygen and water free conditions. Argon was used as inert atmosphere in the reaction flask. The reaction flask was placed into an acetone/liquid nitrogen mixture while adding the *n*-BuLi. The reaction mixture was stirred for 2 h and was subsequently allowed to thaw to ambient temperature. Once at ambient temperature,  $\text{CO}_{(g)}$  was percolated through the reaction flask for approximately 45 min. A color change from red/brown to dark green occurs as soon as the CO is introduced into the reaction mixture. After the CO percolation, saturated  $\text{NH}_4\text{Cl}$  solution was added drop-wise to the reaction flask, which was subsequently separated into an aqueous and organic phase. The organic phase was dried over  $\text{MgSO}_4$  followed by the evaporation of all solvent. Primary purification is achieved *via* column chromatography using a 1:4 mixture of ethyl acetate/hexane. The first column chromatography results in a crude product and a second column chromatography is carried out on the collected crude product to further purify the compound. Recrystallization in ethanol gives the final mesityl product in the form of orange plate crystals. ESI-MS: 294.2 Da (found), 294.16 Da (calculated).  $^1\text{H-NMR}$  (300 MHz,  $\text{CDCl}_3$ ): 2.20 (s, 12H), 2.30 (s, 6H), 6.88 (s, 4H).

### 3.3.4 UV Spectra

UV/Vis spectra were recorded at ambient temperatures using a Varian Cary 300 Bio photospectrometer.

### 3.3.5 Electrospray Ionization Mass Spectrometry

ESI-MS experiments were carried out using a Thermo Finnigan LCQ Deca quadrupole ion-trap mass spectrometer (Thermo Finnigan, San Jose, CA) as well as a Thermo Finnigan LXQ linear quadrupole ion-trap mass spectrometer (Thermo Finnigan, San Jose, CA) in positive ion mode. The ESI-MS is equipped with an atmospheric pressure ionization source which operates in nebulizer assisted electrospray mode. The instrument was calibrated with caffeine, MRFA, and Ultramark 1621 (all from Aldrich) in the mass range 195-1822 amu. All spectra were acquired over the mass to charge range ( $m/z$ ) of 150-2000 Da with a spray voltage of 5 kV, a capillary voltage of 39 V and a capillary temperature of 275 °C. Nitrogen was used as sheath gas (flow: 40 % of maximum) while helium was used as auxiliary gas (flow: 5 % of maximum in all experiments). The eluent was a 3:1 v/v mixture of dichloromethane:methanol with polymer concentration being around 0.4 mg·mL<sup>-1</sup>.

## 3.4 Pulsed Laser Polymerization (PLP) for the Determination of $k_p$ of 2-Ethyl Hexyl Acrylate and MA beyond Ambient Temperature

The materials and conditions outlined in this section relate to work in the second part of Chapter 6, where PLP is employed to determine  $k_p$  of MA and 2-EHA beyond room temperature. Furthermore, triple detection SEC is performed to investigate possible effects of branching on SEC results, which directly impact  $k_p$  evaluation.

### 3.4.1 General PLP procedure

Neat monomer, or monomer/solvent solutions, and photo-initiator were combined to give a photo-initiator concentration of 5·10<sup>-3</sup> mol L<sup>-1</sup>. Samples, ~ 0.3 mL, were deoxygenated by purging with nitrogen gas for approximately 2 min and irradiated at energies of 1.0-1.5 mJ·pulse<sup>-1</sup>. The sample vial was placed into a sample holder and brought to the required temperature by a re-circulating bath (VWR 1196D) including a feedback loop through a thermocouple attached to the side of the sample holder. The temperature was monitored directly at the sample. The samples were allowed to equilibrate at the reaction temperature for 5 min and were subsequently initiated by laser pulsing at repetition rates of

up to 500 Hz. Laser initiation was achieved by a Xantos XS-500; a compact version of the ExciStar™ EXS-500; operated at the XeF-line of 351 nm. The vial was irradiated from the bottom. Conversion was determined by gravimetry. Typical conversions were in the range 2-9 %. Immediately following irradiation, 2 drops of hydroquinone solution in methanol were added to stop further reaction.

### 3.4.2 Size Exclusion Chromatography

Molecular weight distributions (MWD) obtained from PLP were determined on a Varian system, comprising an auto injector, a Polymer Laboratories 5.0 µm bead-size guard column, followed by three linear PL columns (PLgel 5 µm MIXEDC) and a differential refractive index detector using THF as the eluent at 40 °C with a flow rate of 1 mL·min<sup>-1</sup>. The SEC system was calibrated using narrow polystyrene standards ranging from 160 to 6·10<sup>6</sup> g·mol<sup>-1</sup> and the resulting molecular weight distributions were recalibrated using the Mark-Houwink parameters of the corresponding polymer and for polystyrene ( $K = 14.1 \cdot 10^{-5} \text{ dL} \cdot \text{g}^{-1}$  and  $\alpha = 0.70$ ).

The triple-detection chromatographic setup used for the determination of the MHKS parameters consisted of a modular system (Polymer Standard Service, PSS, Mainz/Agilent 1200 series) incorporating a ETA2010 viscometer (WGE Dr. Bures) and a light-scattering unit (PSS SLD7000/BI-MwA, Brookhaven Instruments) and a differential refractive index detector (Agilent 1200 series). Sample separation was achieved on two linear columns provided by PSS (SDV-Lux-1000 Å and 105 Å, 5 µm) with THF as the eluent at 25 °C with a flow rate of 1 mL·min<sup>-1</sup>. The system was calibrated using polystyrene standards (PSS).

### 3.4.3 Mark-Houwink-Kuhn-Sakurada Parameter Determination for 2-Ethyl Hexyl Acrylate

Samples prepared *via* PLP were analyzed in the triple detection system described in the previous section. For the theory pertaining to triple detection SEC please refer to section 2.4. Absolute molecular weights were determined by light scattering and intrinsic viscosity from viscometer measurements. This data was linearly plotted and fitted with  $\alpha$  being the slope and  $\log K$  the y-intercept of the fit, according to the following equation:

$$\log [\eta] = \log K + \alpha \log M \quad \text{Equation 3-3}$$

### 3.5 PREDICI®

Initial work is presented in Chapter 7 on a proposed method of determining the reaction rate coefficients of  $\beta$ -scission, backbiting and termination of midchain radicals, using the commercial software package PREDICI®, obtained from Computing in Technology GmbH (CIT). PREDICI® (Polyreaction Distributions by Countable System Integration) is a simulation package for the investigation of macromolecular reactions *via* the input of kinetic equations. The kinetic equations represent a model of the polymerization as a whole, and PREDICI® allows the computation of chain length distributions (molecular weight distributions) of macromolecules generated in polymerizations under various conditions. It is also possible to employ PREDICI® as a tool for advanced kinetic coefficient extraction and an outline of the methodology is presented in Chapter 7.

Input of a complete reaction model including kinetic parameters and the initial values of all reaction components and reactor variables must be provided and PREDICI® performs a numerical time integration of the resulting systems of differential equations for a given reaction time. Results that can be obtained from these simulated polymerization reactions include approximations of the chain length distributions of the polymer products and/or the respective moments and mean values, the concentrations of the remaining components in the reaction, other additives such as chain transfer agents, resulting polymer concentrations, and balances of the reactor variables temperature, volume and mass. PREDICI® was used to simulate the outcome of bulk *n*-butyl acrylate polymerizations in the presence of varying amounts of 1-octanethiol as transfer agent.

### 3.6 References

- 1 Penzel, E.; Goetz, N. *Angew. Makromol. Chem.* 1990, 178, 191-200.
- 2 Strazielle, C.; Benoit, H.; Vogl, O. *Eur. Polym. J.* 1978, 14, 331-334.
- 3 Castignolles, P.; Graf, R.; Parkinson, M.; Wilhelm, M.; Gaborieau, M. *Polymer* 2009, 50, 2373-2383.
- 4 Rathman, T. L.; Woltermann, C. J. *Pharma. Chem.* 2003, 2, 6-8.
- 5 Nudelman, N.; Schulz, H. J. *Chem. Res.* 1999 422-423.

## 4 In-depth Probing of the Product Spectrum of High Conversion *n*-Butyl Acrylate Free Radical Polymerization Mediated by 1-Octanethiol

### 4.1 Introduction

As discussed in section 2.4.2, backbiting and  $\beta$ -scission play an important role in acrylate polymerizations at moderate to high temperatures, e.g. > 60 °C, and have been accepted as the cause of deviation between ideal kinetics and those observed. From an industrial perspective, production techniques which form highly uniform product are exceedingly sought after, as they reduce the number of post polymerization purification steps required and thus lead to lower production costs. If it were possible to reduce or prevent the formation of these MCRs, this could provide important information on acrylate reactions which have until now eluded study (as a result of current technological limitations). Alternatively, removing MCRs from the polymerization system as they form is another method which could be used to eliminate their effect in polymerization reactions. This is an area of high interest both from a fundamental and from an industrial perspective; yet to date very few studies have been conducted to investigate MCR formation and the subsequent reaction pathways that MCRs undergo once they are created. Such knowledge is paramount to further current understanding of the outstanding problems arising from MCR formation, but only limited research efforts have so far been directed at this area. One of these studies is that of Farcet *et al.* to trace the number of nitroxide end groups in the SG1-mediated polymerization of BA and to detect the branching consequences of intermolecular transfer to polymer *via* the MALDI-TOF technique as this potentially leads to more than one active centre on the polymer chain.<sup>1</sup>

However, technological limitations at the time prevented more detailed information on the product spectrum from being obtained from these MALDI-TOF MS spectra.<sup>2</sup> In the context of investigating acrylate specific reactions, the current study is the only high-resolution MS study that has been performed with the exception of studies of the high-temperature polymerization of BA in xylene solution.<sup>3-4</sup>

Suppression of MCR side reactions is possible by adding a thiol chain transfer agent to the polymerizable reaction mixture. The chain transfer agent can transfer its proton from the thiol functionality to a growing radical site, and this becomes the dominant chain terminating event. The sulfur-centered radical that is produced in the same instance subsequently reinitiates polymerization such that most polymer that is formed contains an alkyl-sulfur endgroup on one side and a proton on the other.

This study shows that the same mechanism also operates for the midchain radicals and hence the amount of reaction side products is significantly reduced. A second benefit of employing a CTA in the polymerization is that the average molecular weight is reduced and thus the resulting polymer can be easily analyzed *via* ESI-MS. The ESI-MS setup used here has an upper operational mass limit of 2000 g·mol<sup>-1</sup> (see Chapter 3 Methods and Materials for a description of setup used), so a reduced average molecular weight is desirable from the perspective of ESI-MS analysis such that the greatest part of the polymer distribution can be observed.

The development of modern soft-ionization mass spectrometry techniques such as matrix assisted laser desorption ionization – time of flight (MALDI-TOF) spectrometry and in particular ESI-MS has given access to a convenient method for the unambiguous determination of the components in the product spectrum and its changes within the chain length distribution.<sup>5-8</sup> These new techniques have created vast opportunities for in-depth polymer characterization at a level of detail previously unavailable. The potential of ESI-MS for exploring mechanistic aspects of radical polymerization has been discussed in a feature article<sup>5</sup> and the impact of ESI-MS on the characterization of synthetic polymers has been reviewed.<sup>9-15</sup> Soft ionization techniques can be problematic in the analysis of polymers under certain circumstances as they may not be fully quantitative when compounds of different ionization potential are analyzed. They are also restricted to lower molecular weight material. Nonetheless, they allow product spectrum imaging in great detail and with high accuracy and hence soft ionization techniques provide information that cannot be obtained by other methods, such as the exact composition and distribution of the polymeric chains. Such knowledge is highly significant when contemplating the unresolved problems arising from mid-chain radical formation.

Size exclusion chromatography (SEC) provides easy access to the molecular weight distribution, but it does not yield any information about the endgroups of the polymer chains. Limited information about the endgroup composition can be obtained by NMR spectroscopy, although it is rather time-consuming and has the notable disadvantage of being widely hindered by the relative insensitivity and frequent low solubility of branched polyacrylates. NMR rapidly loses sensitivity with increasing  $DP_n$  because the endgroup signal becomes weaker compared to the backbone signals. Hence, quantitative endgroup information, especially at larger  $DP_n$ , is associated with high experimental errors. As an example, if a polymer with an average chain length of 10 is analyzed and an error in the NMR signal of 5 % is assumed (compared to the main peaks) then the endgroup compositions are derived with higher absolute errors. In contrast, with mass spectrometry, the resulting uncertainty in endgroup composition is directly given by the error of signal intensity. So even if the primary experimental error might be higher in ESI-MS due to ionization effects, more accurate composition data for the single species can be derived from ESI-MS spectra.

Another disadvantage of NMR is that no coupled information on endgroup chemistry and molecular weight can be obtained. While soft ionization techniques have a drawback in that they may not be fully quantitative and/or in that they are restricted to relatively low molecular weight material, they allow product spectrum imaging in great detail and with high accuracy and are able to provide information that cannot be obtained by other techniques, such as the exact composition of the polymeric chains. Since soft ionization mass spectrometry allows for very detailed characterization and mapping of what reactions take place during polymerization, it appears of high priority to carry out a systematic MS study directed towards investigating the effects that MCR reactions have on overall product spectrum distributions in acrylate polymerizations and the behavior of MCRs in the presence of thiol as CTA.

The mechanistic reaction steps that MCRs can follow are generally agreed upon, but the kinetic coefficients associated with these reactions are only partially known and often associated with high uncertainties. Conversely, the rate parameters for the propagation and termination of the SPR are accurately known.<sup>16-17</sup> Various techniques have been used to determine individual rate coefficients, notably electron spin resonance (ESR) detection of

the MCR concentration,<sup>18-24</sup> determination of branching points in the residual polymer<sup>25-29</sup> and kinetic modeling of high-temperature polymerizations.<sup>30-32</sup> However, for precise determination of the kinetic rate coefficients governing acrylate polymerizations, it is compulsory to separate the individual reaction steps to be able to study their rates. To date a range of studies employing ESI-MS to investigate the mechanism and kinetics of free radical polymerization have been carried out, ranging from the analysis of RAFT polymers to photo- and thermally initiated systems. Most recently, photo-initiation processes in methacrylate, acrylate and itaconate systems<sup>33</sup> as well as complex macromolecular architecture formation<sup>34-35</sup> have been studied *via* ESI-MS. Contemporarily, Buback and coworkers studied initiation pathways using peroxides.<sup>36-38</sup>

The study presented here stems from a search for experimental conditions and analytical methods that can distinguish the effects and contributions of all reactions occurring in an acrylate free radical polymerization reaction, with the aim of determining the kinetic rate coefficients which govern acrylate polymerizations, and in summary presents a convenient methodology to (i) fully characterize the polymer product *via* soft-ionization mass spectrometry, and to (ii) significantly reduce the concentration of midchain radicals during polymerization, to achieve conditions where no side products from transfer to polymer reactions can be found in the post polymerization product and thus resulting in the formation of highly uniform polyacrylate with respect to the endgroup chemistry. This two part study provides a detailed assignment of MCR derived products in butyl acrylate polymerizations *via* ESI-MS and implements a novel method to quantify the various species obtained at varying conditions of temperature and thiol concentration.

In the broader scope this knowledge would increase current understanding of MCR formation processes and their subsequent reaction pathways. First, the influence of a chain-transfer agent that allows efficient suppression of secondary reactions of MCRs is examined and discussed in the context of being a possible means to obtain highly uniformly structured poly(acrylates). The second part of this work then enhances the study to provide the first quantitative ESI-MS study of a thiol mediated acrylate polymerization. This product distribution data can subsequently be used in a kinetic modeling analysis, which is discussed in Chapter 7. The ultimate purpose of this approach and the related quantitative information is to use this information to develop a method for deducing kinetic information;

that is, the  $\beta$ -scission rate, MCR termination rate and backbiting rate, pertaining to acrylate polymerizations that have thus far proven difficult to access.

## 4.2 Integration of Mass Spectra – Some considerations

Before the results of the ESI-MS can be presented, the validity of the spectra with respect to the analyses conducted must be established. To make qualitative and quantitative assessments of the spectra it is important to first exclude the possibility of biased results due to ionization suppression of the different endgroup functionalities, as a result of varying the acquisition parameters or as a result of bias introduced when tuning for the optimum signal intensity for one product peak over another. ESI-MS is a powerful tool to identify polymeric species with respect to endgroup analysis, but information derived from the mass spectra must be treated with care. Varying endgroups and functionalities can significantly affect the ionization of the molecules and therefore the observed spectra. For example, a product that is more easily ionized than another species can exhibit a higher relative abundance when observed *via* ESI-MS as compared to its relative amount when based on concentration. This would lead to an incorrect assessment of the relative amounts of species in the sample. Moreover, the instrument can be optimized for specific species, and therefore endgroup functionalities, so erroneous relative abundances are potentially obtained when instrument settings such as the capillary voltage are changed.

Although complete or near-complete suppression of any species is unlikely as very high ion counts were achieved when analyzing the poly(*n*-BA) samples, the extent of ionization differences was nevertheless tested as the results are based on the assumption that the ionization properties of the molecules are mostly dependent on the polymer backbone and hence on the type of monomer, rather than on the endgroups. This assumption was evaluated by mixing a high temperature 1-octanethiol-mediated poly(*n*-BA) sample with BA macromonomer obtained by a slightly modified procedure outlined by Chiefari *et al.*<sup>39</sup> BA macromonomer is of known structure, in fact corresponding to structure  $\beta^1$  in Scheme 2-7, and more importantly, concomitantly has the same backbone as poly(*n*-BA) samples. This implies that any observed variance in ionization would stem from differences in endgroups. An ESI-MS spectrum was obtained where the mixing ratio was satisfactorily reflected when comparing the relative abundance of the peaks. An absolute error in the determination of peak abundances, and hence product composition, of less than 20 % is assumed. Other

studies<sup>36,40</sup> have shown that ionization occurs on the polymer backbone and thus endgroups have relatively little effect on ionization ability. It can therefore be presumed with a high degree of confidence that ionization suppression due to differing endgroup functionalities does not prove to be a significant constraint or limitation in undertaking a quantitative analysis of the data presented herein.

The impact of varying the tuning files on the measurement was evaluated by optimizing the instrument settings for each peak found in the spectrum (within the monomer repeat unit as displayed in Figure 4-6). As depicted in Figure 4-1, no significant change in the spectrum can be identified. This indicates that tuning on different peaks also has no significant impact on the abundances found for the various species within one monomer repeat unit, and that integration of the so obtained mass spectra is feasible.

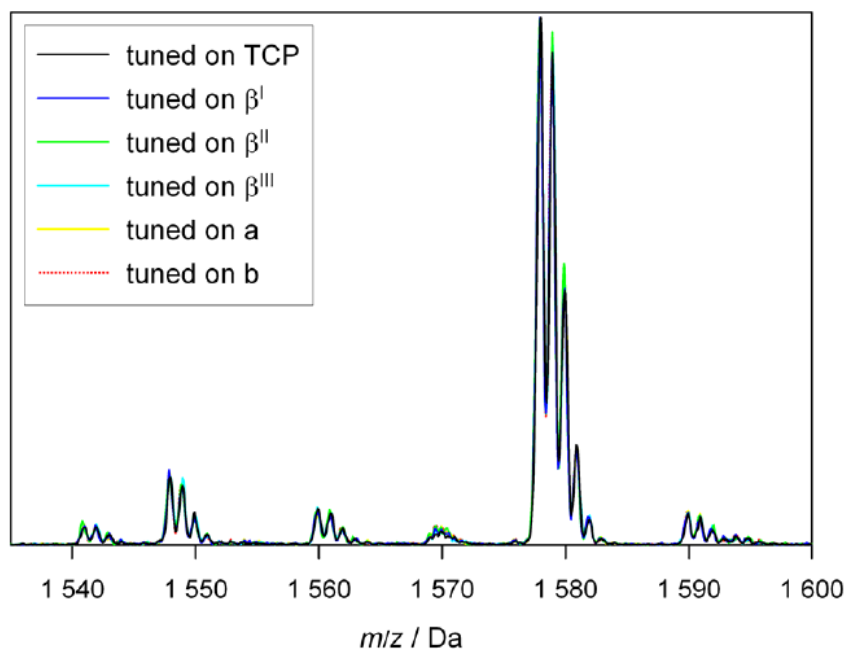


Figure 4-1: ESI-MS spectra of a poly(butyl acrylate) sample under different optimizations of the ESI-MS instrument on the various peaks. Please refer to Figure 4-6 for peak assignments.

#### 4.2.1 Integration

Integrations of all peaks of interest in the mass spectrum distribution were made using an appropriate spreadsheet number analysis package, using the principle of area calculation *via* the trapezoidal rule, by which incremental areas formed under the peaks of the mass

spectrum were calculated and summed up over the relevant mass ranges to provide a measure of area.

$$Area = \int_a^b f\left(\frac{m}{z}\right) d\frac{m}{z} \approx \Delta \frac{m}{z} \left( \frac{A_0}{2} + A_1 + A_2 + A_3 + \dots + \frac{A_n}{2} \right)$$

Equation 4-1

A limitation of the trapezoidal rule for calculating areas is that a positive slope on the peak being integrated will yield an overestimation of the actual area just as conversely a negative slope will yield an underestimation of the actual area. This is an error inherent in the trapezoidal rule algorithm used to compute areas. Thus, all sample analysis proportions derived from integrals have been rounded to the nearest percent. Any attempt to increase accuracy to finer detail is unwise. The mass spacing for data acquisition in the mass spectrometer is 0.0667 Da, and corresponds to the variable  $\Delta m/z$  in equation 4-1. This is of consequence only to point out that a larger spacing would result in larger errors while a smaller spacing would reduce these errors.

The area of each relevant peak in the mass spectrum is individually calculated as follows. The entire isotopic pattern of a species is integrated as one whole, rather than each peak in the isotopic pattern being integrated individually and then summed for one species. This constitutes the integral of one peak in one repeat unit. The integral area of each species in each repeat unit is determined, and subsequently summed up to provide the total area of that species over the entire spectrum. This area is directly proportional to the concentration of the species, as MS provides a number distribution. The proportion of that species within the entire spectrum is calculated by dividing the area of that species by the total area of all species present. Data presented in the results section refer to the proportion, i.e. the mole fraction, of that particular species.

A complete spectrum integration includes the full accessible spectral range from 150 - 2000 Da. Multiply charged species are not considered as they occur as singly charged species elsewhere in the spectrum and are accounted for in that instance. Comparison of values obtained in the integration of only a single repeat unit leads to erroneous results as the species composition changes with polymer chain length. Such changes are caused by relative shifts of the various product distributions relative to each other and thus make ratio determination at the repeat unit level meaningless. This is graphically demonstrated in

Figures 4-2 to 4-4. It is clear by mere inspection that both the relative peak heights and the offset of one distribution relative to another both affect the product proportions when considering individual repeat units. Thus there exists no single repeat unit which can be taken as representative of product distributions in the entire sample. Instead, an accurate analysis must consider every repeat unit and average proportions must be calculated on the basis of the entire spectrum as seen *via* ESI-MS.

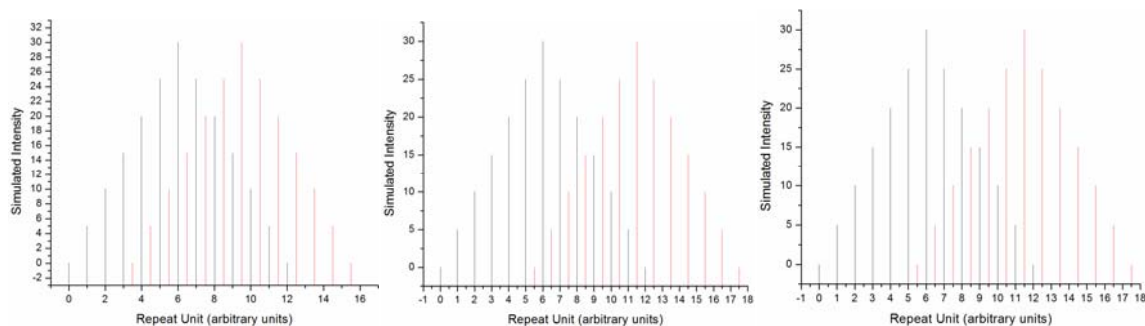


Figure 4-2: Simulation of two product distributions with varying degrees of overlap. Both product distributions are of the same intensity.

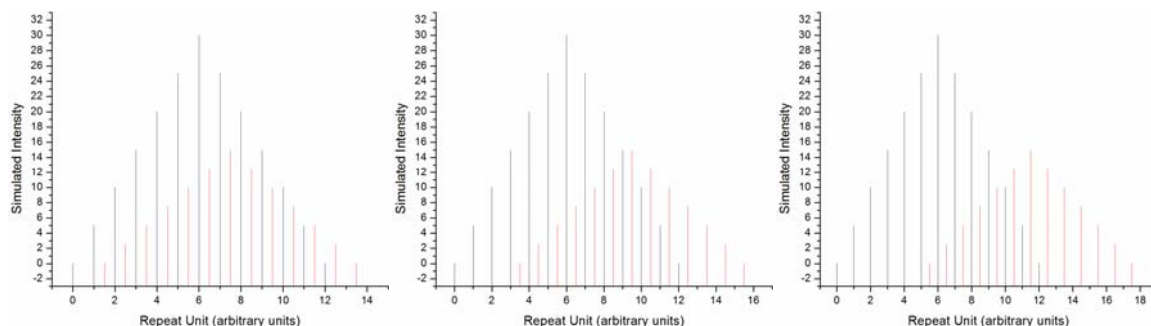


Figure 4-3: Simulation of two product distributions with varying degrees of overlap. The smaller product distribution is half the intensity of the other.

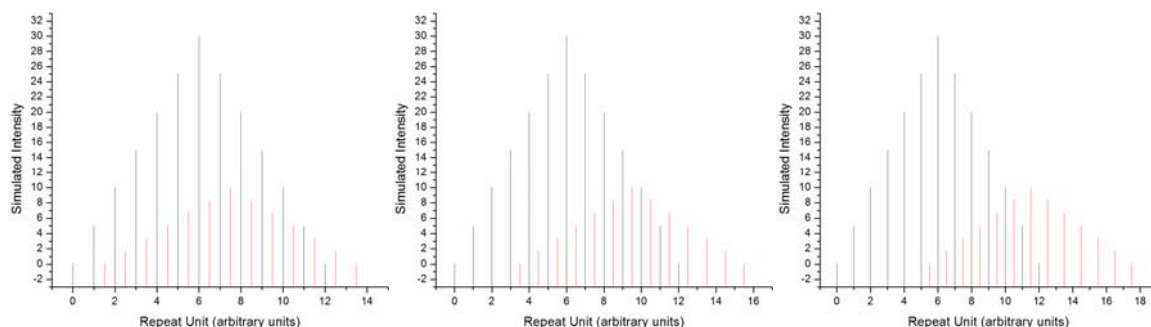


Figure 4-4: Simulation of two product distributions with varying degrees of overlap. The smaller product distribution is one third the intensity of the other.

Figure 4-5 presents an actual TCP peak in the sample prepared at 100 °C in the presence of 0.005 mol·L<sup>-1</sup> 1-octanethiol, with appropriate labels to indicate the values corresponding to variables in equation 4-1. *a* and *b* are the limits of integration, and correspond to the end values that enclose the peak and its isotopic pattern. The dark grey area is one incremental area; many such small areas are summed to provide the area of this TCP peak.

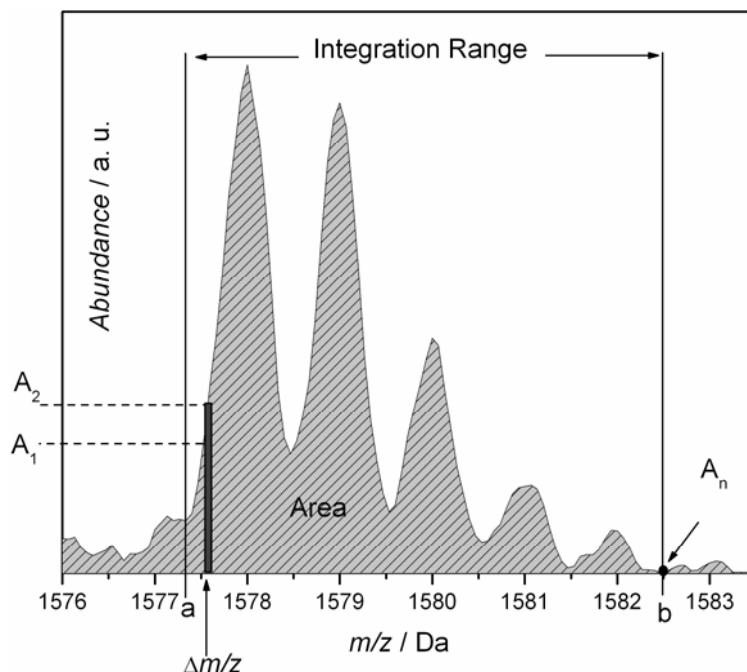


Figure 4-5: One TCP peak from the sample prepared at 100 °C in the presence of 0.005 mol·L<sup>-1</sup> 1-octanethiol and initiated by 5·10<sup>-3</sup> mol·L<sup>-1</sup> AIBN, showing how the integral of this peak was determined. The dark shaded area represents one incremental area and the light shaded area within the range *a*-*b* is the total area for this peak. All labels correspond to variables in equation 4-1.

### 4.3 Experimental Results – Thiol Mediated *n*-BA Polymerizations

The SPRs in the present system can undergo the reactions of: chain propagation, termination *via* combination/disproportionation and transfer to a CTA. Species β<sup>I</sup> (see section 2.6.4 for the accompanying scheme and structures) is most probably congruent with polymer that is formed after transfer to monomer has taken place. Since no such peak is identified for polymer synthesized at lower temperature, and hence no production of β<sup>I</sup>

either, this reaction seems to play a minor role at the most in the systems studied and was hence not included in the scheme. The occurrence of H-abstractions by the MCR from the CTA is the main reaction investigated in this study, and the effects may not be immediately apparent and the consequences of this reaction on the endgroup chemistry and branching levels in acrylate polymerization have not yet been explored. The thiol group could alternatively be an AIBN or ACHN initiating fragment. In this case,  $\beta$ -scission results in the formation of species  $\beta^{\text{II}}_{\text{AIBN}}$  or  $\beta^{\text{II}}_{\text{ACHN}}$ . In addition other reactions may occur, such as radical addition to the  $\beta^{\text{I}}$  and  $\beta^{\text{II}}$  species. Also, the radical scission product that leads to the formation of  $\beta^{\text{III}}$  may undergo its specific scission and transfer reactions. However, in all these reactions, no further structurally different species are generated.

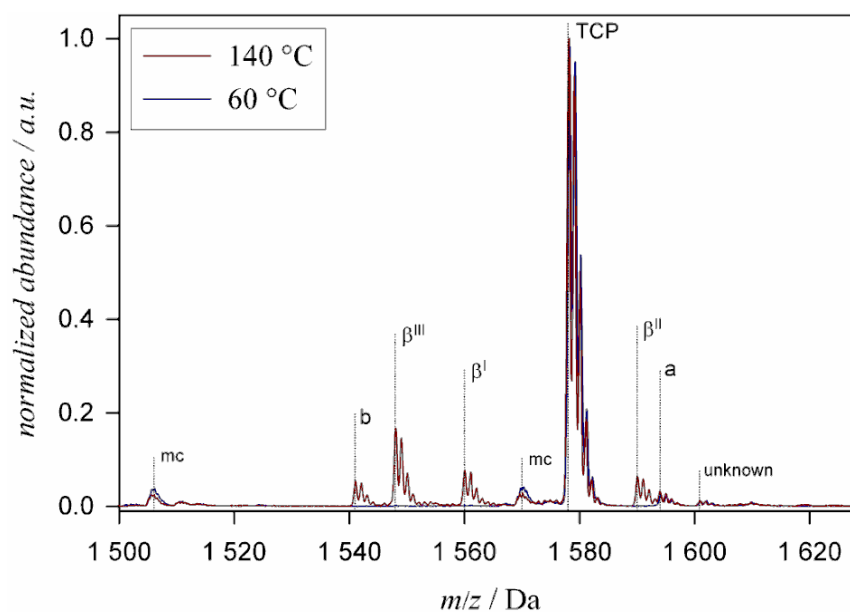


Figure 4-6: ESI-MS spectrum of polymer obtained from bulk polymerization of butyl acrylate at 60 °C and 140 °C, respectively, in the presence of 0.4 mol·L<sup>-1</sup> 1-octanethiol initiated by 5·10<sup>-3</sup> mol·L<sup>-1</sup> AIBN (60 °C) or ACHN (140 °C). Each polymerization was carried out until almost full conversion of monomer was reached. The labels correspond to species appearing in Scheme 4-1 and 4-2 (where T represents an octyl-S group) and the vertical dotted lines indicate the theoretical *m/z*. mc denotes peaks which are multiply charged.

Looking into a single monomer repeat unit of the spectrum, depicted in Figure 4-6, reveals the presence of a very small quantity of termination by combination product a which is not immediately apparent upon cursory inspection. No mass peak corresponding to a

disproportionation product can be identified which suggests that combination is the primary mode of termination in the system. This observation does not fully agree with a previous MS study on poly(*n*-BA) produced under pulsed laser polymerization conditions at low temperatures.<sup>33</sup> However, the ratio between combination and disproportionation is known to change with temperature.<sup>41-42</sup> The ratio could also have been influenced in the previous study by the very high radical concentrations, in combination with the highly different reaction conditions that occur under laser irradiation. It should be noted that *b* coincides in mass with the three and four arm stars as shown in Scheme 2-7.

Unfortunately, mass spectrometry is unable to distinguish between the star/long chain branch structure and the normal combination product *b*, so no clear conclusion can be drawn from the spectrum as to whether this species is a star. Only star polymers that carry more than two non-proton endgroups, formed after *intermolecular* transfer to polymer reactions, can be clearly distinguished and identified as branched polymers. However, as the vast majority of polymer material consists of the TCP species, it is highly unlikely that such products form in this system. Regardless of whether the backbiting reaction takes place, it is remarkable to observe such a clean spectrum of poly(*n*-BA), where a plethora of products is usually expected. It is known from low conversion ESR experiments that under normal reaction conditions, meaning without addition of a CTA, at 60 °C the majority of radicals are MCR species.<sup>23</sup> It was also shown that the MCR concentration is likely to further increase as the polymerization proceeds since monomer concentration decreases, which is followed by a decrease of the probability of chain propagation of the MCR. The increasing polymer concentration also favors *intermolecular* transfer.

As shown in Scheme 2-7, MCRs not only undergo chain propagation or termination forming long or short-chain branches, but they can also undergo  $\beta$ -scission reactions to yield unsaturated polymer endgroups. The formation of unsaturated polymer species was reported for temperatures as low as 80 °C and their presence is easy to establish *via* <sup>1</sup>H-NMR.<sup>31,39</sup> No such macromonomeric species can be identified at 60 °C or at 140 °C, neither in the ESI-MS spectrum, nor by NMR spectroscopy, although its formation is likely to occur at 60 °C under normal reaction conditions.<sup>43</sup>

It may then be concluded that the presence of the CTA very effectively suppresses the secondary reactions of the MCR such as  $\beta$ -scission under the given conditions. While the  $\beta$ -scission reactions are associated with a rather high activation energy and hence are not expected to manifest themselves to any great degree at 60 °C, measurable amounts of  $\beta$ -scission products would nevertheless be expected under the chosen conditions.<sup>43</sup> The absence of these  $\beta$ -scission species is explained by the intervention of the CTA before any scission reaction may take place. The CTA acts as an effective repair device that mends the MCR, forming a dead linear chain.

Experiments at elevated temperatures were then designed to confirm the hypothesis of a self-repairing acrylate system. Figure 4-6 also contains a spectrum of the polymerization product obtained from bulk polymerization at 140 °C. All experimental conditions were maintained as that of the 60 °C sample, other than a temperature increase to 140 °C and 1,1'-azobis(cyclohexanecarbonitrile) being used as initiator. AIBN decays too fast at 140 °C to allow the reaction to proceed to almost full conversion. Decomposition constants for the initiators AIBN and ACHN are given in Table 4-1.

Table 4-1: Decomposition Arrhenius parameters for AIBN and ACHN<sup>44</sup>

Initiator	$A \times 10^{-8} / s^{-1}$	$E_A / J \cdot mol^{-1}$
AIBN	7.03	84319
ACHN	6.23	93561

Examination of the ESI-MS spectrum of polymer produced at 140 °C reveals four new products when compared to the analogous sample at 60 °C, three of which are products of  $\beta$ -scission reactions. The scission reactions yield four different fragments but the fourth fragment is identical to a normal propagating chain and hence does not appear as a distinctly separate peak. The fourth fragment b is consistent with the mass of an azo-fragment initiated polymer chain. The appearance of b in the spectrum indicates the much higher average radical concentration at 140 °C compared to 60 °C even when a different initiator is used. A peak according to the mass of b' is also found in AIBN-initiated polymerization when the reaction temperature, and thus radical concentration, is increased, see Figure 4-6. Only one peak remains unassigned, at an *m/z* ratio of approximately 1601 Da. The same peak also appears in the same quantity in the 60 °C spectrum, but it is

too low in abundance for an unambiguous assignment and is not considered significant. All assigned species match the experimental data with an accuracy of 0.1 Da; the accepted accuracy limit of the quadrupole ion-trap ESI-MS. Theoretical and experimental  $m/z$  ratios for the monoisotopic peak are given in Table 4-2.

Table 4-2: Theoretical and experimental masses of the monoisotopic peaks of products occurring in the chain-transfer polymerization of *n*-BA with 1-octanethiol in the  $m/z$  range of 1500 and 1630 Da, in the presence of either AIBN (60 °C – 100 °C) or ACHN (120 °C -140 °C) as initiator. All masses correspond to sodium adducts. The given values refer to data obtained for the sample made at 100 °C and a 1-octanethiol concentration of 0.005 mol·L<sup>-1</sup> and in case of the ACHN-specific product to a sample prepared at 140 °C and otherwise identical conditions. Virtually identical  $m/z$  are found in all spectra.

species	$m/z_{\text{theoretical}} / \text{Da}$	$m/z_{\text{experimental}}^a / \text{Da}$	$ \Delta m/z $
TCP	1578.02	1578.0	0.02
$\beta^{\text{I}}$	1560.00	1560.07	0.07
$\beta^{\text{II}}$	1590.02	1590.07	0.05
$\beta^{\text{III}}$	1547.99	1548.07	0.08
a	1594.04	1593.93	0.11
b	1541.00	1541.07	0.07
b'	1500.97	1500.93	0.04
$\beta^{\text{II}}_{\text{AIBN}}$	1512.96	1512.93	0.03

The  $\beta$ -scission reaction does not take place to one specific side of the MCR over the other side, with respect to the position of the radical moiety, since the fragments  $\beta^{\text{I-III}}$  appear in almost equal amounts. This can be expected because the electronic nature of both sides is virtually identical. It should be noted that in principle two different macromonomers plus two corresponding fragments are formed. As it is of no concern in rate-based investigations, this distinction is not always made and therefore some literature studies only focus on the scission reaction forming  $\beta^{\text{II}}$ .<sup>3-4,30</sup> The presence of relatively large quantities of  $\beta^{\text{I}}$  is more revealing and indicates that *intermolecular* transfer to polymer and *intramolecular* transfer to polymer to remote backbone positions both occur to significant extents. If backbiting *via* a six-membered ring was the only active pathway available to MCRs this fragment would consist of only two monomeric units and hence would not appear in the displayed monomer

repeat unit where  $DP_n = 12$ . Such species may be present, but are not found in larger quantities, which suggests that at least at high monomer conversion, other transfer to polymer pathways, that is, inter and intramolecular transfer to remote backbone locations, are as important as the backbiting reaction that is dominant in low conversion systems. This finding is in good agreement with studies carried out in the context of RAFT-star polymerization, where star-star coupling upon intermolecular transfer is clearly observed.<sup>34,45</sup>

The amount of the unsaturated  $\beta$ -scission products relative to the main product peak also provides interesting information about the BA/1-octanethiol system. The most abundant  $\beta$ -scission peak,  $\beta^{III}$ , is less than 20 % of the TCP signal strength and the peak of the second unsaturated product  $\beta^I$  shows slightly less than 10 % abundance. Such amounts are significant, but both are nevertheless minor products. Chiefari *et al.* reported formation of macromonomer in quantities above 90 % at the same reaction temperature,<sup>39</sup> albeit at low monomer concentrations, which indubitably favor scission reactions over short-chain branching formation *via* MCR propagation. Furthermore, in the BA polymerization in xylene at high temperatures, macromonomers have been identified as the main product as a result of NMR and ESI-MS characterization.<sup>3-4,46</sup> Although scission products are clearly visible, their amount is greatly reduced in the CTA system, again demonstrating the repairing function of the thiol.

#### 4.4 Intermezzo – <sup>13</sup>C-Nuclear Magnetic Resonance for Quantitative Determination of Branching

An alternative way to test for suppression of secondary MCR reactions is quantitative <sup>13</sup>C-NMR spectroscopy. Such data are complementary to the ESI-MS data as they provide the number of branch points in the polymer. Quantitative <sup>13</sup>C NMR spectroscopy of polymers is not a routine method. There have been several attempts to quantify the degree of branching in poly(acrylates) synthesized under various conditions, with various NMR methods.<sup>27,47-48</sup> Both resolution and sensitivity are required for a reliable quantification of the degree of branching. Initial attempts were carried out either on polymer solutions<sup>47</sup> or on swollen samples.<sup>27</sup> These samples exhibited high resolution (owing to high sample mobility) but suffered from limited sensitivity (and thus low precision) partly due to limited sample concentration. Moreover, polyacrylates often contain a significant gel fraction and

only the soluble fraction of the sample is measured in some cases.<sup>48</sup> The soluble fraction presumably consists of polymer with fewer branches. A method was recently proposed and validated to estimate the precision of the determined degree of branching from the signal-to-noise ratio of the quaternary carbon at the branching point,<sup>48-49</sup> allowing for a meaningful comparison of samples, along with a reliable melt-state <sup>13</sup>C NMR method for the quantification of the degree of branching in polyacrylates was developed to allow this measurement.<sup>48</sup> Melt-state NMR (using solid-state NMR equipment) is more sensitive than solution- or gel-based methods as it measures the pure (undiluted) sample. It yields sufficient resolution for branching quantification through the high mobility of polymer chains in the melt. The accuracy of measured degrees of branching is ensured by full relaxation of the relevant signals between pulses.<sup>48</sup> The NMR results that follow were acquired *via* this new methodology.

NMR measuring parameters were chosen to match those previously used in the literature (see section 3.1.4) which are thought to yield adequately quantitative spectra. Regardless, the determination of number of branches per chain *via* this method does not indicate whether the branching belongs to a short or a long chain branch and is therefore incapable of distinguishing between *inter*- and *intramolecular* transfer. Despite this shortcoming, ESI-MS in conjunction with <sup>13</sup>C-NMR allows for an almost complete mapping of the secondary MCR reactions. Branch points are identified by observing the characteristic peak of the quaternary backbone carbon. The mol-percentage of branch points in the sample is obtained by comparing the integral of the quaternary carbon peak ( $\delta = 47.5-49.1$  ppm) to the integral of one of the ester side chain peaks such as the carbon closest to the ester function ( $\delta = 63.5-66.0$  ppm). The degree of branching (DB) was quantified in percents of the monomer units from the integrals *I* of the signals of the quaternary carbons at 49 ppm and of the -OCH<sub>2</sub> moiety at 63 ppm, following the equation below:

$$DB (\%) = \frac{I(C_q) \cdot 100}{I(OCH_2)} \quad \text{Equation 4-2}$$

Note that due to a signal from 1-octanethiol overlapping with the backbone signal of poly(*n*-BA), the latter could not be used for quantification. The relative standard deviation

*SD* of *DB* was calculated from the signal-to-noise ratio of the quaternary carbon *SNR* using the following equation:<sup>48</sup>

$$SD(\%) = \frac{238}{SNR^{1.28}} \quad \text{Equation 4-3}$$

As the chain length of the polymer is expected to influence the local chain dynamics, which may influence the conditions for recording quantitative <sup>13</sup>C melt-state NMR spectra, all spectra were recorded at exactly 150 °C above the *T<sub>g</sub>*. Table 4-3 presents *M<sub>n</sub>* and *M<sub>w</sub>*, for the thiol (0.4 mol·L<sup>-1</sup>) and non-thiol containing poly(*n*-butyl acrylates) synthesized at various temperatures that were characterized by <sup>13</sup>C NMR analysis to determine degree of branching.

Table 4-3: Number-average molecular weights, *M<sub>n</sub>*, and weight-average molecular weights, *M<sub>w</sub>*, for the thiol (0.4 mol·L<sup>-1</sup>) and non-thiol containing poly(*n*-butyl acrylates) synthesized at various temperatures that were subjected to <sup>13</sup>C NMR analysis to determine degree of branching.

<i>T</i> / °C	<i>C</i> <sub>thiol</sub> / mol·L <sup>-1</sup>	<i>M<sub>n</sub></i> / g·mol <sup>-1</sup>	<i>M<sub>w</sub></i> / g·mol <sup>-1</sup>
60	0	55 200	425 000
100	0	85 900	825 000
140	0	60 200	825 000
60	0.4	1 830	10 100
100	0.4	3 810	26 300
140	0.4	2 500	18 800

The <sup>13</sup>C melt-state NMR spectra of the samples exhibiting the lowest and the highest *DB* are shown in Figure 4-7. Figure 4-7 presents the <sup>13</sup>C-NMR spectrum of the sample obtained at 140 °C discussed with respect to the ESI-MS data. The full chemical shifts assignment is known from literature for both poly(*n*-butyl acrylate)<sup>48</sup> and 1-octanethiol and are shown in Figure 4-8.<sup>50</sup> Small peaks appear in the double-bond region at 127 and 138 ppm which are consistent with the observation of some β-scission products. Integration of the quaternary carbon peak and the ester side chain peak at 65 ppm yields a mol percentage of 1.37 of branched monomer units. With the number average molecular weight of 1720 g·mol<sup>-1</sup>, the

number of branches per chain is calculated to be close to 0.2. This level of branching is close to the level reported for 60 °C RAFT polymerization up to almost full conversion again indicating the MCR-suppressing ability of the CTA as much higher levels of branching are to be expected when the temperature is increased.<sup>43</sup> Even higher values, up to nearly 5 %, were reported for 70 °C<sup>25</sup> at lower monomer concentrations, which favors  $\beta$ -scission to some degree. Most other literature data deal with lower conversion systems and the numbers are thus hardly comparable. Nevertheless, most other literature data suggest much higher branching levels than what is identified for these 1-octanethiol mediated samples.

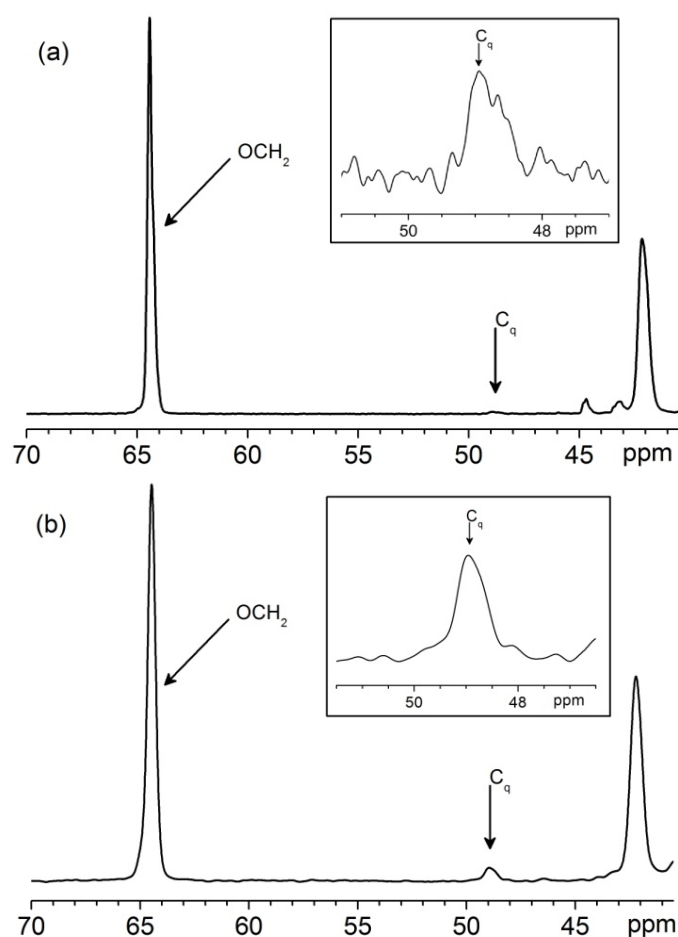
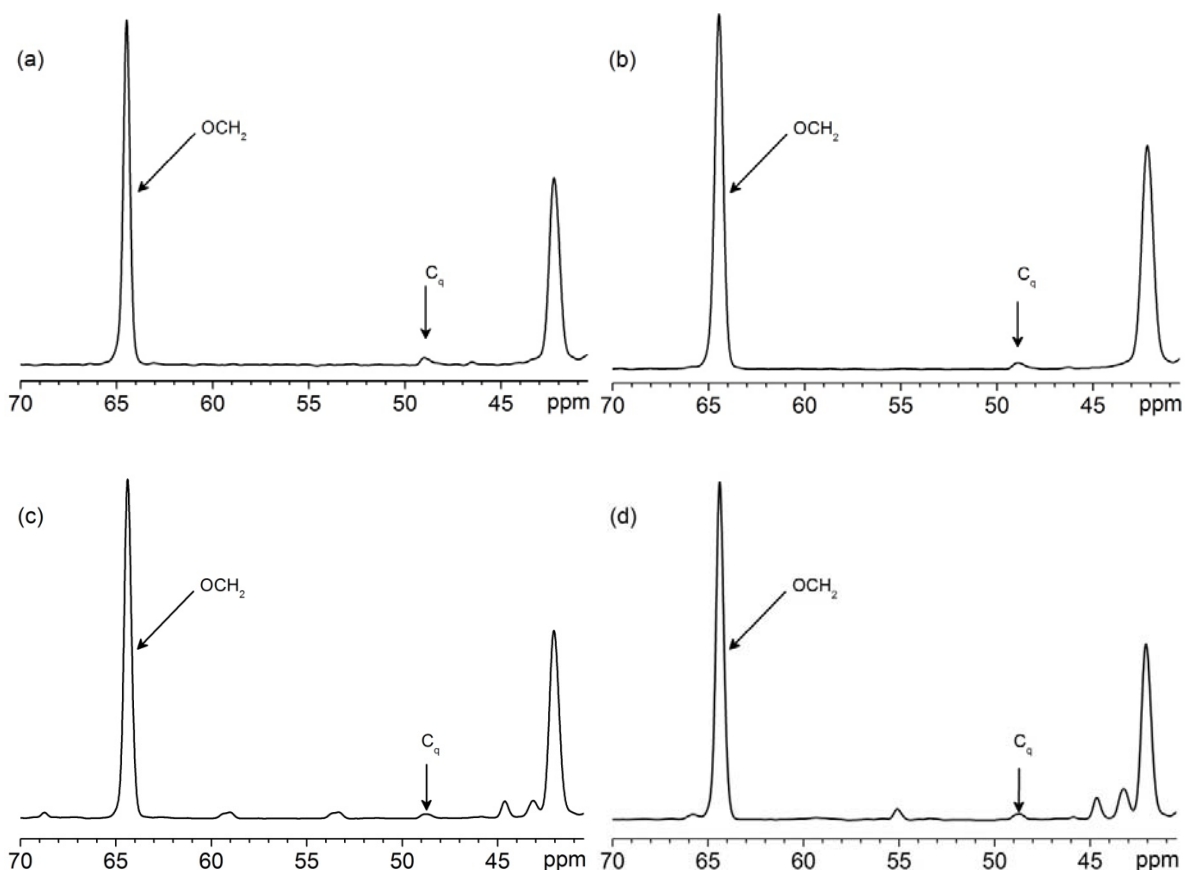


Figure 4-7: Melt-state <sup>13</sup>C SPE-MAS NMR spectra recorded at  $T_g+150$  °C for poly(*n*-butyl acrylate) samples synthesized at 60 °C with  $C_{AIBN} = 5 \cdot 10^{-3} \text{ mol} \cdot \text{L}^{-1}$  and  $C_{SH} = 0.4 \text{ mol} \cdot \text{L}^{-1}$  (a) and at 140 °C without thiol and  $C_{AIBN} = 5 \cdot 10^{-3} \text{ mol} \cdot \text{L}^{-1}$  (b). Both polymerizations were carried out to almost full conversion. For an assignment of the relevant peaks in the spectrum see Table 4-4. The relevant peak of the quaternary backbone peak is marked C<sub>q</sub>.

Table 4-4: Complete  $^{13}\text{C}$  chemical shifts assignment for  $^{13}\text{C}$  NMR spectra of poly(*n*-butyl acrylates) (PBA) synthesized with and without 1-octanethiol (OctSH).<sup>25</sup>

$\delta$ (ppm)	Assignment
14	$\text{CH}_3$ of side chain of PBA, $\text{CH}_3$ of OctS-
20	$\text{CH}_2\text{-CH}_3$ of side chain of PBA
23	$\text{CH}_2\text{-CH}_3$ of OctS-
31	$\text{CH}_2\text{-CH}_2\text{-CH}_3$ of side chain of PBA
25-36	other $\text{CH}_2$ of OctS-
36	$\text{CH}_2$ of main chain of PBA
42	$\text{CH}$ of main chain of PBA
49	$\text{C}_q$ of main chain of PBA
64	$\text{O-CH}_2$ of side chain of PBA
130	$\text{C=C}$ of PBA or residual monomer
172.1, 174.4	$\text{C=O}$ of PBA

Figure 4-8: Melt-state  $^{13}\text{C}$  SPE-MAS NMR spectra recorded at  $T_g + 150$  °C for samples synthesized at 60 °C without thiol (a), at 100 °C without thiol (b), at 100 °C with thiol (c), at 140 °C with thiol (d).

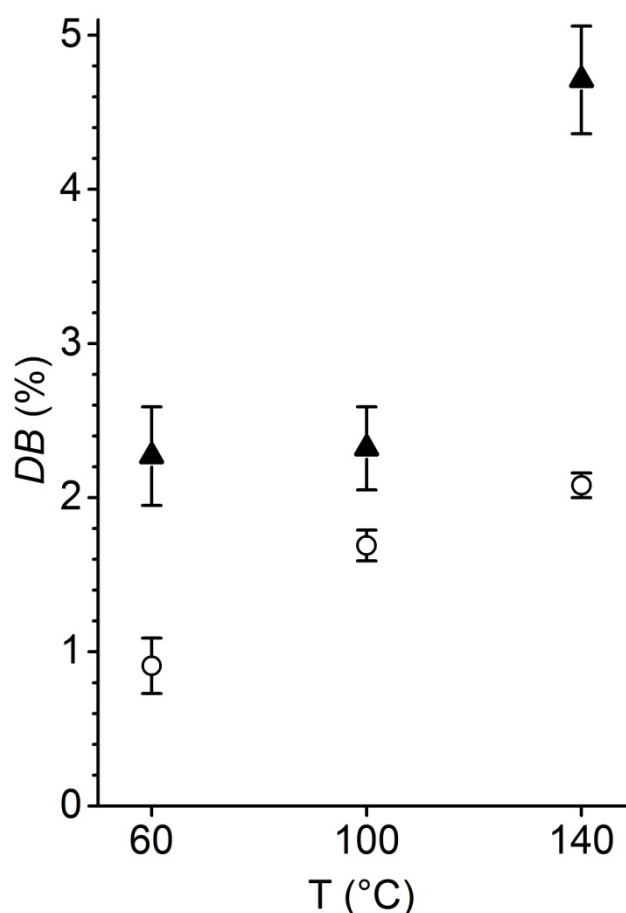


Figure 4-9: Degree of branching (in percent of monomers units) as a function of the reaction temperature for poly(*n*-butyl acrylates) polymerized in bulk in the absence (solid triangles) or presence (empty circles) of  $0.4 \text{ mol}\cdot\text{L}^{-1}$  1-octanethiol as transfer agent. The error bars given for each measurement were calculated according to Equation 4-3.

The degree of branching values measured for all samples are shown in Figure 4-9 with their precision. Figure 4-9 clearly indicates that the degrees of branching obtained in the thiol-containing systems are significantly lower than those obtained in the conventional system for all temperatures. The ‘patching’ effect of tertiary mid-chain radicals by the thiol can thus be confirmed to be operational. In addition, the degree of branching significantly increases with increasing temperature for both the thiol and non-thiol containing systems. Such an observation is explained by the increased frequency of the reactions that lead to the formation of MCRs, i.e. inter-molecular chain transfer as well as random intra-molecular transfer and backbiting. Typical activation energies for the rate coefficients governing these reactions may be 20 to 25  $\text{kJ}\cdot\text{mol}^{-1}$  higher than that of propagation.<sup>51</sup> Concomitantly, the

transfer rate of the thiol onto the MCR may be hypothesized to be similar to the one of propagation. Therefore, although the thiol is capable of reducing the amount of branching significantly, its effectiveness decreases with increasing temperature.

Looking at this system from a different perspective, if the thiol repairs the midchain radical functionality, it follows that decreasing the thiol concentration should then increase the amount of side products as the absolute rate of transfer is reduced. Indeed, when the thiol concentration is reduced from 0.4 to 0.1 mol·L<sup>-1</sup>, the number average molecular weight increases from 2200 to 4500 g·mol<sup>-1</sup>. At the same time, as seen from mass spectra depicted in Figure 4-10, an increase in  $\beta$ -scission products as well as termination product a is seen.

Table 4-5: Glass transition temperature ( $T_g$ ) and degrees of branching ( $DB$ ) for the thiol (0.4 mol·L<sup>-1</sup>) and non-thiol containing poly(*n*-butyl acrylates) synthesized at various temperatures.

$T / ^\circ\text{C}$	$c_{\text{thiol}} / \text{mol}\cdot\text{L}^{-1}$	$T_g / ^\circ\text{C}$	SNR	DB / %
60	0	-46	8.99	2.27 ± 0.32
100	0	-54	10.4	2.32 ± 0.27
140	0	-51	15.1	4.71 ± 0.35
60	0.4	-71	6.99	0.91 ± 0.18
100	0.4	-73	18.6	1.69 ± 0.10
140	0.4	-72	24.7	2.08 ± 0.08

However, it should be noted that although the total amount of side products increases, this total amount is still much lower than in the sample taken at 140 °C. This shows that even at reduced thiol concentrations, the patching effect on secondary MCR reactions is still considerable. Again, no disproportionation product can be identified in the spectrum. In addition to the peaks identified above in the spectra shown in Figure 4-6, product peaks corresponding to the structures  $b'$  and  $\beta_{\text{AIBN}}^{\text{II}}$  (see Scheme 4-2) appear. The presence of  $b'$  is a direct consequence of the increased radical concentration at 80 °C compared to 60 °C. At the same time, as significant amounts of  $b'$  are present in the system, the  $\beta$ -scission product carrying an AIBN endgroup instead of a thiol group is also formed. However, one more peak appears at 1521.9 Da that is not present in the system at the highest thiol concentration. Unfortunately no structure could be assigned to this  $m/z$  ratio, even considering macromonomer insertion into other chains which is assumed to occur in some butyl acrylate

polymerizations.<sup>4,43</sup> Samples obtained with even lower thiol concentrations cannot be analyzed at this time as the MWD shifts significantly to larger molecular weight and not enough material is available for ionization in the ESI mass range to produce clear spectra. The same effect is already evident in the present data, because the absolute abundance is much lower in the ESI-MS mass range for samples containing lower thiol concentrations. Multiple charged species appear more abundantly than they actually are as they reflect higher molecular weight species. Comparison of the amounts of single-charged species nevertheless remains valid because  $\beta$ -scission and ‘normal’ transfer should in principle occur to similar extents irrespective of chain length.

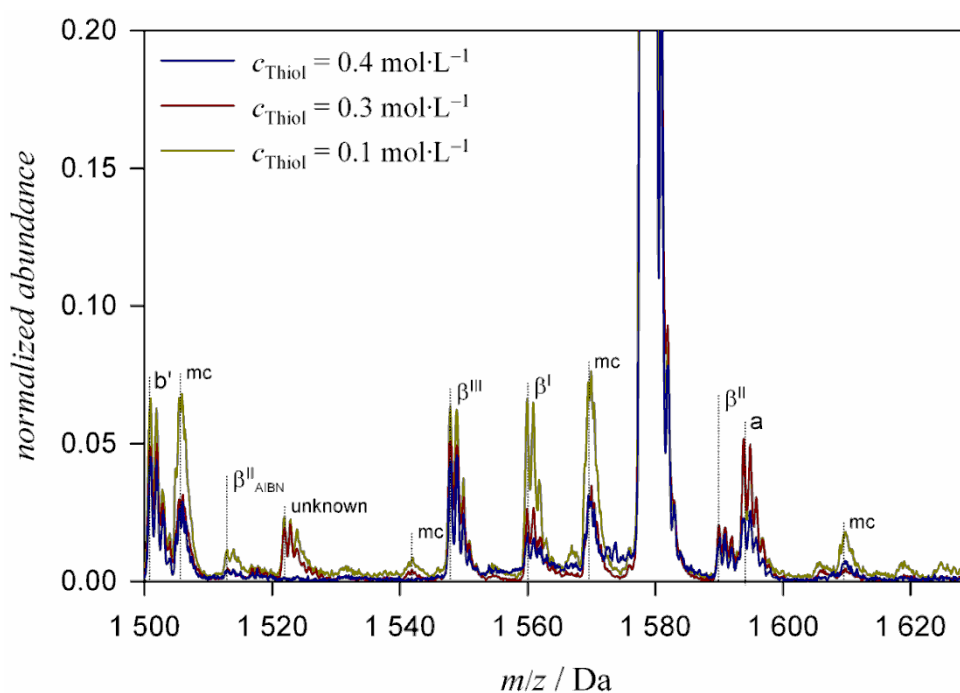


Figure 4-10: ESI-MS spectra of poly(*n*-BA) obtained from bulk polymerization at 80 °C in the presence of 1-octanethiol at the indicated concentrations. Polymerization was initiated by  $5\cdot 10^{-3} \text{ mol}\cdot\text{L}^{-1}$  AIBN. The spectra are normalized on the main product peak at 1578.1 Da such that the amounts of side products formed are able to be compared from one sample to the next.





exactly 0.5  $m/z$ . Formation of these multiply charged peaks is a result of the high molecular weight of this sample. Schemes 4-1 and 2-7 present the structures of these species. Without the effects of the transfer agent, the main species ( $\beta^I$ ) is formed by  $\beta$ -scission and comprises the vast majority of product seen, i.e. 60 % of the total product.  $\beta$ -scission products  $\beta^{I-III}$  make up a total of 78 % of the whole sample. It is not possible to determine how much of the SPR species originates from  $\beta$ -scission as it is not known how many chains undergo backbiting and subsequently how many of those MCRs undergo  $\beta$ -scission to yield the SPR and  $\beta^I$  species. Furthermore, *intramolecular* transfer is an isobaric transformation, so it is fundamentally not possible to determine how many backbiting steps one growing chain has already undergone in its lifetime.

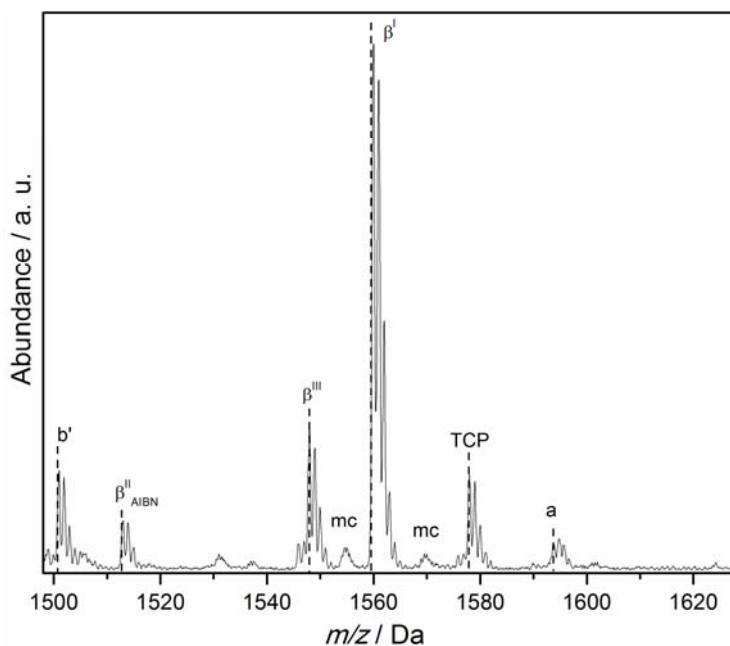


Figure 4-13: One repeat unit in the ESI-MS spectrum of polymer obtained from bulk polymerization of butyl acrylate at 100 °C in the presence of  $5 \cdot 10^{-3} \text{ mol} \cdot \text{L}^{-1}$  1-octanethiol initiated by  $5 \cdot 10^{-3} \text{ mol} \cdot \text{L}^{-1}$  AIBN. This is a repeat unit in the range 1498-1628 Da with assigned species. The dashed lines represent the  $m/z_{\text{theoretical}}$  and mc denotes multiply charged peaks. Please refer to Schemes 2-7 and 4-1 for structures of the individual species depicted in this figure.

Comparing Figure 4-11 and Figure 4-13, it can be seen that at lower concentrations of 1-octanethiol, smaller amounts of TCP are identified in the mass spectrum. At low concentrations of thiol and relatively high temperatures, e.g.  $c_{\text{thiol}} < 0.05 \text{ mol}\cdot\text{L}^{-1}$  and  $T > 80 \text{ }^\circ\text{C}$ ,  $\beta$ -scission reactions dominate transfer and conventional termination.  $\beta$ -scission products constitute 78 % of the whole product spectrum depicted in Figure 4-10. In Figure 4.6, where  $0.4 \text{ mol}\cdot\text{L}^{-1}$  thiol was employed, the TCP product accounts for 81 % of the product while the  $\beta$ -scission products account for only 11 %. This is a trend seen in all samples whereby higher concentrations of 1-octanethiol produce higher amounts of TCP in the final polymer. Generally, small amounts of termination *via* combination product a (see Scheme 2-7 for structure) are found in all samples.

#### 4.5 Determination of the Transfer Constant of 1-Octanethiol Towards *n*-BA

Thiols are known to be very good transfer agents, but nevertheless in the course of the current thesis, the transfer constant of 1-octanethiol was determined according to the Mayo Method, outlined in section 2.2.4.  $C_{\text{tr}}$  was found to be 1.05.

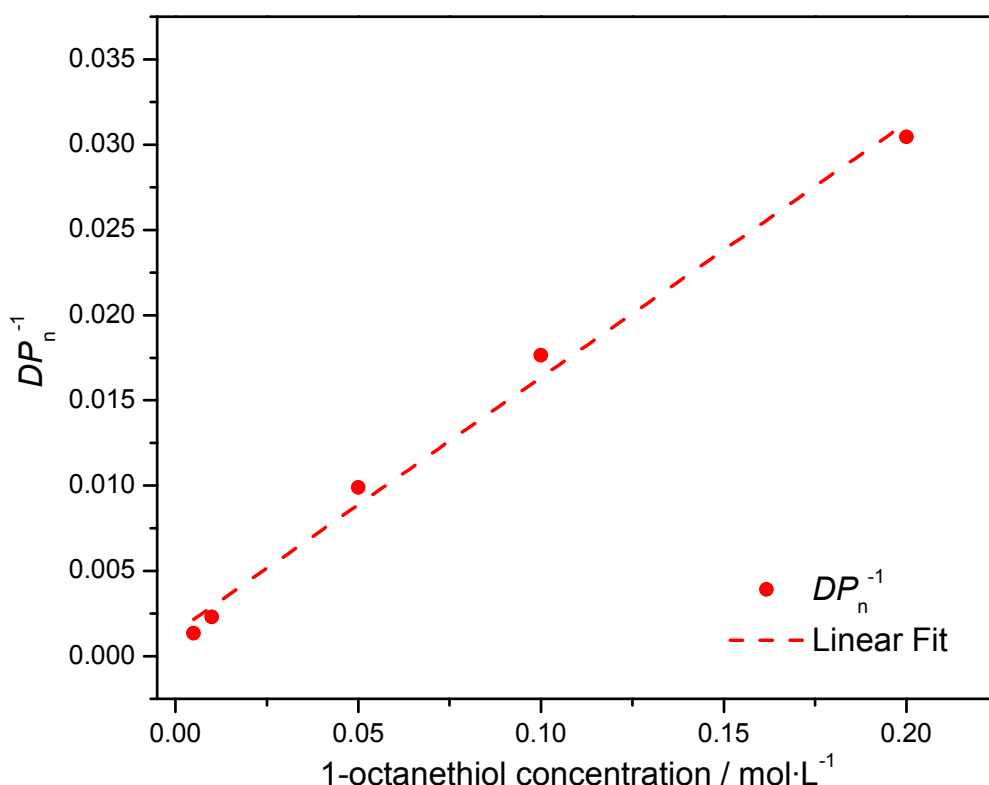


Figure 4-14: Variation of  $DP_n$  with concentration of 1-octanethiol concentration. The transfer constant of 1-octanethiol was determined from the slope of the graph. The data displayed in this graph is tabulated in Table 4-6.

Table 4-6:  $M_n$  and  $DP_n^{-1}$  information for poly(*n*-BA) synthesized with the specified amounts of 1-octanethiol.

[1-octanethiol] / mol·L <sup>-1</sup>	$M_n$ / g·mol <sup>-1</sup>	$DP_n^{-1}$
0.2	4 209	0.0305
0.1	7 264	0.0176
0.05	12 969	0.0099
0.01	55 945	0.0023
0.005	95 353	0.0013

#### 4.6 Quantitative Evaluation of the Poly(*n*-BA) Product Spectrum via ESI-MS

It has now been established that employing 1-octanethiol as a CTA in the thermal polymerization of *n*-BA does have an effect on the product spectrum and these effects have been globally discussed. In what follows, a finer quantitative evaluation of the effects of varying thiol concentration and the accompanying changes in the mole fractions of the various species will be discussed.

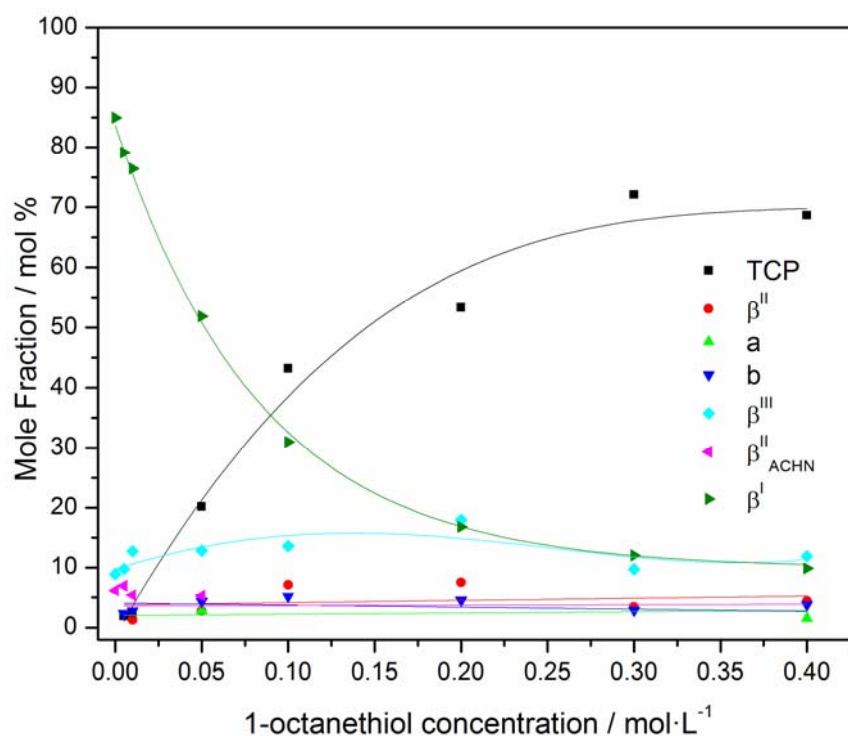


Figure 4-15: Change in mole fraction of individual polymer species from *n*-BA polymerizations in experiments conducted at 140 °C at varying concentrations of 1-octanethiol. Please refer to Schemes 2-7 and 4-1 for structures of the individual species depicted in this figure.

Figure 4-15 depicts a graph of the mole fraction of all species found as a function of the concentration of 1-octanethiol for samples prepared at 140 °C. Butyl acrylate boils at 144 °C at ambient pressure so 140 °C is the highest temperature studied. This temperature was also chosen because  $\beta$ -scission occurs profusely under these conditions and is thus the best way to assess the effect of adding 1-octanethiol on product constituents. From Figure 4-15 the variation of the proportion, and hence mole fraction, of the different species as the concentration of 1-octanethiol is changed can be seen.

The graph emphasizes trends and highlights the species most sensitive to increasing thiol concentration. Figure 4-15 undoubtedly reveals that at high temperatures, TCP and  $\beta^1$  show the largest variation in mole fraction and are therefore the main products of interest with respect to the thiol concentration variation. In addition, all other species do not show significant variation in mole fractions with increasing thiol concentration. The formation of species  $\beta^1$  is highly sensitive to the thiol concentration. Increasing thiol concentration from 0.01 to 0.05 mol·L<sup>-1</sup> results in the TCP proportions rising from 2 % to 20 %, and the  $\beta^1$  proportions decreasing from 76 % to 52 %. At a concentration of 0.4 mol·L<sup>-1</sup>,  $\beta^1$  becomes a minor product, constituting 10 % of the product spectrum. The decrease of TCP with decreasing thiol concentration is an obvious effect of having less chain transfer activity during polymerization.

Concomitantly, the relative amounts of the  $\beta^1$  species increase as  $\beta$ -scission is predominant in the absence of transfer, as mentioned above. In principle, similar amounts of the individual  $\beta$ -scission products are expected as the scission is not favored to occur to either side of the MCR. The much higher concentrations of  $\beta^1$  that are found can be explained by a complex set of equilibria between the scission products and the midchain radicals as  $\beta$ -scission is in principle a reversible reaction. Note that  $\beta^1$  is the unsaturated polymer carrying only a proton endgroup on the saturated chain end. As demonstrated in Chapter 6, such equilibria favor the formation of  $\beta^1$  due to the additional driving force of the backbiting reaction.<sup>52</sup> In fact, in the high-temperature initiator-free solution polymerization of butyl acrylate, where polymerization occurs under conditions of a very low radical flux, solely  $\beta^1$  can be found in the product. This observation fits to the experimental finding of almost equal amounts of all scission products in the case of high thiol content, as the ‘patching’ of the MCR *via* proton transfer from the thiol interrupts such equilibria. At lower thiol

concentrations, disparate amounts of  $\beta^I$  to  $\beta^{II}$  and  $\beta^{III}$  are identified under all conditions investigated.

Trends for minor species are difficult to discern, so the following discussion on changing reaction temperature will focus on the species  $\beta^I$  and TCP as these show the largest variation in relative product concentrations. A large data basis was obtained for this study but for the sake of clarity not all data are displayed and discussed in all detail. However, all important kinetic effects are explained on selected representative data sets while the full data have been tabulated in Table 4-7 to Table 4-11. All listed polymer samples for a large number of different reaction conditions were obtained and subjected to MS analysis.

Table 4-7: Polymer product composition and  $M_n$  data derived by integration for all samples prepared at 60 °C.  $M_n$  is provided in  $\text{g}\cdot\text{mol}^{-1}$ .

$T / ^\circ\text{C}$	$c_{\text{thiol}} / \text{mol}\cdot\text{L}^{-1}$	TCP	$b'$	$\beta^{II}_{\text{AIBN}}$	$\beta^{II}$	$\beta^I$	$\beta^{II}$	a	Total	$M_n$
60	0	0.000	0.170	0.118	0.147	0.564	0.000	0.000	1	69680
60	0.005	0.048	0.132	0.067	0.180	0.532	0.000	0.042	1	46130
60	0.01	0.107	0.151	0.084	0.173	0.486	0.000	0.000	1	34580
60	0.05	0.446	0.100	0.025	0.091	0.226	0.016	0.095	1	10180
60	0.2	0.510	0.076	0.046	0.096	0.211	0.061	0.000	1	4630
60	0.3	0.827	0.046	0.000	0.048	0.079	0.000	0.000	1	2860
60	0.4	0.973	0.000	0.000	0.000	0.000	0.000	0.027	1	1470

Table 4-8: Polymer product composition and  $M_n$  data derived by integration for all samples prepared at 80 °C.  $M_n$  is provided in  $\text{g}\cdot\text{mol}^{-1}$ .

$T / ^\circ\text{C}$	$c_{\text{thiol}} / \text{mol}\cdot\text{L}^{-1}$	TCP	$b'$	$\beta^{II}_{\text{AIBN}}$	$\beta^{III}$	$\beta^I$	$\beta^{II}$	a	Total	$M_n$
80	0	0.000	0.000	0.000	0.125	0.875	0.000	0.000	1	80210
80	0.005	0.104	0.101	0.065	0.136	0.520	0.019	0.055	1	58010
80	0.01	0.058	0.107	0.072	0.130	0.548	0.016	0.068	1	20440
80	0.05	0.416	0.092	0.015	0.101	0.265	0.024	0.086	1	11250
80	0.1	0.760	0.056	0.000	0.054	0.068	0.016	0.046	1	9480
80	0.2M	0.756	0.060	0.000	0.064	0.054	0.025	0.041	1	4370
80	0.3M	0.809	0.042	0.000	0.045	0.037	0.019	0.047	1	3440
80	0.4M	0.830	0.043	0.000	0.045	0.036	0.017	0.029	1	2750

Table 4-9: Polymer product composition and  $M_n$  data derived by integration for all samples prepared at 100 °C.  $M_n$  is provided in  $\text{g}\cdot\text{mol}^{-1}$ .

$T / ^\circ\text{C}$	$c_{\text{thiol}} / \text{mol}\cdot\text{L}^{-1}$	TCP	$b'$	$\beta^{\text{II}}_{\text{AIBN}}$	$\beta^{\text{III}}$	$\beta^{\text{I}}$	$\beta^{\text{II}}$	a	Total	$M_n$
100	0	0.000	0.114	0.079	0.162	0.645	0.000	0.000	1	86570
100	0.005	0.080	0.098	0.051	0.118	0.596	0.013	0.044	1	57040
100	0.01	0.059	0.101	0.050	0.109	0.627	0.022	0.033	1	22010
100	0.05	0.119	0.042	0.058	0.139	0.596	0.047	0.000	1	11030
100	0.2	0.209	0.047	0.05	0.143	0.488	0.064	0.000	1	4760
100	0.3	0.402	0.107	0.000	0.111	0.249	0.031	0.099	1	3490
100	0.4	0.805	0.049	0.000	0.055	0.042	0.016	0.032	1	2450

Table 4-10: Polymer product composition and  $M_n$  data derived by integration for all samples prepared at 140 °C.  $M_n$  is provided in  $\text{g}\cdot\text{mol}^{-1}$ .

$T / ^\circ\text{C}$	$c_{\text{thiol}} / \text{mol}\cdot\text{L}^{-1}$	TCP	b	$\beta^{\text{II}}_{\text{ACHN}}$	$\beta^{\text{III}}$	$\beta^{\text{I}}$	$\beta^{\text{II}}$	a	Total	$M_n$
140	0	0.000	0.000	0.062	0.089	0.849	0.000	0.000	1	44720
140	0.005	0.019	0.023	0.070	0.097	0.791	0.000	0.000	1	18500
140	0.01	0.021	0.027	0.053	0.126	0.760	0.013	0.000	1	12340
140	0.05	0.201	0.043	0.053	0.128	0.519	0.027	0.028	1	7780
140	0.1	0.432	0.051	0.000	0.136	0.310	0.071	0.000	1	6200
140	0.2	0.533	0.045	0.000	0.179	0.168	0.075	0.000	1	3830
140	0.3	0.721	0.028	0.000	0.097	0.120	0.034	0.000	1	2450

Table 4-11: Polymer product composition and  $M_n$  data derived by integration for all other samples prepared.  $M_n$  is provided in  $\text{g}\cdot\text{mol}^{-1}$ .

$T / ^\circ\text{C}$	$c_{\text{thiol}} / \text{mol}\cdot\text{L}^{-1}$	TCP	b or $b'$	$\beta^{\text{II}}_{\text{ACHN}}$ or $\beta^{\text{II}}_{\text{AIBN}}$	$\beta^{\text{III}}$	$\beta^{\text{I}}$	$\beta^{\text{II}}$	a	Total	$M_n$
70	0.4	0.963	0.000	0.000	0.000	0.000	0.000	0.037	1	2120
90	0.4	0.813	0.048	0.000	0.051	0.042	0.017	0.029	1	2700
120	0.4	0.765	0.032	0.000	0.083	0.072	0.021	0.028	1	2520

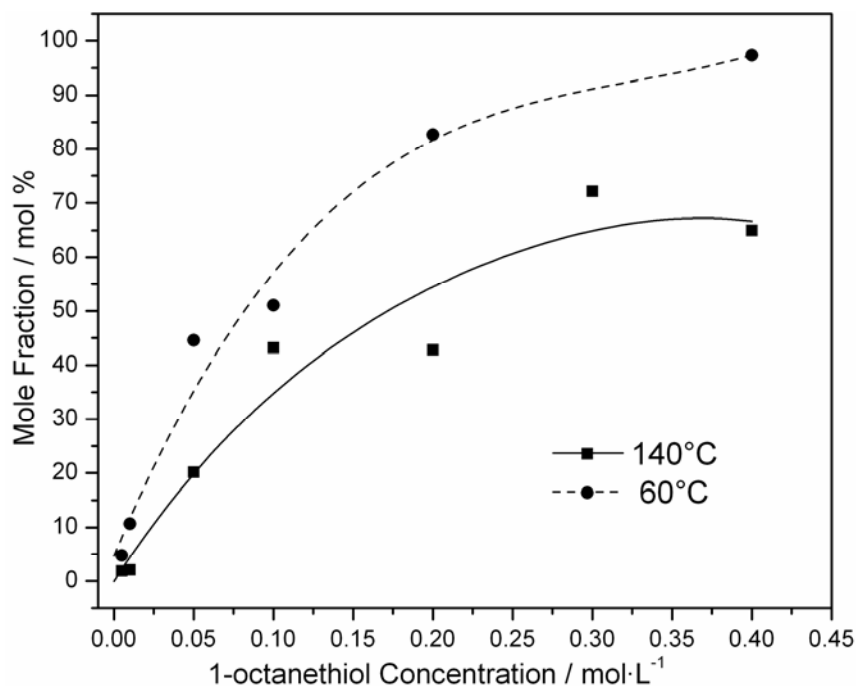


Figure 4-16: Mole fraction of TCP product formed at various concentrations of 1-octanethiol at 140 °C and at 60 °C. At 60 °C, AIBN was used as initiator, whereas at 140 °C ACHN was used. TCP and  $\beta^1$  structures can be seen in Schemes 2-7 and 4-1.

Figure 4-16 demonstrates how the mole fraction of TCP product changes when increasing amounts of 1-octanethiol are added to the reaction mixture at different temperatures. As more thiol is added, more TCP product is found in the final polymer since the thiol is a highly effective chain transfer agent. Furthermore, it can be seen that at 140 °C less TCP is found when compared to the respective samples containing the same concentrations of thiol at 60 °C.

Figure 4-17 shows the mole fractions of the most abundant  $\beta$ -scission species  $\beta^1$  at 60 °C, and at 140 °C. Accordingly, less scission products are found at high thiol content at lower temperatures. About 10 % of the final product consists of  $\beta^1$  at the highest thiol concentration at 140 °C, whereas almost none can be found at 60 °C. As  $\beta$ -scission reactions are predominant at higher temperatures, such an observation comes as no surprise and shows that the CTA cannot prevent all side reactions from occurring at higher temperatures even though proton transfer onto the MCRs is still highly effective as pointed out previously.

As can be expected due to backbiting and  $\beta$ -scission, significantly more  $\beta^1$  product is formed at 140 °C (85 %), compared to the respective samples at 60 °C (56 %).

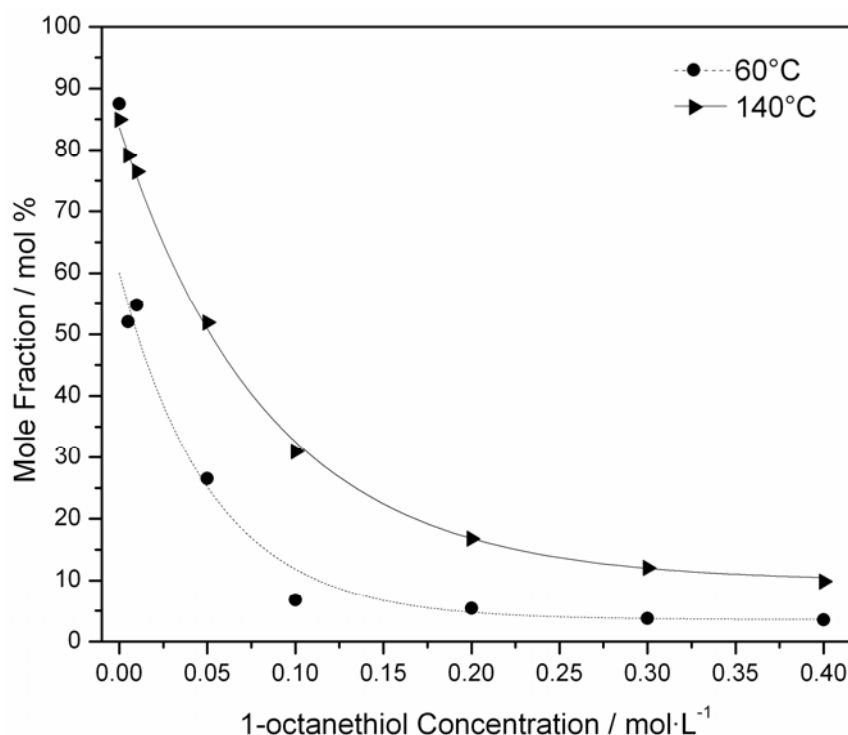


Figure 4-17: Mole fraction of  $\beta^1$  product formed at various concentrations of 1-octanethiol at 140 °C and at 60 °C. At 60 °C, AIBN was used as initiator, whereas at 140 °C ACHN was used. TCP and  $\beta^1$  structures can be seen in Schemes 2-7 and 4-1.

In addition, it can be observed that as thiol concentration increases, an almost exponential decrease is seen in the amount of  $\beta^1$ . TCP is the main species seen at thiol concentrations above 0.05 mol·L<sup>-1</sup>, irrespective of the temperature at which the sample was prepared; however its mole fraction increases with increasing thiol concentration. This is most evident when looking at the TCP peaks in Figures 4-11 and 4-13. Conversely,  $\beta^1$  is the main product seen at all thiol concentrations below 0.05 mol·L<sup>-1</sup>, irrespective of synthesis temperature. In this case, the mole fraction of  $\beta^1$  increases with *decreasing* thiol concentration indicating that  $\beta$ -scission plays an important role even at moderate polymerization temperatures. Lastly, it is of interest to examine the effect of temperature on the formation of various species. It must be noted that two initiators were used as no suitable initiator with reasonable half-lives for conducting experiments in the range between 60°C and 140 °C is

available. For this reason, AIBN was used as initiator for all experiments up to and including 100 °C. Above 100 °C, 1,1-azobis(cyclohexanecarbonitrile) was used.

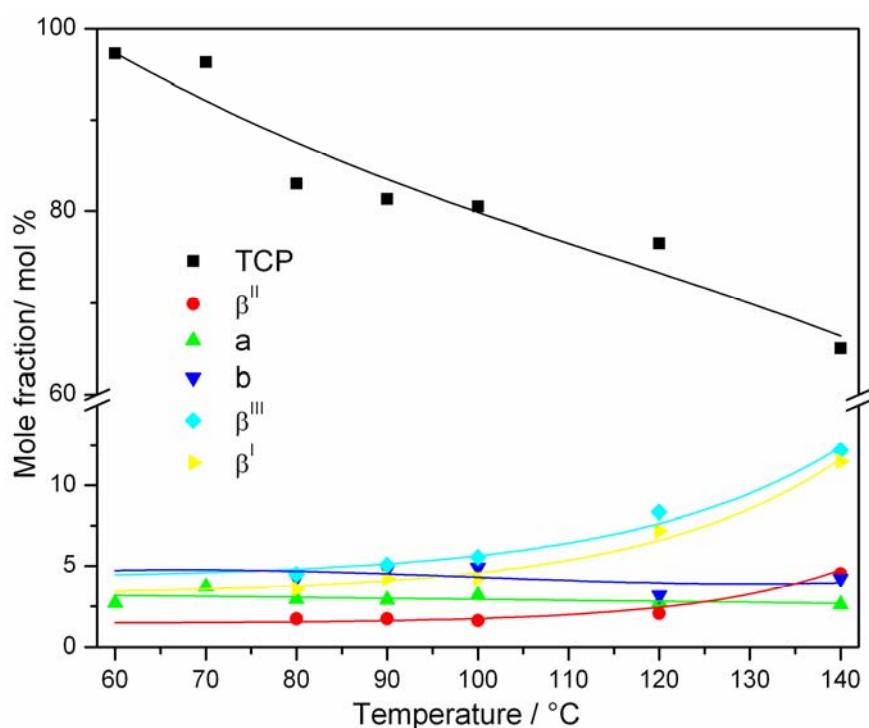


Figure 4-18: Figure shows the variation in proportion of species present over a range of temperatures when all samples contain  $0.4 \text{ mol}\cdot\text{L}^{-1}$  1-octanethiol. Note the break in the vertical axis. All chemical structures of species present can be seen in Schemes 2-7 and 4-1.

Figure 4-18 presents data illustrating the change in product composition with temperature at a fixed thiol concentration of  $0.4 \text{ mol}\cdot\text{L}^{-1}$ . Making note of the break in the vertical axis of Figure 4-18 clarifies that the apparently large increase of  $\beta^{\text{I}}$  and  $\beta^{\text{III}}$  is still comparatively small when compared to changes in the TCP product. The proportion of TCP decreases from 97 % to 67 % as temperature is increased. Such a shift with temperature is caused by increasing  $\beta$ -scission reactions as was already identified in the context of Figure 4-16 and Figure 4-17. In the present case the minor products  $\beta^{\text{I}}$  and  $\beta^{\text{III}}$  double in amount as the temperature is increased from 100 °C to 140 °C due to the overall increased importance of  $\beta$ -scission at higher temperatures. Closer inspection of Figure 4-18 shows that there is 2 % to 5 % more  $\beta^{\text{I}}$  than  $\beta^{\text{II}}$  according to general dominance of  $\beta^{\text{I}}$ .

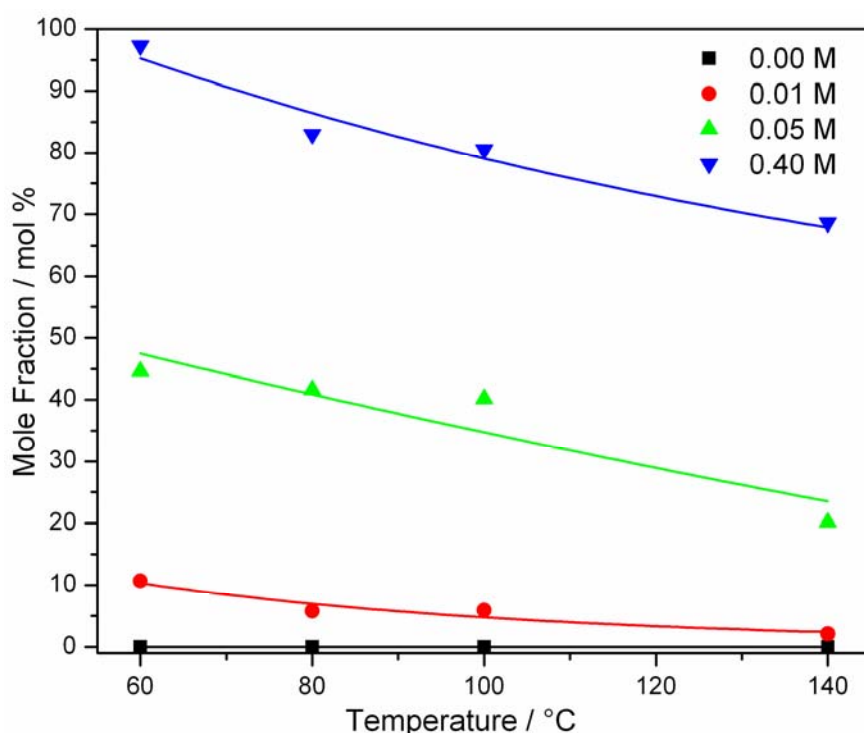


Figure 4-19: Figure represents proportions of the main TCP product at varying temperatures and varying concentrations of 1-octanethiol. The chemical structures of species TCP can be seen in Scheme 2-7.

Figure 4-19 shows the proportions of the main TCP product from 60 °C to 140 °C at four incremental concentrations of 1-octanethiol, varying from 0 to 0.4 mol·L<sup>-1</sup>. It is clear that irrespective of thiol concentration the proportion of TCP product decreases as the temperature increases. This trend is again readily explained as increasing amounts of  $\beta$ -scission products are formed with increasing temperature. At 0 mol·L<sup>-1</sup> concentration of thiol, obviously no TCP product is found.

Figure 4-20 presents the amounts of  $\beta^I$  formed at varying concentrations of thiol. It is not surprising to see the trend of decreasing overall  $\beta^I$  amounts with increasing thiol concentrations. Examination across the temperature range shows an increase of  $\beta^I$  with increasing temperature, again an observation that can be hypothesized by looking at Figure 4-18, as TCP and  $\beta^I$  are the complementary major products.

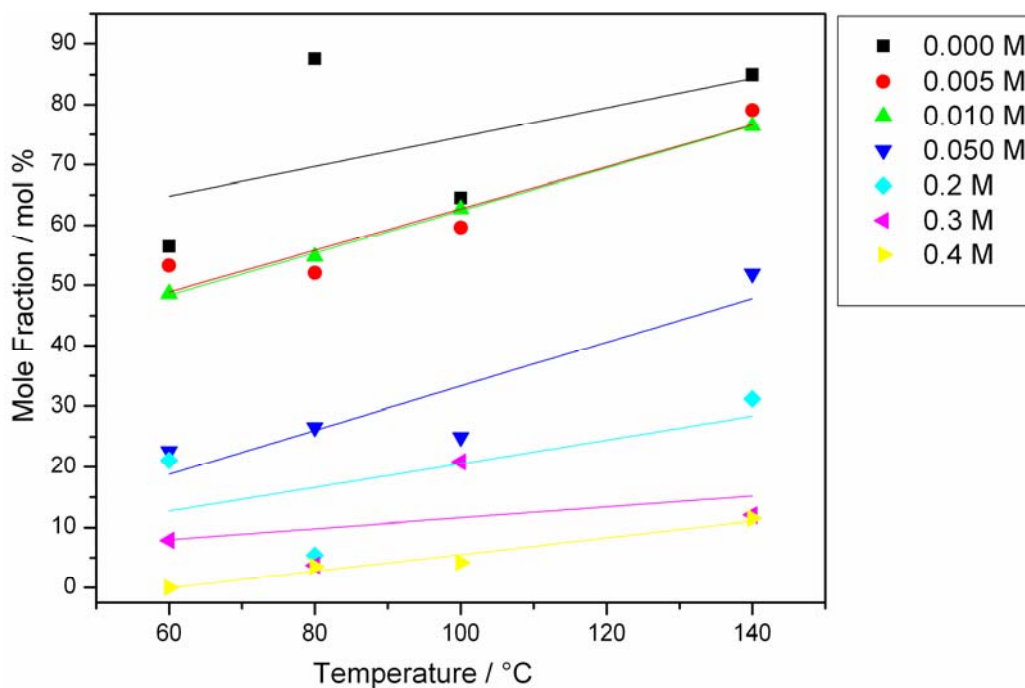


Figure 4-20: Mole fractions of the product  $\beta^I$  at varying temperatures and varying concentrations of 1-octanethiol.

#### 4.6.1 Survey of Data and Consideration of Less Abundant Side Products

Chain transfer agent concentration and temperature are counteracting forces when it comes to controlling the amounts of side products formed *via*  $\beta$ -scission. On the one hand, increasing the reaction temperature creates a greater variety of different types of species, as well as increasing the amount of  $\beta$ -scission products formed, while on the other hand increasing the concentration of 1-octanethiol added to reaction mixtures leads to increasing amounts of TCP product formation and suppresses the formation of  $\beta$ -scission products. The products found are TCP (if thiol is present), conventional termination products a, b or b', and  $\beta$ -scission products  $\beta^I$ ,  $\beta^{II}$ ,  $\beta^{III}$ , as well as  $\beta^{II}_{AIBN}$  or  $\beta^{II}_{ACHN}$  at higher temperatures. The composition of a particular polymer sample depends on a combination of the effects of thiol concentration and reaction temperature. The two parameters determine which products are found and in what concentrations. However, information regarding general trends can be gleaned from the samples prepared at the extremes of the selected conditions. At low temperature and high concentration of thiol, i.e. the sample prepared at 60 °C with addition of 0.4 mol·L<sup>-1</sup> 1-octanethiol, 97 % of polymer formed is the TCP species, with the remaining 3 % being species a. At high temperature (140 °C) and high concentration of thiol

(0.4 mol·L<sup>-1</sup>), only 69 % of the total product spectrum is TCP product. Species a (1 %), b (4 %), β<sup>I</sup> (10 %), β<sup>II</sup> (4 %), and β<sup>III</sup> (12 %) are also found, and these constitute the remaining proportions in the sample. At 0.005 mol·L<sup>-1</sup> thiol concentration and 140 °C, TCP is a mere 2 % of the total, with β<sup>I</sup> being the major product at 79 %, β<sup>II</sup><sub>ACHN</sub> (7 %), with β<sup>III</sup> (10 %) and b (2 %) being the remaining constituents. The last extreme is at low thiol concentration (0.005 mol·L<sup>-1</sup>) and low temperature (60 °C). This sample contains 5 % TCP, 4 % a, 13 % b', 7 % β<sup>II</sup><sub>AIBN</sub>, 18 % β<sup>III</sup> and 53 % β<sup>I</sup>. Samples with 0 mol·L<sup>-1</sup> thiol do not contain any TCP product, rather they contain amounts of b' (17 %), β<sup>II</sup><sub>AIBN</sub> (12 %), β<sup>III</sup> (15 %) and β<sup>I</sup> (56 %) in the case of low temperature, i.e. 60 °C; and β<sup>II</sup><sub>ACHN</sub> (6 %), β<sup>III</sup> (9 %) and β<sup>I</sup> (85 %) at high temperature, i.e. 140 °C.

#### 4.7 Summary of Results

Electrospray ionization mass spectrometry allows detailed mapping of the product spectrum in acrylate polymerization giving access to mechanistic information that are complementary to the molecular weight distribution and branching level data obtained by size exclusion chromatography and <sup>13</sup>C-NMR, respectively.

The main product peak found in the ESI-MS spectra obtained from polymer made by 1-octanethiol mediated polymerization at higher thiol concentrations is the expected transfer to thiol product, TCP, with small amounts of termination products also present. A complete assignment of the MCR derived products obtained *via* ESI-MS of various butyl acrylate polymerizations was also conducted as part of this study. From the myriad data provided by the initial qualitative analysis, a quantitative analysis was deemed pertinent to further explore this acrylate and CTA system. Thiol transfer systems are well known<sup>53-61</sup> and a quantitative assessment of gathered data provides valuable information on the effects of 1-octanethiol addition to a butyl acrylate thermal polymerizing system. The chain transfer agent is able to patch the midchain radical by transferring its proton to the backbone radical, so mostly unbranched polymer chains are formed and the secondary reactions, such as β-scission are (partially) suppressed, providing access to more uniform poly(*n*-BA) than would be obtained under the same conditions by conventional polymerization. The novel quantitative integration method identifies clear trends for all species with variation of temperature and thiol concentration and demonstrates the robustness of the integration method applied when issues of ionization are dealt with.

At lower thiol concentrations, predominant species are the products of  $\beta$ -scission reactions, even at a moderate reaction temperature of 60 °C. At all thiol concentrations the expected  $\beta$ -scission products are identified with  $\beta^1$  being by far the most abundant product under all conditions. This disparity is explained by equilibration of the scission products with the midchain radicals. At elevated temperatures,  $\beta$ -scission products are generally more prevalent, and between the extremes (from 60 °C to 140 °C and 0 to 0.4 mol·L<sup>-1</sup> chain transfer agent) a comprehensive exploration of the product spectra is conducted, providing a detailed quantitative examination of the influence of temperature and presence of varying amounts of CTA 1-octanethiol in thermal butyl acrylate polymerization. This work shows that ESI-MS spectra can indeed be integrated in a quantitative fashion when the ionization potential of all present species are similar. Such an approach can not only be applied to the present line of work, but has potential for quantitative analysis of other polymer product spectra and therefore represents an important advance for ESI-MS analysis in general.

Degrees of branching for selected samples were measured with <sup>13</sup>C melt-state NMR in poly(*n*-butyl acrylates) synthesized in both the presence and absence of 1-octanethiol at various temperatures, and their precision calculated. A significant decrease of branching was observed in the presence of a thiol during the polymerization process, experimentally confirming the ‘patching’ effect of mid-chain tertiary radicals by the thiol. Thus, the addition of a chain transfer agent not only controls the chain length of the poly(acrylate), but also the complexity of its microstructure is significantly reduced. The NMR study illustrates the potential of melt-state NMR for the quantitative determination of the degrees of branching, with precision, for example for kinetic studies.<sup>62</sup>

The melt-state <sup>13</sup>C NMR results support the mass spectrometric findings relating to the  $\beta$ -scission products as the reduction in degree of branching and the reduction in the amount of  $\beta$ -scission product correlate well to each other. The degrees of branching obtained moreover allow for detailed investigations into the kinetics and mechanism of acrylate polymerizations. The highly complementary mass spectrometric and NMR spectroscopic data provide a complete micro-structural image of the obtained polymer chains.

---

## 4.8 References

- 1 Farcet, C.; Bellenev, J.; Charleux, B.; Pirri, R. *Macromolecules* 2002, 35, 4912-4918.
- 2 McEwen, C. N.; Jackson, C.; Larsen, B. S. *Int. J. Mass Spectrom. Ion Processes* 1997, 160, 387-394.
- 3 Grady, M. C.; Simonsick, W. J.; Hutchinson, R. A. *Macromolecular Symposia* 2002, 182, 149-168.
- 4 Quan, C.; Soroush, M.; Grady, M. C.; Hansen, J. E.; Simonsick, W. J. *Macromolecules* 2005, 38, 7619-7628.
- 5 Barner-Kowollik, C.; Davis, T. P.; Stenzel, M. H. *Polymer* 2004, 45, 7791-7805.
- 6 Szablan, Z.; Lovestead, T. M.; Davis, T. P.; Stenzel, M. H.; Barner-Kowollik, C. *Macromolecules* 2007, 40, 26-39.
- 7 Lovestead, T. M.; Hart-Smith, G.; Davis, T. P.; Stenzel, M. H.; Barner-Kowollik, C. *Macromolecules* 2007, 40, 4142-4153.
- 8 Szablan, Z.; Junkers, T.; Koo, S. P. S.; Lovestead, T.; Davis, T. P.; Stenzel, M. H.; Barner-Kowollik, C. *Macromolecules* 2007, 40, 6820-6833.
- 9 Hanton, S. D. *Chem. Rev.* 2001, 101, 527-569.
- 10 Prokai, L. *Int. J. Polym. Anal. Charact.* 2001, 6, 379-391.
- 11 Montaudo, G. *Trends in Polymer Science* 1996, 4, 81-86.
- 12 Scrivens, J. H.; Jackson, A. T. *International Journal of Mass Spectrometry* 2000, 200, 261-276.
- 13 McEwen, C. N.; Peacock, P. M. *Analytical Chemistry* 2002, 74, 2743-2748.
- 14 McEwen, C. N.; Simonsick, W. J. J.; Larsen, B. S.; Ute, K.; Hatada, K. *Journal of the American Chemical Society Mass Spectrometry* 1995, 6, 906-911.
- 15 Peacock, P. M.; McEwen, C. N. *Analytical Chemistry* 2006, 78, 3957-3964.
- 16 Junkers, T.; Theis, A.; Buback, M.; Davis, T. P.; Stenzel, M. H.; Vana, P.; Barner-Kowollik, C. *Macromolecules* 2005, 38, 9497-9508.
- 17 Asua, J. M.; Beuermann, S.; Buback, M.; Castignolles, P.; Charleux, B.; Gilbert, R. G.; Hutchinson, R. A.; Leiza, J. R.; Nikitin, A. N.; Vairon, J. P.; van Herk, A. M. *Macromol. Chem. Phys.* 2004, 205, 2151-2160.
- 18 Kajiwara, A. *Macromol. Rapid Commun.* 2009, 30, 1975-1980.
- 19 Azukizawa, M.; Yamada, B.; Hill, D. J. T.; Pomery, P. J. *Macromol. Chem. Phys.* 2000, 201, 774-781.
- 20 Sato, E.; Emoto, T.; Zetterlund, P. B.; Yamada, B. *Macromol. Chem. Phys.* 2004, 205, 1829-1839.
- 21 Yamada, B.; Azukizawa, M.; Yamazoe, H.; Hill, D. J. T.; Pomery, P. J. *Polymer* 2000, 41, 5611-5618.
- 22 Barth, J.; Buback, M.; Hesse, P.; Sergeeva, T. *Macromol. Rapid Commun.* 2009, 30, 1969-1974.
- 23 Willemse, R. X. E.; Herk, A. M. v.; Panchenko, E.; Junkers, T.; Buback, M. *Macromolecules* 2005, 38, 5098-5103.
- 24 Buback, M.; Hesse, P.; Junkers, T.; Sergeeva, T.; Theis, T. *Macromolecules* 2007, 41, 288-291.
- 25 Ahmad, N. M.; Heatley, F.; Lovell, P. A. *Macromolecules* 1998, 31, 2822-2827.
- 26 Plessis, C.; Arzamendi, G.; Alberdi, J. M.; Herk, A. M. v.; Leiza, J. R.; Asua, J. M. *Macromol. Rapid Commun.* 2003, 24, 173-177.
- 27 Plessis, C.; Arzamendi, G.; Leiza, J. R.; Schoonbrood, H. A. S.; Charmot, D.; Asua, J. M. *Macromolecules* 2000, 33, 5041-5047.

- 
- 28 Gaborieau, M.; Koo, S. P. S.; Castignolles, P.; Junkers, T.; Barner-Kowollik, C. Submitted 2010.
  - 29 Castignolles, P.; Graf, R.; Parkinson, M.; Wilhelm, M.; Gaborieau, M. *Polymer* 2009, 50, 2373-2383.
  - 30 Peck, A. N. F.; Hutchinson, R. A. *Macromolecules* 2004, 37, 5944-5951.
  - 31 Rantow, F. S.; Soroush, M.; Grady, M. C.; Kalfas, G. A. *Polymer* 2006, 47, 1423-1435.
  - 32 Junkers, T.; Barner-Kowollik, C. *Macromol. Theory Simul.* 2009, 18, 421-433.
  - 33 Szablan, Z.; Junkers, T.; Koo, S. P. S.; Lovestead, T. M.; Davis, T. P.; Stenzel, M. H.; Barner-Kowollik, C. *Macromolecules* 2007, 40, 6820-6833.
  - 34 Hart-Smith, G.; Chaffey-Millar, H.; Barner-Kowollik, C. *Macromolecules* 2008, 41, 3023-3041.
  - 35 Chaffey-Millar, H.; Hart-Smith, G.; Barner-Kowollik, C. *J. Polym. Sci., Part A: Polym. Chem.* 2008, 46, 1873-1892.
  - 36 Buback, M.; Frauendorf, H.; Gunzler, F.; Vana, P. *J. Polym. Sci., Part A: Polym. Chem.* 2007, 45, 2453-2467.
  - 37 Buback, M.; Frauendorf, H.; Gunzler, F.; Vana, P. *Polymer* 2007, 48, 5590-5598.
  - 38 Buback, M.; Frauendorf, H.; Janssen, O.; Vana, P. *J. Polym. Sci., Part A: Polym. Chem.* 2008, 46, 6071-6081.
  - 39 Chiefari, J.; Jeffery, J.; Mayadunne, R. T. A.; Moad, G.; Rizzardo, E.; Thang, S. H. *Macromolecules* 1999, 32, 7700-7702.
  - 40 Buback, M.; Frauendorf, H.; Vana, P. *J. Polym. Sci., Part A: Polym. Chem.* 2004, 42, 4266-4275.
  - 41 Zammit, M. D.; Davis, T. P.; Haddleton, D. M.; Suddaby, K. G. *Macromolecules* 1997, 30, 1915-1920.
  - 42 Buback, M.; Günzler, F.; Russell, G. T.; Vana, P. In *29th Australian Polymer Symposium: Hobart, Tasmania, 2007*, p 51.
  - 43 Postma, A.; Davis, T. P.; Li, G.; Moad, G.; O'Shea, M. S. *Macromolecules* 2006, 39, 5307-5318.
  - 44 Fabiano, A. N. F. In *J. Appl. Polym. Sci.*, 2005, p 2088-2093.
  - 45 Boschmann, D.; Vana, P. *Macromolecules* 2007, 40, 2683-2693.
  - 46 Penzel, E.; Goetz, N. *Angew. Makromol. Chem.* 1990, 178, 191-200.
  - 47 Ahmad, N. M.; Heatley, F.; Lovell, P. A. *Macromolecules* 1998, 31, 2822-2827.
  - 48 Castignolles, P.; Graf, R.; Parkinson, M.; Wilhelm, M.; Gaborieau, M. *Polymer* 2009, 50, 2373-2383.
  - 49 Klimke, K.; Parkinson, M.; Piel, C.; Kaminsky, W.; Spiess, H. W.; Wilhelm, M. *Macromol. Chem. Phys.* 2006, 207, 382-395.
  - 50 National Institute of Advanced Industrial Science and Technology AIST Japan. Spectral database for organic compounds SDBS, [http://www.aist.go.jp/RIODB/SDBS/cgi-bin/cre\\_index.cgi](http://www.aist.go.jp/RIODB/SDBS/cgi-bin/cre_index.cgi), Accessed 2009.
  - 51 Junkers, T.; Barner-Kowollik, C. *J. Polym. Sci. Pol. Chem.* 2008, 46, 7585-7605.
  - 52 Junkers, T.; Bennet, F.; Koo, S. P. S.; Barner-Kowollik, C. *J. Polym. Sci., Part A: Polym. Chem.* 2008, 46, 3433-3437.
  - 53 Damico, J. J.; Jackson, D. *Abstracts of Papers of the American Chemical Society* 1979, 248-248.
  - 54 Mallik, K. L. *Naturwissenschaften* 1958, 45, 385-385.
  - 55 Lee, K.-C.; Wi, H.-A. *J. Polym. Sci., Part A: Polym. Chem.* 2008, 46, 6612-6620.

- 
- 56 Sorokina, L. I.; Radbil, T. I.; Sorokina, G. N.; Shtarkman, B. P. *Polymer Science U.S.S.R.* 1983, 25, 2414-2418.
  - 57 Matsumoto, A.; Tanno, R.; Aota, H.; Ikeda, J.-i. *Eur. Polym. J.* 2001, 37, 1071-1074.
  - 58 Gugliotta, L. M.; Salazar, A.; Vega, J. R.; Meira, G. R. *Polymer* 2001, 42, 2719-2726.
  - 59 Jahanzad, F.; Kazemi, M.; Sajjadi, S.; Taromi, F. A. *Polymer* 1993, 34, 3542-3544.
  - 60 Podosenova, N. G.; Lachinov, M. B.; Revnov, B. V.; Cherep, Y. I.; Zubov, V. P.; Budtov, V. P. *Polymer Science U.S.S.R.* 1985, 27, 2822-2830.
  - 61 Madruga, E. L.; Malfeito, J. J. *Eur. Polym. J.* 1992, 28, 863-866.
  - 62 Plessis, C.; Arzamendi, G.; Alberdi, J. M.; van Herk, A. M.; Leiza, J. R.; Asua, J. M. *Macromol. Rapid Commun.* 2003, 24, 173-177.



## 5 Butyl Acrylate Macromonomer Synthesis & Its Application in Radical Catalyst-Free Polymer-Polymer Conjugation *via* Thiol-ene Coupling

This chapter presents work pertaining to the synthesis of *n*-butyl acrylate macromonomers, and the subsequent attempt to conjugate these macromonomers to form star polymers *via* radical thiol-ene chemistry. The Polymer Chemistry Research (PCR) group at Ghent University simultaneously attempted to make functional polymers and PS-*b*-PVAc block copolymers by UV-initiated, metal-free thiol-ene chemistry, thus a collaboration was set up with the PCR group. The results on conjugation efficiency are compared with the results obtained by PCR to give a broader understanding on the limitations of thiol-ene for polymer-polymer conjugation.

Macromonomers are polymers or oligomers that carry a polymerizable unsaturated endgroup, either of a 1,2-disubstituted structure, resulting in a vicinal double bond, or of the more readily polymerizable 1,1'-disubstituted structure with a geminal double bond. A method was developed to form *n*-butyl acrylate macromonomer with surprisingly high uniformity under very simple conditions of high temperature and very dilute monomer concentrations. An investigation was undertaken into the formation mechanism to better understand the formation processes behind such a consistent product spectrum in a system where no control agents or synthesis methods are employed. Macromonomers are in general useful in the development and synthesis of complex architectures, such as homo- or block copolymers that, for example, are branched, comb-like or star shaped. The potential application of these *n*-butyl acrylate macromonomers is then explored *via* thiol-ene chemistry in the second section of this chapter.

The thiol-ene reaction has experienced a resurgence in polymer chemistry and some scientists have gone so far as to categorize it as a *click* reaction. There is no immediate reason to suppose failure of the polymer – polymer conjugation process, and the literature is replete with examples of small molecule conjugation (see section 5.2 for details). In the

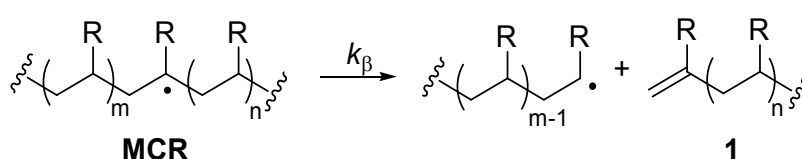
case of the conjugation of macromonomers, the reality of the situation is much more complex and to date there are no cases where polymer chains have been coupled *via* radical thiol-ene chemistry. This work explores the limitations of the radical, metal-free thiol-ene reaction with respect to constructing star shaped polymers. The ability of the radical thiol-ene reaction to serve as a *click* reaction for polymer-polymer conjugation was tested on various systems.

## 5.1 Self-Directed Formation of Uniform Unsaturated *n*-Butyl Acrylate Macromonomers at High Temperatures

Modern polymer chemistry focuses largely on the synthesis of complex architectures, aiming for homo- or (block) co-polymers that, for example, are branched, comb-like or star shaped. However, to obtain such structures, sophisticated methods must be used to functionalize polymer chains and subsequent reactions are required to obtain the desired structures. Various approaches are used to obtain functionalized polymers, including controlled radical/living polymerization methods<sup>1</sup> such as atom transfer radical polymerization (ATRP),<sup>2-3</sup> nitroxide mediated polymerization (NMP)<sup>4-5</sup> or reversible addition fragmentation chain transfer (RAFT)<sup>6-7</sup> polymerization, sometimes combined with *click* chemistry (see ref.<sup>8</sup> and literature cited within). A different approach makes use of macromonomers (MM), which are polymers or oligomers that carry a polymerizable unsaturated endgroup, either of a 1,2-disubstituted structure or of the more readily polymerizable geminal structure **1** as shown in Scheme 5-1. Brush polymers can be easily obtained by radical polymerization of such macromonomers. If a co-monomer is added, graft polymers can also be made with ease.<sup>9</sup> However, synthesis of macromonomers of the general structure **1** usually requires elaborate functionalization of polymers previously containing other endgroups.

This work demonstrates that the growing radicals in acrylate polymerization at temperatures well above 120 °C undergo a series of transfer and  $\beta$ -scission reactions, which are interconnected *via* several complex dynamic equilibria. The synthesis is based on a modified procedure initially described by Chiefari *et al.*<sup>10</sup> The proposed reaction mechanism demonstrates the high complexity of side reactions in acrylate polymerizations and it is noteworthy to add that the participating chemical reactions are not polymer specific reactions and may hence be of interest on a wider scope. Highly uniform MM with defined

polymer endgroups are obtained, rather than the expected variety of products, without the need to employ additives such as mediating agents or even a radical initiator. This particular ability to obtain such highly uniform MM is a result of a distinct chemical self-organization or self-direction of the system. The term *chemical self-organization* (or *self-direction*) is used here to distinguish the proposed reaction from controlled/living polymerization techniques (e.g. ATRP or RAFT) from which similarly uniform products are obtained. In controlled/living radical polymerizations, initiators, and more importantly, mediating agents, are generally required. This work demonstrates that the assembly of monomer molecules into highly ordered macromonomers takes place without any specific stimuli apart from temperature.



Scheme 5-1:  $\beta$ -scission reaction of a midchain radical

Chiefari *et al.* introduced a procedure to generate macromonomers of high purities directly from the monomer without the need for endgroup modification.<sup>10</sup> They homo-polymerized butyl acrylate at low initiator concentrations in solution at very high temperatures and obtained relatively short macromonomers **1**, with the size of the molecules depending on temperature and monomer concentration. They obtained MMs in the range of  $10^3$  to  $10^4$  g·mol<sup>-1</sup> at temperatures in the range of 80 to 240 °C. As the dominant mechanism they proposed formation of midchain radicals (MCR) *via* intra- or intermolecular transfer to polymer followed by  $\beta$ -scission reactions (see Scheme 5-1). The work presented in this chapter uses the kinetic information known about MCRs to harness the  $\beta$ -scission reaction and produce essentially pure MM as the main product, thus bridging the gap from fundamental kinetic investigations to the development of straightforward synthetic strategies.

### 5.1.1 Macromonomer Synthesis

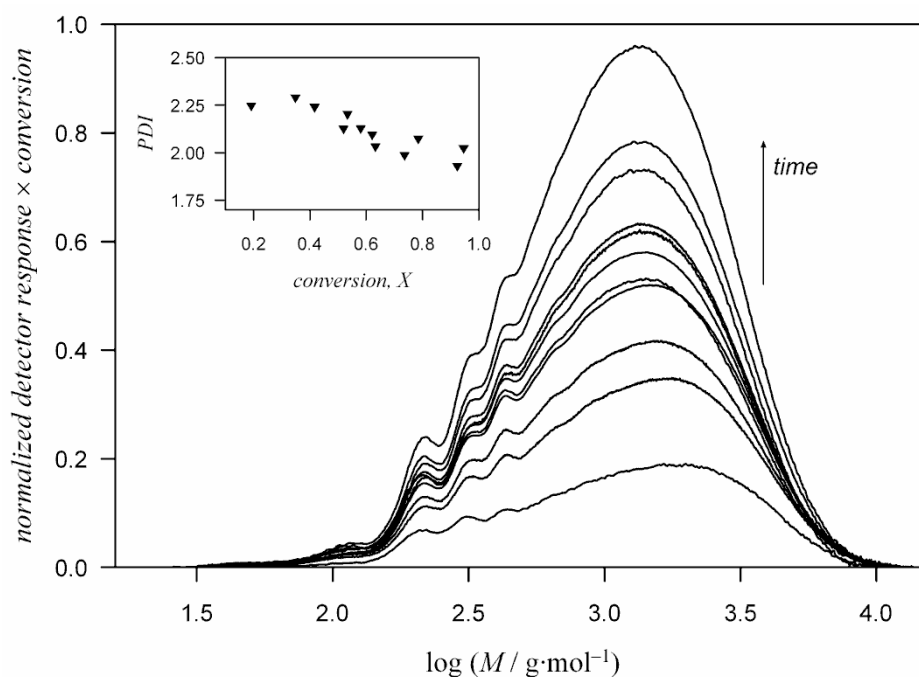
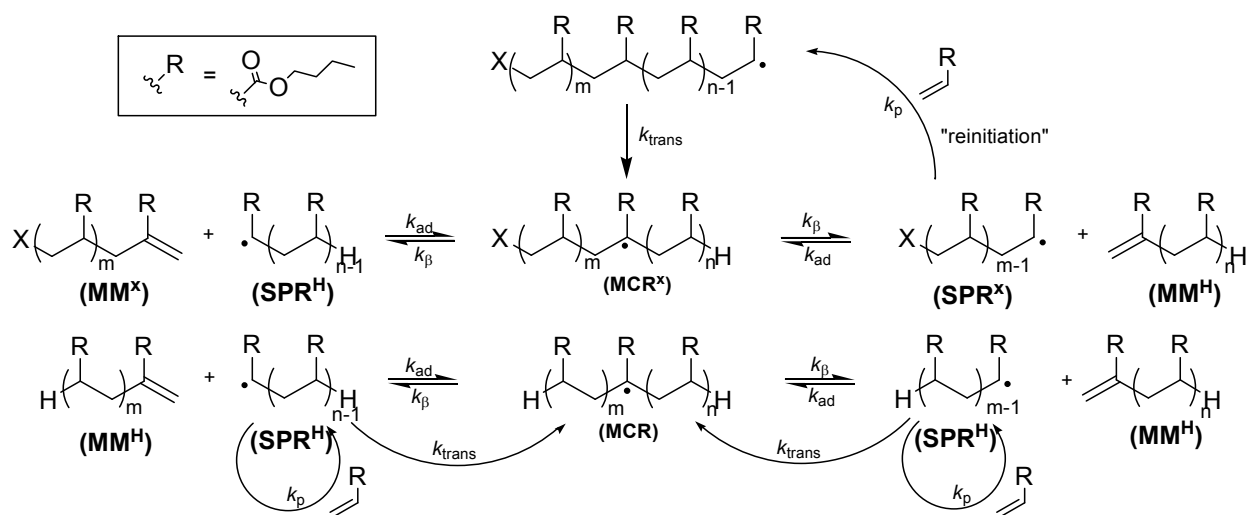


Figure 5-1: Evolution of molecular weight distributions in auto-initiated butyl acrylate polymerization in hexyl acetate solution (5 wt %) at 140 °C. Samples were taken over a period of 14 hours and conversion was determined by gravimetry.

Auto-initiation of free radical polymerizations is known to occur with several monomers at increased temperatures. Acrylates and methacrylates are known to self-initiate,<sup>11</sup> and until recently it was speculated that peroxides present in the reaction mixture or the solvent used could be responsible for the start of the reaction.<sup>11-13</sup> Alternatively the decomposition of impurities was also proposed as a means of initiating MMA polymerization.<sup>14</sup> Srinivasan *et al.*<sup>15</sup> performed a computational study to investigate the mechanism of spontaneous initiation in thermal polymerization of alkyl acrylates, and they propose a mechanism of spontaneous thermal initiation of methyl acrylate *via* first the formation of di-radicals according to the Flory di-radical mechanism. Subsequent hydrogen transfer from a triplet di-radical to a monomer causes monoradical generation which initiates the polymerization. In a study on thermally-initiated MMA polymerization, it was reported that MMA could also undergo reaction with air to form macromolecular peroxides.<sup>16</sup>

As auto-initiation certainly provides a low radical flux which aids the formation of MM, no initiator was used in the present study. Poly(*n*-BA) macromonomers were synthesized in two solvents; at 140 °C in hexyl acetate and at 128 °C in butyl acetate at boiling point. Figure 5-1 depicts the change in the molecular weight distribution with increasing monomer conversion from samples taken over a period of 14 hours. All samples exhibit an average number-average molecular weight  $M_n$  of 850 g·mol<sup>-1</sup> while a shift of the peak maximum to slightly lower values is observed with increasing conversion. This reproducible shift reflects a decrease in polydispersity with increasing conversion as depicted in the insert of the figure. Over the course of the reaction, the polydispersity of the sample (PDI) decreases from almost 2.3 to 1.9 at full conversion. It should be noted here that some variations in the reaction rate can occur whereas the change in PDI with conversion is almost identical for the different reactions. Those rate variations range from as little as 2 h, up to 14 h, to reach full monomer conversion under otherwise identical reaction conditions. Consequently, no kinetic analysis could be carried out. These significant differences in the rate of polymerization can be attributed to the very low radical concentrations present at all times during the reaction. Thus, the smallest impurities may quench radicals or alternatively be an additional source of radicals and eventually slow down or accelerate the reaction. It should be noted that the monomer and solvent used in the current study were carefully purified and passed over a column of basic alumina. However, as stated above, this change in the number of radicals seems to have very minor impact on the product formed, if any.

Interestingly, when the reaction mixture is held at reaction temperature for an extended time, a further decrease in PDI is observed, regardless of the actual rate of polymerization. After stirring and heating of the sample that took 14 h to reach close to full conversion for more than 24 h, PDIs of 1.5 to 1.6 are obtained at otherwise unchanged average molecule size. The end group composition also remains unchanged as can be confirmed *via* mass spectrometric monitoring. Rather narrow distributions are formed compared to normal radical polymerization systems and approaching the polydispersity limit characteristic for controlled or living polymerization systems. The observation of an ongoing reaction even after (almost) all monomer has been consumed leads to the conclusion that MMs are not just dead polymeric material, but actively take part in the reaction. In principle, addition of an unsaturated MM to a secondary propagating radical (SPR) is likely to occur.



Scheme 5-2: Macromonomer Formation Mechanism

However, such a reaction forms a radical of an MCR structure as is shown in Scheme 5-2, and hence the growing chains and MMs are in equilibrium with the MCR species. The equilibrium is largely shifted to the side of the macromonomers  $\text{MM}^{\text{H}}$  (in Chapter 4  $\text{MM}^{\text{H}}$  is referred to as  $\beta^{\text{I}}$ ) because the radical product that is formed at the same time as  $\text{MM}^{\text{H}}$  is structurally identical to the  $\text{SPR}^{\text{X}}$  species that may again form a  $\text{MCR}^{\text{X}}$  *via* backbiting. It should be noted that X refers to the fragment that initiated the polymerization. The equilibrium is thus shifted following Le Chatelier's principle; the backbiting reaction is the driving force of the reaction and leaves the equilibrium to act as a macromonomer production machine.

In a second step, the short-chained  $\text{MM}^{\text{H}}$ , predominantly of chain length 3, generated by the first equilibrium, enters into a second equilibrium with the radical  $\text{SPR}^{\text{H}}$  that then yields identical products on either side. Hence production of  $\text{MM}^{\text{H}}$  is further accelerated with the propagation/backbiting reaction being the driving force. It should be noted that the  $\text{SPR}^{\text{X}}$  can also enter into an equilibrium with its corresponding MM. However, as backbiting is such a fast reaction, any SPR species is more likely to yield  $\text{MM}^{\text{H}}$  than a macromonomer with an endgroup X. The system thus exhibits strong similarities to the equilibria governing the reversible-addition-fragmentation transfer (RAFT) polymerization process,<sup>12</sup> with the major difference that the concentration of the MM changes during the course of the reaction

while its counterpart, the macroRAFT agent, remains at constant concentration. Further complexity is added by the fact that there is no corresponding reaction for backbiting. The narrowing of the molecular weight distributions over time may hence be explained by the RAFT effect of the propagation probability being equally distributed over all chains which allows for self-organization of the system. Moreover, the two depicted equilibria may be regarded as the equivalent to the pre- and main RAFT equilibria. Thus the original initiating fragment may be found only in small quantities or not at all in the final product due to the constant reinitiation of the system.

Similarly to RAFT, chain extension of the macromonomer should be feasible by adding fresh monomer after the reaction is completed. A simple increase in the starting monomer concentration, however, also leads to higher molecular weights due to the increased probability of chain propagation. Zorn *et al.*<sup>17</sup> have since synthesized macromonomers of many other acrylate monomers, including methyl, ethyl, *n*-butyl, *t*-butyl, 2-ethyl hexyl, isobornyl and 2-[[[(butylamino)carbonyl]oxy]ethyl acrylate. They obtained between 82 and 95 % yield of macromonomers containing the geminal double bond, as analyzed *via* ESI-MS, with molecular weights of between 800 and 2000 g·mol<sup>-1</sup> and polydispersities close to 1.6.<sup>17</sup>

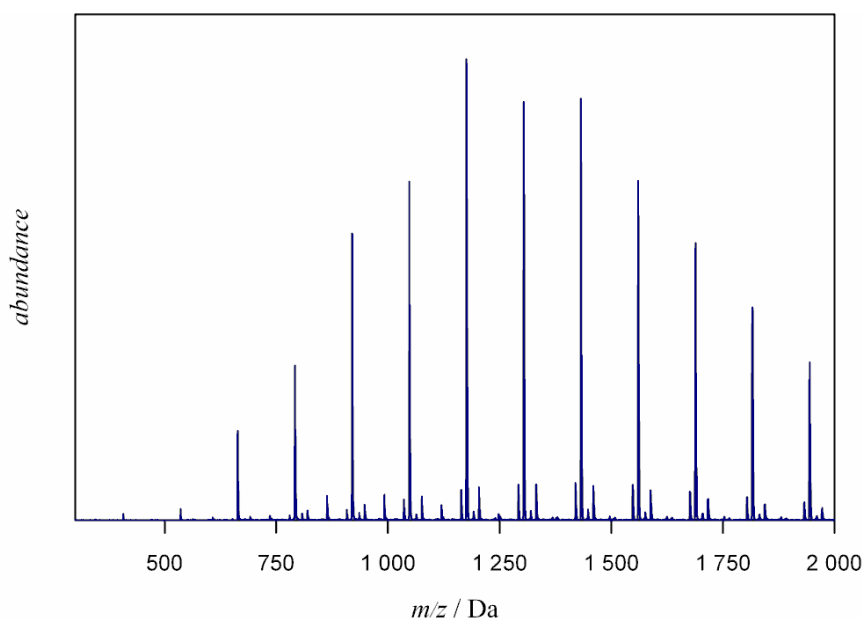


Figure 5-2: Full ESI-MS spectrum of macromonomer obtained from *n*-BA auto-initiated polymerization to full monomer-to-polymer conversion in 5 wt % solution in hexyl acetate at 140 °C.

The proposed mechanism of MM formation, Scheme 5-2, was verified by analyzing the macromonomer samples *via* ESI-MS.

Figure 5-2 and Figure 5-3 depict the full product spectra obtained when BA macromonomer is synthesized in hexyl acetate and butyl acetate respectively at 140 °C and 128 °C. Both spectra are very uniform in product and while a small amount of side products can be seen, the macromonomer is by far the major species in both cases.

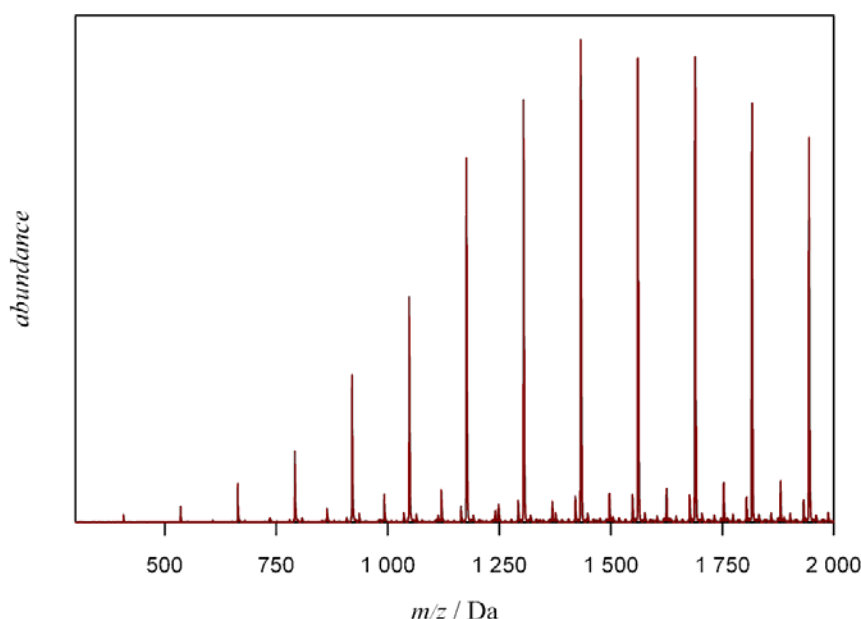


Figure 5-3: Full ESI-MS spectrum of macromonomer obtained from *n*-BA auto-initiated polymerization to full monomer-to-polymer conversion in 5 wt % solution in butyl acetate at 128 °C.

The product spectra for the auto-initiated MM synthesis in butyl acetate and hexyl acetate solutions at the level of one repeat unit are presented in Figure 5-4. In both cases, one main product is observed that is congruent with the structure of MM<sup>H</sup> as expected. Apart from this peak, only very low abundant species are identified, none of them congruent with a termination product. For the reaction in hexyl acetate, a small peak is visible that can be assigned to a MM that carries a hexyl side chain on one of the ester moieties and is most likely formed during a transfer to solvent reaction resulting in a hexyl acetate radical initiating the polymerization (and hence X = HAc). Table 5-1 presents the experimental and

theoretical  $m/z$  ratios for species found in the mass spectra. All values agree well within the experimental resolution of the employed set-up.

Table 5-1: The experimental and theoretical  $m/z$  ratios for species found in the mass spectra of BA MM.

	$m/z_{\text{theo}} / \text{Da}$	$m/z_{\text{exp (BuAc)}} / \text{Da}$	$m/z_{\text{exp(HexAc)}} / \text{Da}$
$\text{MM}^{\text{H}} [\text{Na}^+]$	1175.74	1175.9	1175.8
$\text{MM}^{\text{H}} [\text{K}^+]$	1191.72	1191.9	1191.7
$\text{MM}^{\text{HAc}} [\text{Na}^+]$	1203.77	---	1203.8
$\text{MM}^{\text{X}} [\text{Na}^+]$	1119.73	1119.9	1119.8
satP $[\text{Na}^+]$	1163.74	1163.9	1163.8
satP <sup>HAc</sup> $[\text{Na}^+]$	1191.78	---	1191.7

In accordance with this observation, saturated polymer chains satP are observed that could potentially have emerged from the same reaction originating from  $\text{SPR}^{\text{H}}$ . A transfer to solvent peak would not appear in the spectrum for the polymer made in butyl acetate as this species is identical to  $\text{MM}^{\text{H}}$ . A transfer reaction product  $\text{satP}^{\text{HAc}}$  may also be identified in the spectrum, however a product peak congruent with this mass is identified in both spectra making it more likely that this peak is actually a potassium adduct of  $\text{MM}^{\text{H}}$ .

This conclusion is supported by the observation that the peak shifts by 2 Da when the polymer is hydrogenated, as opposed to the satP peak.<sup>18</sup> The peak labelled dc refers to doubly-charged  $\text{MM}^{\text{H}}$ . A peak at 1119.8 Da is observed that cannot be assigned to any termination product and is known from the above mentioned hydrogenation experiment to carry one unsaturated group. Hence it is assigned to  $\text{MM}^{\text{X}}$  with X potentially being of the structure 2 (see Scheme 5-4) or, in principle, a structural isomer of it. However, 2 is only a suggestion and any isomer with the formula  $\text{C}_{10}\text{H}_{10}\text{O}_3$  or, in principle any structure that coincides with the mass of 2 or 2 plus any number of monomer units may be assigned to X. No further information on the auto-initiation mechanism could be obtained. In fact, a larger variety of peaks is observed in the ESI-MS spectra of macromonomer taken at earlier stages of polymerization, at times before the second equilibrium dominates the process, indicating that more than one radical fragment is involved in initiation.

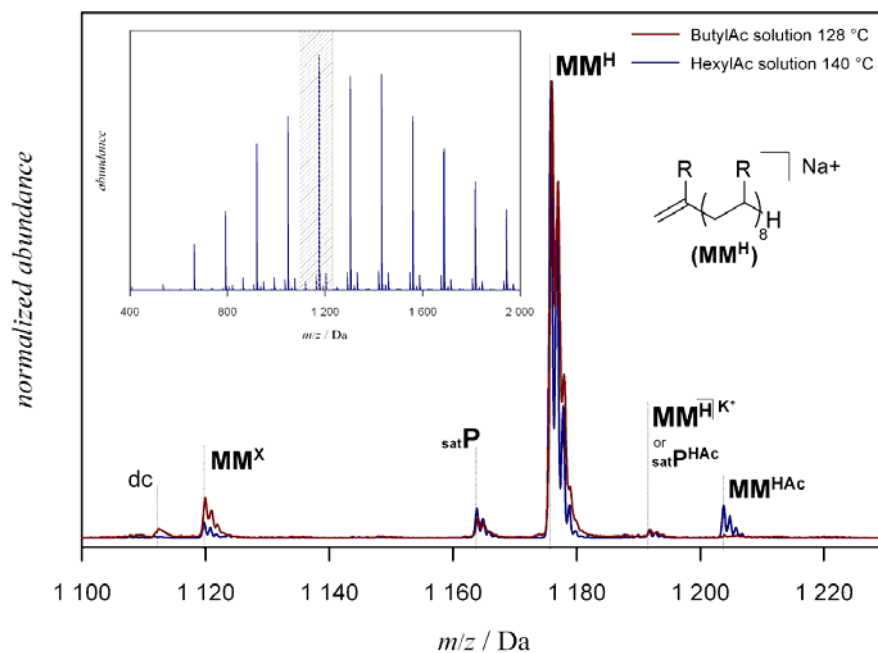
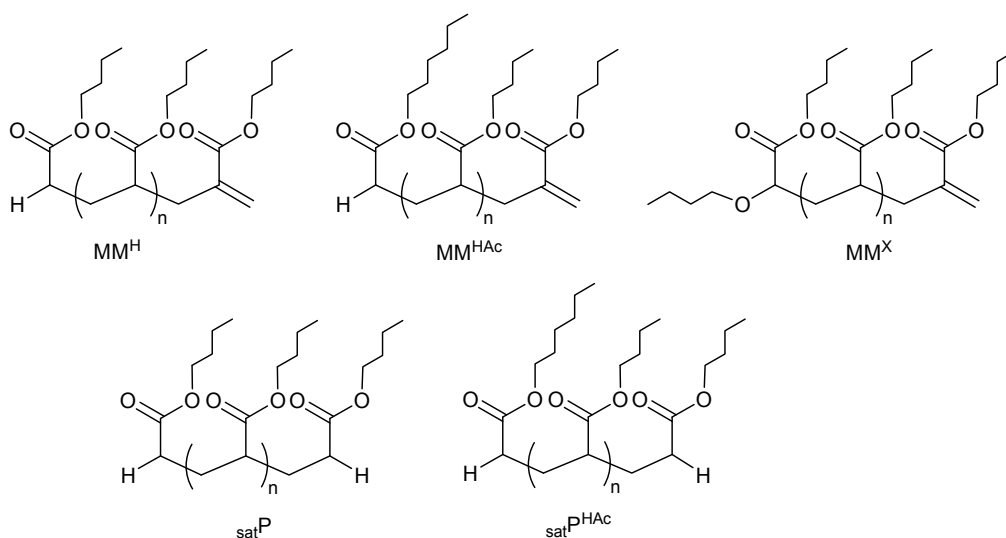
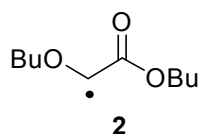


Figure 5-4: ESI-MS spectrum of poly(*n*-BA) macromonomers synthesized to full conversion in solutions of butyl acetate (at 128 °C) and of hexyl acetate (at 140 °C) with 5 wt % BA. The insert shows the full spectrum for the sample prepared in hexyl acetate.



Scheme 5-3: Chemical structures of the species found in the mass spectra of BA MM.



Scheme 5-4: Structure of the apparent initiating species

Zorn *et al.*<sup>17</sup> employed the same method of dilute monomer concentration (5 wt %) and high temperature (140 °C) and obtained MM with molecular weights ranging from 800 to 2000 g·mol<sup>-1</sup> with a terminal geminal double bond. Coupling experiments were also successfully carried out using BA MM and EA MM, to form a copolymer. The success at coupling two separately synthesized macromonomers indicates the reactivity of the terminal double bond, an important property when complex architectures are targeted. The synthesis and subsequent chain extension of macromonomers has the potential to become an important synthetic tool to build graft polymers or other polymer architectures more readily than with current strategies.

### 5.1.2 Summary – Synthesis of Butyl Acrylate Macromonomer

High temperature auto-initiated polymerization of butyl acrylate yields a highly ordered product that consists almost quantitatively of uniform macromonomeric structures that may be further used to build complex molecular architectures. The self-organized synthesis itself is highly efficient, simple and, except for the high temperature, cost and time-effective as no purification and/or isolation steps either during or after the reaction are required. Zorn *et al.*<sup>17</sup> have since synthesized a library of various acrylate macromonomers and shown that these MMs have the potential to be conjugated to form copolymers and may lead to new synthetic strategies for the formation of complex macromolecular architectures. The next section of work employs the MM species in an attempt at polymer-polymer conjugation utilizing the thiol-ene coupling reaction, to investigate recent claims that the thiol-ene coupling reaction can be considered a *click* reaction.<sup>19-24</sup>

## 5.2 Limitations of the Thiol-ene Coupling Reaction for Polymer-Polymer Conjugation

The facile production of butyl acrylate macromonomers inspired the idea of employing these macromonomers in a further reaction, for polymer-polymer conjugation using radical thiol-ene chemistry. Thiol-ene coupling reactions are not new chemistry, but have been rather extensively studied over the last century,<sup>25-27</sup> and were described as early as 1926 by Braun and Murjahn.<sup>28</sup> Hoyle *et al.* have presented a detailed review on thiol-ene reactions from recent historical and on-going industrial perspectives, as well as discussing thiol-ene reactions in great detail as a newly rediscovered pathway to affording novel polymeric materials with specific properties.<sup>29</sup> Radical addition of thiols onto the vinyl double bonds of

poly[2-3-butenyl)-2-oxazoline], initiated by UV light has also been recently reported.<sup>30</sup> While thiol-ene polymerizations are commonly used for the formation of networks<sup>31-32</sup> or for the purpose of controlling molecular weight in radical polymerizations, thiol-ene coupling has more recently also been referred to as a *click* reaction.<sup>22</sup>

The concept, or rather philosophy, of *click* chemistry, established by Sharpless not too long ago,<sup>33</sup> has rapidly triggered profound interest in the polymer community. Complex macromolecular products are often accessed *via* sequential chain extension of polymers prepared from multi-functional controlling agent cores<sup>34-41</sup> but the sequential chain extension process often does not proceed entirely efficiently and thus residues of both the initial block as well as the second block can remain at the end of the reaction. As a result, the product compositions of such macromolecular designs are often complex and difficult to purify. Also, sequential synthesis sets limitations on the choice of polymerizable monomers as the reactivity of the control agents towards the different blocks must be considered. The advent of the *click* philosophy has highlighted an efficient modular pathway to construct polymer materials enabling the synthesis of complex molecular architectures, including compositions that were previously inaccessible.

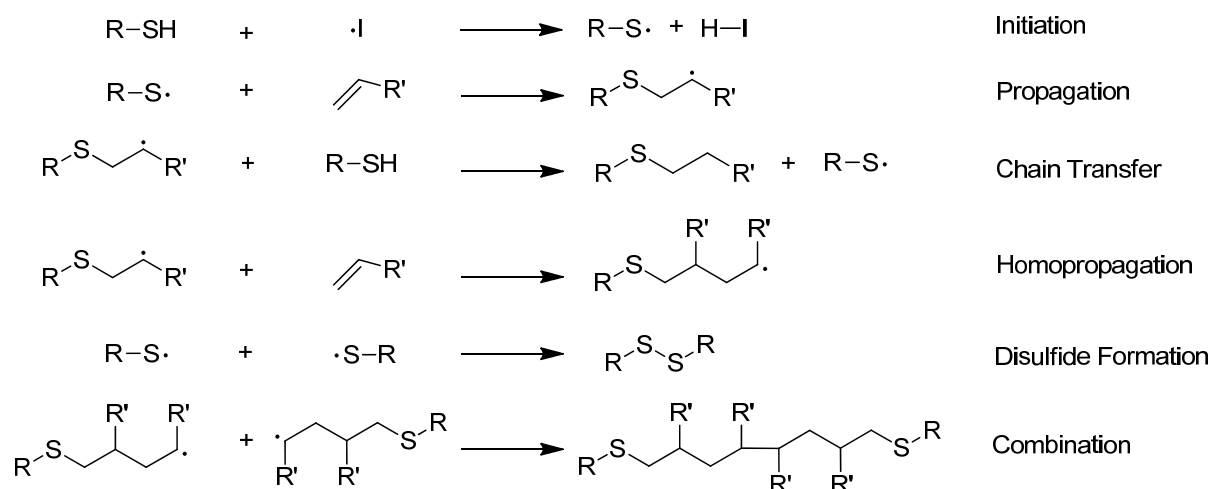
There exist several excellent reviews on the topic and the underpinning details of *click* chemistry will not be reiterated here.<sup>42-46</sup> It is sufficient to state that from the variety of *click* reactions available, the copper-catalyzed azide-alkyne 1,3-dipolar cycloaddition<sup>47</sup> has thus far proven to be the most popular. Nevertheless, the use of a toxic metal catalyst, i.e. copper(I), remains a main drawback, especially for bio-related applications. Although a number of strategies have been developed to avoid the use of copper for azide-alkyne *click* reactions, it is often argued that in the near future at least these approaches will not be able to replace the copper(I) catalyzed coupling reaction.<sup>45</sup> A number of alternative *click* strategies have been recently proposed to avoid the use of a copper catalyst,<sup>48</sup> and in particular (hetero) Diels-Alder cycloaddition reactions<sup>39,49</sup> as well as thiol-ene reactions<sup>19,32,50-52</sup> are becoming increasingly widespread. Among these, the thiol-ene radical addition reactions are believed to have significant potential to become as popular as the Cu(I)-catalyzed azide-alkyne *click* cycloaddition reaction, CuAAC, since the introduction of terminal alkene and thiol groups is straightforward and the coupling procedure can be conducted without a catalyst in the presence of UV light.<sup>48</sup> As an example, this strategy has

been employed as part of a facile method for the construction of various dendritic thioether structures,<sup>24</sup> where thiol-ene chemistry is used to functionalize the chain ends and to create a dendritic backbone. As a result, the potential of thiol-ene to be classified as a representative of the *click* class of reactions was recognized.

When discussing conjugation *via* thiol-ene chemistry, it is important to distinguish radical thiol-ene from the catalyzed Michael addition of thiols onto vinyl groups, a reaction that has also been applied to polymeric compounds.<sup>53,57-59</sup> The present work does not focus on the Michael-type addition reaction but only on the thermally induced or UV light initiated thiol-ene coupling reaction involving radicals where no catalysts are employed. Radical thiol-ene coupling proceeds *via* a mechanism that is similar to that of a chain-transfer polymerization mechanism (see Scheme 5-5). In a first step, a thiyl radical is generated from a thiol functionalized molecule *via* hydrogen abstraction from an initiator-derived radical, which subsequently readily reacts with both electron rich and electron poor carbon-carbon double bonds. This reaction is referred to as propagation (not to be confused with the homopropagation of the chain growth mechanism in conventional radical polymerization). In the next step, the radical adduct abstracts a proton from another thiol, thus forming the reaction product and recovering a thiyl radical (chain transfer reaction). Frequently, side reactions have been observed.<sup>21</sup> It should be noted here, that in cases where thiol-ene chemistry exhibits significant side reactions, the whole process may not be considered to be a *click* reaction, as the occurrence of secondary reaction pathways is in direct contradiction to the *click* concept. Thus, thiol-ene may only serve as an efficient conjugation tool if such reactions can be largely avoided. One known side reaction is thiyl-thiyl radical coupling, which leads to disulfide formation; another is head to head coupling of the carbon centered radicals. These two reactions are arguably the most prominent reactions terminating the thiol-ene cycle, but in principle, any bimolecular spin-annihilation reaction can of course occur. Additionally, the step-mechanism of thiol-ene conjugation is in competition with the chain growth mechanism of a transfer polymerization if a (homo)polymerizable ene is used.

Several studies reporting successful functionalization of polymers *via* radical-initiated thiol-ene conjugation with small molecules have been performed. However, no example exists where two polymer chains were coupled and even with the Michael addition type reaction, only few examples of such an attempt can be found in the literature to the best of

our knowledge. This lack of (radical) thiol-ene chemistry as a tool for polymer conjugation was also most recently noted by Sumerlin and Vogt.<sup>60</sup> One example of polymer-polymer conjugation has been presented by Li *et al.*, where a maleimide end group functionalized poly(*N*-isopropylacrylamide) was coupled to thiol end group functionalized poly(styrene) *via* a Michael addition reaction.<sup>61</sup> However, an excess of the thiol-functionalized poly(styrene) and its subsequent removal was required.



Scheme 5-5: Generalized radical thiol-ene *click* reaction: possible reaction pathways for the generated radicals.

The current study attempts polymer-polymer conjugation reactions using radical-initiated thiol-ene chemistry. Surprisingly, the thiol-ene approach was found to be relatively unsuccessful when targeting polymer-polymer conjugation reactions and only showed success to some extent when polymers were functionalized with small molecules. Justifying why some reactions do not work is always challenging as ultimate proof might not be achievable. Still, radical thiol-ene cannot be considered a *click*-type reaction for polymer-polymer conjugation, contrary to the impression given by a large number of papers and therefore this work is an important accomplishment to highlight this significant deviation from expected outcomes.

### 5.2.1 Implications of the *Click* concept for Polymer Conjugation Reactions

The success of *click* chemistry within the polymer community lies in the fact that reactions which follow the *click* philosophy provide reaction pathways that would otherwise be inaccessible with conventional methodologies. Following the original definition by Sharpless,<sup>33</sup> a *click* reaction must, among other requirements, proceed with a high thermodynamic driving force to allow for high yields and reasonable reaction times without the formation of problematic side products. The purification of the products should be simple and not require chromatographic separation. These requirements in particular make *click* chemistry very attractive for polymer chemists. When working with polymers, preparative chromatography is tedious if not often impossible. Reactions that proceed with close to 100 % selectivity and at the same time employ the starting materials in equimolar amounts allow for polymer-polymer reactions without the necessity for a product purification step, other than perhaps removal of a potential catalyst or other additives. Without such reactions, modular approaches for the synthesis of complex macromolecules could not be taken.<sup>62</sup> Consequently, even though equimolar amounts of reactants are not strictly required based on the original definition of *click* type reactions, it is the 'equimolarity feature' of efficient *click* reactions that creates their high value in polymer chemistry. Regardless, the *click* definition dictates that if one reaction partner is used in excess, or if significant side products are formed during the reaction, these components must be easily removable by non-chromatographic methods, i.e. recrystallization or distillation.

When dealing with two polymeric reactants one can easily rule out distillation as a separation method. The analog to crystallization would be precipitation in the case of polymers. Thus, if one cannot use precipitation (or fractional precipitation for that matter) to separate the reaction product from excess starting material or by-products, the original *click* definition is not fulfilled for a polymer conjugation reaction. It should be mentioned that when two polymer chains are coupled, the reaction product will always, at least partially, reflect the physical characteristics of the starting material. Thus complete separation based on solubility will always be hard to achieve.

In the context of polymer conjugation, two requirements that directly follow from the original *click* philosophy can be defined, for which polymer reactions must be tested in order to assess their ability to be used in modular transformations: (i) Endgroup transformation

without any presence of significant side products and (ii) high conjugation efficiency when at least two polymer chains are coupled to each other, i.e. the completion of the reaction on a reasonable time scale without employing an excess of one reaction partner. Violation of any of the above two requirements will inevitably lead to complex product mixtures that in the worst case are non-separable. Despite these strict requirements, there indeed exist very successful cases that fulfill the *click* criteria for polymer-polymer ligation as described above.<sup>60,63-65</sup>

The current work presents results obtained in collaboration with the Polymer Chemistry Research group from Ghent University (PCR – UGent). The PCR group was also inspired to devote research time to thiol-ene reactions based on the encouraging results from other groups claiming *click*-status for radical thiol-ene reactions. While their synthetic targets were distinctly different, the goal was identical; namely, to use radical thiol-ene chemistry in a modular approach to link individual polymer chains. The combination of both projects allows the study of a very broad range of reaction conditions using different thiols as well as enes. The work was carried out entirely independently, but for completion and a deeper exploration of the possibilities as well as the limitations afforded by thiol-ene reactions, the results from Ghent will also be discussed. However, the synthesis strategies are outlined and discussed separately. This work aimed for the synthesis of star polymers employing sequential radical thiol-ene coupling reactions using macromonomers and multifunctional thiols, while the UGent group aimed to couple two different polymer chains containing either thiol or ene functionalities to form block copolymers.

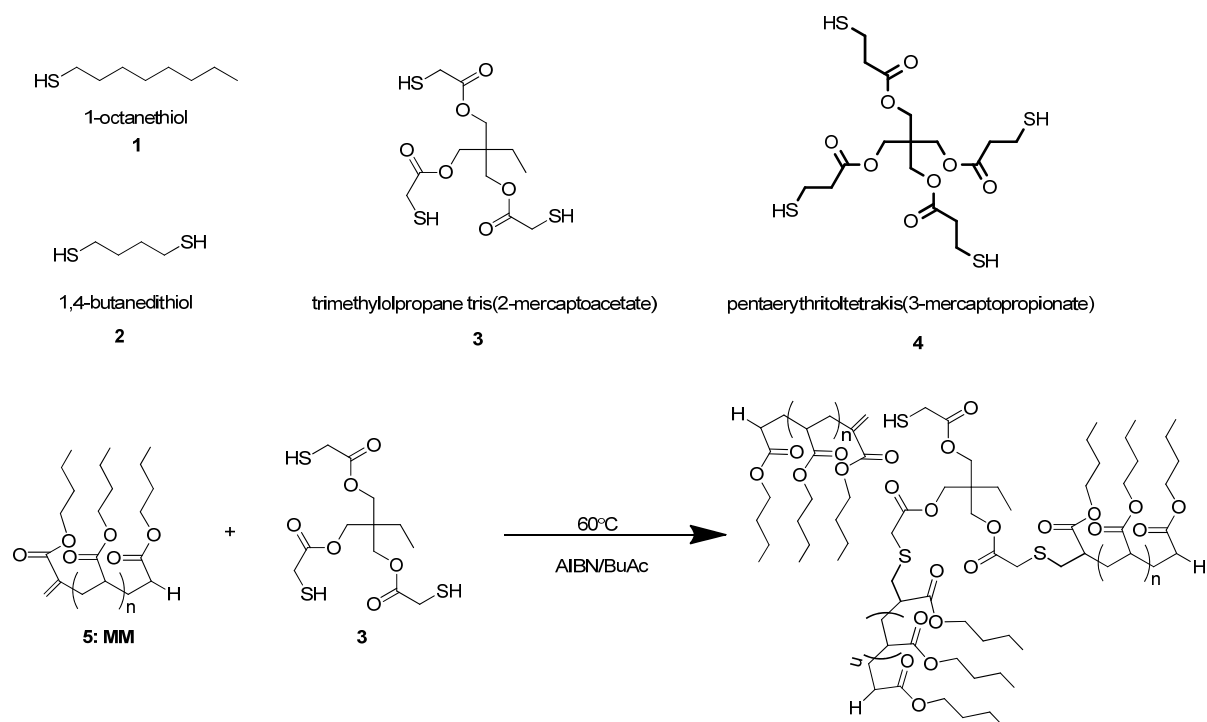
A joint discussion of the results from both groups can be found at the end of the chapter where the results are put into the context of the limitations of the thiol-ene reaction. As part of this extensive combined study, thermal and UV initiation methods are also compared with respect to thiol-ene chemistry. Evaluation of the efficiency of radical thiol-ene chemistry for polymer conjugation is based on the possibility of performing polymer endgroup modifications and polymer conjugation reactions without forming of any side products in the process.

### 5.2.2 Star polymers *via* Thiol-ene Chemistry

If thiol-ene was a method that comes close in its efficiency to the well known *click* conjugation methods such as the copper catalyzed azide-alkyne coupling or (hetero) Diels-Alder reactions, then assembly of star molecules from specific core molecules with end-functional polymers should be feasible. Thus, the aim was to synthesize multi-arm acrylates from linear macromonomers with commercially available multifunctional thiols that are often used in the synthesis of polymer networks from traditional thiol-ene reactions (see Scheme 5-6).

The ene employed in this study is the MM synthesized in the first section of the chapter. The synthetic method does not require any purification or post-modification steps and gives high yields, so the thiol-ene strategy was based on this type of compound. The MM possesses an unsaturated endgroup that can form relatively stable radicals upon addition of e.g. a thiyl radical, while not undergoing homopropagation due to steric reasons. This feature makes the poly(*n*-butyl acrylate) type MM an excellent choice for thiol-ene conjugations: the double bond is relatively accessible and due to the 1,1'-disubstituted nature combined with the ester substituent, a relatively stable tertiary radical is formed upon radical addition, giving rise to a high driving force behind the addition reaction of the thiyl radicals to the ene. At the same time, no homopropagation can occur, in contrast to similarly reactive enes like for example methacrylates, which would readily form oligomers when monomer and thiol were employed in equimolar amounts. Also, acrylates show good solubility in most solvents so that solvent effects can largely be excluded and the choice of solvent is only limited with respect to radical transfer to solvent rates, and furthermore butyl acetate does not show a high tendency to undergo radical transfer.<sup>17,66</sup> The ESI-MS spectrum of the MM synthesized and subsequently employed in thiol-ene reactions is shown in Figure 5-4.

The mass spectrum of the starting BA MM that was employed is shown in Figure 5-4. It is also labelled as spectrum 4 in Figure 5-5. One major peak associated with structure **5** (Scheme 5-6) can be found, corresponding to the macromonomer that is subsequently used as the ene in the thiol-ene reaction.



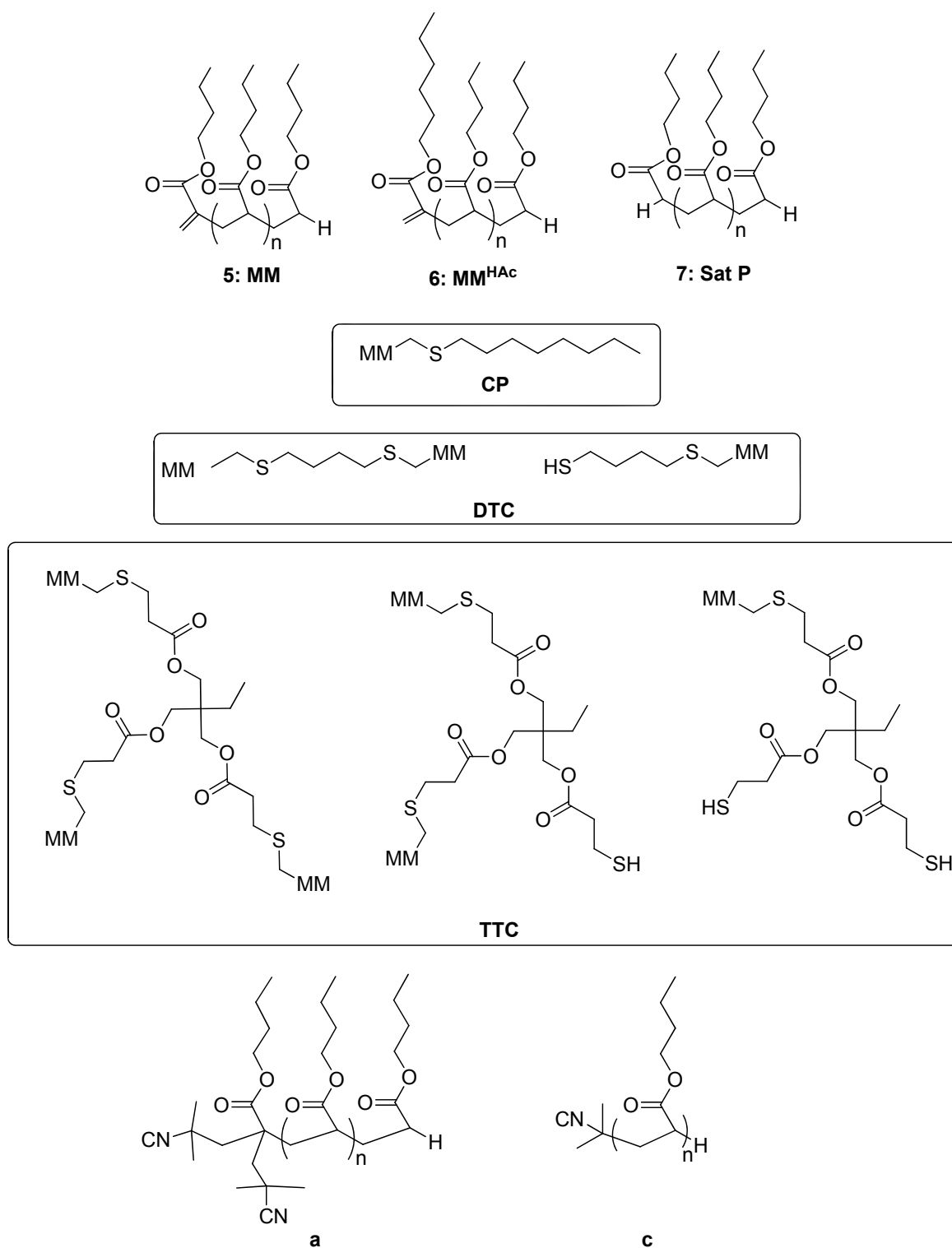
Scheme 5-6: (a) Multifunctional thiols employed in the current study, (b) Typical reaction scheme.

Trace amounts of structures 6 and 7 can also be seen (for structures see Scheme 5-7), which correspond to a macromonomer molecule resulting from transfer to solvent (6), carrying a hexyl group, since MM synthesis was performed in hexyl acetate solution, and a saturated species (7). The structures of all species that appear in the macromonomer product mix are given in Scheme 5-7. The employed high temperature macromonomer synthesis<sup>66</sup> is clearly a very selective reaction, with over 95 % of the product constituting the required starting material structure for the thiol-ene reaction.<sup>17</sup> Thus, this starting material is comparable to macromonomers prepared *via* classical controlled radical polymerization, and are of equally high overall functionality.

Alongside size exclusion chromatography, mass spectrometry is a powerful tool in investigations on the efficiency of *click* reactions as the product is directly observable from the spectra, even in cases where no change in the size distribution can be expected (for example, when conjugating a polymer chain with a small molecule) or where the elugram of the conjugated polymers is expected to be complex.<sup>67</sup> For observation of changes in

polymer endgroups and conjugation points, no better analytical method presently exists. This characterization approach is also especially useful for the current study where the macromonomers are conjugated *via* multi-thiol core molecules (see Scheme 5-6), thus leading to the formation of homopolymers with distinct topology. For coupling of the macromonomers with polymer chains of different types to form di-block copolymers, this technique is less appropriate, as the mass spectra of copolymers are far more complicated. As previously demonstrated,<sup>68,69</sup> mass spectra can be analyzed in a quantitative fashion if some prerequisites are fulfilled, i.e. when the ionization of the polymer mainly depends on the backbone rather than on the endgroups.

Hence, the occurrence of the saturated and therefore unreactive species 7 may be used to compare the product spectra from conjugation reactions under different reaction conditions. The saturated macromonomer product is not expected to – and indeed does not – participate in any reactions; therefore all spectra in the following discussion have been normalized with respect to the peak corresponding to 7 as a reference point.



Scheme 5-7: Main structures found in the product mixture of starting macromonomer material, numbered **5**, **6** and **7**, and other products as labeled in all mass spectra.

### 5.2.2.1 Thiol-ene Reaction Conjugation of Butyl Acrylate Macromonomer and Trimethylolpropane tris(2-mercaptoacetate)

In a first step, the butyl acrylate macromonomer was reacted with a multifunctional thiol core molecule in a one-to-one ratio with macromonomer based on concentration of the complementary functionalities. The result from such a coupling reaction is depicted in Figure 5-5. Inspection of the mass spectrum reveals that most of the initial macromonomer is converted in the reaction and formation of some of the desired product **TTC** (**TriThiol Coupling product**) is observed. However, three additional products (denoted as **a**, **b** and **c** in the mass spectrum) are also observed, each in higher quantities than the desired reaction product. It can thus be concluded that the conjugation attempt, at least under the chosen conditions, was not successful.

To evaluate whether the reaction conditions were unreasonably chosen, further experiments were performed with an excess of thiol compared to ene, following conditions typically applied for thiol-ene reactions found in the literature. Following the procedure of Campos *et al.*,<sup>19</sup> reactions were carried out with 5-10 equivalents of thiol initiated by 0.5 eq. AIBN. Results for the trifunctional thiol species are presented alone Figure 5-5 for clarity and results for the bifunctional thiol species are provided in Figure 5-6, with the corresponding trifunctional thiol results added to the figure for comparison.

With a 5-fold excess of thiol, almost quantitative conversion of the MM into coupling products **DTC** (**DiThiol Coupling product**) or **TTC** (see Scheme 5-7 for structures), respectively, is observed. It should be noted that DTC and TTC refer to different thiols as core molecules (difunctional thiol or trifunctional thiol) and not to the number of MMs attached as mass spectrometry cannot distinguish between the different DTC or TTC products. (A discussion on the limitations of mass spectrometry in the detection of the number of arms follows shortly.) Further raising the thiol content results in slightly improved yields, however, both reactions can be considered successful transformations from the viewpoint of endgroup transformations.

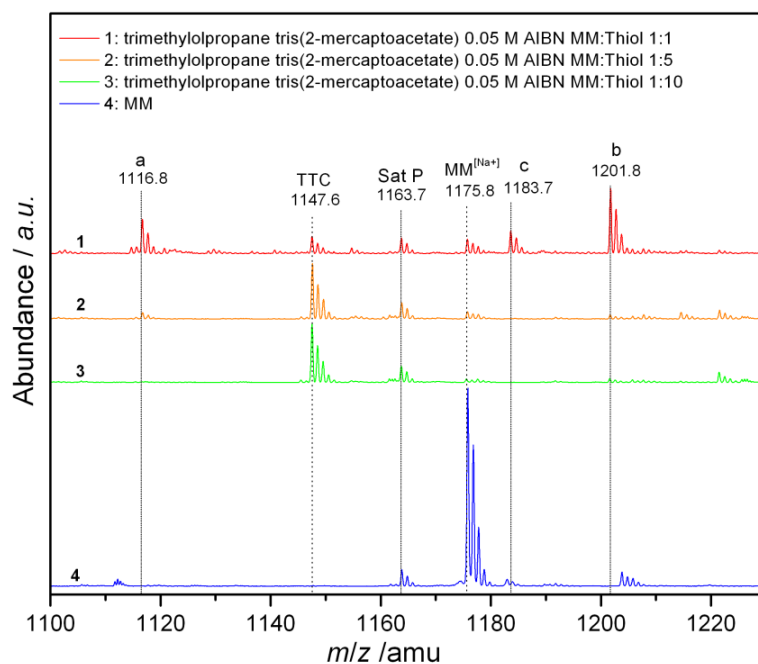


Figure 5-5: Thiol-ene coupling reactions carried out with 5 and 10 equivalents of thiol with respect to MM end groups, employing trimethylolpropane tris(2-mercaptoacetate). Samples were heated for 16 h at 60 °C, in butyl acetate as solvent.

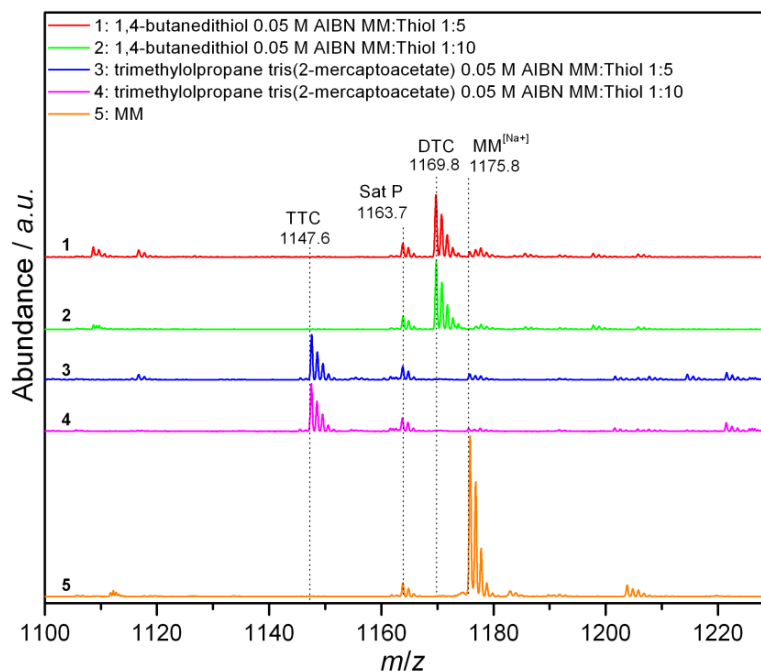


Figure 5-6: ESI-MS spectra of a series of experiments conducted with 1,4-butanedithiol and trimethylolpropane tris(2-mercaptoacetate), employing 0.05 mol·L<sup>-1</sup> AIBN with varying ratios of excess thiol.

Very small amounts of side products are observed in all cases, supporting the apparent efficiency of radical thiol-ene conjugations. Though the results are encouraging, further analysis of the products is nevertheless disappointing. Alongside the mass spectra presented in Figure 5-5, Figure 5-7 presents the resulting SEC traces of the reaction products. In all cases, no significant shift in molecular weight can be observed and the reaction products all have virtually the same molecular weight as the starting material. Such results are – judging from the overall good result from the mass spectrometric analysis – surprising only at first glance.

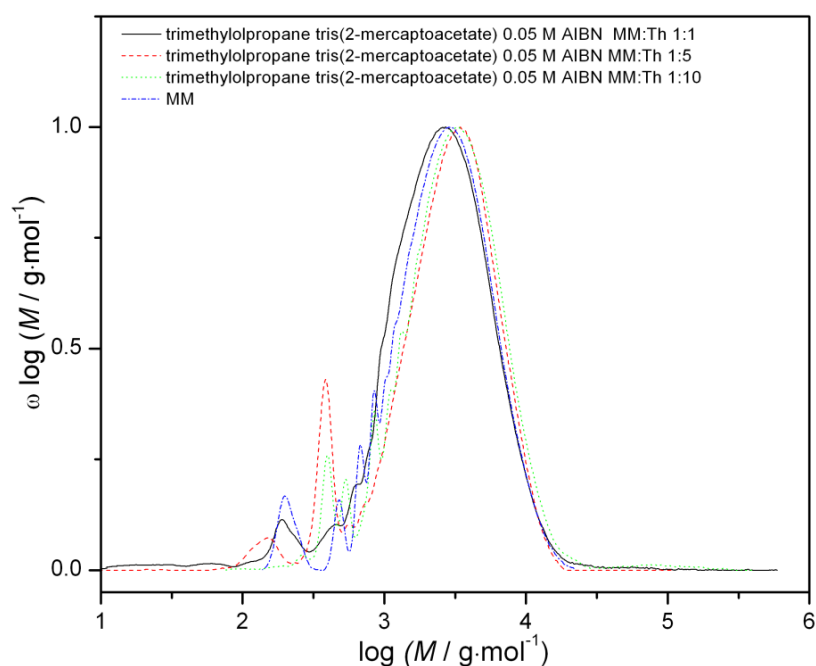


Figure 5-7: SEC elugrams of thiol-ene coupling reactions carried out with 5 and 10 equivalents of thiol with respect to MM end groups, employing trimethylolpropane tris(2-mercaptoacetate). Samples were heated for 16 h at 60 °C, in butyl acetate solution.

The macromonomer employed in the reactions is produced from auto-initiated polymerization, i.e. its molecular weight is an exact multiple of the monomer molar mass. Thus, mass spectrometry is able to show the conversion of double bonds, but based on the obtained  $m/z$  it is impossible to elucidate how many arms of the core molecule have reacted. Addition of one macromonomer onto a core molecule results in isobaric species compared to addition of  $n$  macromonomers to the  $n$ -functional thiol. Thus, taking the DTC species as an example, the reaction product where two macromonomers are attached to

the original dithiol compound and the product where only a single macromonomer chain was conjugated to the dithiol both appear at the same  $m/z$ , depending on the length of the macromonomer arm length, and are thus indistinguishable. Therefore, the results from mass spectrometry and SEC are not contradictory. As can be expected, the conversion of the alkene was successful, but due to the large excess of thiol, formation of star structures did not occur. Nevertheless, such experiments were mandatory to see if thiol-ene conjugation can be achieved under conditions reported in the literature. These conditions can hence subsequently be used as a starting point for a systematic investigation to refine reaction conditions to meet the needs of polymer-polymer conjugation. If essentially pure star structures are targeted, the thiol-ene reactions must be carried out in a true 1:1 ratio of starting materials as only under such conditions is it assured that little starting material remains at the end of the reaction and that all individual chains have been assembled into larger star structures. Slight excesses of the double bond-species may also be used, resulting in a product mixture of star polymers with some residual linear macromonomer chains. If the excess is small, i.e. in the order of a few percent only, such results might be tolerable from a materials point of view.

#### 5.2.2.2 Thiol-ene Conjugation of Butyl Acrylate Macromonomer and 1-Octanethiol

In order to optimize conditions for an equimolar conversion of thiol and ene, the system under investigation was switched to the simpler reaction of macromonomer with 1-octanethiol as this reduces the number of potential reactions and hence simplifies the interpretation of the mass spectra. If conditions can be identified under which such small monofunctional thiols can be conjugated onto a macromonomer in a 1:1 ratio, then one may proceed to more complex systems; a task that is demonstrated to be unachievable under the studied conditions.

Reaction conditions were systematically varied to find optimum conditions for quantitative conversion of thiols. Reactions were carried out with variations in thiol to ene ratios (both excesses of thiol groups to macromonomer groups and vice versa were studied), and finally variation in the concentration and type of initiator were carried out. The initiator was varied from a concentration of  $1.56 \cdot 10^{-3}$  to  $0.5 \text{ mol} \cdot \text{L}^{-1}$ , and the thiol was again reacted with macromonomer excesses ranging from 1 to 2 equivalents. Selected samples were carried

out with excess macromonomer, ranging from 1.1 to 2 equivalents of macromonomer with respect to thiol ratio.

Figure 5-8 presents the mass spectra of the final product mixtures after a thiol-ene reaction between the butyl acrylate macromonomer with varying equivalents of macromonomer to 1-octanethiol, initiated by  $0.05 \text{ mol}\cdot\text{L}^{-1}$  AIBN. All reactions employ a slight excess of macromonomer, as such conditions were deemed to be the most likely to produce the targeted star product. The goal was to keep the excess of macromonomer as low as possible, as remaining, unreacted linear chains are difficult to remove from the resulting product mixture. Thus, large excesses are not practical when a pure end product is required, even though it would facilitate generation of the desired star structures when the multifunctional cores are used.

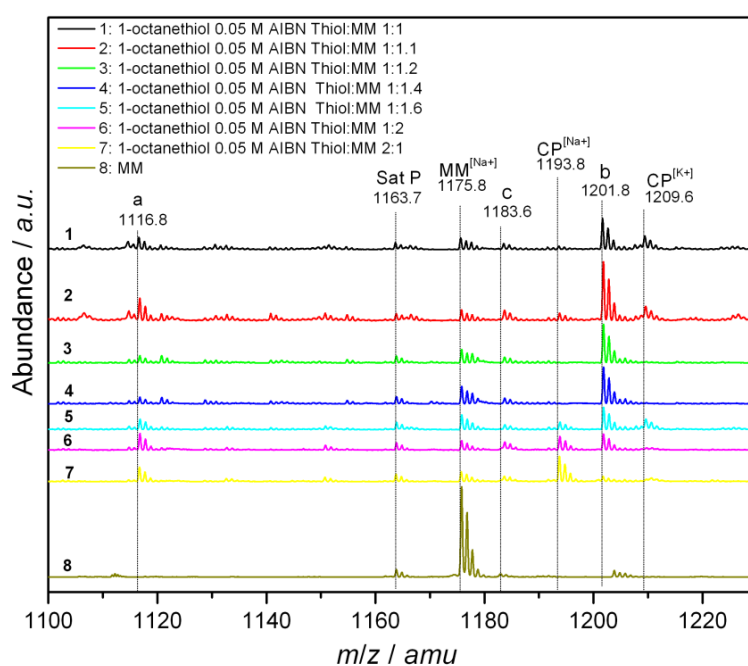


Figure 5-8: ESI-MS spectrum of the reaction between 1-octanethiol and butyl acrylate macromonomer showing one polymer repeat unit in the  $m/z$  range 1100 to 1230  $\text{g}\cdot\text{mol}^{-1}$  of the reaction mixture containing varying ratios of thiol to ene endgroups, initiated by  $0.05 \text{ mol}\cdot\text{L}^{-1}$  AIBN, after a reaction time of 16 h at  $60^\circ\text{C}$ . The spectra have been normalized relative to the Sat P peak.

Inspection of Figure 5-8 indicates that under the applied reaction conditions very little, if any, macromonomer-thiol conjugate is formed. However, when an excess of 2 equivalents of thiol to 1 equivalent of macromonomer ene groups is employed, conversion to the desired conjugate product is achieved (over 50 % of MM to the thiol-coupled species conversion is estimated).

Under all conditions, a number of side products do occur in the product spectra. Product **a** is a result of an AIBN radical reacting with a macromonomer chain to form an initiator fragment (i.e. cyano-isopropyl) terminated species. Identification of such a product in the reaction mixture is not surprising considering the large amounts of AIBN employed to initiate the thermal thiol-ene reaction; a concentration of  $0.05 \text{ mol}\cdot\text{L}^{-1}$  represents 0.5 equivalents in the reaction mixture. Small amounts of side product **c** can also be observed, the  $m/z$  value of which can be assigned to a macromonomer species carrying two initiator-derived fragments. The masses of both **a** and **c** are thus independent of the thiol employed. Another unidentified side product is found at 1201.8 Da, labeled **b**. This side product is possibly formed in a reaction resulting from the high concentration of AIBN. It should be noted that **b** is the main product observed under all conditions other than when 2 eq. of thiol are used, and therefore it is of critical importance to identify and/or minimize the extent of the reaction leading to **b**. To investigate its origin and to elucidate the reaction pathway by which it forms, further experiments were conducted with variations in the concentration of the employed AIBN initiator. Interestingly, under no conditions is (polymeric) disulfide observed, even though such coupling is known to occur in thiol-ene reactions. It may thus be concluded that once a thiyl radical has reacted with a macromonomer, the macroradical formed is unlikely to react with another thiyl radical but will almost certainly abstract a proton from any surrounding source (a coupling of a thiyl radical with primary initiator fragments can be excluded based on their absence in the mass spectra).

### 5.2.2.3 Variation of AIBN Initiator Concentration

Figure 5-9 presents the results of a series of experiments where the effect of initiator concentration on the resulting product mixture was explored, now using 1,4-butanedithiol as the conjugation point. AIBN has a half life of 10 h at 66 °C, and in the context of these experiments (having been conducted at 60 °C for 16 h), one would expect that the

concentration of AIBN would affect the final product composition, since just under half of the AIBN is still present after the first 10 h of reaction. Figure 5-9 illustrates clearly that the initiator concentration is, within broad limits ( $1.6 \cdot 10^{-3} \text{ mol} \cdot \text{L}^{-1}$  to  $1.25 \cdot 10^{-2} \text{ mol} \cdot \text{L}^{-1}$ ), not a factor in determining the composition of the final product. The spectra are almost identical in all respects and following these observations, it was concluded that a minimum concentration of  $0.05 \text{ mol} \cdot \text{L}^{-1}$  AIBN is required for conversion of the macromonomer into – at least some amounts – of the desired conjugate product. In agreement with this observation, comparable trends in the product spectra are observed, when a variation of the thiol:MM ratio is performed as in Figure 5-8 at a lowered initiator concentration. Increasing the thiol:initiator ratio appears to be slightly beneficial, but the amount of side products being formed does not change significantly.

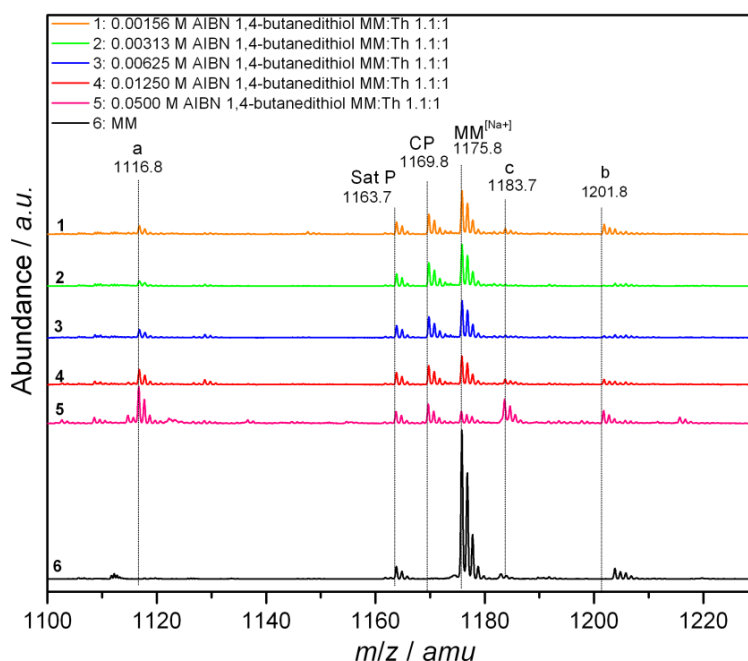


Figure 5-9: ESI-MS spectrum of the reaction between 1,4-butanedithiol and butyl acrylate macromonomer showing one polymer repeat unit in the  $m/z$  range 1100 to 1230  $\text{g} \cdot \text{mol}^{-1}$  of the reaction mixtures containing varying concentrations of AIBN initiator, after a reaction time of 16 h at 60 °C. The spectra have been normalized relative to the Sat P peak.

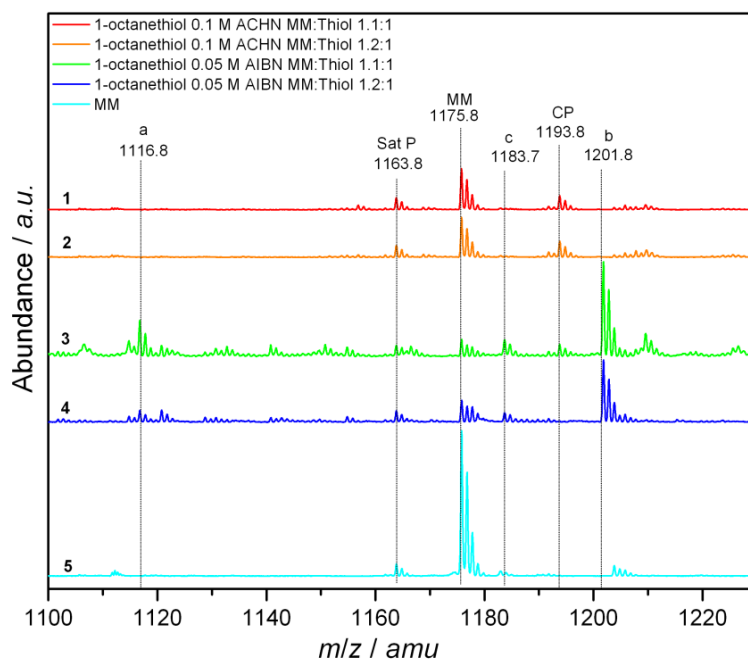


Figure 5-9: ESI-MS spectrum of the reaction between 1-octanethiol and butyl acrylate macromonomer showing one polymer repeat unit in the  $m/z$  range 1100 to 1230  $\text{g}\cdot\text{mol}^{-1}$  of the reaction mixtures containing AIBN or ACHN initiator, after a reaction time of 16 h at 60 °C. The spectra have been normalized relative to the Sat P peak.

As no plausible structure can yet be assigned to species **b**, experiments were conducted using 1,1-azobis(cyclohexanecarbonitrile), ACHN, to investigate whether a change in initiator affects the positioning of **b** on the  $m/z$  axis, and to confirm whether the side products are a result of the particular initiator utilized (if **b** was formed upon reaction with initiator fragments, a shift in mass should be observed when changing the initiator). The resulting mass spectra are presented in Figure 5-10. In fact, **b** is absent in the product spectra when ACHN is employed. However, as ACHN has a longer half life compared to AIBN, the change in initiator also caused a change in radical flux, and the absence of **b** indicates that the origin of this species is initiator-related, but does not entirely prove this hypothesis. ACHN was employed at twice the concentration of AIBN to attempt to somewhat equalize the radical flux, although no quantitative assessment of the radical flux was attempted. Nevertheless, the fact that **b** occurs at the same  $m/z$  regardless of the thiol employed also supports the hypothesis of this species being dependent on the type of initiator.

## 5.2.2.4 Excess Macromonomer to Thiol

The effect of increasing the macromonomer content was also investigated to determine if the increased macromonomer would facilitate the synthesis of the desired products, even if the amount of leftover macromonomer after the reaction would not be tolerable for most purposes. From a scientific point of view, it is however an important question whether an excess of alkene has similar benefits as an excess of thiol. Thus, reactions with the multifunctional thiols in a ratio of MM:thiol of 2:1 were performed. ESI-MS spectra can be seen in Figure 5-8, graph 6 (1-octanethiol); Figure 5-11 (l.h.s) graph 1 (1,4-butanedithiol) and Figure 5-11 (r.h.s), graph 6 (trimethylolpropane tris(2-mercaptoacetate)).

In such cases where there is a significant excess of MM in relation to thiol, a complete disappearance of the MM species cannot be expected when looking at the mass spectra and at best a one to one ratio of starting material to conjugation product can be envisaged if the initial ratio was a two-fold excess of MM with respect to thiol. Analysis of the spectra immediately indicates that while the desired product is formed, large amounts of **a**, **b** and **c** are also formed in significant amounts, demonstrating the repeated failure of the procedure.

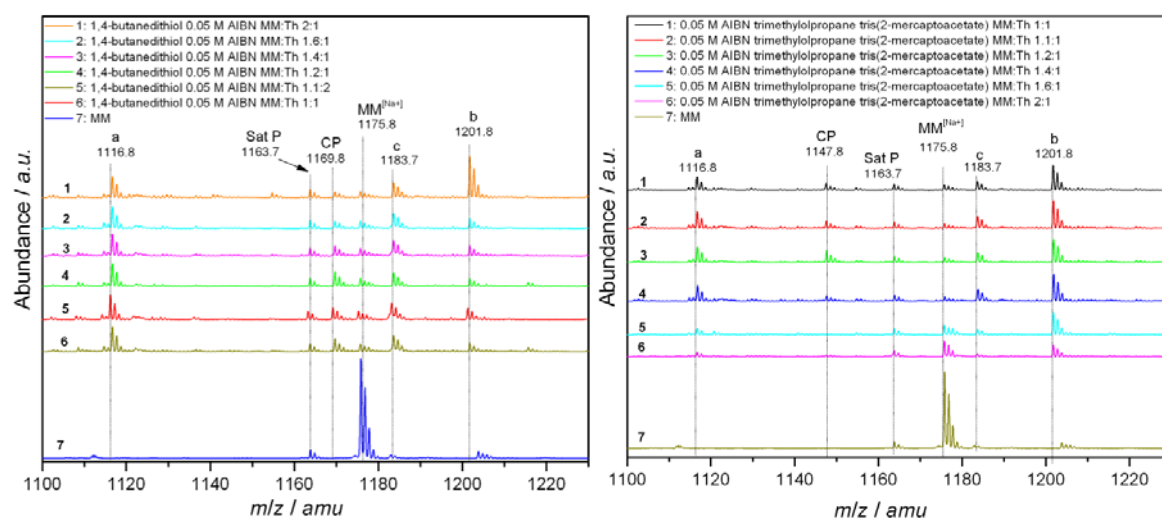


Figure 5-10: (l.h.s) ESI-MS spectra of a series of experiments conducted using 1,4-butanedithiol, employing 0.05 M AIBN with varying ratios of excess macromonomer to thiol. (r.h.s) ESI-MS spectra of a series of experiments conducted using trimethylolpropane tris(2-mercaptoacetate), employing 0.05 mol·L<sup>-1</sup> AIBN with varying ratios of excess MM to thiol.

It must however be noted that the analysis by ESI-MS may be misleading. If star-polymer assembly was indeed successful, significantly higher  $m/z$  values are reached and the reaction product might not be as clearly identifiable in the spectra due to the limited accessible molar mass range. As a consequence, the mass spectrometric data might overemphasize side products, which is supported by the apparent improvement in results for the difunctional thiol compared to the trifunctional thiol (where significantly higher masses are potentially formed). Therefore, the reaction products have also been subjected to SEC analysis to analyze the molecular weight of the product.

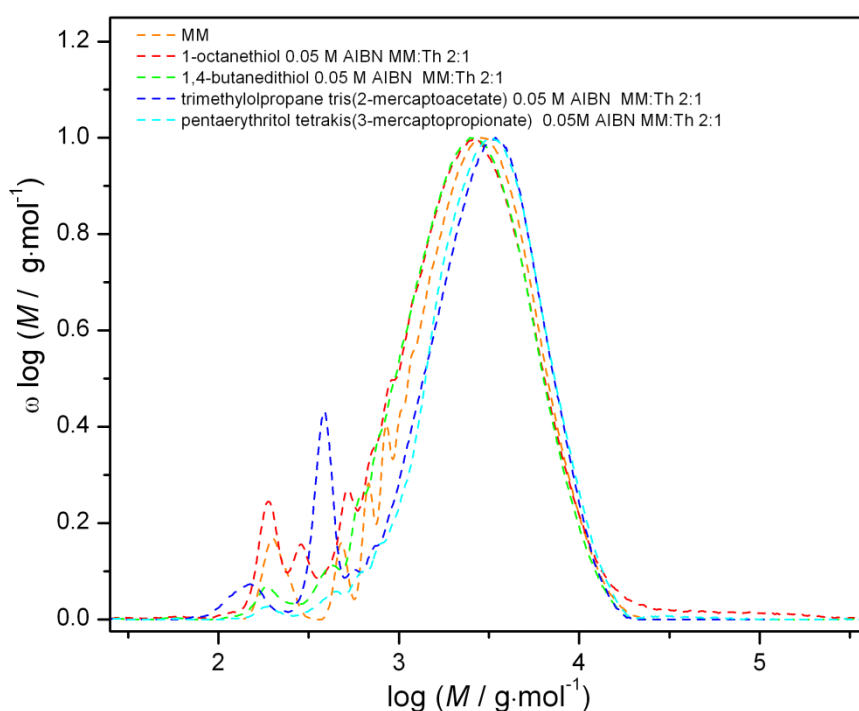


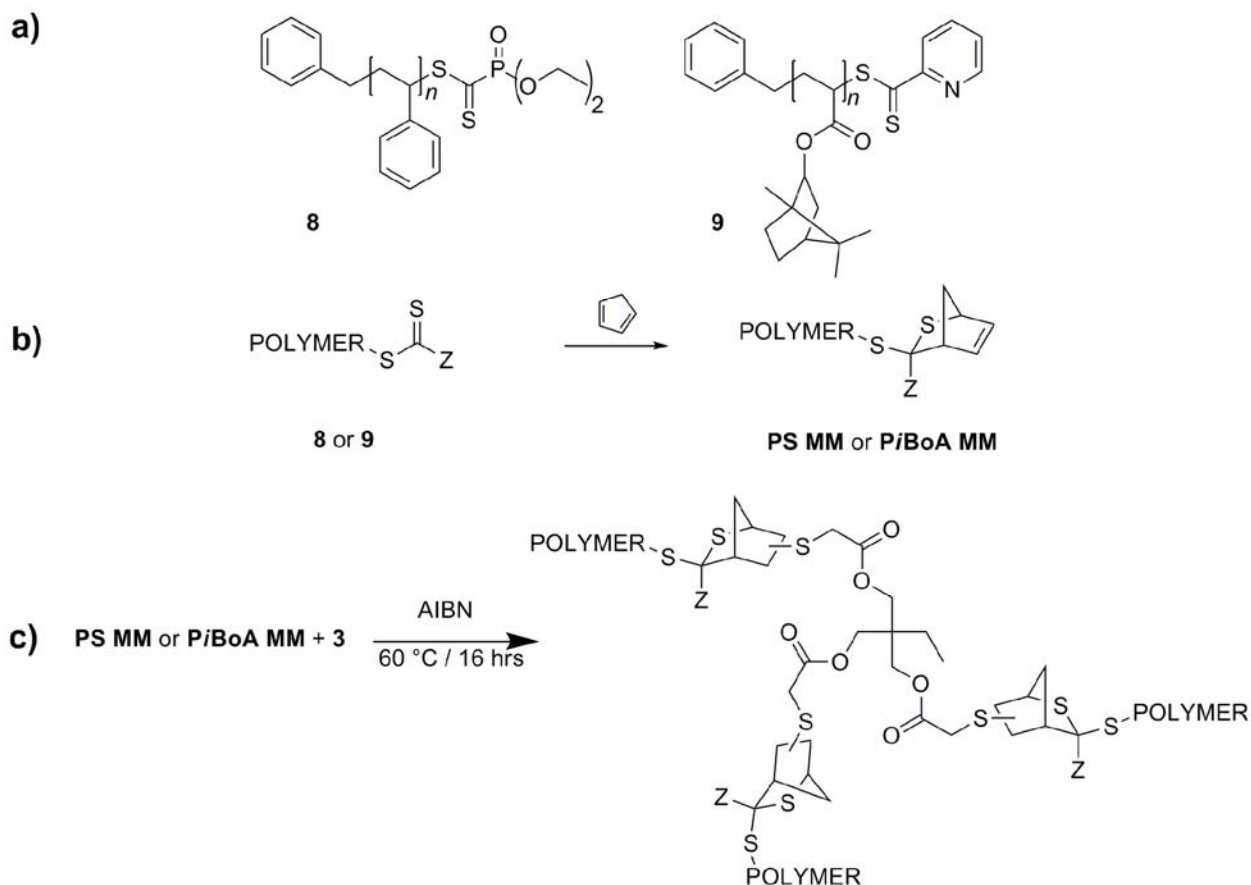
Figure 5-11: Molecular weight distributions of the starting macromonomer material, and product mixtures after the thiol-ene reaction with 1-octanethiol, 1,4-butanedithiol, trimethylolpropane tris(2-mercaptoacetate) and pentaerythritol tetrakis(3-mercaptopropionate). All samples were prepared using  $0.05 \text{ mol}\cdot\text{L}^{-1}$  AIBN, and heated for 16 h at  $60 \text{ }^\circ\text{C}$ , in butyl acetate solution, with the MM to thiol ratio as specified in the graph. One representative elugram was selected for each thiol studied as no significant shift was observed in any sample.

Figure 5-12 presents the SEC traces after the reaction of a two-fold excess of macromonomer for the different thiols employed in this work. Although a slight shift in the traces is observed with increasing number of available arms on the core molecule, no significant increase in  $M_n$  of the samples can be observed. As mentioned above, a two-fold increase in molecular weight is not expected due to the leftover starting material. However, as SEC yields a weighted distribution, a clear shift of the distributions (with an increased polydispersity) should be seen if the star formation was indeed successful. Thus, the SEC results confirm the observation made by mass spectrometry that some star polymer product is formed as evidenced by the presence of a congruent species in the mass spectrum and the slight shift observed by chromatography. However, conversion of the macromonomer *and* of the thiol is far from complete and side products seem to be formed in at least similar numbers as the targeted structures.

#### 5.2.2.4.1 Polystyrene and poly(isobornyl acrylate) Thiol-ene Star Polymer Assembly

To eliminate the possibility that the polydispersity of the MM species is masking any shift in the SEC chromatogram, a narrowly distributed polymer system, in the form of low PDI poly(isobornyl acrylate) with a terminal vinyl function was prepared and subjected to radical thiol-ene coupling in a separate small study by Andrew Inglis at the Macroarc group at the KIT. The data will now be presented, however the results remain – qualitatively – identical to those described above.

Poly(styrene) **8** and poly(isobornyl acrylate) **9** were synthesized by RAFT polymerization (Scheme 5-8a). These two polymers were subsequently modified *via* a hetero Diels-Alder cycloaddition with cyclopentadiene to produce a structure analogous to the BA MM which contains an unsaturated bond that can be further reacted (Scheme 5-8b).<sup>70</sup> Thiol-ene reactions were attempted with these modified polymers using the same thiol containing molecules as were used in the BA MM experiments (Scheme 5-8c). The advantage of using these RAFT prepared polymers is the reduction in *PDI*, which in turn allows any increases in molecular weight to be more clearly observed.



Scheme 5-8: a) Synthesized RAFT polymerization poly(styrene) (**8**) and poly(isobornyl acrylate) (**9**), (b) Hetero Diels-Alder cycloaddition of cyclopentadiene with dithioester-terminated polymers. (c) Final star structure after thiol-ene reaction of modified PS and PiBoA RAFT polymers.

Figure 5-13 presents the molecular weight distributions of the starting RAFT-HDA prepared macromonomers in comparison to those of their respective thiol-ene coupling products under varying macromonomer to thiol ratios using trimethylolpropane tris(2-mercaptoacetate). The left side of Figure 5-13 clearly demonstrates the effect of varying PS MM to thiol concentration on the conjugation product molecular weight distribution. In the most favorable scenario, when a 1:1 PS MM to thiol ratio is employed, a multi-modal molecular weight distribution is observed, with each of the modal peaks corresponding to starting product, 2-arm and 3-arm star material.

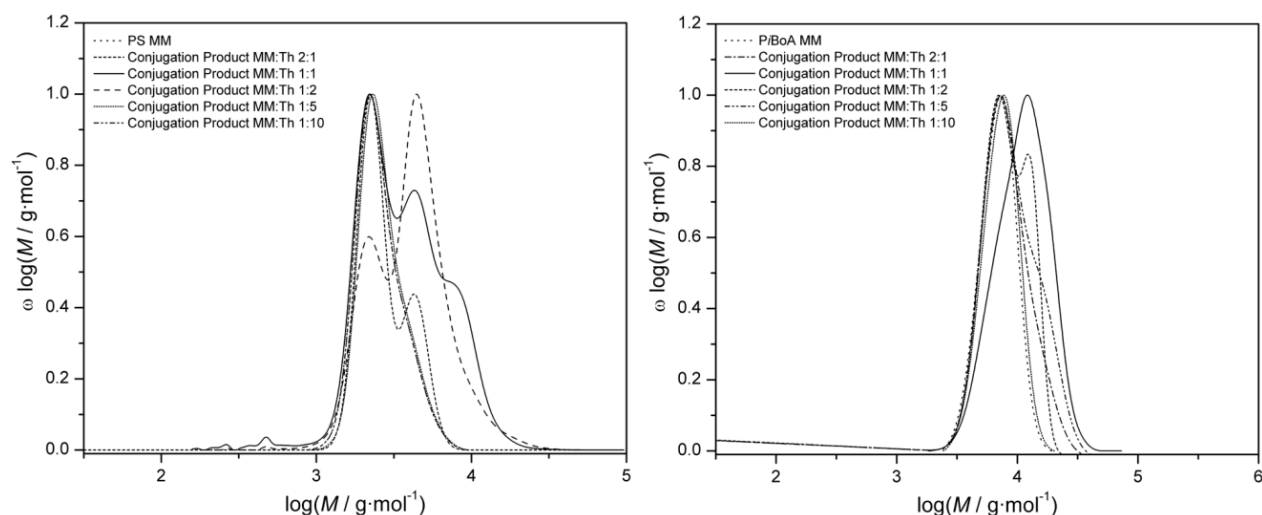


Figure 5-12: Comparative molecular weight distributions of poly(styrene) (l.h.s) and poly(isobornyl acrylate). (r.h.s) after thiol-ene coupling reactions performed with varying polymer to thiol ratio. The thiol core molecule used was trimethylolpropane tris(2-mercaptoacetate).

It is also worthwhile to note that from these distributions a clear distinction between starting material and the result of a single conjugation of a PS MM to the thiol core molecule cannot be made. When the PS MM to thiol ratio was changed to 1:2, as expected, more starting material appears to have been consumed. Furthermore, the predominant product appears to be a thiol core bearing two polymer arms. When the amount of thiol was further increased, the resulting product distribution closely resembles that of the starting material, indicative of the lack of star formation. The right side of Figure 5-12 shows the analogous results of the P/BoA MM thiol-ene coupling experiment. The molecular weight distributions are broader than in the case of the PS MM and thus provide data of lower resolution. However, it can still be discerned that the major product resulting from a coupling utilizing a 1:1 P/BoA MM to thiol ratio is the core bearing two polymeric arms. It cannot, however, be determined whether any 3-arm star material has been formed. Despite demonstrating a somewhat improved performance in the coupling reactions when compared to the BA MM, Figure 5-12 still provides proof that the thermal thiol-ene conjugation is far from quantitative in terms of achieving macromolecular star formation.

Variations of the reaction conditions were carried out beyond the above described experiments and that the presented data represents a cross-section of results for the sake of brevity. Duplicates of the reactions were performed to test for the reproducibility of the results. Furthermore, different reaction vessels, different amounts and types of solvent and methods for de-oxygenation were tested but without improvement on the results presented in Figure 5-12. This section was a summary of work carried out by Andrew Inglis at the Macroarc Group at the KIT.

### 5.2.3 Comparison – Functional and Block Copolymers, and Star Polymers *via* Radical Thiol-ene Chemistry

Independently from the research efforts presented above, the Polymer Chemistry Research group at UGhent focused on photo-initiated thiol-ene chemistry in the synthesis of functional polymers and amphiphilic block copolymers consisting of a poly(styrene) (PS) and a poly(vinyl acetate) (PVAc) segment, as a precursor of hydrophilic poly(vinyl alcohol) PVA. The results obtained by the PCR group will now be compared to the work describing attempted star synthesis in the previous section of this chapter.

The PCR group from Ghent University attempted the preparation of functional polymers as well as PS-*b*-PVAc block copolymers by UV initiated, metal-free thiol-ene chemistry. The strategy consisted of the independent synthesis of well-defined PS and PVAc homopolymers *via* RAFT, bearing thiol and allyl functional groups respectively, and further post-polymerization conjugation reactions *via* thiol-ene radical addition reaction. Although photo-initiation was employed in contrast to the thermally induced experiments of this thesis, the reaction proceeds *via* the same radical mechanism (Scheme 5-5). Campos *et al.* reported that thiol-ene photo-coupling was found to proceed with higher efficiency, in a shorter time, and with higher tolerance to various functional groups in comparison with its thermal counterpart.<sup>19</sup> The following section summarizes the work conducted by researchers at Ghent University.

The attempt to prepare PS-*b*-PVAc polymers by coupling PS-SH with PVAc containing an allyl end-group (PVAc=) was initially deemed successful when analyzed *via* SEC and FT-IR, indeed excellent agreement was found between the peak molecular weight  $M_p$  and number average molecular weights  $M_n$  of the homopolymers and the corresponding block copolymers. Quantitative <sup>1</sup>H-NMR (500 MHz, CDCl<sub>3</sub>, acetone-*d*<sub>6</sub>, DMSO-*d*<sub>6</sub> and THF-*d*<sub>8</sub>)

surprisingly revealed a conjugation efficiency of only 25 % and a variation of solvent did not provide different conjugation efficiency values. Elemental analysis was then performed to verify the results obtained by  $^1\text{H}$  NMR analysis, which were in conflict with the SEC and FT-IR results. The exact carbon, hydrogen, oxygen and sulfur content of the purified product was determined and results obtained for the oxygen content were consistent with the  $^1\text{H}$ -NMR results (3.3 % oxygen content measured compared to the theoretically expected 14 %, indicating a 23 % conjugation efficiency), thus leading the PCR group to the conclusion that (radical) thiol-ene reactions are not efficient for polymer conjugation reactions, if a one to one thiol-to-ene initial ratio is used.

Blank reactions consisting of the application of the typical thiol-ene coupling conditions (irradiation time of 1 h, DMPA photo-initiator present) to a reaction mixture containing only PS-SH (no PVAc= was present) were performed to reveal the cause of the clear shift that was observed in SEC analysis. After irradiation for 1 hour, a slight shift toward higher molecular weights was noticed in the chromatogram, which was attributed to the formation of disulfide species. Thus, while the initial SEC analysis of the reaction product from the attempt to conjugate the PS-SH and PVAc= blocks indicated a success of the reaction, closer analysis revealed that the reaction was not at all successful but rather that the product mixture contained mostly random termination products. The PCR group concluded that coupling reactions *via* bimolecular termination reactions occur as competitive side reactions in thiol-ene polymer conjugation reactions of PS-SH and PVAc=, underpinning that thiol-ene chemistry has severe limitations when targeting polymer-polymer conjugation reactions. It is interesting to note that in the case of star formation, no disulfide species were seen in the mass spectra.

The Ghent group in Belgium also conducted experiments with an excess of 5 equivalents of PS-SH to try to increase the efficiency of the conjugation reaction, but however the coupling efficiency remained the same. Moreover, longer irradiation times also did not improve the conjugation yield. In the work pertaining to star formation, using excess equivalents improved the thiol-ene coupling, but however, with excess equivalents of thiol star formation is unlikely to occur and many unreacted thiol groups remain at the end of the reaction.

#### 5.2.4 Summary – Radical Thiol-ene Coupling as a *Click* Reaction

The results from both the work carried out in this thesis and the investigation carried out by the PCR group in Ghent are generally in good agreement with each other despite their relatively large difference in synthetic scope, starting materials and method of initiation employed. Even though the initial experiments undertaken in Ghent at first glance indicated success of the reaction and are seemingly in disagreement with the results from the star polymer formation experiments, both studies come to the same conclusion when the conjugation product mixtures are characterized in-depth. From all the experiments carried out, it is abundantly clear that considerable difficulties are present in both thermally and photo-chemically induced radical thiol-ene reactions when polymer-polymer conjugations are targeted in quantitative conversions. Neither variation of the initiator concentration (and type of initiator/initiation method), nor variation of the macromonomer to thiol concentration ratio or type of macromonomer lead to optimized conditions of the reaction allowing for quantitative formation of the desired conjugation products. It seems that only a large excess of thiol allows for the formation of the targeted structures without significant amounts of side products.

Generally, the similarity between thermal and photo-chemical initiation is not surprising. From a kinetic point of view, the applied radical source is more or less irrelevant as the competing reactions are chain stopping events *vs* the propagation and the ene-addition reactions, thus comprising reactions that do not directly involve initiator fragments.

In summary, it can be stated that:

- (i) conjugation of a polymer with a small molecule counterpart works reasonably well, even if an excess of the low molecular weight compound must be used to achieve high conjugation efficiencies.
- (ii) polymer-polymer conjugation largely fails if the starting materials are employed in (or close to) equimolar ratios.
- (iii) the radical flux has only a limited effect on the outcome of the coupling reaction as a change in initiator concentration on one hand and a switch from dedicated UV-lamp irradiation towards sunlight as UV-source on the other hand did not have a critical influence on the product.

- (iv) the reason for failure in both research strands are qualitatively similar, i.e. head-to-head coupling reactions that stop the propagation cycle of the thiol-ene process.

Only one small difference exists, which might explain why frequently better conjugation efficiencies are observed from photochemical thiol-ene reactions. Ideally, the primary radicals would only abstract protons from the thiol. However, a fraction of the initiator fragments will add to the ene as a competitive side reaction, which in turn can start a thiol-ene reaction cycle, but finally leads to the formation of an undesired (non-conjugated) product. Thus, in principle, radical initiators should be employed that are comparatively slow in adding to the ene. For the photo-initiator DMPA it is known that its benzoyl fragment is a fast initiator whereas the second fragment might only be available for termination or proton abstraction, potentially aiding the overall process.<sup>71</sup> However, as only very limited data on initiation efficiencies are available to date, such a hypothesis remains speculative and an extensive experimental series would be required to confirm it.

Regardless, as the initiation rate depends on the type of initiator and the ene (and of course the thiol with respect to the rate of proton abstraction), this implies that suitable initiators must be evaluated for each particular system, an approach that is not very promising if thiol-ene is proposed as a universal conjugation tool. Independent of the choice of initiator, an increase in the thiol to initiator concentration will have a beneficial effect, because transfer of the initiator fragment radicals onto a thiol will become more likely. In addition, termination of initiator fragments, as observed by ESI-MS, will occur to a lesser extent. The fact that functionalization of the chain ends *via* radical thiol-ene is largely successful, when the thiol is employed in excess, can be explained by this effect. For polymer-polymer conjugation, where the thiol concentration cannot be increased, a similar effect can only be reached by reducing the initiator concentration. This reduced initiator concentration, however, also leads to a significantly reduced rate of reaction and consequently unfeasibly long reaction times are required to reach full conversions while at the same time side reactions are not completely eliminated.

Any radical reaction proceeds to a certain extent with the formation of side reaction due to the high reactivity of the radicals and the sequential nature of the reaction. The termination reactions as observed in both investigations appear to be unavoidable. Moreover, both cases show that it is not possible to suppress these side reactions to a sufficient degree if

the thiol and ene compound are employed in equimolar ratios and in particular if polymeric starting materials are used. The somewhat better efficiencies that are observed for the coupling reactions with small molecules might indicate that the thiol-ene propagation reaction is subject to a diffusional control mechanism.

Ultimately, radical thiol-ene may only be used as a polymer conjugation tool if either the thiol or the ene is used in excess or if substantial side product formation is acceptable. Both approaches require tedious additional work-up procedures, which is a direct violation of the *click* concept.<sup>33</sup> Only for small molecules is such a purification potentially easily performed (for example by precipitation or evaporation). Thus, radical thiol-ene is only effective if one can sacrifice efficiency and is satisfied with only partial conjugation, for example when grafting to surfaces or microspheres.<sup>72</sup>

Based on the findings as well as the definition of *click* chemistry, its implications and requirements for polymer-polymer conjugation, the conclusion is that *radical* thiol-ene conjugation chemistry should not be referred to as a *click* reaction. The criterion of a high reaction efficiency is clearly not fulfilled as a significant number of polymer byproducts must be expected when trying to conjugate two polymer blocks. Even if reaction conditions should exist under which successful polymer conjugation may be performed, the reaction clearly cannot serve as a general chemical tool. The *click* philosophy implies that the window of reaction conditions under which a reaction can be applied must be relatively wide and this is certainly not the case for radical thiol-ene chemistry polymer conjugation.

### 5.3 Conclusions

The first part of this section of work detailed the facile synthesis of butyl acrylate macromonomers in high yield. High temperature auto-initiated polymerization of butyl acrylate affords a highly ordered product that consists almost quantitatively of uniform macromonomeric structures that may be further used to build complex molecular architectures. The self-organized synthesis itself is highly efficient, simple and, except for the high temperature required, the synthesis is cost and time-effective as no purification and/or isolation steps are required either during or after the reaction.

The second part of this section of work employs the butyl acrylate macromonomers to attempt the formation of 4 arm star polymers *via* the grafting to approach, employing thermal radical thiol-ene chemistry to produce the coupling. The results are confirmed by

experiments carried out at the PCR group at Ghent University, where they investigated the functionalization and production of block copolymers *via* UV-initiated radical thiol-ene chemistry. The overall success of the coupling reaction was low, and as a result, it is clear that *radical* thiol-ene conjugation chemistry should not be referred to as a *click* reaction. Radical thiol-ene, as a polymer conjugation tool, is only successful if either the thiol or the ene is used in large excess or if substantial side product formation is acceptable. Furthermore, for the purpose of polymer-polymer conjugation for star formation, where the thiol concentration cannot be increased, a similar effect can only be reached by reducing the initiator concentration. This, however, also leads to greatly reduced rates of reaction and unfeasibly long reaction times are thus required to reach full conversions. At the same time side reactions are not completely eliminated so radical thiol-ene cannot be considered a useful reaction for polymer-polymer conjugations. Therefore, while functionalization of polymer chains with small molecules can be carried out without many problems, polymer-polymer conjugation can only be achieved when the thiol is in excess of the ene component. Thus, radical thiol-ene cannot be considered to be an efficient *click* reaction in a polymer chemistry context.

The conclusions arrived at by the PCR group in Ghent are that, in cases where block copolymers are sought, bimolecular termination reactions occur as competitive side reactions in thiol-ene polymer conjugation reactions (of PS-SH and PVAc=), underpinning that thiol-ene chemistry has severe limitations when targeting polymer-polymer conjugation reactions.

The two studies concur with each other and together they show conclusively that radical thiol-ene chemistry is not and cannot be classified as a *click* reaction when polymer-polymer conjugation is attempted, despite having proven itself a highly expedient method in small molecule chemistry.

---

## 5.4 References

- 1 Hadjichristidis, N.; Iatrou, H.; Pitsikalis, M.; Pispas, S.; Avgeropoulos, A. *Prog. Polym. Sci.* 2005, 30, 725-782.
- 2 Wang, J.-S.; Matyjaszewski, K. *J. Am. Chem. Soc.* 1995, 117, 5614-5615.
- 3 Matyjaszewski, K. *Prog. Polym. Sci.*, 30, 858-875.
- 4 Hawker, C. J.; Bosman, A. W.; Harth, E. *Chem. Rev.* 2001, 101, 3661-3688.
- 5 Dufils, P.-E.; Chagneux, N.; Gimes, D.; Trimaille, T.; Marque, S. R. A.; Bertin, D.; Tordo, P. *Polymer* 2007, 48, 5219-5225.
- 6 Chiefari, J.; Chong, Y. K.; Ercole, F.; Krstina, J.; Jeffery, J.; Le, T. P. T.; Mayadunne, R. T. A.; Meijs, G. F.; Moad, C. L.; Moad, G.; Rizzardo, E.; Thang, S. H. *Macromolecules* 1998, 31, 5559-5562.
- 7 Moad, G.; Rizzardo, E.; Thang, S. H. *Aust. J. Chem.* 2006, 59, 669-692.
- 8 Evans, R. A. *Aust. J. Chem.* 2007, 60, 384-395.
- 9 Boutevin, B.; David, G.; Boyer, C. In *Advances in Polymer Science*; Springer Berlin, 2007, p 31-135.
- 10 Chiefari, J.; Jeffery, J.; Mayadunne, R. T. A.; Moad, G.; Rizzardo, E.; Thang, S. H. *Macromolecules* 1999, 32, 7700-7702.
- 11 Yamada, B.; Zetterlund, P. B. *Handbook of Radical Polymerization*; Wiley, 2002.
- 12 Moad, C. L.; Barner-Kowollik, C. *Handbook of RAFT Polymerization*; Wiley-VCH, 2008.
- 13 Lehrle, R. S.; Shortland, A. *Eur. Polym. J.* 1988, 24, 425-429.
- 14 Clouet, G.; Chaumont, P.; Corpart, P. *J. Polym. Sci., Part A: Polym. Chem.* 1993, 31, 2815-2824.
- 15 Srinivasan, S.; Lee, M. W.; Grady, M. C.; Soroush, M.; Rappe, A. M. *Journal of Physical Chemistry A* 2009, 113, 10787-10794.
- 16 Nising, P.; Meyer, T.; Carloff, R.; Wicker, M. *Macromol. Mater. Eng.* 2005, 290, 311-318.
- 17 Zorn, A.-M.; Junkers, T.; Barner-Kowollik, C. *Macromol. Rapid Commun.* 2009, 30, 2028-2035.
- 18 Bennet, F.; Lovestead, T. M.; Barker, P. J.; Davis, T. P.; Stenzel, M. H.; Barner-Kowollik, C. *Macromol. Rapid Commun.* 2007, 28, 1593-1600.
- 19 Campos, L. M.; Killips, K. L.; Sakai, R.; Paulusse, J. M. J.; Damiron, D.; Drockenmuller, E.; Messmore, B. W.; Hawker, C. J. *Macromolecules* 2008, 41, 7063-7070.
- 20 Chan, J. W.; Yu, B.; Hoyle, C. E.; Lowe, A. B. *Chem. Commun.* 2008, 4959-4961.
- 21 Chan, J. W.; Yu, B.; Hoyle, C. E.; Lowe, A. B. *Polymer* 2009, 50, 3158-3168.
- 22 Dondoni, A. *Angew. Chem., Int. Ed. Engl.* 2008, 47, 8995-8997.
- 23 Hoyle, C. E.; Lowe, A. B.; Bowman, C. N. *Chem. Soc. Rev.* 2010, 39, 1355-1387.
- 24 Killips, K. L.; Campos, L. M.; Hawker, C. J. *J. Am. Chem. Soc.* 2008, 130, 5062-5064.
- 25 Posner, T. *Berichte der deutschen chemischen Gesellschaft* 1905, 38, 646-657.
- 26 Mayo, F. R.; Walling, C. *Chem. Rev.* 1940, 27, 351-412.
- 27 Griesbaum, K. *Angew. Chem., Int. Ed. Engl.* 1970, 9, 273-287.
- 28 Braun, J. v.; Murjahn, R. *Berichte der deutschen chemischen Gesellschaft (A and B Series)* 1926, 59, 1202-1209.
- 29 Hoyle, C. E.; Lee, T. Y.; Roper, T. *Journal of Polymer Science Part A: Polymer Chemistry* 2004, 42, 5301-5338.
- 30 Gress, A.; Volkel, A.; Schlaad, H. *Macromolecules* 2007, 40, 7928-7933.
- 31 Carioscia, J. A.; Stansbury, J. W.; Bowman, C. N. *Polymer* 2007, 48, 1526-1532.

- 
- 32 Cook, W. D.; Chen, F.; Pattison, D. W.; Hopson, P.; Beaujon, M. *Polymer International* 2007, 56, 1572-1579.
- 33 Kolb, H. C.; Finn, M. G.; Sharpless, K. B. *Angew. Chem., Int. Ed. Engl.* 2001, 40, 2004-2021.
- 34 Unal, S.; Lin, Q.; Mourey, T. H.; Long, T. E. *Macromolecules* 2005, 38, 3246-3254.
- 35 Kadokawa, J.-i.; Kaneko, Y.; Yamada, S.; Ikuma, K.; Tagaya, H.; Chiba, K. *Macromol. Rapid Commun.* 2000, 21, 362-368.
- 36 Singh, R.; Verploegen, E.; Hammond, P. T.; Schrock, R. R. *Macromolecules* 2006, 39, 8241-8249.
- 37 Jo, Y. S.; van der Vlies, A. J.; Gantz, J.; Antonijevic, S.; Demurtas, D.; Velluto, D.; Hubbell, J. A. *Macromolecules* 2008, 41, 1140-1150.
- 38 Abraham, S.; Choi, J. H.; Ha, C.-S.; Kim, I. J. *Polym. Sci., Part A: Polym. Chem.* 2007, 45, 5559-5572.
- 39 Dag, A.; Durmaz, H.; Tunca, U.; Hizal, G. J. *Polym. Sci., Part A: Polym. Chem.* 2009, 47, 178-187.
- 40 Kaur, I.; Misra, B. N.; Gupta, A.; Chauhan, G. S. J. *J. Appl. Polym. Sci.* 1998, 69, 599-610.
- 41 Lima, V.; Jiang, X.; Brokken-Zijp, J.; Schoenmakers, P. J.; Klumperman, B.; Linde, R. V. D. J. *Polym. Sci., Part A: Polym. Chem.* 2005, 43, 959-973.
- 42 Lutz, J.-F. *Angew. Chem., Int. Ed. Engl.* 2007, 46, 1018-1025.
- 43 Angell, Y. L.; Burgess, K. *Chem. Soc. Rev.* 2007, 36, 1674-1689.
- 44 Moses, J. E.; Moorhouse, A. D. *Chem. Soc. Rev.* 2007, 36, 1249-1262.
- 45 Lutz, J. F.; Schlaad, H. *Polymer* 2008, 49, 817-824.
- 46 Iha, R. K.; Wooley, K. L.; Nyström, A. M.; Burke, D. J.; Kade, M. J.; Hawker, C. J. *Chem. Rev.* 2009, 109, 5620-5686.
- 47 Johnson, J. A.; Finn, M. G.; Koberstein, J. T.; Turro, N. J. *Macromol. Rapid Commun.* 2008, 29, 1052-1072.
- 48 Becer, C. R.; Hoogenboom, R.; Schubert, U. S. *Angew. Chem., Int. Ed. Engl.* 2009, 48, 4900-4908.
- 49 Sinnwell, S.; Inglis, A. J.; Davis, T. P.; Stenzel, M. H.; Barner-Kowollik, C. *Chem. Commun.* 2008, 2052 - 2054.
- 50 Carioscia, J. A.; Lu, H.; Stanbury, J. W.; Bowman, C. N. *Dent. Mater.* 2005, 21, 1137-1143.
- 51 Campos, L. M.; Meinel, I.; Guino, R. G.; Schierhorn, M.; Gupta, N.; Stucky, G. D.; Hawker, C. J. *Adv. Mater.* 2008, 20, 3728-3733.
- 52 Chen, G.; Amajjahe, S.; Stenzel, M. H. *Chem. Commun.* 2009, 1198-1200.
- 53 Bickel, C. L. J. *Am. Chem. Soc.* 1950, 72, 1022-1023.
- 54 Wu, D.-C.; Liu, Y.; He, C.-B. *Macromolecules* 2008, 41, 18-20.
- 55 Liu, Y.-L.; Tsai, S.-H.; Wu, C.-S.; Jeng, R.-J. *J. Polym. Sci., Part A: Polym. Chem.* 2004, 42, 5921-5928.
- 56 Maraval, V.; Laurent, R.; Donnadiou, B.; Mauzac, M.; Caminade, A.-M.; Majoral, J.-P. *J. Am. Chem. Soc.* 2000, 122, 2499-2511.
- 57 Moszner, N.; Rheinberger, V. *Macromol. Rapid Commun.* 1995, 16, 135-138.
- 58 Mantovani, G.; Lecolley, F.; Tao, L.; Haddleton, D. M.; Clerx, J.; Cornelissen, J. J. L. M.; Velonia, K. J. *Am. Chem. Soc.* 2005, 127, 2966-2973.
- 59 Nurmi, L.; Lindqvist, J.; Randev, R.; Syrett, J.; Haddleton, D. M. *Chem. Commun.* 2009, 2727-2729.
- 60 Sumerlin, B. S.; Vogt, A. P. *Macromolecules* 2009, 43, 1-13

- 
- 61 Li, M.; De, P.; Gondi, S. R.; Sumerlin, B. S. J. *Polym. Sci., Part A: Polym. Chem.* 2008, 46, 5093-5100.
  - 62 Barner-Kowollik, C.; Inglis, A. J. *Macromolecular Chemistry and Physics* 2009, 210, 987-992.
  - 63 Inglis, Andrew J.; Sinnwell, S.; Stenzel, Martina H.; Barner-Kowollik, C. *Angew. Chem., Int. Ed. Engl.* 2009, 48, 2411-2414.
  - 64 Inglis, A. J.; Pierrat, P.; Muller, T.; Brase, S.; Barner-Kowollik, C. *Soft Matter* 2010, 6, 82-84.
  - 65 Becer, C. R.; Hoogenboom, R.; Schubert, Ulrich S. *Angew. Chem., Int. Ed. Engl.* 2009, 48, 4900-4908.
  - 66 Junkers, T.; Bennet, F.; Koo, S. P. S.; Barner-Kowollik, C. *J. Polym. Sci., Part A: Polym. Chem.* 2008, 46, 3433-3437.
  - 67 Barner-Kowollik, C. *Macromol. Rapid Commun.* 2009, 30, 1625-1631.
  - 68 Koo, S. P. S.; Junkers, T.; Barner-Kowollik, C. *Macromolecules* 2009, 42, 62-69.
  - 69 Günzler, F.; Wong, E. H. H.; Koo, S. P. S.; Junkers, T.; Barner-Kowollik, C. *Macromolecules* 2009, 42, 1488-1493.
  - 70 Inglis, A. J.; Sinnwell, S.; Stenzel, Martina H.; Barner-Kowollik, C. *Angew. Chem.* 2009, 121, 2447-2450.
  - 71 Szablan, Z.; Junkers, T.; Koo, S. P. S.; Lovestead, T.; Davis, T. P.; Stenzel, M. H.; Barner-Kowollik, C. *Macromolecules* 2007, 40, 6820-6833.
  - 72 Goldmann, A. S.; Walther, A.; Joso, R.; Ernst, D.; Loos, K.; Nebhani, L.; Barner-Kowollik, C.; Barner, L.; Müller, A. H. E. *Macromolecules* 2009, 42, 3707-3714.

## 6 Quantifying the Efficiency of Photo-Initiation Processes in Methyl Methacrylate *via* Pulsed Laser Polymerization and the Determination of $k_p$ for Methyl Acrylate and 2-Ethyl Hexyl Acrylate beyond Ambient Temperature

This section is comprised of work involving the use of photo-initiation *via* laser pulsing to investigate the radical reactivity of 1,2-dimesitylethane-1,2-dione relative to that of benzoin. In the first section pulsed laser polymerization (PLP) combined with the technique of electrospray ionization mass spectrometry (ESI-MS) are employed to generate and then quantitatively assess the ability of two specific photolytically generated radical fragments to initiate the bulk free radical polymerization of methyl methacrylate (MMA) at 5 °C. The second part is concerned with the use of pulsed laser polymerization as a tool to determine the propagation coefficients of methyl acrylate and 2-ethyl hexyl acrylate beyond ambient temperature. The issues concerning the continuing difficulties encountered in acrylate PLP-SEC experiments are outlined and as a result an analysis of branching is conducted on the aforementioned PLP samples of both MA and 2-EHA.

### 6.1 Photo-polymerizations

Photo-polymerizations represent an important avenue for the preparation of synthetic polymers in both industry and academia and can be achieved through the use of photo-initiators, photo-crosslinkable polymers and/or photo-crosslinking agents.<sup>1</sup> Photo-initiators are used for the polymerization of functional monomers, oligomers and polymers<sup>2</sup> for applications including UV-curing<sup>2</sup> of coatings and inks, as well as in more specialized applications such as dental restorative materials<sup>3-4</sup> and biomaterials.<sup>5-6</sup> In the first part of this chapter electrospray ionization mass spectrometry (ESI-MS) is employed to quantitatively assess the ability of two specific photolytically generated radical fragments to initiate the bulk free radical polymerization of methyl methacrylate (MMA) at 5 °C. Despite a range of studies on photo-initiation processes of various photo-initiators, there is almost no quantitative information available on the initiation efficiency of photo-initiators obtained

from polymerizing systems, which provides concrete numbers on the effectiveness of one radical species over another as an initiating species. Such quantitative information is of significant help when choosing optimum radical fragment combinations for applications ranging from photo-curing in the realm of material science to mechanistic and kinetic investigations, where the selection of radical fragments that exclusively terminate polymerization activity can be of importance.<sup>7</sup> For the present initial quantitative study MMA is selected as the monomer, as it is a key monomer in several UV-curing applications, photo-imaging, and kinetic studies.<sup>8-11</sup> In previous investigations employing mass spectrometry to qualitatively study photo-initiation processes *via* ESI-MS mass spectrometry,<sup>12-14</sup> the reaction products which are generated during the pulsed laser induced photo-initiation employing variable acetophenone-type initiators were mapped in great detail.

The investigations were conducted with a wide range of monomer classes including acrylates, methacrylates as well as itaconates. Such detailed polymer endgroup analysis has become feasible by the development of soft-ionization mass spectrometry techniques; notably MALDI-ToF-MS<sup>15-16</sup> and ESI-MS coupled with quadrupole ion trap and/or time of flight detectors.<sup>17-19</sup> The potential of mass spectrometric analysis for synthetic polymers has been discussed in numerous publications and review articles.<sup>20-23</sup> ESI-MS is one of the most powerful mass spectrometry techniques as it provides very soft ionization conditions and has been employed to study the mechanism and kinetics of a wide range of polymer systems, ranging from living/controlled radical polymerizations<sup>24-25</sup> to thermal initiation processes.<sup>26-28</sup>

The reason for employing a pulsed laser as UV radiation source in the present study to deposit photons into the polymerization system is two-fold: firstly, and most importantly, the rapid pulse frequency of the laser allows excellent control over the molecular weight of the generated polymers. The length of the generated polymer chains is essentially controlled by the time a polymer chain has to grow between two consecutive laser pulses; in other words a higher pulsing frequency leads to a lower  $DP_n$ . Thus, the use of a pulsed laser system is a convenient tool for studying photo-initiation processes in acrylates *via* ESI-MS, as it represents a simple and practical avenue for providing low molecular weight polymers which fall within the ESI-MS  $m/z$  window of  $< 4000 m/z$  for analysis. Secondly, the

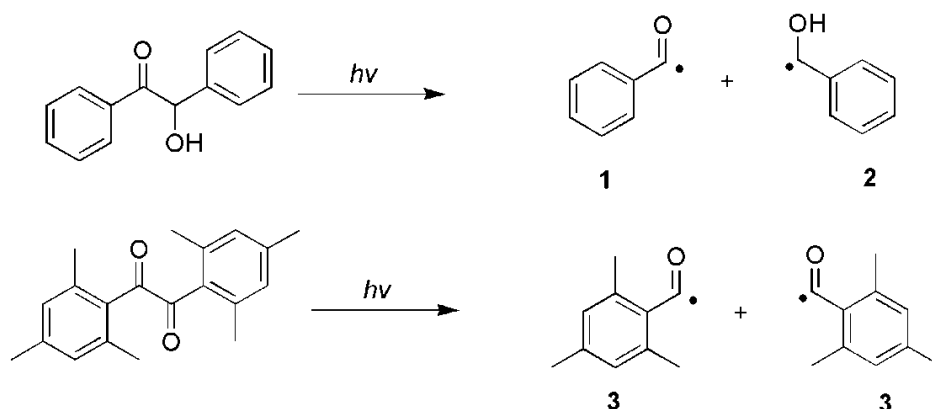
laser light is highly monochromatic, employing the XeF line of an excimer laser at a wavelength of 351 nm, and provides a defined and stable energy input into the polymerization system.

The choice to study the comparative reactivity of benzoyl vs mesitoyl radicals is driven by a previous qualitative finding that the mesitoyl fragment seems to display a very poor ability to react with MMA or other monomers after its generation from a phosphoryl-type photo-initiator and thus initiate its polymerization.<sup>29</sup> This finding is in contrast to the generally high ability of benzoyl radical fragments to initiate macromolecular growth.<sup>29</sup> The primary aim of the study is thus to quantify this efficiency difference observed when using benzoin and mesitil initiators, respectively *via* the following experimental strategy: mixtures of benzoin and mesitil, ranging from equimolar composition to a large excess of mesitil, are prepared and subjected to pulsed laser initiation. The generated polymer is isolated and subjected to direct infusion ESI-MS.<sup>23</sup> *Via* the mass spectral evaluation procedure described in detail below, the ratio of benzoyl to mesitoyl radical fragments that have initiated macromolecular growth is plotted as a function of the ratio of both initiators in the reaction mixture. Interpretation of such a plot provides a quantitative measure of the ratio of the initiation ability of both radical fragments. Within the present study a methodology that may be employed to quantitatively assess comparative radical reactivities for a range of photo-initiators is introduced.

## 6.2 Quantifying the Efficiency of Radicals Generated from Benzoin (2-hydroxy-1,2-diphenylethanone) and Mesitil (1,2-dimesitylethane-1,2-dione)

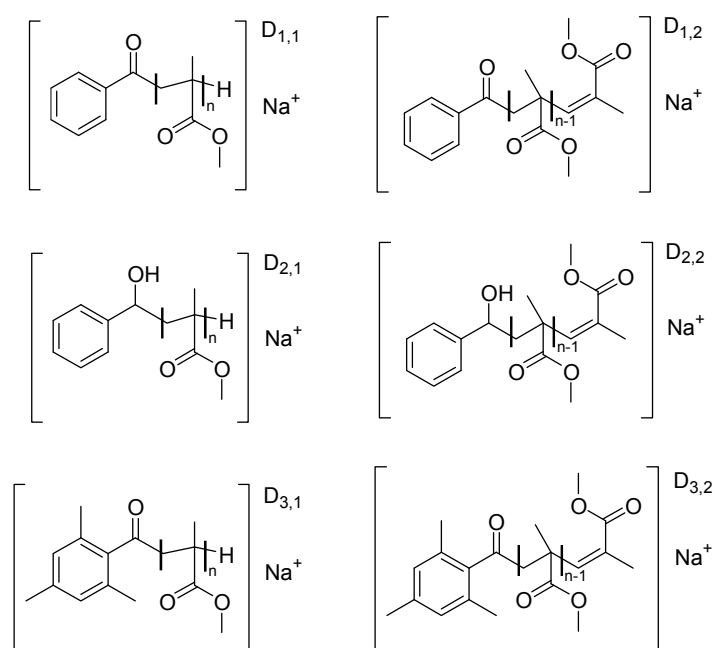
Scheme 6-1 shows the chemical structure of both initiators employed as well as their UV light induced radical decomposition products. Scheme 6-2 depicts the expected disproportionation products which are almost exclusively formed at this temperature in the presence of MMA as monomer. Note that the disproportionation product having radical fragment (2) as end group is not subject of the present study. Details on why this is the case are given further in the text. Before discussing the results of the investigation in detail, it is important to clarify a particular aspect of the present work. This work is concerned with

determining in a quantitative manner the ratio in which the benzoyl and the mesitoyl radical fragments are initiating macromolecular growth.



Scheme 6-1: Photolytic decomposition pattern of benzoin and mesitil into their radical fragments. The efficiency of the benzoyl fragment (1) to initiate the free radical bulk polymerization of methyl methacrylate (MMA) is quantitatively compared to that of the mesitoyl (3) fragment. Mixtures of benzoin and mesitil are employed, see Figure 6-5 for details.

However, knowledge of this ratio does not necessarily allow conclusions to be drawn about the reactivity of both fragments towards MMA, because it is possible that the observed ratio of the initiation ability is a reflection of the fact that the number of each radical species that is available to react with MMA is different. It is well-known that an initiator's ability to absorb UV light, the primary quantum yields, as well as cage reactions directly after the birth of the individual radical fragments may be different for both initiators so that the number of radicals generated from each initiator may significantly diverge. Thus a different number of radicals are available to initiate macromolecular growth. It is, however, very important to note that beyond the difficulty in clarifying the actual individual radical reactivity towards a vinyl monomer, the data presented here may be viewed from the perspective of the employed initiators rather than from the perspective of the generated radicals. *Via* such an approach, the data presented provide an unambiguous value for the effectiveness of the benzoin *vs* mesitil initiators to provide benzoyl and mesitoyl radicals to initiate the free radical polymerization of methyl methacrylate.



Scheme 6-2: Expected polymeric disproportionation peaks in the photo-chemically initiated bulk free radical polymerization of methyl methacrylate (MMA) in the presence of a cocktail of the benzoin and mesitol photo-initiators depicted in Scheme 6-1. Note that the position of the double bond in the unsaturated disproportionation product may also be at the site of the (former)  $\alpha$ -methyl group. See Table 6-1 for the masses of the individual radical fragments.

The top of Figure 6-1 depicts the entire ESI mass spectrum recorded from a polymer sample generated *via* the pulsed laser polymerization of MMA in the presence of a 1:2.5 mixture of benzoin and mesitol. The bottom the figure shows a representative repeat unit from the full mass spectrum, with every peak labeled according to the following nomenclature: Disproportionation peaks occur in pairs separated by 2 Da. Thus, each peak is labeled  $D_{n,1 \text{ or } 2}$  where  $n$  denotes the radical fragment that has initiated the polymerization. The expected and experimental masses for the depicted representative repeat unit are collated in Table 6-1. The minor combination products can be found at double the molecular weight of the disproportionation products.

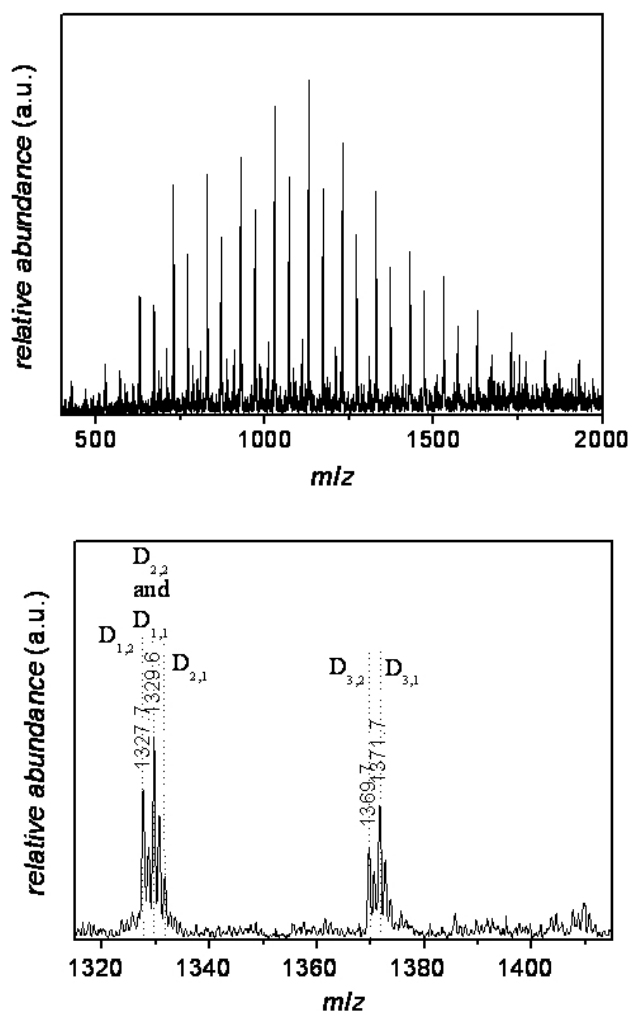


Figure 6-1: ESI-MS spectra of the polymeric material obtained from the benzoin/mesitol-initiated ( $c_{ini,0} = 5 \cdot 10^{-3} \text{ mol} \cdot \text{L}^{-1}$ ) PLP of MMA in bulk at 5 °C at a laser intensity of 5 mJ and a frequency of 100 Hz. *Top*: Full scan between 400 and 2000  $m/z$ . *Bottom*: Zoom scan of one monomer repeat unit from 1315 to 1415  $m/z$ . The nomenclature employed to identify the individual disproportionation products is provided in Scheme 6-2.

Inspection of Table 6-1 shows that the experimental and theoretically expected masses agree well within the accuracy of the mass spectrometric analysis ( $\pm 0.2 \text{ Da}$ ). Such excellent agreement is found in every repeat unit and is representative for any initiator cocktail composition employed within the current study. Before proceeding to a quantitative analysis of the individual disproportionation peaks, a brief qualitative description of how the ESI-MS spectrum changes with increasing amounts of mesitol in the initiation cocktail will be given.

Table 6-1: Polymeric product signals observed during ESI-MS of poly(methyl methacrylate) samples generated during the pulsed laser initiated bulk free radical polymerization of MMA at ambient temperature. The table provides experimentally observed as well as theoretically expected masses for the disproportionation products that consist of 11 monomer units, i.e. for  $n = 11$  in Scheme 6-2. The structures corresponding to the individual peaks are depicted in Scheme 6-2. The tabulated values correspond to the peaks displayed in Figure 6-1.

Species	Ionization	$(m/z)_{\text{theo}} / \text{Da}$	$(m/z)_{\text{exp}} / \text{Da}$	$ \Delta m/z $
D <sub>1,2</sub>	Na <sup>+</sup>	1327.6	1327.7	0.1
D <sub>1,1</sub> and D <sub>2,2</sub>	Na <sup>+</sup>	1329.7	1329.6	0.1
D <sub>2,1</sub>	Na <sup>+</sup>	1331.7	1331.7	0
D <sub>3,2</sub>	Na <sup>+</sup>	1369.7	1369.7	0
D <sub>3,1</sub>	Na <sup>+</sup>	1371.7	1371.7	0

Figure 6-2 depicts the  $m/z$  region from a representative repeat unit, of the disproportionation peaks D<sub>3,1</sub> and D<sub>3,2</sub> as a function of the initiator cocktail composition. For each cocktail composition, the spectrum was normalized (within the repeat unit under consideration) to the peak D<sub>1,2</sub>, which occurs at 1127.7 Da, i.e. the disproportionation product peak corresponding to polymer chains initiated by a benzoyl fragment. This peak is more importantly free from isobaric interference, a crucial element in the analysis.

More details on why absence of isobaric interference is given shortly. Inspection of Figure 6-3 shows that with increasing amounts of mesitol in the reaction mixture, the number of chains carrying a mesitoyl end group increases. Qualitatively, relatively large amounts of mesitol in the initiation cocktail need to be present to achieve a significant signal intensity. To put this qualitative observation into a quantitative basis, the disproportionation peaks corresponding to the chains initiated with mesitoyl radicals (3) depicted in Figure 6-3 are placed in relation to the peaks associated with chains initiated by benzoyl fragments (1). The specific evaluation procedure applied to arrive at quantitative ratios of (1) to (3) as species that have started macromolecular growth is detailed below. Before progressing to the particulars of the analysis procedure, the following should be noted: The signals which are

directly compared *via* Equation (1) and/or Equation (2) to (4) must not show isobaric overlap with any other peak.

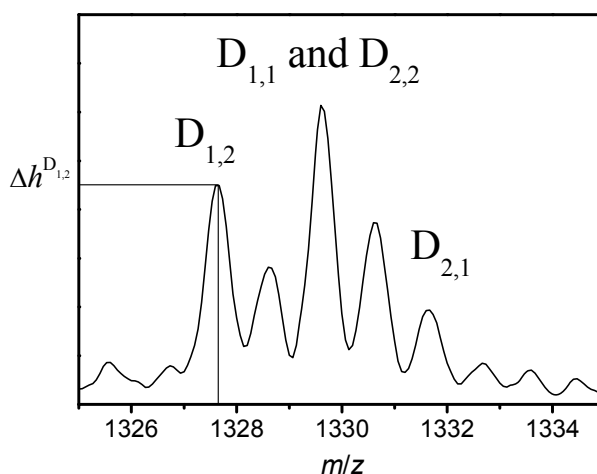


Figure 6-2: Enlarged section of the disproportionation peak ensemble associated with polymer chains initiated by radical fragment (1) or radical fragment (2). The signal employed for evaluation purposes is  $D_{1,2}$  as it is the only isotopically non-overlapping signal.

The disproportionation peak ensemble, see Figure 6-2, for chains initiated with (1) or (2) demonstrates that only the peak labeled  $D_{1,2}$  is free from isobaric interference. The isotopic pattern associated with  $D_{1,1}$ ,  $D_{2,2}$  and  $D_{2,1}$  all overlap with each other, making their quantitative evaluation non-feasible. These isobaric overlaps also do not allow quantitative information about the initiation ability of (2) to be evaluated. In addition, it is important to compare disproportionation products that carry the same end group, i.e. saturated or non-saturated. Given the isobaric overlap of  $D_{2,1}$  with  $D_{2,2}$ , the only option for quantitatively evaluating the mass spectra is a comparison between  $D_{1,2}$  and  $D_{3,2}$ . Figure 6-2 shows how the height  $\Delta h_{1,2}^D$  is defined which is employed in the mass spectrometric data evaluation procedure. This procedure will now be described in detail.

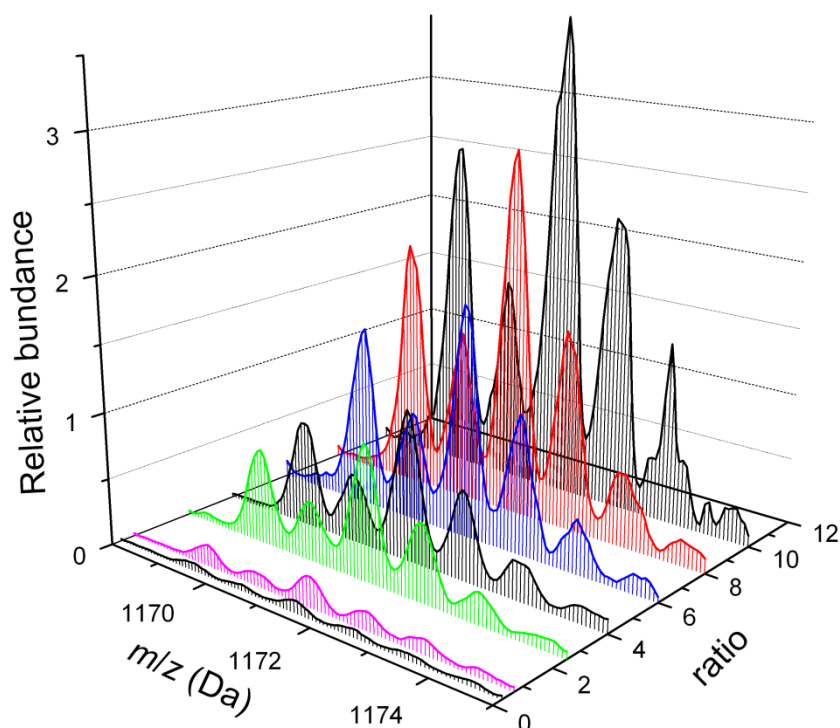


Figure 6-3: 3-Dimensional plot of the variation of intensity observed in the mass spectroscopic signal of the disproportionation peak  $D_{3,1}$  and  $D_{3,2}$  (i.e. chains which have been initiated *via* a mesityl radical) as a function of the composition of the photo-initiator cocktail ( $ratio = n_{mesityl} : n_{benzoin}$ ). The constant increase of the amount of mesityl initiated polymer chains with increasing amounts of mesityl in the cocktail is clearly visible. The relative abundance is determined by normalizing each individual spectrum with respect to the (benzoin derived) peak at 1127.7 Da ( $D_{1,2}$ ).

### 6.3 Data Analysis and Evaluation of the ESI-MS Spectra

The procedure for evaluating the obtained ESI-MS spectra will be detailed in this section. Ideally, mass spectra would display no mass bias at all. In reality, there may always a certain amount of mass bias present and it is important to test for its occurrence. In the most simple and straight forward approach for evaluating the mass data in the present study, the height of the only two peaks that do not show isobaric overlap (i.e.  $D_{1,2}$  and  $D_{3,2}$ , the species of interest),  $\Delta h_{n,2}^D$  is evaluated in each repeat unit. Figure 6-2 provides a graphical representation on how  $\Delta h_{n,2}^D$  is determined. As the height of peak, or alternatively the integral could be employed,<sup>30</sup> is proportional to the number of molecules corresponding to

the associated mass, the individual peak heights can be analyzed to arrive at the mole fraction of the disproportionation product  $D_{1,2}$ ,  $F$ , *via* Equation 6-1. Note that  $F$  is given as  $F(i)$ , as it can be evaluated for every repeat unit, with  $i$  being the chain length to which the repeat unit corresponds. It is important to note that this mole fraction does not consider the entirety of all disproportionation products generated during the polymerization (i.e.  $D_{1,2}$ ,  $D_{1,1}$ ,  $D_{2,2}$ ,  $D_{2,1}$ ,  $D_{3,1}$  and  $D_{3,2}$ , see Scheme 6-2 for the corresponding structural definitions), but only  $D_{1,2}$  and  $D_{3,2}$ . The factor 2 in front of  $\Delta h_{1,2}^D$  arises because each mesityl initiator yields two mesityl radicals, whereas each benzoin fragment only generates one benzoyl radical fragment. A detailed description is provided on the results of evaluating the mass spectrometry data *via* Equation 6-1 further on.

$$F(i) = \frac{\Delta h^{D_{3,2}}(i)}{\Delta h^{D_{3,2}}(i) + 2 \cdot \Delta h^{D_{1,2}}(i)} \quad \text{Equation 6-1}$$

While Equation 6-1 can be a valuable tool, it does not take into account any potential chain length dependent ionization mass biases other than evaluation of every repeat unit. However, there exists another approach which can be employed to try to eliminate the mass biases. We have adopted and modified for our purposes the elegant approach taken by Günzler *et al.* in previous quantitative mass spectrometric evaluations.<sup>30</sup> The modified approach taken here is as follows: Let  $G(i)$  be the ratio of the peak heights of  $D_{3,2}$  and  $D_{1,2} \forall i$ . *Nota bene*: This ratio may directly be plotted against chain length,  $i$ , and yields identical information to  $F(i)$  as  $F(i) = G(i) \cdot (G(i) + 1)^{-1}$ . Now define  $G'(i, i-1)$ ,  $G''(i, i+1)$  in a similar manner to  $G(i)$ , however taking the height of  $D_{3,2}$  ( $\Delta h_{3,2}^D$ ) from one repeat unit higher than  $D_{1,2}$  (Equation 6-3) or lower than  $D_{1,2}$  (Equation 6-4). Thus, the vectors  $G(i)$ ,  $G'(i, i-1)$  and  $G''(i, i+1)$  are obtained.

$$G(i) = \frac{\Delta h^{D_{3,2}}(i)}{2 \cdot \Delta h^{D_{1,2}}(i)} \quad \text{Equation 6-2}$$

$$G'(i, i-1) = \frac{\Delta h^{D_{3,2}}(i)}{2 \cdot \Delta h^{D_{1,2}}(i-1)} \quad \text{Equation 6-3}$$

$$G''(i, i+1) = \frac{\Delta h^{D_{3,2}}(i)}{2 \cdot \Delta h^{D_{1,2}}(i+1)} \quad \text{Equation 6-4}$$

In a subsequent step,  $G(i)$ ,  $G'(i,i-1)$  and  $G''(i,i+1)$  are individually averaged  $\forall i$ , yielding the average values  $\langle G \rangle$ ,  $\langle G' \rangle$  and  $\langle G'' \rangle$ .  $\langle G \rangle$  corresponds to the average ratio of  $\Delta h^D_{n,2}$  within the same repeat unit (mass difference between the compared peaks is  $\Delta m/z = 42$  Da),  $\langle G' \rangle$  corresponds to the average ratio of  $\Delta h^D_{n,2}$  within two repeat units with the second repeat unit being at smaller molecular weights ( $\Delta m/z = -58$  Da) and  $\langle G'' \rangle$  corresponds to the average ratio of the  $\Delta h^D_{n,2}$  within two repeat units with the second repeat unit being at larger molecular weights ( $\Delta m/z = +142$  Da). With  $\langle G \rangle$ ,  $\langle G' \rangle$  and  $\langle G'' \rangle$  now obtained, these values can be plotted against  $\Delta m/z$ . The  $y$ -intercept ( $\Delta m/z = 0$ ) of such a plot yields  $\langle G \rangle_{\Delta m/z,0}$ , which represents the mass bias free ratio of the two disproportionation products  $D_{3,2}$  and  $D_{1,2}$  in the polymer sample. In systems where the mass bias is negligible, all the evaluation procedures, i.e. averaging  $F(i)$ ,  $G(i)$  and calculating  $\langle G \rangle_{\Delta m/z,0}$  should give (near) identical results. In the present system, nearly ideal conditions are observed, as described presently.

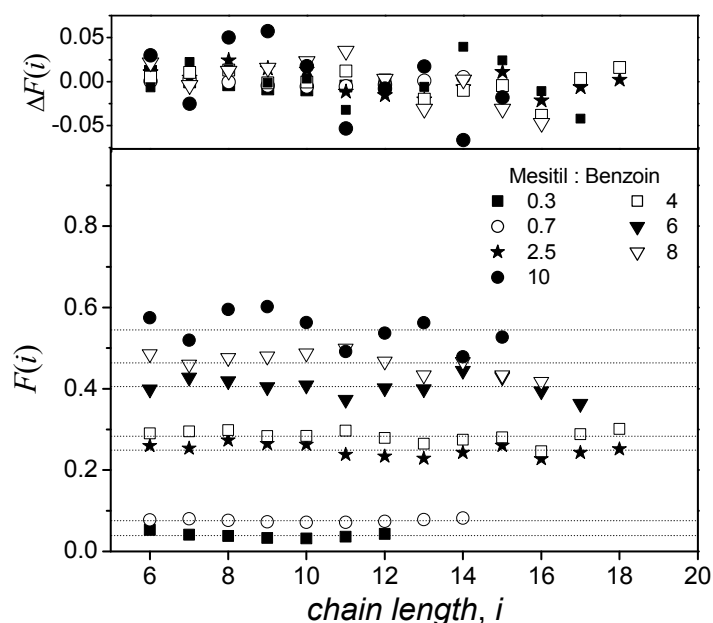


Figure 6-4: Intensity derived mole fractions of polymer chains initiated with mesityl radicals,  $F(i)$ , vs. the chain length,  $i$ . The dotted lines give the average of the mole fraction over the entire chain length range. The upper part of the figure depicts the residual demonstrating that  $F(i) = F$ .  $\Delta F(i)$  is the deviation of each  $i$  measured data point from the average value derived from all data points as a function of chain length for a given ratio of mesitol to benzoin.

As shown in the data analysis section above, it is relatively simple to arrive at Equation 6-1 that gives the mole fraction,  $F(i)$ , of mesityl radicals that have initiated the polymerization process as a function of the analyzed chain length,  $i$ . Figure 6-4 depicts how  $F(i)$  varies with increasing amounts of mesityl initiator in the initiator cocktail. Two important observations can be made from Figure 6-4: i)  $F(i) = F$ , indicating no dependence of  $F$  on the mass range that has been analyzed, which implies that mass bias effects are not pronounced.

The upper part of Figure 6-4 shows the residual  $\Delta F(i)$  and that all data points can be seen scattered around the zero line, indicating that no systematic dependence of  $F$  on  $i$  is observed; ii) Between 8 and 10 times excess of mesityl over benzoin is required to produce an identical number of chains initiated by mesityl and benzoyl radical fragments. Note that equal initiation ability would be observed at  $F = 0.5$ , which lies between the data series representing the ratios of 10:1 (closed circles) and 8:1 (open triangles). As has been detailed previously, it is possible to plot not  $F$  but rather  $G$  (or more correctly  $\langle G \rangle_{\Delta m/z, 0}$ , the mass bias corrected variant of  $G(i)$ ) vs the initiator cocktail composition. Such a plot (which gives the direct ratio of chain initiated with mesityl fragments over those initiated with benzoyl radicals) allows a direct and quantitative comparison of the initiation efficiency of benzoin and mesityl with respect to the derived benzoyl and mesityl radicals to be made.

Figure 6-5 depicts such a plot. Inspection of Figure 6-5 immediately reveals that a linear correlation exists between the ratio of benzoin to mesityl in the reaction mixture and the mass bias corrected ratio,  $\langle G \rangle_{\Delta m/z, 0}$ , of the benzoyl and mesityl radicals that have initiated the polymerization process. Parity in the initiation between mesityl and benzoin derived fragments ( $\langle G \rangle_{\Delta m/z, 0} = 1$ ) occurs at an initiator cocktail composition of 8.6. Upon inspection of Figure 6-5, the conclusion that benzoyl radicals are a factor 8.6 more efficient in reacting with MMA monomer units and initiating macromolecular growth could be easily deduced at first glance. However, it is also possible that the number of radicals which are available to initiate macromolecular growth differs for both photo-initiators. Two main factors can contribute to this: i) The efficiency with which both initiators absorb the incident UV light differs and thus a different number of radicals is generated for each photo-initiator per laser pulse and ii) the quantum yield for primary radical production,  $\Phi$ . The primary quantum yield is composed of processes that occur after irradiation and absorption has taken place and consists of several deactivation mechanisms including the quantum yield for

intersystem crossing  $\Phi_{ISC}$  (going from an  $S_1$  state to a  $T_1$  state), the radical quantum yield,  $\Phi_R$  (i.e. efficiency with which the triplet state of the photo-initiator molecule is deactivated by processes that do not lead to the formation of primary radicals), as well as the efficiency at which the generated radicals escape solvent cage reactions,  $\Phi_{RM}$ . The quantum yield for intersystem crossing is rather high for ketones,<sup>31</sup> so that  $\Phi_{ISC}$  can be set to unity as a good approximation. Thus, the overall quantum yield of the initiation process only depends on  $\Phi_R$  and  $\Phi_{RM}$ . In free radical polymerization, these reactions include deactivation by molecular oxygen. In the present study, the reaction mixture was carefully freed from oxygen prior to laser irradiation and thus a significant deviation of  $\Phi_R$  from unity is unlikely. In addition, the shorter the lifetime of the triplet state  $T_1$ , the fewer the chances that deactivation processes can reduce  $\Phi_R$ .

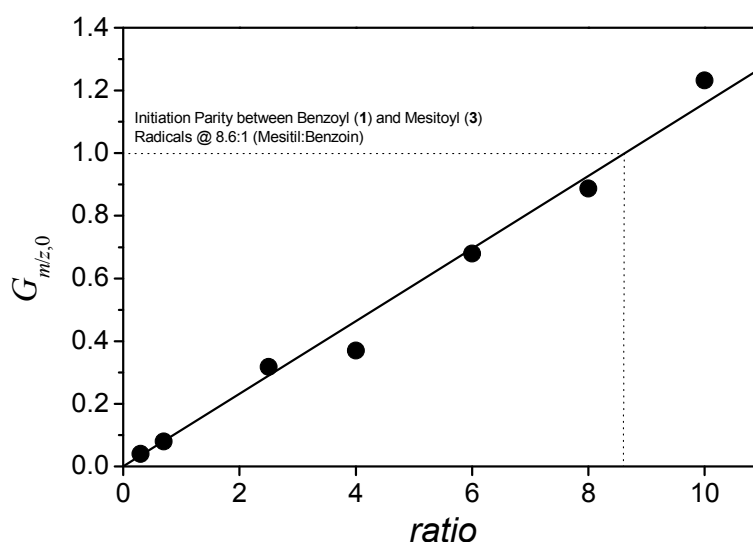


Figure 6-5: Ratio of the intensities of the disproportionation signals corresponding to polymer chains initiated with a benzoyl and a mesityl radical vs. the ratio of both initiators in the reaction mixture ( $ratio = n_{mesityl} : n_{benzoil}$ ). An evaluation procedure has been adopted, which allows for the minimization of mass bias and yields the mass bias free intensity ratio  $\langle G \rangle_{\Delta m/z,0}$  (refer to the section 0 for a detailed description of the evaluation procedure).

An initiator similar to benzoin and mesitil is 2,2-dimethoxy-2-phenylacetophenone (DMPA), which features a rather short triplet lifetime of  $\tau < 0.1$  ns.<sup>32</sup> Given these short triplet lifetimes coupled with the fact that the reaction solutions were freed of oxygen suggests that  $\Phi_R$  is quite likely close to unity. The quantum yield  $\Phi_{RM}$ , which governs the formation of the available initiating radicals, is often termed the initiator efficiency. The initiator efficiency (i.e.  $\Phi_{RM}$ ) is influenced by the ability of the nascent radicals to diffuse from their birth solvent cage to the reaction site, i.e. the monomer units. For both initiators, there is currently no information available on the value of  $\Phi_{RM}$  and it is highly likely that this value is unity. However, the absolute value of  $\Phi_{RM}$  is irrelevant for the present study as the comparison here is between the efficiency of two radicals to initiate macromolecular growth. Since both the benzoin and mesitil photo-initiators are structurally similar, one could expect that the difference in  $\Phi_{RM}$  may not be overly large and may be not as large as the factor of 8.6 observed in the initiating end group amounts. Clearly, a definite statement on  $\Phi_{RM}$  and its difference for both initiators is not possible, however, two points should be kept in mind. First, the value of  $\Phi_{RM}$  will depend strongly on the solvent environment and nature of the solvent cage, as this will determine the radicals' ability to escape and initiate the polymerization process. Second, the rate of recombination of the nascent radical fragments within the solvent cage may differ for the mesitoyl and the benzoyl radicals. Within the solvent cage, these reactions are governed by the individual radical reactivities, determined by the electronic and steric conditions at the radical site, which may indeed be different for both fragments and thus lead to different  $\Phi_{RM}$  values.

The possibility that both initiators absorb UV light with a very different efficiency at 351 nm has not yet been considered in detail and thus the observed end group difference is a reflection of the initiators' ability to absorb photons. To some extent, it can be estimated whether an absorption phenomenon can contribute to the difference: if benzoin and mesitil have different absorptivities at 351 nm, at equal concentrations, then it is a corollary that they also have a different efficiency in absorbing the photons. At a concentration of  $10^{-3}$  mol·L<sup>-1</sup> (in methanol) and an optical path length of 10 mm, both benzoin and mesitil have an absorption of 0.09 and 0.9, respectively, as measured and shown in Figure 6-6. This result is a highly interesting: the initiator (mesitil) which absorbs *more* photons by a factor of 10, yields radicals that are a factor of 8.6 *less* likely to be found as initiating groups in the

polymer. Under the premise that  $\Phi_{RM}$  is equal for both initiators, it could be tempting to multiply both factors, and obtain a factor of 86 in reactivity difference, to arrive at the true reactivity of the mesityl vs. the benzoyl radicals towards MMA. However, it suffices note that on the balance of the above arguments, it is very likely that a significant part of the observed difference in the ability of benzoin and mesitil respectively to provide benzoyl and mesityl initiated chains is caused by a difference in their reactivity towards the monomer MMA and not solely by a potential difference in the respective  $\Phi_{RM}$  values. To even achieve parity in radical reactivity, the primary radical yield of mesitil would have to be a factor of 86 less than that of benzoin which is a highly unlikely scenario.

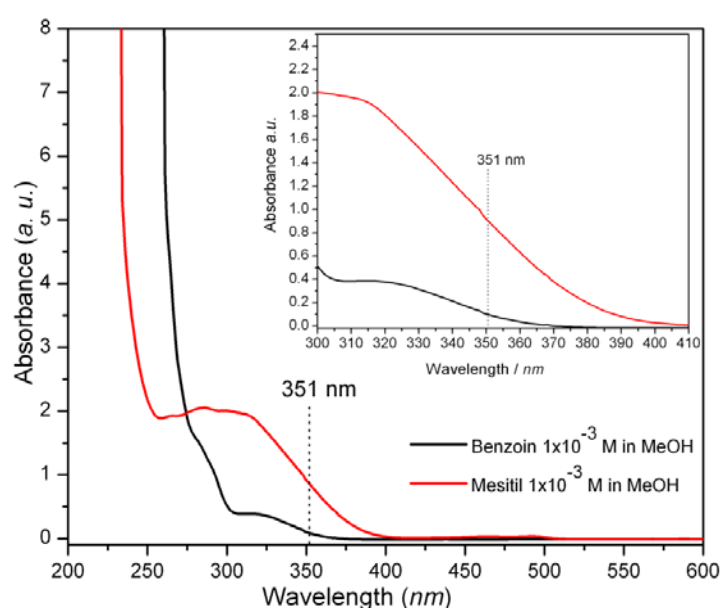


Figure 6-6: UV Vis spectra of Benzoin and Mesitil. Inset shows an enlarged section of full spectrum with the relevant wavelength of 351 nm at the centre, showing the large difference in absorption for the respective photo-initiators.

#### 6.4 Summary - Quantifying the Efficiency of Radicals Generated from Benzoin (2-hydroxy-1,2-diphenylethanone) and Mesitil (1,2-dimesitylethane-1,2-dione)

Quantitative information on the initiation abilities of two radicals moieties commonly contained in acetophenone photo-initiators was provided for an MMA polymerizing system, utilizing benzoin and mesitil as sources for benzoyl and mesityl radicals. To quantitatively

assess the relative efficiency of each radical fragment to initiate macromolecular growth, pulsed laser polymerizations of MMA were initiated at 351 nm with cocktails of benzoin and mesitol of varying composition (1:0.3 to 1:10 benzoin vs. mesitol). A plot of the relative amounts in which both fragments were found in the disproportionated chains in the polymer indicates that benzoyl radicals are close to a factor 8.6 more likely to initiate macromolecular growth than mesitoyl radicals. This quantitative finding is in good agreement with earlier qualitative observations that mesitoyl radicals may be poor initiating entities. It is also satisfying to note that mass dependent ionization biases are minimal, at least in the present system. For MMA, it can be concluded that initiators containing mesitoyl (such as 2,4,6-trimethylbenzoyldiphenyl-phosphin oxide) may be improved by exchanging the mesitoyl moiety with a benzoyl fragment.<sup>29,33</sup> Considering all available data, the strong discrepancy in initiating macromolecular growth is due to a significant part to the reactivity difference between mesitoyl and benzoyl radicals and probably only to a lesser degree to different effective radical concentrations generated from mesitol and benzoin.

## 6.5 Pulsed Laser Polymerization for the Determination of Propagation Coefficients for MA and 2-EHA above Ambient Temperature

The development of novel synthesis strategies and refinement of existing procedures utilizing radical polymerization requires precise knowledge of the individual rate coefficients for the initiation, propagation, termination and transfer reaction. Among these parameters, the propagation rate coefficient  $k_p$  is perhaps the most important as the determination of all other rate coefficients is often carried out relative to the propagation reaction. Since the Pulsed Laser Polymerization-Size Exclusion Chromatography (PLP-SEC) technique was developed in the late eighties,<sup>34</sup> it has become the IUPAC-recommended method<sup>35</sup> for determination of propagation rate coefficients,  $k_p$ , due to its relative precision, reliability, and simplicity. A large number of monomers has been investigated to determine their propagation rate coefficients, both commodity and specialty monomers,<sup>36</sup> and benchmark values for the most important compounds have been published, including the most relevant monomers from an industrial point of view.<sup>37-38</sup> Pulsed laser polymerization (PLP) allows the determination of the propagation rate coefficient  $k_p$  utilizing a simple method and with unparalleled accuracy. Pulsed laser polymerization was first described by Genkin and Sokolov in 1977 and became the IUPAC recommended standard for determination of

propagation coefficients in 1988<sup>39</sup> after being experimentally verified by Olaj and Schnöll-Bittai.<sup>40</sup> It is a technique that has been widely employed particularly for the determination of effective propagation rate coefficients,  $k_p$ , and the IUPAC working party on free radical kinetics considers this method to be the benchmark technique for the determination of  $k_p$ .<sup>35</sup> It involves the exposure of a monomer solution with photo-initiator to repeated laser pulses of known frequency and energy. At each pulse a population of new radicals is formed and begins propagating. Between pulses, propagation of live radicals continues, while the overall concentration of radicals decreases due to radical-radical termination. Termination of these radicals is instantaneous at the next pulse because of the increase in radical concentration which occurs as the next generation of radicals is created. The intermittent laser illumination effectively starts and stops polymer chain growth and initiation. PLP has been used successfully to evaluate  $k_p$  for styrene,<sup>35</sup> the acrylate and methacrylate family,<sup>41-50</sup> *N*-isopropyl acrylamide,<sup>51</sup> *N*-vinyl formamide,<sup>52</sup> *N*-vinyl pyrrolidone,<sup>53</sup> acrylamide,<sup>54</sup> acrylic acid,<sup>55-56</sup> *N*-vinyl carbazole,<sup>57</sup> vinyl acetate<sup>58-59</sup> and even in copolymerizing systems such as styrene and glycidyl methacrylate<sup>60</sup> amongst many other systems. Despite these successes, quantifying  $k_p$  in fast monomer systems such as the acrylates has proven difficult,<sup>41</sup> except at low temperatures.

Key assumptions in this technique are:<sup>35,61-63</sup>

- Termination is almost instantaneous after a pulse
- The propagation rate coefficient is independent of chain length
- The production of radicals is instantaneous upon laser pulse irradiation
- The primary radicals should undergo a fast initiation reaction with monomer
- In the dark time (time interval between two successive pulses) the polymer radical concentration decays homogeneously with time according to a second order rate law
- The experimentally-measured  $k_p$  value must be independent of pulse frequency, initiator concentration and incident pulse energy

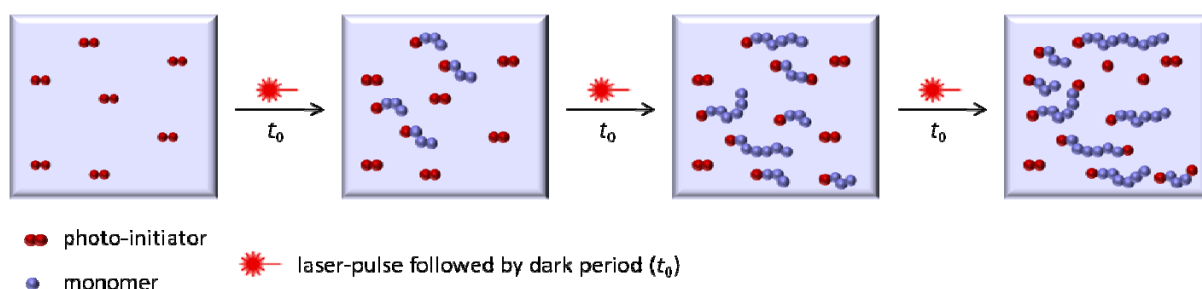
The length of polymer chains that grow between two successive laser pulses is measured and the effective propagation rate coefficient is thus determined. A limitation in the  $k_p$  values obtained in this way is the dependence on determination of a characteristic chain

length ( $L_i$ ) from the polymer molecular weight distribution.  $L_i$  is related to the number of propagation events which a radical undergoes in the time between two laser pulses ( $t_0$ ):

$$L_i = i \cdot k_p \cdot [M] \cdot t_0 \quad \text{where } i = 1, 2, 3, \dots \quad \text{Equation 6-5}$$

where  $[M]$  is the monomer concentration.  $L_i$  denotes the chain length at the characteristic inflection points of the molecular weight distribution (MWD), determined by identifying the maxima of the first derivative of the distributions, which is generally measured by size exclusion chromatography (SEC) and calculated using the principle of universal calibration, and  $t_0$  the dark time between two consecutive laser pulses. The accuracy of  $k_p$  determinations is thus directly dependent upon the accuracy of Mark-Houwink-Sakurada (MHS) calibration constants used for SEC analysis.<sup>44</sup>

For some systems up to four points of inflection can be observed; the presence of two characteristic points in the MWD is however sufficient to obtain reliable  $k_p$  (technically, if other criteria are fulfilled, even the second point of inflection is not strictly required). From these two characteristic points two rate coefficients can be obtained that ideally are identical. As the second point of inflection is however often not as easily determined, usually only  $L_1$  is used and  $L_2$  only serves as a verification of  $L_1$ . Other experiments that may be performed to check the reliability of the results is to determine the dependence of the results on experimental parameters such as initiator concentration and pulse frequency. If no interfering effects exist, for example with acrylate monomers,<sup>47</sup> a variation of these reaction parameters should not change the resulting  $k_p$ .



Scheme 6-3: Schematic representation of the technique of Pulsed Laser Polymerization (PLP) to generate polymer.

Scheme 6-3 graphically depicts the processes which lead to formation of PLP polymer, which is polymer of a particular molecular weight distribution, from which  $k_p$  may be evaluated. The PLP technique has been successfully applied to many propagating monomers,<sup>35,38,43,64-68</sup> but PLP of faster propagating systems such as the acrylates is difficult due to the presence of branching and secondary reactions such as combinations of transfer to monomer and transfer to polymer reactions.<sup>69</sup> At temperatures above 30 °C and pulsing frequencies not exceeding 100 Hz, the results show broad featureless molecular weight distributions and concentration dependent solution PLP results.<sup>69</sup> Additionally, pulse energy and photo-initiator concentration seem to have an effect on the product obtained.

Experimental conditions for the polymerization must be selected so that laser pulses are the dominant chain-starting and chain-stopping events. Interference from excessive chain-transfer reactions, or from termination reactions which are either too fast or too slow, results in molecular weight distributions which do not exhibit PLP structure. Beuermann *et al.*<sup>43,70</sup> have successfully carried out PLP of butyl, and dodecyl acrylates, with the purpose of determining their propagation rate coefficients.

The main source of experimental error that limits the accuracy of a pulsed laser polymerization experiment is the mass detection of the employed chromatographic setup. The method of choice for the evaluation of molecular weight distributions is size exclusion chromatography, which is discussed in section 2.3. If standard instruments are used, i.e. chromatographs equipped with a refractive index (RI) detector, a calibration of the system is required on the basis of the universal calibration principle or, if available, *via* direct calibration. Zammit *et al.*<sup>71</sup> found that SEC results are strongly influenced by the MHKS parameters employed. There are often significant errors in the MHKS constants when they are selected from the literature and employed to characterize the same polymer but which is potentially structurally very different, see section 2.3.5.1.1 on MHKS calibration for a discussion of the pitfalls of using MHKS parameters from the literature. This is exemplified in the wide discrepancies between MHKS constants for the same polymer that may be found in the literature, and these errors produce a hidden systematic error in the molecular weights, and thus  $k_p$  values, measured by this technique.

## 6.6 Problems Encountered in PLP of Acrylates and their Causes

A molecular weight distribution (MWD) is described as a PLP distribution if it satisfies all the criteria defined by the IUPAC, notably that the distribution should satisfy the criterion  $L_2 = 2 L_1$  at all frequencies. This is demonstrated in Figure 6-7, from a study carried out by Barner-Kowollik *et al.*<sup>72</sup> where the right hand side of the figure depicts a successful PLP experiment, as all peak maxima of the first derivative curve are clearly identifiable to  $L_3$ . The left hand figure shows a clear  $L_1$ , but  $L_2$  on the other hand is ambiguous because the shoulder of the molecular weight distribution leads to an inflection point that converges into a saddle point, making the exact location of the maximum difficult to determine.

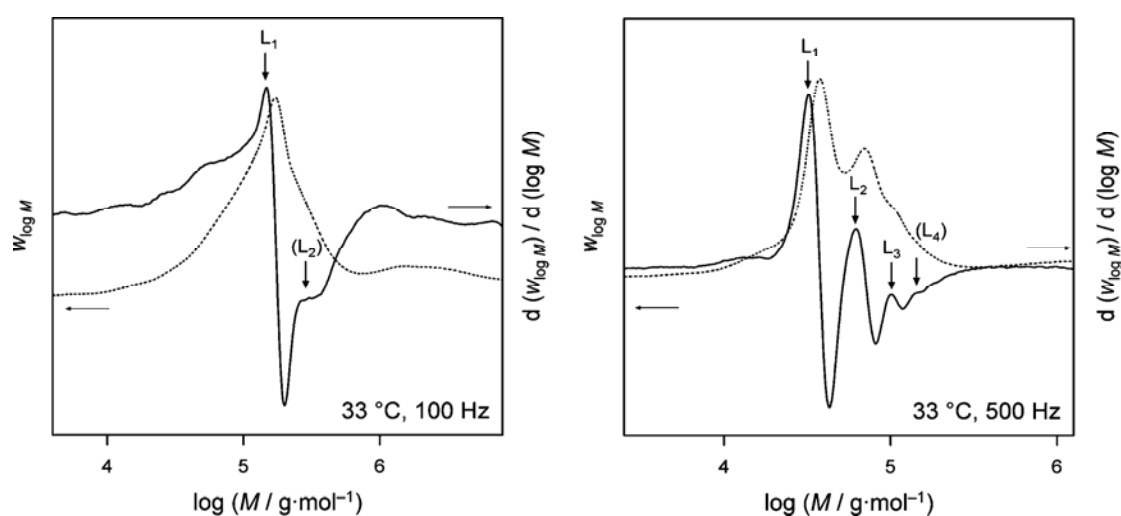


Figure 6-7: Molecular weight distributions and their derivatives from polymer generated by PLP of *n*-butyl acrylate at 33 °C. The left hand side depicts a sample from laser pulsing at 100 Hz and the right hand side from pulsing with 500 Hz and otherwise identical conditions. The dotted line represents the MWD as obtained *via* SEC, and the solid line represents the first derivative curve of the respective MWD.<sup>72</sup>

Davis *et al.* attempted without success to determine  $k_p$  values for methyl acrylate and *n*-butyl acrylate at 25 °C and 50 °C at 10 Hz pulse frequency at high dilutions (95 %).<sup>73</sup> The obtained MWDs were broad and without PLP characteristics, while in the copolymerization of acrylates and styrene PLP distributions could be seen, even at relatively high acrylate composition. Buback *et al.* were unable to obtain PLP distributions of methyl acrylate, *n*-butyl acrylate or dodecyl acrylate above 20 °C in liquid CO<sub>2</sub>.<sup>67,74-75</sup> This difficulty was

addressed in 2005 in a joint publication by the IUPAC working party ‘Modeling of Polymerization Kinetics and Processes’, which identified that the cause of PLP experimental failures stems from the extensive occurrence of transfer to polymer reactions, in particular backbiting reactions.<sup>76-83</sup> These transfer to polymer reactions are responsible for the loss of PLP structuring of samples obtained at technically relevant temperatures.<sup>41,43,46</sup> The transfer to polymer reaction only becomes relevant at higher temperatures due to its relatively high activation energy relative to the activation energy of the propagation reaction.<sup>81</sup> The propagating radicals are converted *via* transfer to polymer into MCRs.<sup>77</sup>

Although monomer addition leads back to a secondary propagating radical chain end, the much slower rate at which those radicals initially propagate<sup>84</sup> causes severe distortion of the chain length distribution and consequently the loss of a clear PLP distribution.<sup>85</sup> If transfer occurs, the approximately monodisperse growth of radicals is disturbed and PLP may thus yield false rate coefficients that do not represent the true  $k_p$ , but a somewhat decreased average rate coefficient, which is influenced by the transfer reaction. The presence of these side reactions destroys the characteristic PLP structure of the SEC chromatogram and is the most significant source of failure of PLP in acrylate monomers. The significance of transfer reactions in PLP experiments of *n*-butyl acrylate has been investigated by Busch,<sup>86</sup> while Olaj *et al.*<sup>87-88</sup> have studied chain length-dependent termination in PLP.

There are myriad reactions that may occur during a PLP experiment, many of which are considered to be side reactions<sup>77</sup> and have received attention in Chapter 4 of this thesis. Furthermore, the presence of these side reactions explains why it has hitherto been difficult to study acrylates by PLP above ambient temperature. In particular, the formation of MCRs *via* a six-membered transition state, also known as backbiting, or *via* inter- or intra-molecular transfer to polymer is prolific at higher temperatures (> 80 °C) and the subsequent reaction pathways that these MCRs can follow present a critical barrier to  $k_p$  determination by the PLP-SEC method. The only way to avoid these problems is by carrying out experiments at low temperatures and high frequencies. Alternatively, one group<sup>47</sup> has reported the propagation rate coefficients of *n*-butyl acrylate by PLP in the presence of intra-molecular chain transfer to polymer. In 2008, Barner-Kowollik *et al.* reported PLP-SEC of *n*-butyl acrylate performed at 500 Hz at temperatures up to 70 °C,<sup>72</sup> while Junkers *et al.* has published work on  $k_p$  of vinyl acetate,<sup>58</sup> and Dervaux *et al.* have reported  $k_p$  values for

isobornyl acrylate, *tert*-butyl acrylate and 1-ethoxyethyl acrylate.<sup>50</sup> The obtained values were in excellent agreement with previous benchmark data obtained in the range -65 to 20 °C. Gruending *et al.* have also proposed a method whereby SEC/ESI-MS is used to precisely determine the molecular weight distribution of the polymer produced by the PLP experiment.<sup>89</sup>

### 6.7 Pulsed Laser Polymerization of Methyl Acrylate beyond 40 °C

To date no PLP data have been provided for the monomers MA or 2-EHA at temperatures above 40 °C despite their extensive use in academia and industry for commodity polymers and copolymers. Other complications arise from the fast termination reaction in MA polymerizations at the routinely applied laser frequencies, such that so far few successful PLP-SEC experiments have been reported.<sup>67,90</sup>

PLP experiments are typically carried out on bulk solutions only containing monomer and initiator. Solvent effects on the propagation rate can then be largely excluded and easily comparable data are thus obtained. It is however noteworthy that while a solvent can have an influence on  $k_p$ <sup>91</sup> its presence does usually not compromise the quality of the PLP experiment.

A PLP-SEC setup was recently introduced that enables laser pulsing at 500 Hz repetition rate.<sup>72</sup> *Via* the rapid pulsing (compared to the 100 Hz laser systems that were in use before), the limitations in acrylate polymerizations at elevated temperatures can be overcome. It was also demonstrated that by using high laser frequencies, the measurement of fast terminating monomers such as vinyl acetate also could be significantly improved.<sup>58</sup> As the quality of data obtained *via* the application of 500 Hz pulsing rate is unsurpassed, high frequency high temperature PLP-SEC of methyl acrylate and 2-ethyl hexyl acrylate was deemed to be an important investigation. The current study provides the first reliable propagation rate coefficients for these monomers at temperatures beyond 40 °C (and up to 80 °C).

### 6.8 Mark-Houwink-Kuhn-Sakurada Parameter Measurements

To ensure correct evaluation of molecular weight values for the calculation of propagation rate coefficients, MHKS parameters were determined for both poly(MA) and poly(2-EHA) PLP samples. No consistent literature values exist in the case of 2-EHA, which has been

attributed to the presence of long chain branching in the polymer. The theory behind inaccurate molecular weight determination when MHKS parameters are employed was briefly touched upon in section 2.3.5.1. Long chain branching has been observed in poly(2-EHA) prepared *via* PLP at temperatures as low as -5 °C.<sup>92</sup> As far back as 1978, Hamielec and Ouano<sup>93-94</sup> demonstrated that for branched poly(vinyl acetate) and for low density poly(ethylene) the error in molecular weight determination by SEC could be very large, due to the elution of polymer with the same hydrodynamic volume ( $V_h$ ) but very different molecular weights in the same elution volume ( $V_e$ ). However, the presence of branching, particularly long chain branching, is extreme in the case of some acrylates, notably 2-EHA.<sup>92,95</sup> Therefore, each reported set of MHKS parameters for poly(2-EHA) are valid for only the samples from which the parameters were derived, as the branching characteristics of a polymer may vary with the conditions (temperature, bulk vs solution) under which it is synthesized. This most likely explains the large discrepancies found in the literature. Section 6.11 introduces the concept of local polydispersity which is a measure of the degree of homogeneity found within one  $V_e$ . An investigation into the local polydispersity of poly(2-EHA) and poly(MA) is undertaken in section 6.12.

The Mark Houwink equation describes the dependence of the intrinsic viscosity,  $[\eta]$ , of a polymer on its molecular weight:<sup>96</sup>

$$[\eta] = K \cdot M_w^\alpha \quad \text{Equation 6-6}$$

Equation 6-6 can be re-arranged and if the log is taken, it now takes the form:

$$\log [\eta] = \log K + \alpha \log M \quad \text{Equation 6-7}$$

From the Mark-Houwink equation, in the form of Equation 6-7,  $\alpha$  and  $K$  can be deduced from a linear fit of the plot of  $\log [\eta]$  vs  $\log M_w$ .

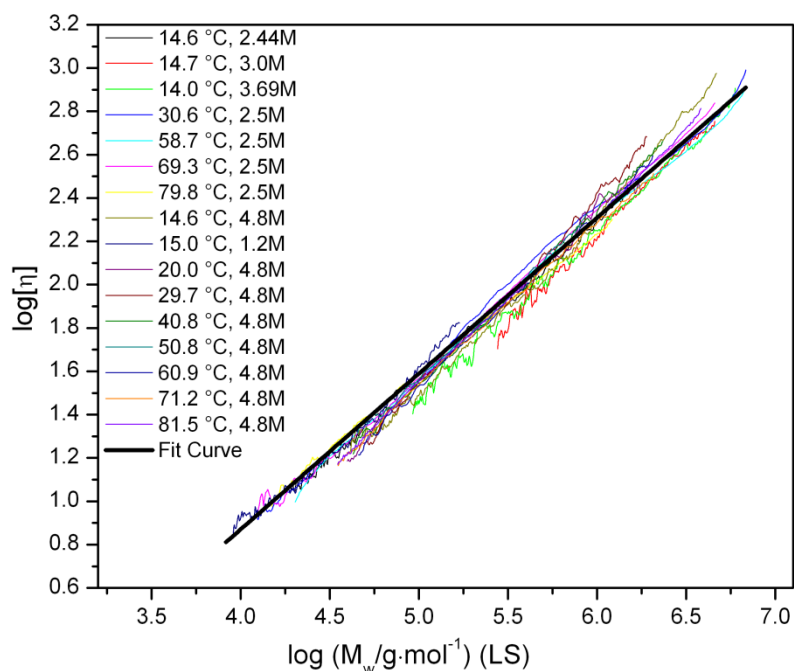


Figure 6-8: Linear regions of intrinsic viscosity for poly(2-EHA) from which the MHKS parameters were determined. The thick black line represents a linear fit of all data presented in the figure. The conditions under which poly(2-EHA) samples were generated can be found in the legend.

Figure 6-8 shows the  $\log [\eta]$  vs  $\log M_w$  plot constructed for poly(2-EHA). All the plots correlate well with each other despite the various conditions under which PLP was performed. The thick black line is a fit of all the plots from which MHKS parameters were calculated. The results are presented in Table 6-2.

The refractive index increment  $dn/dc$  (where  $n$  is the refractive index and  $c$  is the concentration) values used in triple detection SEC were as follows: for poly(MA), a value of  $0.068 \text{ mL}\cdot\text{mg}^{-1}$ , as determined by Penzel and Goetz,<sup>97</sup> while for poly(2-EHA), a value of  $0.070 \text{ mL}\cdot\text{mg}^{-1}$ , determined by Lathova *et al.*<sup>98</sup> The Mark-Houwink parameters determined and used in the PLP analyses that follow are presented in Table 6-2.

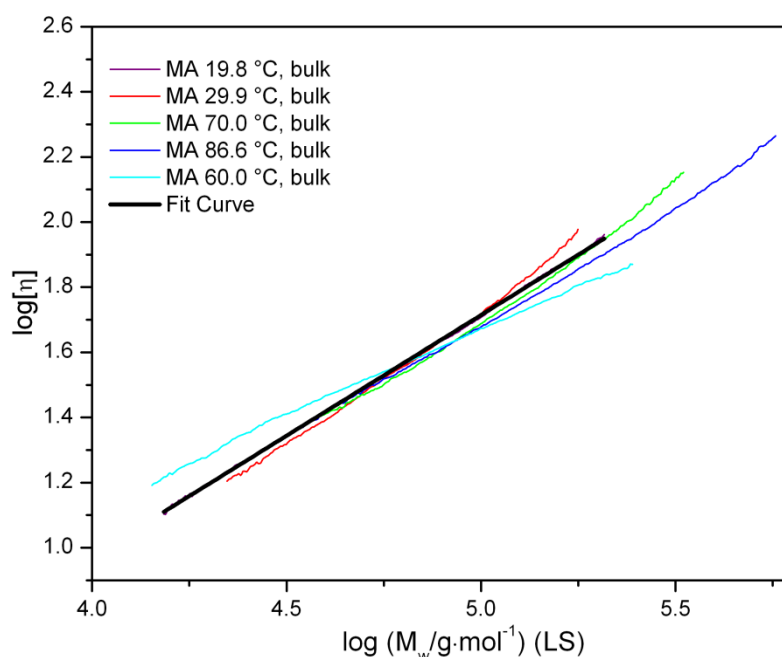


Figure 6-9: Linear regions of intrinsic viscosity for poly(MA) from which MHKS parameters were determined. The thick black line represents a linear fit of all data presented in the figure. The conditions under which poly(MA) samples were generated can be found in the legend.

Figure 6-9 depicts the Mark-Houwink plot for bulk MA PLP samples. The fit was performed with all data presented in the figure. Despite the sample prepared at 60 °C having a different slope relative to other samples, the final fit and calculation of MHKS parameters and the subsequent PLP analysis does not produce markedly different results whether or not the 60 °C sample is included in the initial determination of MHKS parameter calculations. The variation is in the order of a difference of  $600 \text{ L}\cdot\text{mol}^{-1}\cdot\text{s}^{-1}$  at 70 °C, which is not significant and represents a difference of  $<2 \%$  since  $k_{p,MA,70^\circ\text{C}}$  was determined to be  $34\,600 \text{ L}\cdot\text{mol}^{-1}\cdot\text{s}^{-1}$ . In the case of poly(MA), the MHKS parameters obtained in this work, while numerically different, do not produce significantly different  $k_p$  results when compared to literature values for the analysis of poly(MA) (by Buback *et al.*)<sup>67</sup> who used a  $K$  value of  $19.5 \text{ dL}\cdot\text{g}^{-1}$  and an  $\alpha$  value of 0.66. See next section for further details and discussion on  $k_p$  values obtained.

Table 6-2: Calculated MHKS parameters for poly(MA) and poly(2-EHA) PLP samples. Poly(MA) parameters were determined from samples prepared in bulk in the temperature range of 20 – 85 °C, with a molecular weight range of 16 000-200 000 g·mol<sup>-1</sup>. Poly(2-EHA) parameters were determined predominantly from samples in bulk, but including a few samples in solution (toluene) in the temperature range of 15-80 °C, with a molecular weight range of 6 500-6·10<sup>6</sup> g·mol<sup>-1</sup>.

	$K / \text{dL}\cdot\text{g}^{-1}$	$\alpha$
Poly(MA)	10.2	0.741
Poly(2-EHA)	8.2	0.695

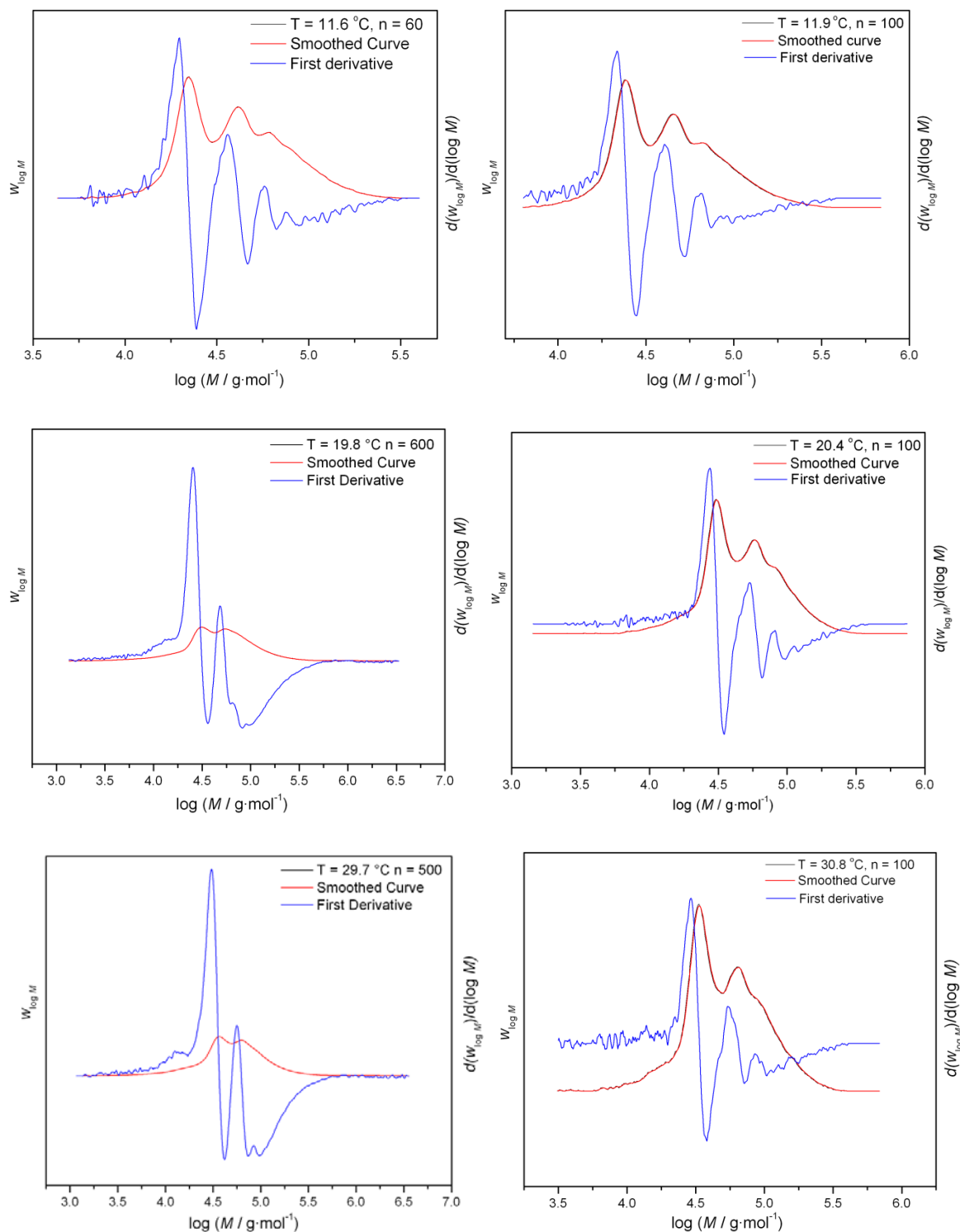
## 6.9 Results and Discussion – PLP of MA beyond 40 °C

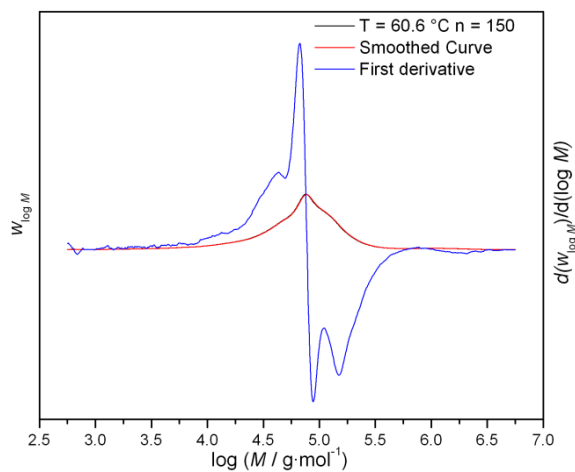
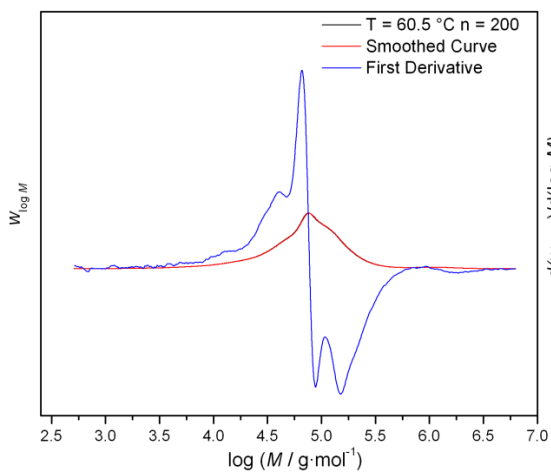
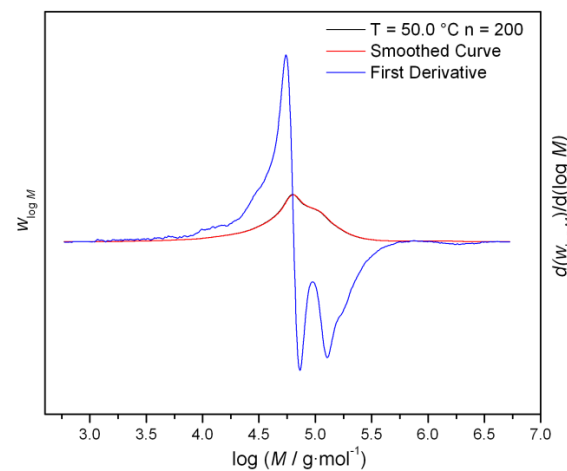
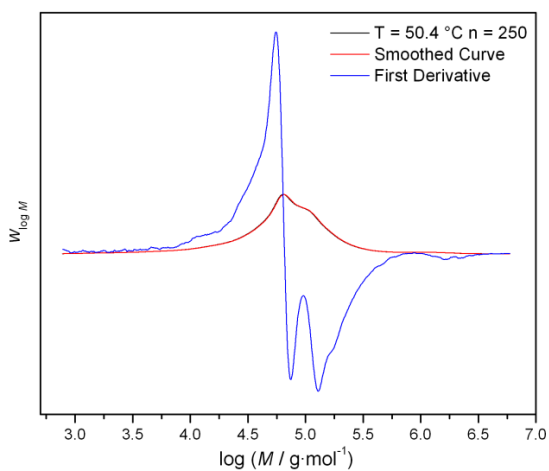
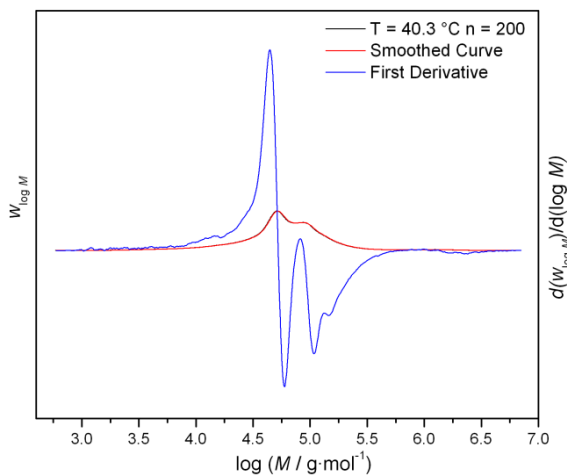
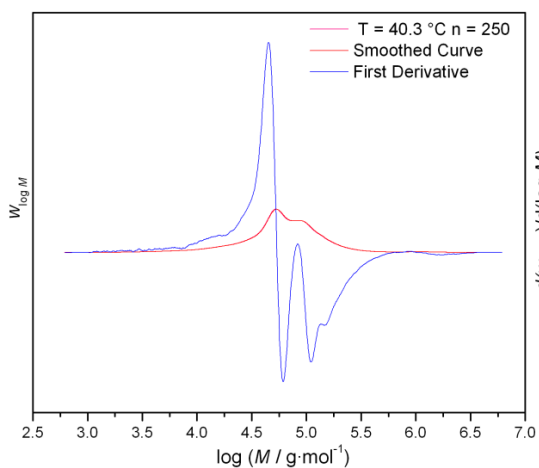
Acrylates are one of the most important type of monomers, however, no satisfactory PLP data could be obtained for temperatures above ambient values until recently.<sup>72</sup> The latest technology in excimer lasers allows pulsing at rates of 500 Hz at the XeF wavelength of 351 nm with energies of several mJ/pulse. There are several benefits of this in relation to acrylate polymerizations: i) high frequency pulsing allows determination of  $k_p$  at higher temperatures, ii) being able to vary pulse frequency creates more degrees of freedom when attempting to generate polymer with lower molecular weights without the need for adding chain transfer agents, and iii) determination of  $k_p$  for fast propagating monomers becomes easier as molecular weights can be more easily controlled *via* shorter dark times.<sup>72</sup>

All following experiments were conducted at 500 Hz, with laser energies of ~1.5 mJ/pulse, with the addition of 5·10<sup>-3</sup> mol·L<sup>-1</sup> DMPA as photo-initiator. The density of MA was calculated according to the equation:<sup>99-100</sup>

$$\rho_{\text{MA}} \left( \text{g}\cdot\text{cm}^{-3} \right) = 0.97196 - 1.11\cdot 10^{-3} (T \text{ } ^\circ\text{C}) \quad \text{Equation 6-8}$$

All molecular weight distributions and their derivatives used for  $k_p$  determination in the framework of the present study are shown in Figure 6-10 over the next three pages.





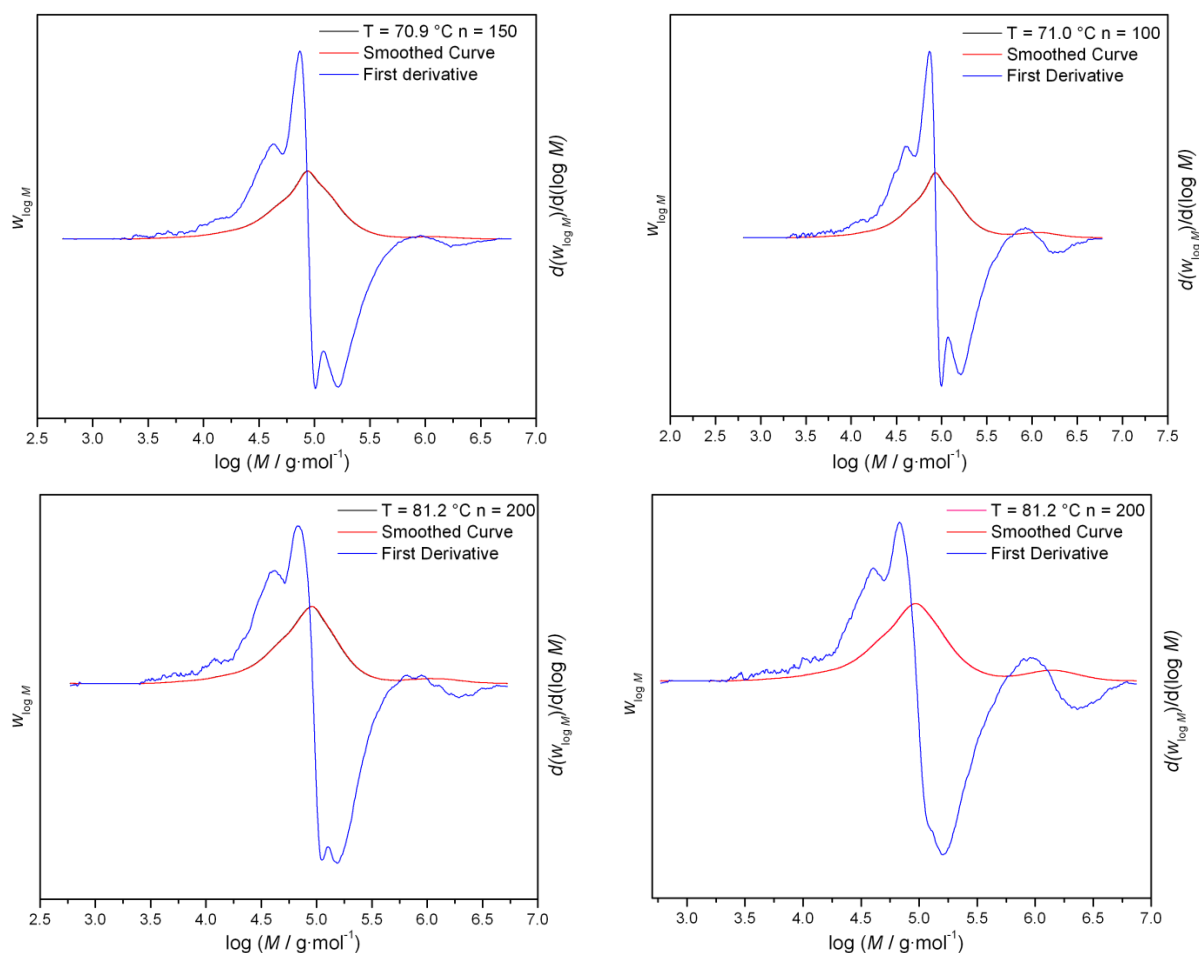


Figure 6-10: Molecular weight distributions and their first derivatives for all samples collated in Table 6-3.

Figure 6-10 depicts all the samples employed in the construction of the Arrhenius plot and the derivation of the Arrhenius parameters. The monomer density  $\rho$  was extrapolated from Equation 6-8. All samples were generated at a 500 Hz pulse repetition rate with a pulse energy of approximately  $1.5\text{ mJ}\cdot\text{pulse}^{-1}$ . The initiator concentration was  $c_{\text{DMPA}} = 5\cdot 10^{-3}\text{ mol}\cdot\text{L}^{-1}$  in all cases.

Table 6-3: Processed data for the  $k_p$ -determination of poly(MA) from PLP–SEC experiments.  $M_1$  and  $M_2$  refer to the molecular weight at the inflection points  $L_1$  and  $L_2$  respectively.  $k_{p,1}$  and  $k_{p,2}$  are the propagation rate coefficients that are derived from  $M_1$  and  $M_2$  respectively,  $n$  denotes the number of pulses applied, and  $X$  denotes overall monomer conversion.

N	$\theta / ^\circ\text{C}$	$n$	$X, \%$	$\rho / \text{g}\cdot\text{mol}^{-1}$	$\log (M_1 / \text{g}\cdot\text{mol}^{-1})$	$\log (M_2 / \text{g}\cdot\text{mol}^{-1})$	$k_{p,1} / \text{L}\cdot\text{mol}^{-1}\cdot\text{s}^{-1}$	$k_{p,2} / \text{L}\cdot\text{mol}^{-1}\cdot\text{s}^{-1}$
1	11.3	60	0.374	0.9664296	4.29631	4.5593	9935	8849
2	11.9	100	0.34	0.9652776	4.33459	4.60576	10899	9799
3	20.4	100	0.55	0.9489576	4.44059	4.72337	13401	12686
4	19.8	600	2.16	0.9501096	4.42667	4.71409	12679	11915
5	29.7	500	2.62	0.9311016	4.50486	4.77839	15361	13722
6	30.8	50	0.75	0.9289896	4.46471	4.73675	14379	13064
7	40.3	200	1.56	0.9107496	4.64747	4.91386	21478	19273
8	40.3	250	1.91	0.9107496	4.65605	4.9183	21886	19462
9	50.0	200	1.86	0.8917416	4.73807	4.97628	26204	22103
10	50.4	250	2.13	0.8913576	4.74242	4.98076	26456	22322
11	60.5	200	1.86	0.8719656	4.82107	5.03462	31442	25124
12	60.6	150	1.78	0.8717736	4.82547	5.04363	31747	25626
13	70.9	150	1.89	0.8519976	4.86512	5.07974	34634	27740
14	71	100	1.06	0.8518056	4.86512	5.07070	34634	27195
15	81.2	200	1.46	0.8322216	4.82986	5.09784	32054	28864
16	81.2	200	1.34	0.8322216	4.82986	-	32054	-

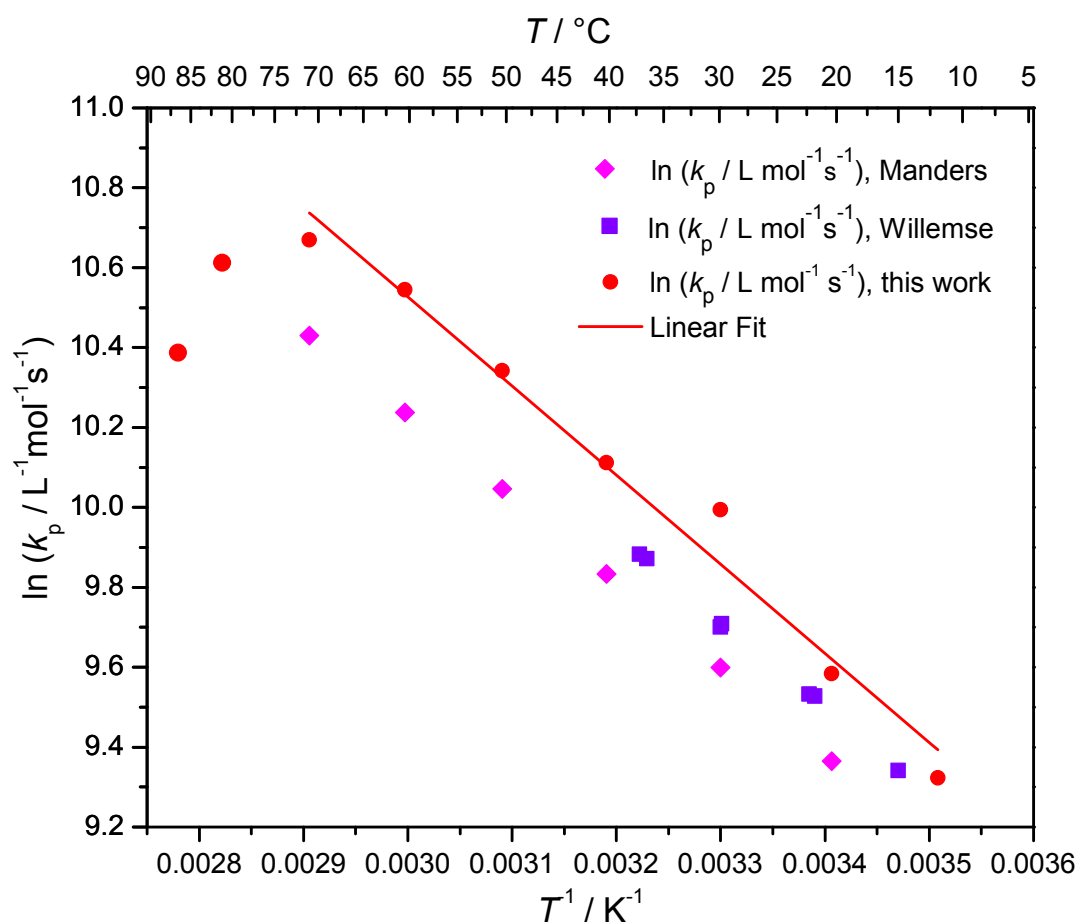


Figure 6-11: Arrhenius plot for the propagation rate coefficient of methyl acrylate in bulk in the temperature range 10-80 °C. The black diamonds represent data obtained by Manders<sup>101</sup> extrapolated to the relevant temperatures, while the black squares represent data obtained by Willemse and van Herk.<sup>102</sup> The red line represents a linear fit of the data obtained in this work.

The linear fit given in Figure 6-11 yields an activation energy of  $E_A = 18.5 (\pm 0.2) \text{ kJ}\cdot\text{mol}^{-1}$  and a frequency factor  $A = 30.0 (\pm 9)\cdot 10^6 \text{ L}\cdot\text{mol}^{-1}\cdot\text{s}^{-1}$ . The errors are determined at the outer limits of a 95 % confidence interval. While values are displayed for PLP experiments conducted at 80 and 85 °C for completeness, they were not considered as part of the Arrhenius calculation due to the pronounced decrease in  $k_p$  values observed. Willemse *et al.*<sup>102</sup> recently reported Arrhenius parameters for a family of acrylates employing MALDI-ToF-MS in conjunction with PLP, including MA, and obtained Arrhenius parameters of  $E_A = 18.3 \text{ kJ}\cdot\text{mol}^{-1}$  and  $A = 24.0\cdot 10^6 \text{ L}\cdot\text{mol}^{-1}\cdot\text{s}^{-1}$  for PLP experiments conducted in the

temperature range of -25 to 37 °C at laser frequencies between 60 to 100 Hz. The activation energy reported ( $18.33 (\pm 0.2) \text{ kJ}\cdot\text{mol}^{-1}$ ) is in very good agreement with the results of this work. At 50 °C, the  $k_p$  value of this work is greater to that of Willemse and van Herk by 15 %. Willemse and van Herk also showed that an increase in the size of the ester side group does indeed cause an increase in the determined  $k_p$ .

The activation energy is in the range typical for acrylate monomers, and agrees well with data obtained by Willemse and van Herk, but is rather different to that obtained by Manders, as discussed presently. Work carried out by Manders<sup>101</sup> yielded an activation energy  $E_A = 17.7 \text{ kJ}\cdot\text{mol}^{-1}$  and frequency factor  $A = 16.6\cdot 10^6 \text{ L}\cdot\text{mol}^{-1}\cdot\text{s}^{-1}$ . Although the Manders data represent one of two comprehensive studies yet attempted at ambient temperature (successful experiments were carried out in the range -19 °C to 32 °C) the data do exhibit some internal discrepancies, such as the observation of higher propagation rates at lower temperatures. One example of this instance is the determined  $k_p$  (50 °C) =  $13\,000 \text{ L}\cdot\text{mol}^{-1}\cdot\text{s}^{-1}$  while  $k_p$  (32 °C) =  $15\,000 \text{ L}\cdot\text{mol}^{-1}\cdot\text{s}^{-1}$ . While the only values retained for final calculation of Arrhenius parameters were in the temperature range -19 °C-32 °C, the Manders experiments were conducted in the range of -25 °C-57 °C, at 80 and 100 Hz, employing DMPA as photo-initiator, mostly in bulk experiments but samples in toluene, methyl propionate and *t*-butylbenzene were also produced. Manders observed a large increase in temperature during the pulsing time; the temperature was seen to rise by 20 °C in 10 s. To eliminate this effect while obtaining sufficient polymer conversion, pulses were applied in consecutive runs of fewer pulses. These conditions are vastly different to the conditions employed in this work where no appreciable increase in temperature was observed during pulsing at 500 Hz with short pulse times, in the range of a few seconds.

Buback *et al.*<sup>64</sup> studied the pressure dependence of  $k_p$  in FRP of MA, and determined  $k_p$  (-28 °C) =  $3\,300 \text{ L}\cdot\text{mol}^{-1}\cdot\text{s}^{-1}$  and  $k_p$  (-15 °C) =  $5\,300 \text{ L}\cdot\text{mol}^{-1}\cdot\text{s}^{-1}$  when extrapolated to ambient pressure. The extrapolation provides values which are ~20 % greater than those obtained by Manders and ~10 % greater than values obtained in this work and by Willemse and van Herk. Due to the limited number of data points no fit of the data was made for determination of Arrhenius parameters.

With increasing temperature, the PLP-derived molecular weight distributions slowly start to lose their characteristic peak maxima in the first derivative. Such behavior is expected, as backbiting and MCR reactions become increasingly influential to the molecular weight distribution and blur the PLP distribution. Even pulsing at 500 Hz is not fast enough to counteract the perturbations caused by MCR formation from a certain point. In this study it is not until 80 °C that no second point of inflection can be observed. However, already at 70 °C, another effect is observable: a shoulder on the low molecular-weight side of the distribution becomes visible. This shoulder is likely caused by the increasing importance of  $\beta$ -scission and/or the termination of radicals that have undergone an intramolecular transfer reaction.

In principle, the second point of inflection could also be used to calculate  $k_p$ . However, an increasing discrepancy between  $k_{p,1}$  and  $k_{p,2}$ , that is,  $k_p$  obtained from  $L_1$  and  $L_2$  respectively, is observed with increasing temperature. This difference is easily explained by the retarding effect that the MCRs induce. As the chains at  $L_2$  grew twice as long as the ones at  $L_1$ , they underwent more transformations into MCRs and back, thus resulting in shorter chains than anticipated. Thus,  $L_2$  does not provide a good measure for  $k_p$  at elevated temperatures, since the difference between  $k_{p,1}$  and  $k_{p,2}$  at 70 °C is already 20 %, which may be regarded to be the largest tolerable difference for a successful PLP-SEC experiment. Typical acceptable discrepancies are in the range of 10 %. Furthermore, at 80 °C the maximum peak of the derivative loses its characteristic sharpness and it becomes difficult to discern a precise maximum. Despite these issues, the values of  $E_A = 18.5 \text{ kJ}\cdot\text{mol}^{-1}$  and a frequency factor of  $A = 30.0\cdot 10^6 \text{ L}\cdot\text{mol}^{-1}\cdot\text{s}^{-1}$  provide a good indication of  $k_p$  of MA above ambient temperature and up to 80 °C and are in good agreement with those obtained by Willemse and van Herk.<sup>102</sup>

Table 6-4 presents some Arrhenius parameters of selected acrylates and is by no means an exhaustive list, but serves as a good general overview of the acrylate monomers which have been examined by PLP-SEC, or PLP-MALDI-ToF-MS in the case of the Willemse and van Herk data. The general trend observed is that  $k_p$  increases with increasing size of the ester side group, as observed repeatedly by various groups.<sup>44,102-103</sup>

Table 6-4: Comparison of Arrhenius parameters for MA and selected other acrylates.

	Monomer	$E_A / \text{kJ}\cdot\text{mol}^{-1}$	$A / 10^{-6} \text{L}\cdot\text{mol}^{-1}\cdot\text{s}^{-1}$
This work	MA	18.5	30.0
Manders <sup>101</sup>	MA	17.7	16.6
Willemse and van Herk <sup>102</sup>	MA	18.33	24.0
Dervaux <i>et al.</i> <sup>50</sup>	<i>i</i> BoA*	17.0	11.22
	<i>t</i> BuA*	17.5	19.05
	EEA*	13.8	6.3
Asua <i>et al.</i> <sup>68</sup>	<i>n</i> -BA	17.9	22.1
Willemse and van Herk <sup>102</sup>	EA*	18.59	26.9
	<i>n</i> -BA	18.55	27.5
	<i>n</i> -HexA*	18.46	27.5
	BenA*	17.38	20.9
Beuermann <i>et al.</i> <sup>43</sup>	<i>n</i> -BA	17.4	18.0
Buback <i>et al.</i> <sup>67</sup>	DA	17.3	17.9

\**i*BoA - isobornyl acrylate, *t*-BA – *tert*-butyl acrylate, EEA – 1-ethoxyethyl acrylate, EA – ethyl acrylate, *n*-HexA – *n*-hexyl acrylate, BenA – benzyl acrylate, DA – dodecyl acrylate

## 6.10 Pulsed Laser Polymerization of 2-Ethyl Hexyl Acrylate beyond 25 °C

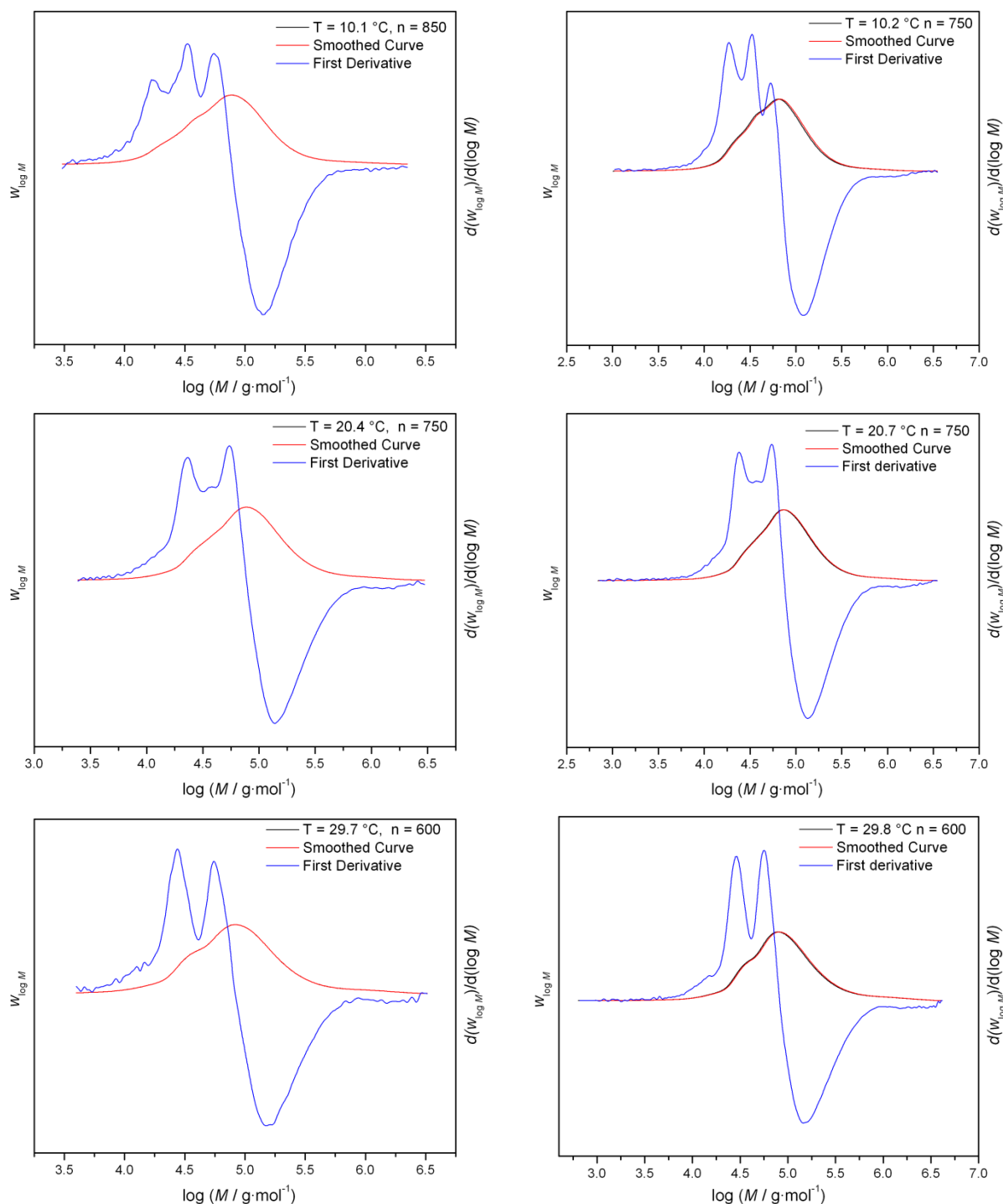
PLP of 2-ethyl hexyl acrylate has previously been studied by Hutchinson and co-workers<sup>43</sup> and by Vairon and co-workers.<sup>104</sup> Hutchinson and co-workers determined twelve values for the PLP of 2-EHA in the temperature range 5 to 25 °C, at 100 Hz pulse frequency employing benzoin as photo-initiator. However, the temperature range examined was too narrow for determination of reliable Arrhenius parameters. Vairon and co-workers studied PLP of 2-EHA in toluene solution where monomer concentration was half of that in bulk. PLP distributions were obtained at low temperatures, in the range -30 °C – 10 °C, at 100 Hz pulse frequency. This work provides for the first time  $k_p$  values for bulk poly(2-EHA) at elevated temperatures, up to 75 °C.

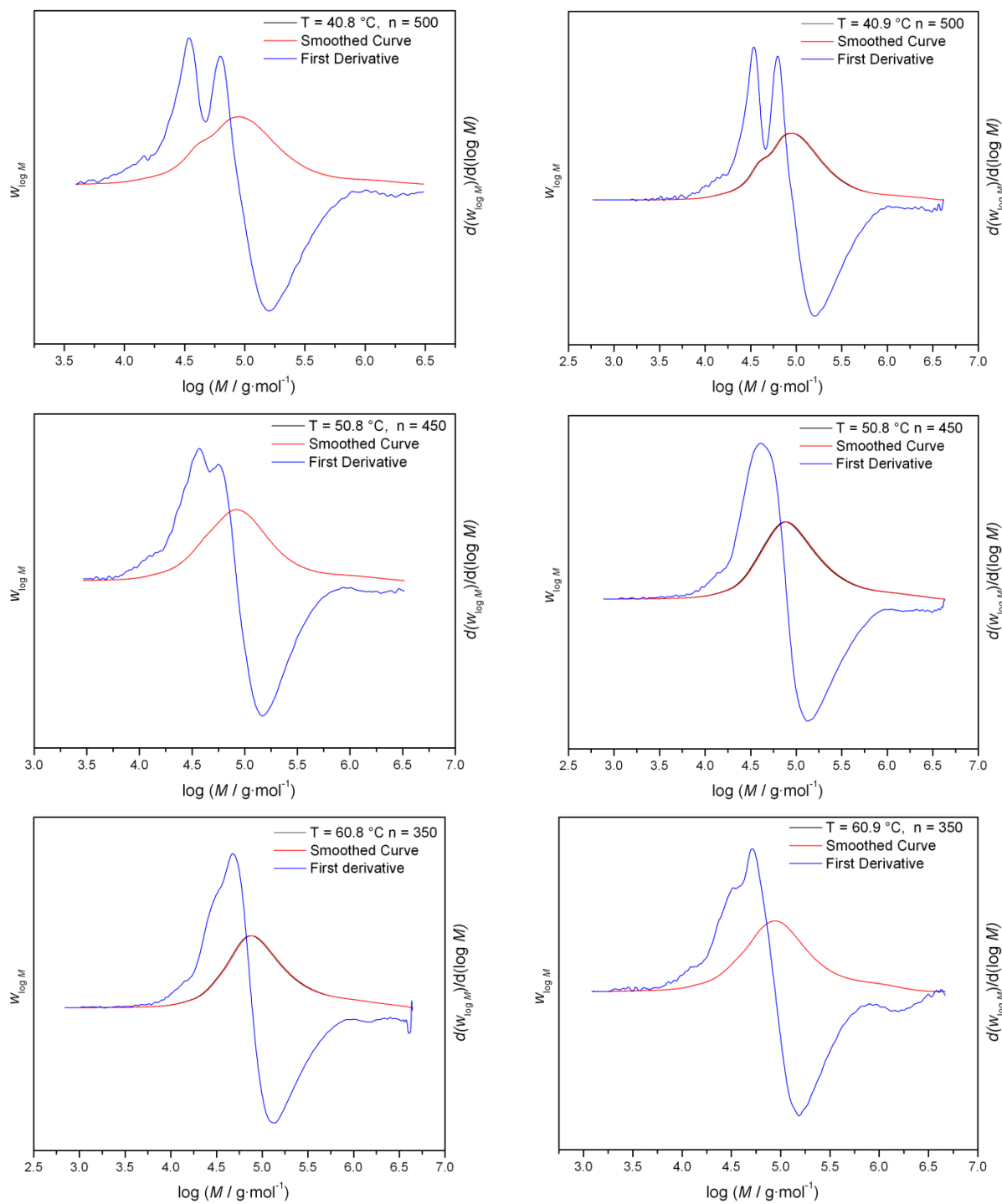
The density of 2-EHA was calculated according to the equation:<sup>104</sup>

$$\rho_{2\text{-EHA}} \left( \text{g}\cdot\text{cm}^{-3} \right) = 0.90056 - 0.00081 (T^\circ\text{C}) \quad \text{Equation 6-9}$$

Figure 6-12 over the next three pages presents the molecular weight distributions and their first derivatives for all samples collated in Table 6-5 which were used to determine Arrhenius parameters for poly(2-EHA).

All samples were measured at 500 Hz pulse repetition rate with a pulse energy of about 1.5 mJ/pulse. The initiator concentration was  $c_{\text{DMPA}} = 5 \cdot 10^{-3} \text{ mol} \cdot \text{L}^{-1}$  in all cases, and the monomer density  $\rho$  was extrapolated from Equation 6-9.





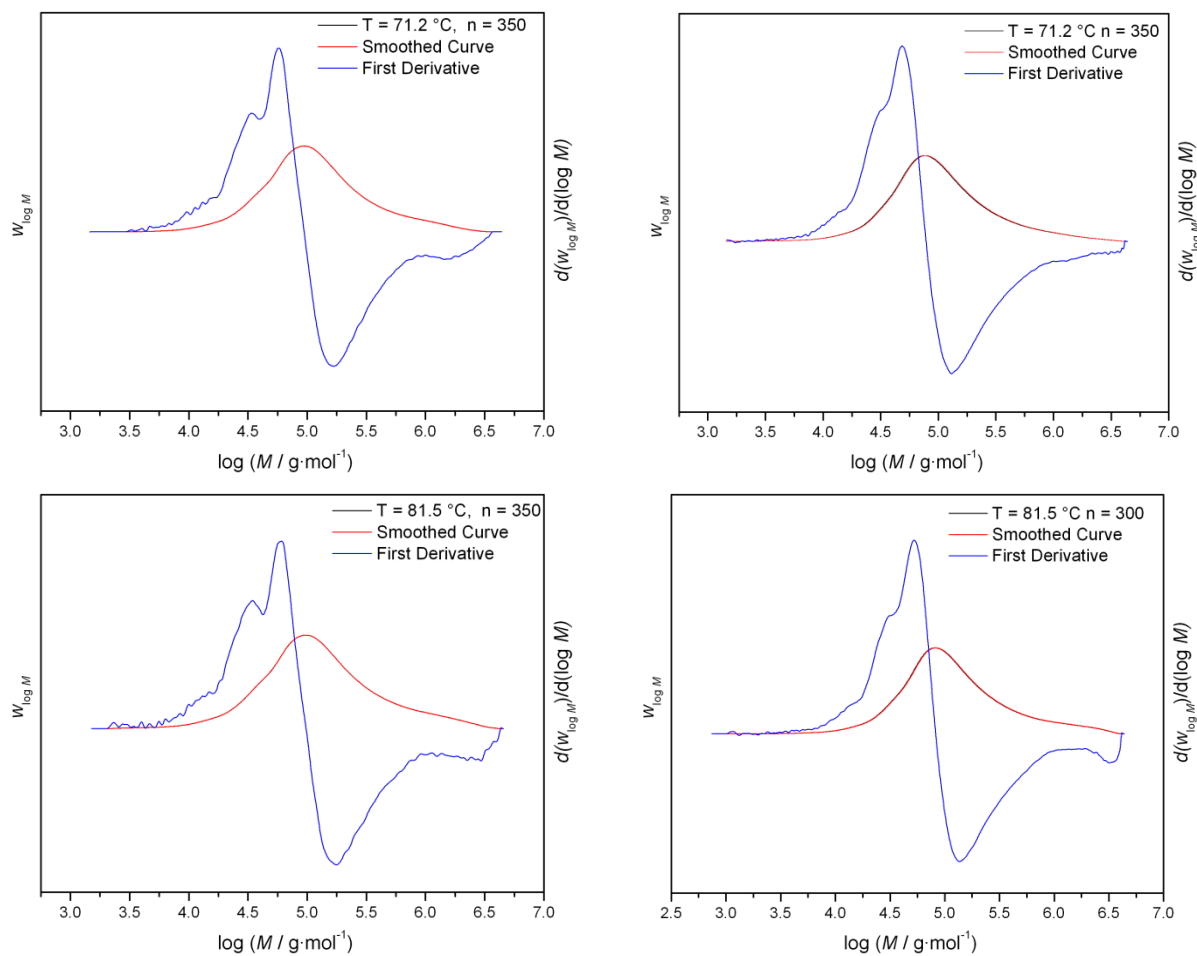


Figure 6-12: Molecular weight distributions and their first derivatives for all samples collated in Table 6-5.

Table 6-5: Processed data for the  $k_p$ -determination of 2-ethyl hexyl acrylate from PLP-SEC experiments.  $M_1$  and  $M_2$  refer to the molecular weight at the inflection points  $L_1$  and  $L_2$  respectively.  $k_{p,1}$  and  $k_{p,2}$  are the propagation rate coefficients that are derived from  $M_1$  and  $M_2$ .  $n$  denotes the number of pulses applied, and  $X$  denotes overall monomer conversion.

N	$\theta / ^\circ\text{C}$	$n$	X %	$\rho / \text{g}\cdot\text{mol}^{-1}$	$\log (M_1 / \text{g}\cdot\text{mol}^{-1})$	$\log (M_2 / \text{g}\cdot\text{mol}^{-1})$	$k_{p,1} / \text{L}\cdot\text{mol}^{-1}\cdot\text{s}^{-1}$	$k_{p,2} / \text{L}\cdot\text{mol}^{-1}\cdot\text{s}^{-1}$
1	10.2	750	1.9	0.892298	4.311874532	4.560531543	11488	10183
2	10.1	850	2.4	0.892379	4.269970268	4.561965266	10433	10218
3	20.7	700	1.8	0.883793	4.424238866	4.773572897	15017	16784
4	20.0	700	2.2	0.88436	4.408220719	4.774462794	14473	16818
5	29.8	600	1.6	0.876422	4.502945316	4.790273299	18811	18227
6	29.7	600	2.0	0.876503	4.480618788	4.778576096	17252	17130
7	40.9	500	1.4	0.867431	4.572179307	4.832385205	21505	19576
8	40.8	500	1.9	0.867512	4.577627454	4.836696261	21793	19786
9	50.8	450	1.5	0.859412	4.651123063		26035	
10	50.8	450	2.1	0.859412	4.605174712		23439	
11	60.8	350	1.4	0.851312	4.719921993		30794	
12	60.9	350	1.9	0.851231	4.749842309		33019	
13	71.2	350	1.5	0.842888	4.724005631		31384	
14	71.2	350	2.0	0.842888	4.799241483		37363	
15	81.5	300	1.8	0.834545	4.824168488		39966	
16	81.5	300	1.5	0.834545	4.756971373		34187	

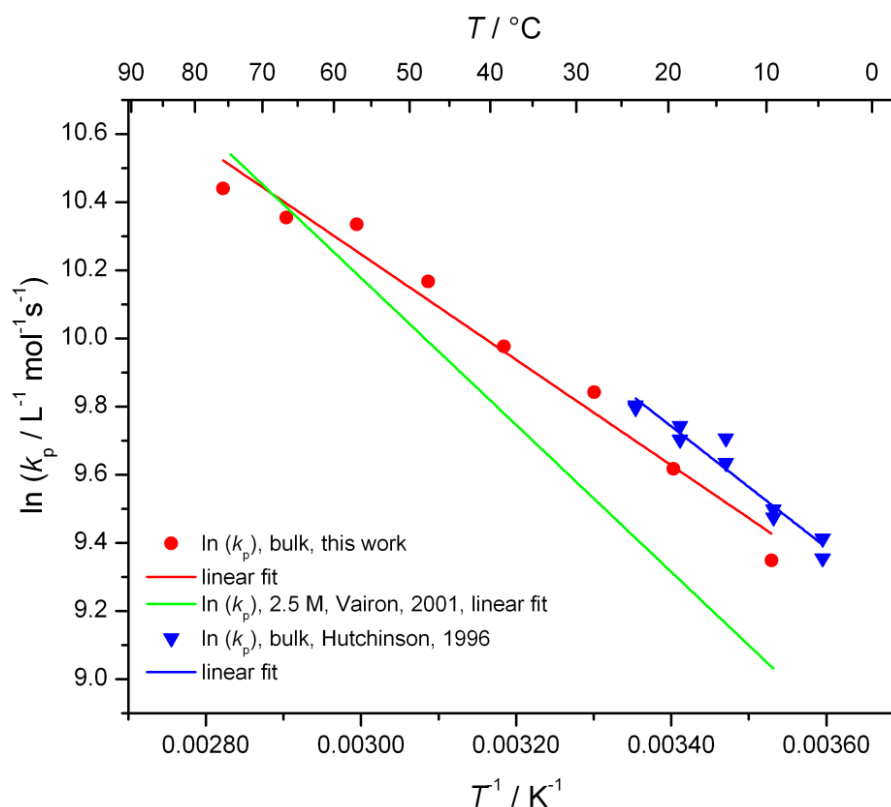


Figure 6-13: Arrhenius plot for poly(2-ethyl hexyl acrylate) showing  $k_p$  data obtained at 500 Hz. The solid line represents the best fit of the data. The dashed line represents a fit of data obtained by Vairon and co-workers.<sup>104</sup> The dotted line represents a fit of data obtained by Hutchinson and co-workers.<sup>43</sup>

A linear fit of all data points indicates an activation energy of  $E_A = 12.9 (\pm 0.8) \text{ kJ}\cdot\text{mol}^{-1}$  and a frequency factor of  $A = 3.0 (\pm 0.8)\cdot 10^6 \text{ L}\cdot\text{mol}^{-1}\cdot\text{s}^{-1}$  for a temperature range of  $10 \text{ }^\circ\text{C} \leq T \leq 75 \text{ }^\circ\text{C}$ . The errors are determined at the 95 % confidence interval. Data by Vairon and co-workers is fitted with  $E_A = 17.93 \text{ kJ}\cdot\text{mol}^{-1}$  and a frequency factor of  $A = 16.98\cdot 10^6 \text{ L}\cdot\text{mol}^{-1}\cdot\text{s}^{-1}$  for the temperature range of  $-25 \text{ }^\circ\text{C} \leq T \leq 10 \text{ }^\circ\text{C}$ . From Figure 6-13 it can already be seen that a significant discrepancy exists between the values determined by Vairon and Hutchinson, values from Vairon are lower by about 30 % in comparison with those obtained by Hutchinson. While values obtained by Hutchinson and co-workers have been inserted into Figure 6-13 for an overview of previously obtained  $k_p$  values, they did not wish to draw any conclusions from this data by reporting activation energies due to the scatter observed in duplicate samples, the narrow temperature range investigated, and the limited number of

values obtained. However, to provide a rough estimate for comparison, the values obtained were fitted as part of this work, resulting in  $E_A = 14.8 \text{ kJ}\cdot\text{mol}^{-1}$  and a frequency factor of  $A = 7.2\cdot 10^6 \text{ L}\cdot\text{mol}^{-1}\cdot\text{s}^{-1}$ .

The results of this work agree more closely with those of Hutchinson and co-workers but exhibit a discrepancy when compared with the data obtained by Vairon and co-workers in terms of activation energy. Since the data obtained in this work and in that of Hutchinson and co-workers was obtained in bulk PLP experiments, this may suggest an effect due to solvent. The present work determines an activation energy approximately  $5 \text{ kJ}\cdot\text{mol}^{-1}$  lower than that obtained by Vairon and co-workers. Possible reasons include the use of a solvent by Vairon and co-workers while samples here were prepared in bulk. Solvent effects with regards to  $k_p$  evaluation are defined as variations in the observed  $k_p$  when monomer concentration and/or the solvent is varied.

Two effects due to solvent addition have been reported in the literature,<sup>105</sup> (i)  $k_p$  and  $E_A$  both vary, and (ii)  $k_p$  values vary while  $E_A$  values remain constant. In the case of variation in both  $k_p$  and  $E_A$ , this can be explained by a complexing effect between the solvent molecules and the propagating radicals. In the second instance, where only  $k_p$  values vary while  $E_A$  values remain constant, the explanation for this behavior lies in the existence of variations in local monomer concentrations, rather than formation of solvent-propagating radical complexation. PLP effectively measures  $k_p\cdot[M]$  and by restricting conversion to low amounts, i.e.  $<10 \%$ , then  $[M]$  can be essentially taken to be equal  $[M]_0$ , the starting monomer concentration, which is a known value, and subsequently allow  $k_p$  values to be calculated. If there is a local monomer concentration at the propagating radical site which is different to the bulk solution monomer concentration, then it follows that varying values of  $k_p$  can be expected. Beuermann<sup>91</sup> determined that  $k_p$  may be enhanced by up to an order of magnitude, depending on the origin of the solvent influence. The solvent influence can have an effect on either or both the pre-exponential or the activation energy of  $k_p$ .

As these new  $k_p$  values provide previously unknown information, there are no other literature values for comparison other than those discussed. However, issues on the effects of branching in 2-EHA, in particular with regards to molecular weight determination, are considered such potential sources of errors that a further investigation into the effects of

branching is of significant importance. The issue of the extent of branching occurring in acrylate systems has further relevance other than the general hindrance of PLP, as chain branches cause changes in the hydrodynamic volume of polymer chains in solution and thus potentially affect SEC analysis.<sup>58,95</sup> Studies have recently begun to measure branching levels in poly(acrylates) with respect to molecular weight determination, with the aim of increasing accuracy of SEC of poly(acrylates).

Table 6-6: Comparison of various activation energies and associated pre-exponential factors for 2-EHA. These data should be examined in conjunction with the values presented in Table 6-4.

	$E_A / \text{kJ}\cdot\text{mol}^{-1}$	$A / 10^{-6} \text{ L}\cdot\text{mol}^{-1}\cdot\text{s}^{-1}$
This work	12.9	3.0
Vairon and co-workers <sup>104</sup>	17.93	16.98
Hutchinson and co-workers <sup>43</sup>	14.8	7.2

It has been firmly established that intra and inter-molecular transfer to polymer is an important reaction pathway in acrylate polymerizations even at moderate temperatures.<sup>77,106</sup> The formation of mid-chain radicals may lead to large errors in  $k_p$  determination<sup>47</sup> and one way to overcome this has been demonstrated in the current work, i.e. the use of ever higher frequency pulsing, and is successful in cases where  $\beta$ -scission is not a significant reaction.<sup>72</sup> Intramolecular transfer stemming from the backbiting reaction produces mainly short chain branching, which is of minor consequence to the viscosity properties of the final polymer. Intermolecular and random intramolecular transfer to polymer on the other hand produce long chain branching, and when this radical terminates it results in the gel formation, which is often observed in radical homopolymerizations of acrylates.<sup>107-108</sup> In relation to determination of molecular weights, which is a critical aspect of PLP-SEC in evaluating  $k_p$ , long chain branching can lead to incomplete separation by SEC; which has been demonstrated both experimentally<sup>92</sup> and by simulation.<sup>109-110</sup> Long chain branching has been observed in PLP of 2-EHA at  $-5\text{ }^\circ\text{C}$ <sup>92</sup> and since it can have a major influence on SEC measurements, it thus also affects  $k_p$  determination. In light of this, a study

into the branching characteristics of the 2-EHA and MA PLP polymer material was conducted. However the concept of local dispersity must be introduced before the results can be presented. The concept of local dispersity is a method that attempts to quantify the error in SEC that is brought about by the presence of long chain branching.

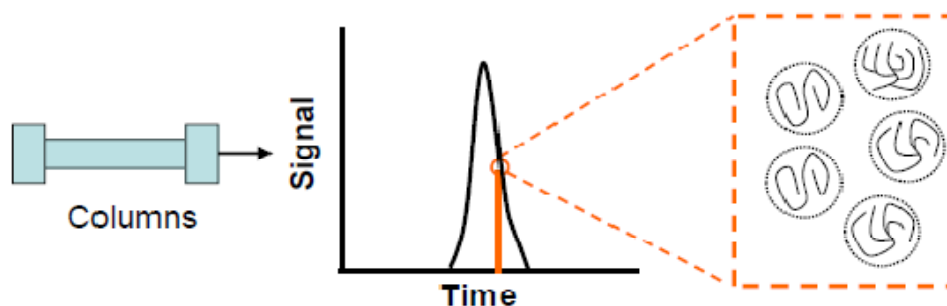
### 6.11 The Concept of Local Dispersity

Multiple detection SEC enables the determination of molecular weights by two independent means, viscometry/universal calibration and light scattering. Benoit<sup>111</sup> as well as other groups<sup>110,112</sup> have provided evidence that SEC separation occurs by the product of  $[\eta] \cdot M$ , where  $[\eta]$  is the intrinsic viscosity and  $M$  the molecular weight, and not only according to molecular weight. Zimm *et al.* demonstrated that the presence of long-chain branches significantly changes the hydrodynamic volume of polymer chains at a given MW.<sup>113-114</sup> For linear polymers a one-to-one relation exists between MW and the elution time when band broadening is neglected (the direct calibration curve), but this is not the case for complex branched polymers. In the case of branched polymers a sample where all chains have the same hydrodynamic volume may contain a distribution of molecular weights.<sup>94,110,115</sup> The distributions obtained from conventional SEC data treatment, as performed by most commercial software, provide distributions of local average molecular weights. Viscometry/universal calibration gives distributions of local number-average molecular weights,  $\overline{M}_n(V_e)$ , while light scattering leads to distributions of local weight-average molecular weight,  $\overline{M}_w(V_e)$ . No relation with the distribution of the true molecular weights  $\omega(\log M)$  is currently known.

A description of the origins of local dispersity will now be provided. Local dispersity is a concept which has existed since Hamielec and co-workers observed incorrect molecular weight determinations for branched poly(vinyl acetate) and low density poly(ethylene)<sup>94,115-116</sup> and which has been examined over the years.<sup>92,109,117-118</sup> Scheme 6-4 graphically shows the concept of local dispersity. Essentially, polymer structures which have the same hydrodynamic volume, but different molecular weights, elute at the same time, creating heterogeneity for a given elution volume. At each elution volume  $V_e$ , viscometry/universal calibration provides local number-average molecular weights  $\overline{M}_n(V_e)$ , while light scattering provides local weight-average molecular weights,  $\overline{M}_w(V_e)$ . The ratio

$\overline{M}_w(V_e)/\overline{M}_n(V_e)$  is defined as corresponding to a local dispersity,  $D(V_e)$ . This is analogous to the concept of polydispersity of a polymer, but here the local dispersity is calculated at each elution volume. Complete separation in terms of molecular weights would correspond to  $D(V_e) = 1$ , that is, at a particular elution volume the  $\overline{M}_n$  and  $\overline{M}_w$  are the same.

Band-broadening<sup>119</sup> is considered negligible in the present case.<sup>117</sup> The premise of local dispersity relies on finding SEC conditions so that  $D(V_e) = 1$  in the case of linear polyacrylates.<sup>92</sup> Significant differences between  $\overline{M}_n(V_e)$  and  $\overline{M}_w(V_e)$  can then be studied using  $D(V_e)$  plots and the domains where  $D(V_e)$  is significantly greater than unity provide information on the heterogeneity of the samples. In the case of branched polyacrylates,  $D(V_e)$  greater than unity have been observed for various polyacrylates not only obtained by conventional or controlled polymerization, but also by PLP.<sup>95</sup> This is attributed to long-chain branching, as previously discussed.<sup>92,109,118</sup> Low signal-to-noise ratios may lead to anomalous molecular weights,<sup>120</sup> so care must be taken to measure samples at high enough concentration to provide strong signals.



Scheme 6-4: Graphical representation of the concept of local dispersity. The presence of various structures of polymer chains leads to different molecular weights chains with the same hydrodynamic volume to be eluted at the same time. Reproduced with permission from the author.<sup>121</sup>

## 6.12 2-Ethyl Hexyl Acrylate and Methyl Acrylate Local Dispersities

To determine  $D(V_e)$ , data treatment is applied as follows to results obtained *via* triple detection SEC: i) The  $\log [\eta]$  is fitted to a degree 6 polynomial and from this fit and in conjunction with universal calibration, values for  $M_n(V_e)$  are obtained *via* calculation of hydrodynamic volume, while  $M_w(V_e)$  values are used directly as observed from light

scattering results. The ratio  $M_w(V_e) / M_n(V_e) = D(V_e)$  is then evaluated. The reason for not fitting both  $M_n(V_e)$  and  $M_w(V_e)$  is that artifacts become apparent in the values of  $D(V_e)$ . This effect was speculated by Castignolles<sup>95</sup> and was confirmed in the course of this investigation. Figure 6-14 clearly shows the significant deviation observed when both  $M_n(V_e)$  and  $M_w(V_e)$  are fitted prior to calculation of  $D(V_e)$ . Fitting only  $M_n(V_e)$  is a compromise that provides smoother  $D(V_e)$  values whilst retaining the essence of the raw data. The  $D(V_e)$  results for each sample of 2-EHA and MA are graphically presented in Figure 6-15.

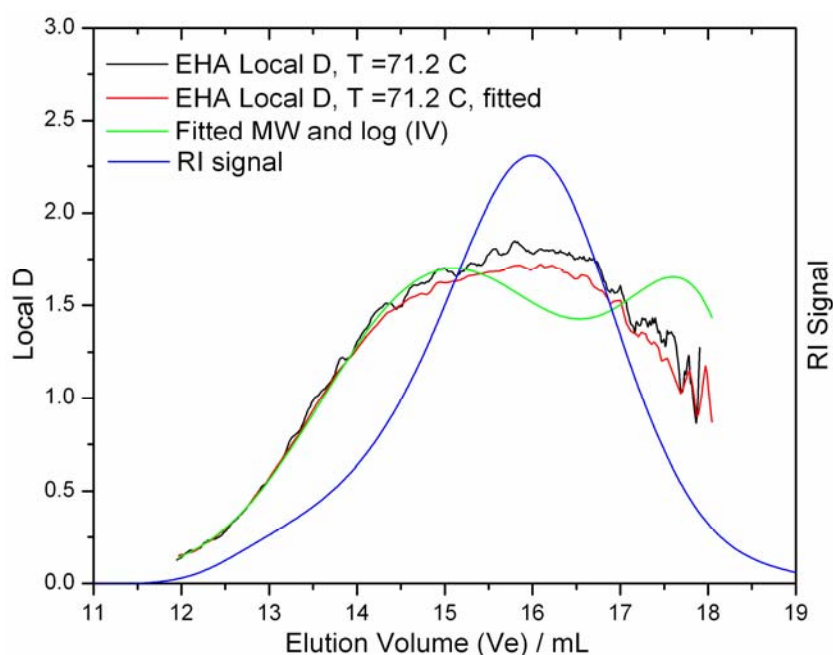
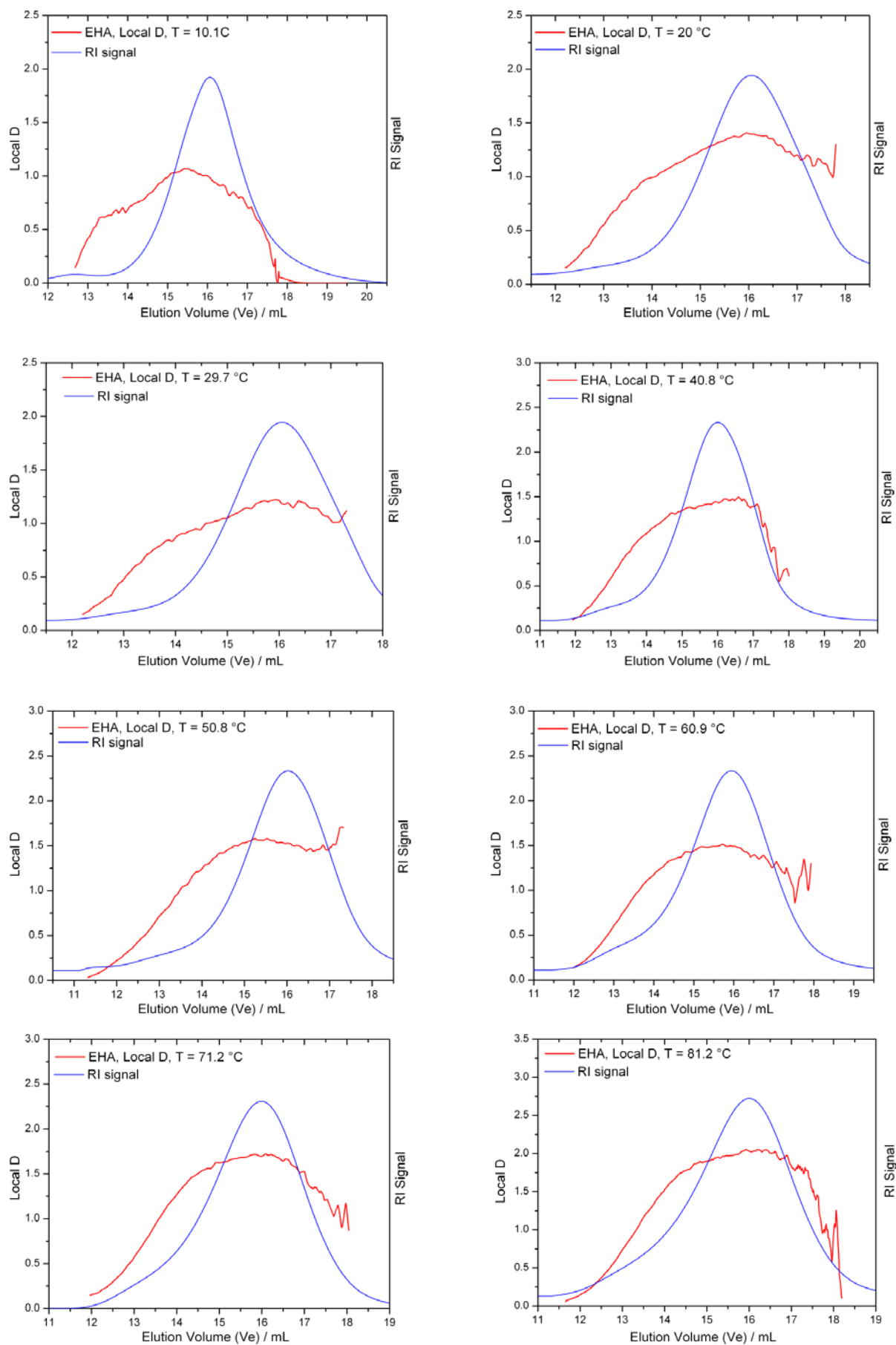


Figure 6-14: The graph depicts the effect of various data treatments on the obtained  $D(V_e)$  values. As an example, the 2-EHA PLP sample prepared at 71.2 °C is considered. The black trace is obtained when no fits are made to either  $M_n(V_e)$  or  $M_w(V_e)$ . The red trace shows  $D(V_e)$  values obtained when only  $M_n(V_e)$  is fitted, and the green trace shows  $D(V_e)$  values obtained when both  $M_n(V_e)$  and  $M_w(V_e)$  values are fitted. Clearly  $D(V_e)$  values obtained when both  $M_n(V_e)$  and  $M_w(V_e)$  values are fitted no longer reflect the original raw values (the black trace) and provide erroneous information on  $D(V_e)$ .

Figure 6-15 over the next two pages graphically depicts the calculated  $D(V_e)$  values for poly(2-EHA) and for poly(MA) over temperatures ranging from 10 – 80 °C.



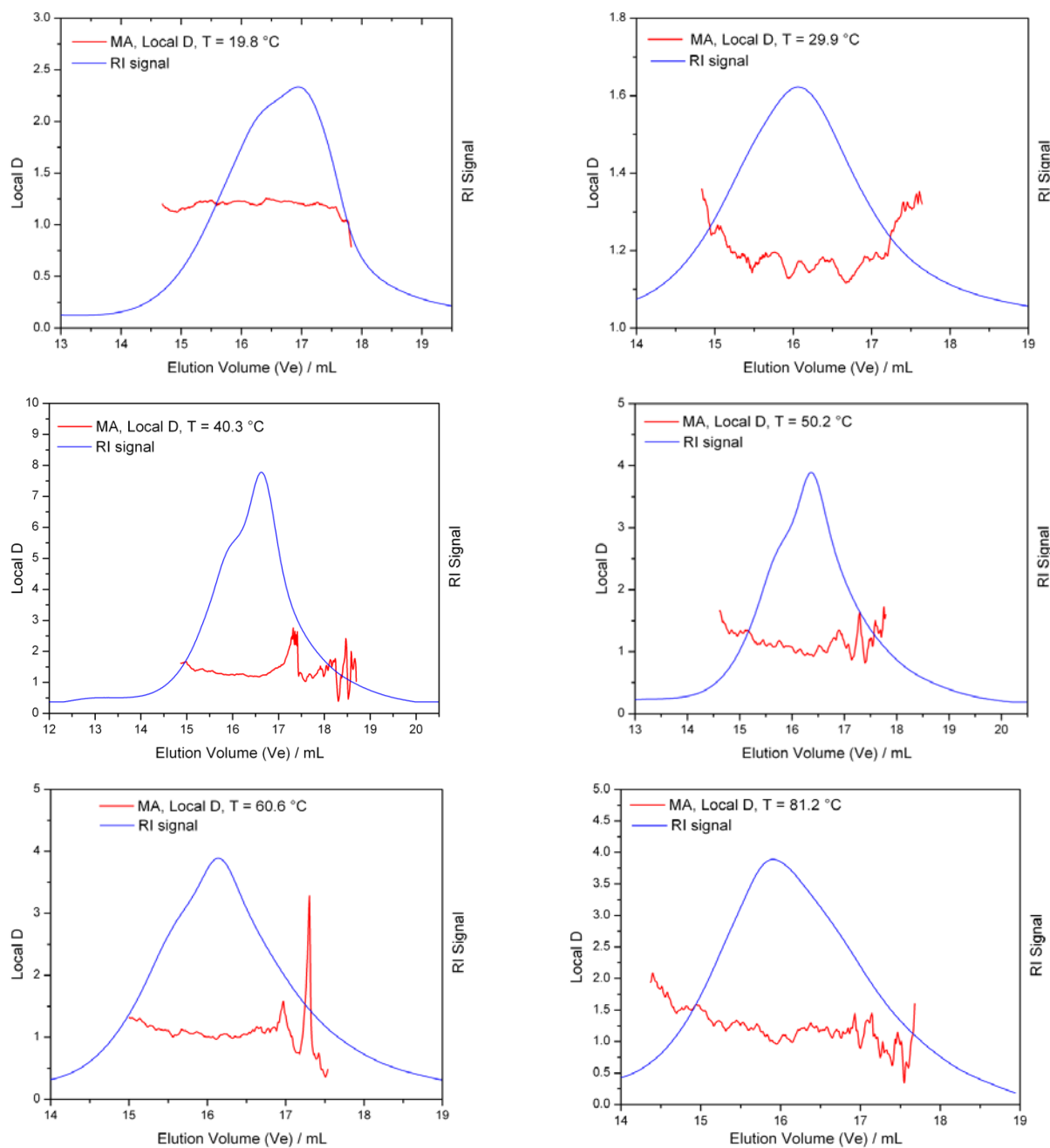


Figure 6-15: Elugrams and corresponding calculated values for  $D(V_e)$  for 2-EHA and MA PLP samples, in the temperature range of 10 °C – 80 °C.

To make comparison of the various  $D(V_e)$  values easier, an average local dispersity is calculated. The average dispersity is taken at half the height of the elugram, and the mean value of  $D(V_e)$  falling in this region is determined. These results are presented in Table 6-7. A graphical representation can be seen in Figure 6-16. It is important to note that although a linear fit of the data has been made, this fit should be considered an aide to guide the eye to

discern trends in the data rather than as a statement that a linear relationship between  $D(V_e)$  and temperature for either poly(2-EHA) or poly(MA) exists. Nevertheless, trends can clearly be observed. Table 6-7 and Figure 6-16 both show the average local dispersities as calculated at half peak height of the corresponding SEC elugram. From both representations, a clear trend is immediately discernible.

Table 6-7: Average Local Dispersities for poly(2-EHA) (left) and poly(MA) (right) PLP samples. Averages are taken at  $\frac{1}{2}$  peak height of the corresponding elugram.

T / °C	Average Local D	T / °C	Average Local D
10.1	0.953	19.8	1.204
20.0	1.310	29.9	1.168
29.7	1.138	40.3	1.304
40.8	1.417	50.2	1.085
50.8	1.516	60.6	1.082
60.9	1.434	70.0	1.148
71.2	1.635	81.2	1.175
81.2	1.956		

It should be noted that a  $D(V_e)$  value of less than one, as calculated for poly(2-EHA) at 10 °C, is theoretically impossible. The value of 0.953 comes into being due to the averaging process but is not the exact  $D(V_e)$  for the sample at 10 °C, as values  $<1$  are meaningless. Rather the value is interpreted to mean that this sample is effectively monodisperse. The  $D(V_e)$  values for MA suggest that, if indeed the cause of heterogeneity is due to long chain branching, either i) long chain branching formation does not occur as a function of temperature or that ii) another aspect of the structure of MA results in relatively similar amounts of LCB being formed irrespective of temperature. However, all but one MA  $D(V_e)$  value is greater than unity, indicating that the samples are still heterogeneous to some extent in the hydrodynamic volume distribution in terms of molecular weights.

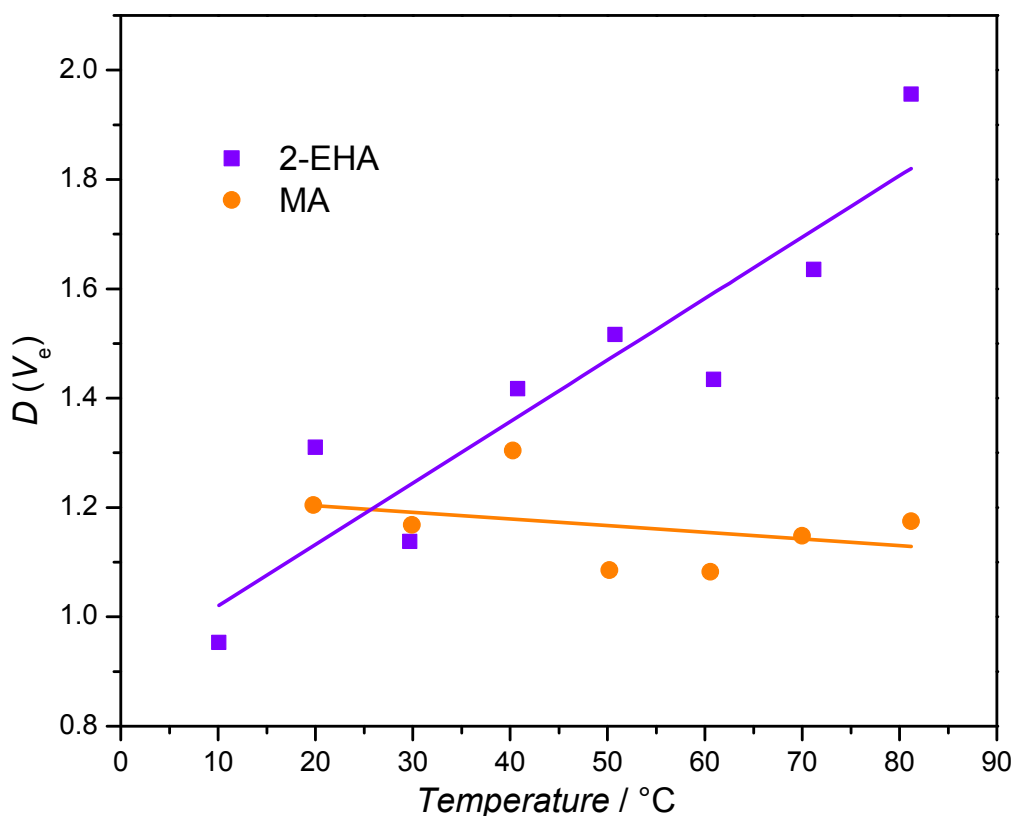


Figure 6-16: Graph shows the clear increase in  $D(V_e)$  with temperature for 2-EHA, while for MA,  $D(V_e)$  values are more stable as temperature increases.

In other words, some poly(acrylate) chains of the same hydrodynamic volume have significantly different molecular weights and this heterogeneity is potentially created by the presence of long-chain branching.  $D(V_e)$  value and heterogeneity do not linearly correlate with the degree of long-chain branching per chain, since low degrees of long-chain branching per chain can create the largest heterogeneity.<sup>95</sup> This is a logical conclusion if it is considered that one or two extra long chain branches have a much more significant impact if there are only few other long chain branches, whereas the presence of a few more long chain branches in a sample which already contains say 100 long chain branches would not lead to much further difference in the polymer properties, in particular viscosity in the case of SEC separation. Low degrees of long-chain branching per chain can thus lead to the worst separation in SEC. Castignolles<sup>95</sup> notes the existence of long chain branching in 2-EHA polymer samples at temperatures as low as -35 °C, as indicated by consistent  $D(V_e)$  values greater than unity and extending beyond 2 at  $V_e = 18$  mL and above. Existing <sup>13</sup>C-NMR

methods are able to detect the total amount of branching in a sample,<sup>118,122-123</sup> however the distinction should be made here that only long chain branching is the focus of this local dispersity study. Currently there is no method of detecting only long chain branches on statistically branched polymers such as the product formed in PLP.<sup>113,124</sup>

The consequence of the current work is to highlight that SEC is one of the largest sources of error in PLP-SEC as in the case of 2-EHA polymer where significant heterogeneity is observed, which leads to erroneous SEC molecular weight determination. The data presented herein was acquired on a triple detection system consisting of only two columns, and already much higher separation can be achieved with an aggregation of more columns, for example, in a 4 or even 5 column set-up employing higher resolution columns, but the current work nevertheless emphasizes difficulties which may not be immediately apparent or deemed to be of concern to the general SEC user. Furthermore, the data is valid on a relative basis to compare polymers produced at varying temperatures. It is generally acknowledged that with poly(acrylate) systems even more caution must be exercised due to the presence of side reactions such as backbiting and inter and intramolecular transfer to polymer which can result in the formation of long chain branching which may be the cause of the heterogeneity observed. Polymer analysis *via* multi detection SEC does not remove the potential error in calculation of molecular weights since incomplete separation occurs on the basis of hydrodynamic volume and a heterogeneous sample will be heterogeneous throughout. This is of particular importance in PLP for determination of rate constants, as the  $k_p$  is usually calculated from the molecular weight at the inflection points of the derivative of the molecular weight distribution.

With the definition of  $D(V_e)$  employed by Castignolles *et al.* to quantitatively assess the degree of heterogeneity, it may be possible to calculate the error associated with SEC molecular weight determination and then correlate this quantitatively to an error in the  $k_p$  values thus calculated. Indeed, Castignolles suggests that an error calculation can be made in a straightforward manner by determining the percentage difference between the calculated  $D(V_e)$  and 1, the expected  $D(V_e)$  if all chains were to be linear. However, a cursory examination of this proposition would imply that at 80 °C, there is an error of 95 % in the  $k_p$  value determined for 2-EHA. Considering the good fit of the data with values obtained at lower temperatures such a high degree of error is highly unlikely to be the case. The current

study therefore refrains from attempting a quantitative error estimation, finding that the error calculation method proposed by Castignolles to be rather simplistic and requiring further refinement to arrive at an equation for error estimation. The current study does however provide an indication of the amounts of heterogeneity introduced into samples prepared *via* radical polymerization and highlights that the larger the local dispersity, the larger is the error associated with the determined molecular weights. This error in molecular weight is then carried on in the calculation of  $k_p$  so care must be taken when interpreting values  $k_p$  of acrylates, in particular with 2-EHA. However, the paradoxical observation is made that in the case of MA, no increase in homogeneity is observed with increasing temperature. This is ground for further investigation into the peculiar polymerizing systems that are the acrylates, with regards to the source of the heterogeneity (perhaps long chain branching created by increased random transfer to polymer as proposed by Castignolles) and the monomers that are susceptible to this effect in the constant search for more accurate and precise kinetic parameters.

### 6.13 Summary of Results

This chapter was concerned with the use of pulsed laser polymerization, in one case as a means of generating photo-initiated methyl methacrylate polymer and combining PLP with the technique of ESI-MS to analyze the polymer end group composition and assess relative efficiencies of two types of initiating radicals, mesityl and benzoyl radicals. For the case of MMA, initiators containing mesityl (such as 2,4,6-trimethylbenzoyldiphenylphosphinoxide) may be improved by exchanging the mesityl moiety by a benzoyl fragment.<sup>29,33</sup> When all available data is considered, the strong discrepancy in initiating macromolecular growth is due significantly to the reactivity difference between mesityl and benzoyl radicals and probably to only a lesser degree to different effective radical concentrations generated from mesityl and benzoin.

The second part of this work employed the PLP-SEC technique to establish  $k_p$  values for methyl acrylate and 2-ethyl hexyl acrylate at temperatures above 40 °C. These two monomers are of industrial importance but as with other acrylates and with the possible exception of *n*-butyl acrylate, they have so far proven notoriously difficult to analyze *via* the PLP-SEC method for reasons discussed in section 6.6 above. For the first time  $k_p$  values above ambient temperature are reported for these two monomers *via* high frequency

pulsing at 500 Hz. An analysis to qualitatively evaluate the effect of branching on molecular weights determined by SEC was also undertaken, to highlight that while advances in laser technology now provide means of generating PLP material for challenging monomers, the technique of SEC is also fraught with difficulties in the analysis of statistically branched acrylate polymers such as those produced *via* PLP. While improved instrumentation allows further probing into acrylate radical systems, this raises many more questions which have until now not been considered, such as the degree of heterogeneity within a particular elution volume of a poly(acrylate) sample. The possibility of incomplete separation even with high resolution columns introduces errors into reported propagation coefficients as the current recommended PLP-SEC methodology is heavily reliant on obtaining as accurate as possible molecular weights. The study that has been presented may lead the way to finding the source of the heterogeneity in acrylate samples, which would be of high interest to kinetic chemists, or may lead to the development of a method for quantitatively assessing the margin of error in SEC separation, which would be useful to any polymer chemist. The ability to assess the quality of the data obtained from SEC would be highly useful to researchers in many areas of polymer research, both to kineticists and to synthetic chemists.

---

## 6.14 References

- 1 Gruber, H. F. *Prog. Polym. Sci.* 1992, 17, 953-1044.
- 2 Kaur, M.; Srivastava, A. K. 2002, 42, 481 - 512.
- 3 Ge, J.; Trujillo, M.; Stansbury, J. *Dent. Mater.* 2005, 21, 1163-1169.
- 4 Anseth, K.; Newman, S.; Bowman, C. In *Biopolymers II*, 1995, p 177-217.
- 5 Fisher, J. P.; Dean, D.; Engel, P. S.; Mikos, A. G. *Annual Review of Materials Research* 2001, 31, 171-181.
- 6 Anseth, K. S.; Metters, A. T.; Bryant, S. J.; Martens, P. J.; Elisseff, J. H.; Bowman, C. N. *J. Controlled Release* 2002, 78, 199-209.
- 7 Junkers, T.; Wong, E. H. H.; Szablan, Z.; Davis, T. P.; Stenzel, M. H.; Barner-Kowollik, C. *Macromol. Rapid Commun.* 2008, 29, 503-510.
- 8 Buback, M.; Feldermann, A.; Barner-Kowollik, C.; Lacik, I. *Macromolecules* 2001, 34, 5439-5448.
- 9 Buback, M.; Junkers, T.; Vana, P. *Macromol. Rapid Commun.* 2005, 26, 796-802.
- 10 Buback, M.; Egorov, M.; Feldermann, A. *Macromolecules* 2004, 37, 1768-1776.
- 11 Szablan, Z.; Stenzel, M. H.; Davis, T. P.; Barner, L.; Barner-Kowollik, C. *Macromolecules* 2005, 38, 5944-5954.
- 12 Szablan, Z.; Junkers, T.; Koo, S. P. S.; Lovestead, T.; Davis, T. P.; Stenzel, M. H.; Barner-Kowollik, C. *Macromolecules* 2007, 40, 6820-6833.
- 13 Vana, P.; Davis, T. P.; Barner-Kowollik, C. *Aust. J. Chem.* 2002, 55, 315-318.
- 14 Szablan, Z.; Lovestead, T. M.; Davis, T. P.; Stenzel, M. H.; Barner-Kowollik, C. *Macromolecules* 2007, 40, 26-39.
- 15 Nielen, M. W. F. *Rapid Commun. Mass Spectrom.* 1999, 13, 826-827.
- 16 Guittard, J.; Tessier, M.; Blais, J. C.; Bolbach, G.; Rozes, L.; Marechal, E.; Tabet, J. C. *Journal of Mass Spectrometry* 1996, 31, 1409-1421.
- 17 Tanaka, K. *Angew. Chem., Int. Ed. Engl.* 2003, 42, 3860-3870.
- 18 Saf, R.; Mirtl, C.; Hummel, K. *Acta polymer.* 1997, 48, 513-526.
- 19 Lovestead, T. M.; Hart-Smith, G.; Davis, T. P.; Stenzel, M. H.; Barner-Kowollik, C. *Macromolecules* 2007, 40, 4142-4153.
- 20 Hanton, S. D. *Chem. Rev.* 2001, 101, 527-569.
- 21 Montaudo, G. *Trends in Polymer Science* 1996, 4, 81-86.
- 22 Scrivens, J. H.; Jackson, A. T. *International Journal of Mass Spectrometry* 2000, 200, 261-276.
- 23 Barner-Kowollik, C.; Davis, T. P.; Stenzel, M. H. *Polymer* 2004, 45, 7791-7805.
- 24 Chaffey-Millar, H.; Hart-Smith, G.; Barner-Kowollik, C. *J. Polym. Sci., Part A: Polym. Chem.* 2008, 46, 1873-1892.
- 25 Hart-Smith, G.; Lovestead, T. M.; Davis, T. P.; Stenzel, M. H.; Barner-Kowollik, C. *Biomacromolecules* 2007, 8, 2404-2415.
- 26 Buback, M.; Frauendorf, H.; Vana, P. *J. Polym. Sci., Part A: Polym. Chem.* 2004, 42, 4266-4275.
- 27 Buback, M.; Frauendorf, H.; Gunzler, F.; Vana, P. *J. Polym. Sci., Part A: Polym. Chem.* 2007, 45, 2453-2467.
- 28 Buback, M.; Frauendorf, H.; Gunzler, F.; Vana, P. *Polymer* 2007, 48, 5590-5598.
- 29 Szablan, Z.; Junkers, T.; Koo, S. P. S.; Lovestead, T. M.; Davis, T. P.; Stenzel, M. H.; Barner-Kowollik, C. *Macromolecules* 2007, 40, 6820-6833.
- 30 Buback, M.; Günzler, F.; Russell, G. T.; Vana, P. *Macromolecules* 2009, 42, 652-662.

- 
- 31 Turro, N. J. *Macromolecular Photochemistry*; University Science Books: Sausalito, 1991.
  - 32 Fouassier, J. P.; Jacques, P.; Lougnot, D. J.; Pilot, T. *Polymer Photochemistry* 1984, 5, 57-76.
  - 33 Wyzgoski, F. J.; Polce, M. J.; Wesdemiotis, C.; Arnould, M. A. J. *Polym. Sci., Part A: Polym. Chem.* 2007, 45, 2161-2171.
  - 34 Olaj, O. F.; Bitai, I.; Hinkelmann, F. *Makromol. Chem.* 1987, 188, 1689-1702.
  - 35 Buback, M.; Gilbert, R. G.; Hutchinson, R. A.; Klumperman, B.; Kuchta, F.-D.; Manders, B. G.; O'Driscoll, K. F.; Russell, G. T.; Schweer, J. *Macromol. Chem. Phys.* 1995, 196, 3267-3280.
  - 36 Yin, M.; Barner-Kowollik, C.; Heuts, Johan P. A.; Davis, Thomas P. *Macromol. Rapid Commun.* 2001, 22, 1035-1040.
  - 37 Beuermann, S.; Buback, M.; Davis, T. P.; Gilbert, R. G.; Hutchinson, R. A.; Olaj, O. F.; Russell, G. T.; Schweer, J.; van Herk, A. M. *Macromol. Chem. Phys.* 1997, 198, 1545-1560.
  - 38 Beuermann, S.; Buback, M.; Davis, T. P.; Gilbert, R. G.; Hutchinson, R. A.; Kajiwarra, A.; Klumperman, B.; Russell, G. T. *Macromol. Chem. Phys.* 2000, 201, 1355-1364.
  - 39 Buback, M.; Garcia-Rubio, L. H.; Gilbert, R. G.; Napper, D. H.; Guillot, J.; Hamielec, A. E.; Hill, D.; Driscoll, K. F. O.; Olaj, O. F.; Jiacong, S.; Solomon, D.; Moad, G.; Stickler, M.; Tirrell, M.; Winnik, M. A. *Journal of Polymer Science Part C: Polymer Letters* 1988, 26, 293-297.
  - 40 Olaj, O. F.; Schnöll-Bitai, I. *Eur. Polym. J.* 1989, 25, 635-641.
  - 41 Lyons, R. A.; Hutovic, J.; Piton, M. C.; Christie, D. I.; Clay, P. A.; Manders, B. G.; Kable, S. H.; Gilbert, R. G. *Macromolecules* 1996, 29, 1918-1927.
  - 42 Jiang, X.; Schoenmakers, P. J.; vanDongen, J. L. J.; Lou, X.; Lima, V.; Brokken-Zijp, J. *Anal. Chem.* 2003, 75, 5517-5524.
  - 43 Beuermann, S.; Paquet, D. A.; McMinn, J. H.; Hutchinson, R. A. *Macromolecules* 1996, 29, 4206-4215.
  - 44 Hutchinson, R. A.; Beuermann, S.; Paquet, D. A.; McMinn, J. H. *Macromolecules* 1997, 30, 3490-3493.
  - 45 Hutchinson, R. A.; Paquet, D. A.; Beuermann, S.; McMinn, J. H. *Ind. Eng. Chem. Res.* 1998, 37, 3567-3574.
  - 46 Castignolles, P.; Nikitin, A. N.; Couvreur, L.; Mouraret, G.; Charleux, B.; Vairon, J.-P. *Macromol. Chem. Phys.* 2006, 207, 81-89.
  - 47 Nikitin, A. N.; Castignolles, P.; Charleux, B.; Vairon, J.-P. *Macromol. Rapid Commun.* 2003, 24, 778-782.
  - 48 Tanaka, K.; Yamada, B.; Fellows, C. M.; Gilbert, R. G.; Davis, T. P.; Yee, L. H.; Smith, G. B.; Rees, M. T. L.; Russell, G. T. *J. Polym. Sci., Part A: Polym. Chem.* 2001, 39, 3902-3915.
  - 49 Siegmann, R.; Beuermann, S. *Macromolecules* 2010, 43, 3699-3704.
  - 50 Dervaux, B.; Junkers, T.; Schneider-Baumann, M.; Prez, F. E. D.; Barner-Kowollik, C. J. *Polym. Sci., Part A: Polym. Chem.* 2009, 47, 6641-6654.
  - 51 Ganachaud, F.; Monteiro, M. J.; Gilbert, R. G. *Macromolecular Symposia* 2000, 150, 275-281.
  - 52 Stach, M.; Lacik, I.; Kasak, P.; Chorvat, D.; Saunders, A. J.; Santanakrishnan, S.; Hutchinson, R. A. *Macromol. Chem. Phys.* 2010, 211, 580-593.

- 
- 53 Stach, M.; Lacik, I.; Chorvat, D.; Buback, M.; Hesse, P.; Hutchinson, R. A.; Tang, L. *Macromolecules* 2008, 41, 5174-5185.
- 54 Seabrook, S. A.; Tonge, M. P.; Gilbert, R. G. *J. Polym. Sci., Part A: Polym. Chem.* 2005, 43, 1357-1368.
- 55 Lacik, I.; Beuermann, S.; Buback, M. *Macromolecules* 2001, 34, 6224-6228.
- 56 Lacik, I.; Beuermann, S.; Buback, M. *Macromolecules* 2003, 36, 9355-9363.
- 57 Yin, M.; Davis, T. P.; Heuts, J. P. A.; Barner-Kowollik, C. *Macromol. Rapid Commun.* 2003, 24, 408-412.
- 58 Junkers, T.; Voll, D.; Barner-Kowollik, C. *e-polymers* 2009, 076.
- 59 Hutchinson, R. A.; Richards, J. R.; Aronson, M. T. *Macromolecules* 1994, 27, 4530-4537.
- 60 Wang, W.; Hutchinson, R. A. *Macromolecules* 2008, 41, 9011-9018.
- 61 Van Herk, A. M. *Macromol. Theory Simul.* 2000, 9, 433-441.
- 62 Olaj, O. F.; Bitai, I. *Angew. Makromol. Chem.* 1987, 155, 177-190.
- 63 Olaj, O. F.; Bitai, I.; Gleixner, G. *Die Makromolekulare Chemie* 1985, 186, 2569-2580.
- 64 Buback, M.; Kurz, C. H.; Schmaltz, C. *Macromol. Chem. Phys.* 1998, 199, 1721-1727.
- 65 Beuermann, S.; Buback, M. *Pure and Applied Chemistry* 1998, 70, 1415-1418.
- 66 Beuermann, S.; Buback, M.; Davis, T. P.; Garcia, N.; Gilbert, R. G.; Hutchinson, R. A.; Kajiwarra, A.; Kamachi, M.; Lacik, I.; Russell, G. T. *Macromol. Chem. Phys.* 2003, 204, 1338-1350.
- 67 Buback, M.; Kurz, C. H.; Schmaltz, C. *Macromol. Chem. Phys.* 1998, 199, 1721-1727.
- 68 Asua, J. M.; Beuermann, S.; Buback, M.; Castignolles, P.; Charleux, B.; Gilbert, R. G.; Hutchinson, R. A.; Leiza, J. R.; Nikitin, A. N.; Vairon, J. P.; van Herk, A. M. *Macromol. Chem. Phys.* 2004, 205, 2151-2160.
- 69 Van Herk, A. M. *Macromol. Rapid Commun.* 2001, 22, 687-689.
- 70 Beuermann, S.; Paquet, D. A.; McMinn, J. H.; Hutchinson, R. A. *Macromolecules* 1997, 30, 194-197.
- 71 Zammit, M. D.; Coote, M. L.; Davis, T. P.; Willett, G. D. *Macromolecules* 1998, 31, 955-963.
- 72 Barner-Kowollik, C.; Günzler, F.; Junkers, T. *Macromolecules* 2008, 41, 8971-8973.
- 73 Davis, T. P.; O'Driscoll, K. F.; Piton, M. C.; Winnik, M. A. *Polymer International* 1991, 24, 65-70.
- 74 Beuermann, S.; Buback, M.; Schmaltz, C. *Macromolecules* 1998, 31, 8069-8074.
- 75 Beuermann, S.; Buback, M.; Schmaltz, C.; Kuchta, F.-D. *Macromol. Chem. Phys.* 1998, 199, 1209-1216.
- 76 van Herk, A. M. *Macromol. Rapid Commun.* 2009, 30, 1964-1968.
- 77 Junkers, T.; Barner-Kowollik, C. *J. Polym. Sci., Part A: Polym. Chem.* 2008, 46, 7585-7605.
- 78 Junkers, T.; Koo, S. P. S.; Davis, T. P.; Stenzel, M. H.; Barner-Kowollik, C. *Macromolecules* 2007, 40, 8906-8912.
- 79 Koo, S. P. S.; Junkers, T.; Barner-Kowollik, C. *Macromolecules* 2009, 42, 62-69.
- 80 van Herk, A. M. *Macromol. Rapid Commun.* 2001, 22, 687-689.
- 81 Arzamendi, G.; Plessis, C.; Leiza, J. R.; Asua, J. M. *Macromol. Theory Simul.* 2003, 12, 315-324.
- 82 Plessis, C.; Arzamendi, G.; Alberdi, J. M.; Herk, A. M. v.; Leiza, J. R.; Asua, J. M. *Macromol. Rapid Commun.* 2003, 24, 173-177.

- 
- 83 Plessis, C.; Arzamendi, G.; Leiza, J. R.; Schoonbrood, H. A. S.; Charmot, D.; Asua, J. M. *Macromolecules* 2000, 33, 4-7.
- 84 Nikitin, A. N.; Hutchinson, R. A.; Buback, M.; Hesse, P. *Macromolecules* 2007, 40, 8631-8641.
- 85 Nikitin, A. N.; Castignolles, P.; Charleux, B.; Vairon, J.-P. *Macromol. Theory Simul.* 2003, 12, 440-448.
- 86 Busch, M.; Wahl, A. *Macromol. Theory Simul.* 1998, 7, 217-224.
- 87 Olaj, O. F.; Vana, P. J. *Polym. Sci., Part A: Polym. Chem.* 2000, 38, 697-705.
- 88 Olaj, O. F.; Vana, P.; Zoder, M. *Macromolecules* 2002, 35, 1208-1214.
- 89 Gruending, T.; Voll, D.; Guilhaus, M.; Barner-Kowollik, C. *Macromol. Chem. Phys.* 2010, 211, 80-90.
- 90 Manders, B. G.; PhD Thesis: Eindhoven, 1997.
- 91 Beuermann, S. *Macromol. Rapid Commun.* 2009, 30, 1066-1088.
- 92 Gaborieau, M.; Nicolas, J.; Save, M.; Charleux, B.; Vairon, J.-P.; Gilbert, R. G.; Castignolles, P. *Journal of Chromatography A* 2008, 1190, 215-223.
- 93 Hamielec, A. E.; Ouano, A. C. J. *Liq. Chromatogr.* 1978, 1, 111 - 120.
- 94 Hamielec, A. E.; Ouano, A. C.; Nebenzahl, L. L. *Journal of Liquid Chromatography & Related Technologies* 1978, 1, 527 - 554.
- 95 Castignolles, P. *Macromol. Rapid Commun.* 2009, 30, 1995-2001.
- 96 McNaught, A. D.; Wilkinson, A. *IUPAC Compendium of Chemical Terminology*; Blackwell Science, 1997
- 97 Penzel, E.; Goetz, N. *Angew. Makromol. Chem.* 1990, 178, 191-200.
- 98 Lathová, E.; Lath, D.; Pavlinec, J. *Polymer Bulletin* 1993, 30, 713-718.
- 99 Lím, D.; Wichterle, O. *Journal of Polymer Science* 1958, 29, 579-584.
- 100 Matheson, M. S.; Auer, E. E.; Bevilacqua, E. B.; Hart, E. J. *J. Am. Chem. Soc.* 1951, 73, 5395-5400.
- 101 Manders, B. G. In *Laboratory of Polymer Chemistry*; Eindhoven University of Technology: Eindhoven, 1997.
- 102 Willemse, R. X. E.; van Herk, A. M. *Macromol. Chem. Phys.* 2010, 211, 539-545.
- 103 Beuermann, S.; Buback, M.; El Rezzi, V.; Jurgens, M.; Nelke, D. *Macromol. Chem. Phys.* 2004, 205, 876-883.
- 104 Couvreur, L.; Piteau, G.; Castignolles, P.; Tonge, M.; Coutin, B.; Charleux, B.; Vairon, J.-P. *Macromolecular Symposia* 2001, 174, 197-208.
- 105 Beuermann, S.; Buback, M. *Prog. Polym. Sci.* 2002, 27, 191-254.
- 106 Willemse, R. X. E.; Herk, A. M. v.; Panchenko, E.; Junkers, T.; Buback, M. *Macromolecules* 2005, 38, 5098-5103.
- 107 Ayrey, G.; Humphrey, M. J.; Poller, R. C. *Polymer* 1977, 18, 840-844.
- 108 Dube, M. A.; Rilling, K.; Penlidis, A. J. *Appl. Polym. Sci.* 1991, 43, 2137-2145.
- 109 Gaborieau, M.; Gilbert, R. G.; Gray-Weale, A.; Hernandez, J. M.; Castignolles, P. *Macromol. Theory Simul.* 2007, 16, 13-28.
- 110 Kostanski, L. K.; Keller, D. M.; Hamielec, A. E. *Journal of Biochemical and Biophysical Methods* 2004, 58, 159-186.
- 111 Benoit, H. C. *Journal of Polymer Science Part B: Polymer Physics* 1996, 34, 1703-1704.
- 112 Sun, T.; Chance, R. R.; Graessley, W. W.; Lohse, D. J. *Macromolecules* 2004, 37, 4304-4312.
- 113 Burchard, W. In *Adv. Polym. Sci.*, 1999, p 113-194.
- 114 Thurmond, C. D.; Zimm, B. H. *Journal of Polymer Science* 1952, 8, 477-494.

- 
- 115 Hamielec, A. E.; Ouano, A. C. *Journal of Liquid Chromatography & Related Technologies* 1978, 1, 111 - 120.
  - 116 Hamielec, A. *Pure Appl. Chem.* 1982, 54, 293-307.
  - 117 Balke, S. T.; Mourey, T. H. *J. Appl. Polym. Sci.* 2001, 81, 370-383.
  - 118 Castignolles, P.; Graf, R.; Parkinson, M.; Wilhelm, M.; Gaborieau, M. *Polymer* 2009, 50, 2373-2383.
  - 119 Baumgarten, J. L.; Busnel, J.-P.; Meira, G. R. *Journal of Liquid Chromatography & Related Technologies* 2002, 25, 1967 - 2001.
  - 120 Tackx, P.; Bosscher, F. *Analytical Communications* 1997, 34, 295-297.
  - 121 Castignolles, P. In *Fraunhofer - Institut für Chemische Technologie ICT Karlsruhe*, 2009.
  - 122 Ahmad, N. M.; Heatley, F.; Lovell, P. A. *Macromolecules* 1998, 31, 2822-2827.
  - 123 Caytan, E.; Botosoa, E. P.; Silvestre, V.; Robins, R. J.; Akoka, S.; Remaud, G. S. *Analytical Chemistry* 2007, 79, 8266-8269.
  - 124 Radke, W.; Muller, A. H. E. *Macromolecules* 2005, 38, 3949-3960.

## 7 Concluding Remarks and Outlook

### 7.1 Concluding Remarks

The ongoing developments in the existing analytical techniques of size exclusion chromatography, mass spectrometry and lasers offer continuing improvement in the area of polymer characterization. Novel methodologies can be established and the extraction of previously inaccessible information regarding kinetic and mechanistic pathways can be performed. The work presented in the current thesis takes advantage of the accuracy and precision of the ESI-MS technique, employing linear quadrupole ion trap detectors, as well as the development of high frequency lasers, to gain insights into the mechanism of acrylate and methacrylate FRP.

A detailed study on the effect of the addition of 1-octanethiol on the product spectrum of poly(*n*-BA) was conducted. All species occurring in the product spectrum were identified; notably combination, termination and transfer products. In particular the MCR derived products as a result of the  $\beta$ -scission reaction were analyzed, and were subsequently quantified to give an in-depth perspective on the kinetics at hand at various temperatures. The main product peak identified in the ESI-MS spectra obtained from polymer made by 1-octanethiol mediated polymerization was assigned to the expected transfer to thiol product, while in the absence of thiol or presence of low amounts of thiol, the predominant species are the vinyl terminated products of  $\beta$ -scission reactions. Thiol capped polymer (TCP) and the main macromonomer product ( $\beta^I$ ) show the largest variation in mole fraction and are therefore the main products of interest with respect to the thiol concentration variation. All other species do not show significant variation in mole fractions with increasing thiol concentration. The formation of species  $\beta^I$  is highly sensitive to the thiol concentration. Without the effects of the transfer agent, the main species ( $\beta^I$ ) is formed and comprises the vast majority of product seen (60 % of the total product).  $\beta$ -scission products  $\beta^{I-III}$  make up a total of 78 % of the whole sample. Increasing thiol concentration from 0.01 to 0.05 mol·L<sup>-1</sup> results in the TCP proportions rising from 2 % to 20 %, and the  $\beta^I$  proportions decreasing from 76 % to 52 %. At a concentration of 0.4 mol·L<sup>-1</sup>,  $\beta^I$  becomes a minor product, constituting 10 % of the product spectrum while the TCP product accounts for 81 % of the product.

Melt state  $^{13}\text{C}$  NMR results supported the mass spectrometric findings relating to the  $\beta$ -scission products as the reduction in degree of branching, as determined from measurements of quaternary carbons on the polymer backbone, and the reduction in the amount of  $\beta$ -scission product correlate well to each other. The highly complementary mass spectrometric and NMR spectroscopic data provide a complete micro-structural image of the obtained polymer chains.

The  $\beta$ -scission reactions which dominate at higher reaction temperatures were exploited to synthesize highly uniform macromonomer and an addition-fragmentation reaction mechanism was proposed to explain the formation of such homogeneous macromonomers. Macromonomers are polymers or oligomers that carry a polymerizable unsaturated endgroup, either of a 1,2-disubstituted structure, resulting in a vicinal double bond, or of the more readily polymerizable 1,1'-disubstituted structure with a geminal double bond. The butyl acrylate macromonomer (MM) was characterized *via* ESI-MS and was found to be of high purity. MM was subsequently employed in a study to form stars *via* radical, catalyst free thiol-ene coupling reactions. Many difficulties were encountered, most importantly the exceedingly low coupling and the necessity of excess thiol to drive the reaction to higher conversion. A detailed exploration of the limitations of the radical, metal-free thiol-ene reaction with respect to constructing star-shaped polymers was consequently performed. Polymer-polymer conjugation could only be achieved when the thiol was in excess of the ene component, which statistically does not result in the formation of star shaped polymers. Rather than 4 arm stars being formed, a statistical distribution of 1, 2 and 3-arm coupled 'stars' are formed. The difficulties encountered highlight that the radical thiol-ene coupling reaction cannot be considered to be an efficient *click* reaction in the context of polymer chemistry.

High frequency laser photo-initiation was used in Chapter 6 to study the comparative reactivity of benzoyl vs mesitoyl radicals, to investigate on a quantitative basis the previously qualitative observation that the mesitoyl fragment displayed a very poor tendency to react with monomers to initiate polymerization after its generation from a phosphoryl-type photo-initiator.<sup>1</sup> In the current thesis the efficiency difference between benzoin and mesitil initiators was evaluated by preparing mixtures of benzoin and mesitil initiator and producing poly(MMA) *via* pulsed laser initiation. Benzoyl radicals were found to

be close to a factor of 8.6 more likely to initiate macromolecular growth than mesityl radicals, as determined by the quantitative evaluation of polymer chains which had undergone disproportionation and furthermore contained the mesityl initiating group. The results were in good agreement with qualitative observations that mesityl radicals might be poor initiating entities. The strong discrepancy in initiating macromolecular growth, as observed by their presence at the chain terminus of chains terminated *via* disproportionation, was attributed to the reactivity difference between mesityl and benzoyl radicals and to a lesser degree to the different effective radical concentrations generated from mesityl and benzoin decomposition.

High frequency laser pulsing was also used to conduct PLP-SEC experiments of methyl acrylate and 2-ethyl hexyl acrylate to determine  $k_p$  values above ambient temperature, which had previously not been reported in the literature. A comparison of the new data acquired for MA  $k_p$  values with literature values showed a divergence of about -15 to -20 %, while a discrepancy of about 15 % was found in the case of the 2-EHA  $k_p$  values. It should be noted that the comparison values were obtained from literature studies where PLP polymer was obtained in very limited temperature ranges, i.e. below 40 °C, and in most cases the Arrhenius plot was extrapolated for comparison with higher temperature  $k_p$  values as obtained in this work. The Arrhenius parameters determined for MA and 2-EHA respectively were  $E_A = 18.5 (\pm 0.2) \text{ kJ}\cdot\text{mol}^{-1}$  and  $A = 30.0 (\pm 9)\cdot 10^6 \text{ L}\cdot\text{mol}^{-1}\cdot\text{s}^{-1}$  up to 80 °C and  $E_A = 12.9 (\pm 0.8) \text{ kJ}\cdot\text{mol}^{-1}$  and a frequency factor of  $A = 3.0 (\pm 0.8)\cdot 10^6 \text{ L}\cdot\text{mol}^{-1}\cdot\text{s}^{-1}$  for the temperature range of  $10 \text{ °C} \leq T \leq 75 \text{ °C}$ . The MA values are in good correlation with recently published data by Willemse and van Herk.<sup>2</sup> The 2-EHA Arrhenius parameters do not correlate well with the two other sets of data for 2-EHA PLP in the literature, namely by Vairon and co-workers<sup>3</sup> and Hutchinson and co-workers<sup>4</sup> but this may be attributed to the existence of high levels of long chain branching observed in 2-EHA polymerizations and the very different conditions under which the various PLP-SEC experiments were conducted. This led to a study of branching characteristics of poly(MA), compared to those of poly(2-EHA) *via* the calculation of local dispersities. It was determined that poly(2-EHA) exhibited a high degree of heterogeneity within each elution volume with increasing temperatures, indicating high levels of branching. Poly(MA) conversely showed no significant variation in local dispersity values, suggesting a much more homogeneous

polymer. The reasons for the discrepancy between the branching behavior of MA and 2-EHA are currently unknown. The study nevertheless reveals that care should be taken in interpreting SEC analysis results especially when there is a possibility that the polymer to be analyzed is highly branched, as SEC separates on the basis of hydrodynamic volume rather than molecular weight. It is possible for some conformations of molecules with vastly differing molecular weights to have the same hydrodynamic volume, which would cause them to be eluted in the same elution volume. Yet, many SEC analyses have as goal the determination of molecular weight averages, particularly so in the case of PLP-SEC, and will lead to the evaluation of erroneous Arrhenius parameters.

The current thesis makes significant contributions to the current knowledge of the kinetics of acrylate FRP, utilizing the technique of ESI-MS as an integral characterization method. A detailed quantitative mechanistic study of the way the final product spectrum may be finely tailored and controlled by manipulating the MCR  $\beta$ -scission reactions is presented, and pulsed laser polymerization is used to gain new insights into radical reactivities, while conventional SEC-PLP provides  $k_p$  values heretofore inaccessible.

## 7.2 Outlook & Future Work

Using the conclusions arrived at in this thesis as a basis, there are several areas which are now open for further study, which are detailed shortly.

A current investigation is underway in the Macroarc group at the KIT to increase the range of photo-initiator radicals studied quantitatively *via* ESI-MS for their relative initiating ability, by much the same method employed in the current thesis. The results of such a study would enable precise tailoring of the endgroups of synthesized polymers by judicious choice of photo-initiator, as it will be known which initiator groups initiate, and are therefore incorporated, into the final polymer. It may lead to a straightforward method of introducing specific end functionalization onto polymers.

An interesting future study could investigate the branching characteristics of the thiol-ene polymers as synthesized in Chapter 4 (potentially *via* LC-ESI-MS or LACCC-SEC) to compare the branching density results with those obtained in the NMR study conducted in this thesis. Since the thiol is speculated to 'patch' the MCRs as they form, linear polymers are expected. The observation of (mostly) linear polymer would lend further credence to the 'patching'

ability of the thiol. Analysis of other branched poly(acrylates) is another interesting area of research, to collate data on the branching characteristics of a family of monomers, analogously to PLP-SEC of a family of monomers, for example ethyl acrylate, butyl acrylate, hexyl acrylate, and dodecyl acrylate. Examination of the branching characteristics may lead to the establishment of trends as yet unidentified. With the methodology employed, more detailed investigations into the branching characteristics of the acrylate family of monomers would provide additional mechanistic information regarding acrylate FRP which may be of great consequence industrially. For example, tailor-made polymers could potentially be made with fewer purification steps or in shorter production times, the former would result in direct cost cutting and the latter would enable faster turn-around of production times, making the process more efficient, and thus also leading to lowered production costs.

Furthermore, the current data obtained *via* ESI-MS analysis has an upper detection limit of 2000 *m/z*. A computational algorithm based on the maximum entropy principle to process the data acquired by coupled ESI-MS and SEC developed by Gruending *et al.*<sup>5</sup> yields accurate molecular weight distributions up to 10 kDa. Using this method, a larger molecular weight range would be observed to provide a better overview of the entire sample.

The limitation in the observable mass range from the ESI-MS technique must also be considered when the quantitative data are used for kinetic modeling. It is imprudent to assume that the accessible low-molecular mass range is representative of the entire molecular weight distribution, which may extend to  $10^6 \text{ g}\cdot\text{mol}^{-1}$  and beyond. In addition, the large library of data accumulated in the detailed investigation presented in this thesis could be used in a modeling study to extract the rate coefficient  $k_{\beta}$ , and possibly  $k_t^{\text{MCR}}$ . The program package PREDICI<sup>®</sup> may be used for such data fitting. The difficulty lies in the development of a model which is endgroup differentiated so that the output might be compared to the quantitative data related to the individual species. The model therefore must be constructed in such a way that allows for output for a specified mass range, to be able to adequately compare the ESI-MS results with those obtained by simulation. An endgroup differentiated model of the thiol mediated polymer system has been constructed, and preliminary work has been carried out to optimize the simulation of the experimental results, but no data comparison has yet been performed between the two sets of data. The endgroup differentiated model was based on a previous model designed to investigate the

formation of MM.<sup>6</sup> The endgroup differentiated model is not only able to provide molecular weight data but also gives information on the specific endgroups on each polymer chain. It can also differentiate between the  $\beta$ -scission product originating from an MCR which underwent backbiting and a  $\beta$ -scission product originating from an MCR which underwent random transfer, since the  $\beta$ -scission product from the backbiting reaction is a small molecule, whereas the  $\beta$ -scission product from a random transfer reaction may be much longer. The model is also able to track the number of short chain branching points and long chain branching points formed during the polymerization. All trials have attempted to simulate actual reaction conditions, so are run up to high conversions. The model allows data extraction for the relevant molecular weights observable *via* ESI-MS, i.e. up to  $2000 \text{ g}\cdot\text{mol}^{-1}$ , but computes molecular weight distributions of the whole sample. Future work utilizing this model would involve comparison of the experimental data with simulated data to obtain statistically identical product spectra, and since the simulation parameters are known, it would provide an indication of the magnitude of  $k_{\beta}$ , and  $k_t^{\text{MCR}}$ . An estimate of  $k_{\beta}$ , and  $k_t^{\text{MCR}}$  would open new avenues of optimizing the synthesis of poly(acrylate)s with much greater control, as currently a paucity of data exists on the subject. The model can of course be extended to other systems, but the acrylates are one class of monomers where knowledge of these significant rate coefficients would be extremely valuable.

With regards to the PLP-SEC experiments presented in the current thesis, reproduction the determined  $k_p$  values herein for MA, 2-EHA, and extension of the study to other monomers in the acrylate series in independent laboratories would help to establish benchmarks for the acrylate series of monomers. Comparison of new data with previously determined values at lower temperatures would provide more information about the acrylate group of monomers, and would also provide information to support or disprove current theories on the behavior of monomers within an analogous series, such as the increase of  $k_p$  with increasing size of the side chain. Inter-laboratory benchmarking may become available if the experiments are reproduced in other working groups, and exploration of a wider range of monomers will generally increase knowledge of acrylates, as to date there have been relatively few kinetic studies performed on a wide range of acrylate monomers, due to the multitude of transfer to polymer reactions that take place at all temperatures, starting as low as  $-34 \text{ }^{\circ}\text{C}$  in the case of poly(2-EHA).<sup>7</sup>

### 7.3 References

- 1 Szablan, Z.; Junkers, T.; Koo, S. P. S.; Lovestead, T. M.; Davis, T. P.; Stenzel, M. H.; Barner-Kowollik, C. *Macromolecules* 2007, 40, 6820-6833.
- 2 Willemse, R. X. E.; van Herk, A. M. *Macromol. Chem. Phys.* 2010, 211, 539-545.
- 3 Couvreur, L.; Piteau, G.; Castignolles, P.; Tonge, M.; Coutin, B.; Charleux, B.; Vairon, J.-P. *Macromolecular Symposia* 2001, 174, 197-208.
- 4 Beuermann, S.; Paquet, D. A.; McMinn, J. H.; Hutchinson, R. A. *Macromolecules* 1996, 29, 4206-4215.
- 5 Gruendling, T.; Guilhaus, M.; Barner-Kowollik, C. *Analytical Chemistry* 2008, 80, 6915-6927.
- 6 Junkers, T.; Barner-Kowollik, C. *Macromol. Theory Simul.* 2009, 18, 421-433.
- 7 Castignolles, P. *Macromol. Rapid Commun.* 2009, 30, 1995-2001.

## 8 Appendix: Proposed PREDICI® Model for Evaluating Acrylate FRP in the presence of a Chain Transfer Agent

model 149

Endtime 21600.00  
Accuracy 1.0000e-01  
Max. chain-length 3  
Library macromonomer.lib  
Compl. distributioncomputing  
Units g l s K

Reactors 1  
Flask  
Type Operation;Controlfile V0 VF VE  
CSTR batch 1.0000e+00 0.0000e+00 0.0000e+00  
controlstream none  
Volumecontraction 0  
RelVol 0  
T0 Model  
140.00 isotherm

Coefficients 23  
kind value k0 energy reactor DV/R temp type  
limit constant 9.900e-01 0  
Ideal Free Radical Polymerization Coefficients  
kd arrhenius 1.580e+15 1.551e+04 Flask 0.000e+00 0 0  
k\_AI constant 1.000e-09 0  
kini constant 1.206e+05 0  
kp arrhenius 2.210e+07 2.153e+03 Flask 0.000e+00 0 0  
kt\_com constant 1.000e+07 0  
kt\_dis constant 0.000e+00 0  
Transfer to Thiol  
ktrans\_thiolSPR arrhenius 2.210e+07 2.153e+03 Flask 0.000e+00 0 0  
ktrans\_thiolMCR arrhenius 1.520e+06 3.476e+03 Flask 0.000e+00 0 0  
kre\_ini constant 1.000e+05 0  
Transfer to Polymer  
kbb arrhenius 4.480e+07 3.813e+03 Flask 0.000e+00 0 0  
k\_intra arrhenius 4.480e+07 3.813e+03 Flask 0.000e+00 0 0  
k\_trans\_inter constant 5.000e+00 0  
MCR Follow up reactions  
kp\_tert arrhenius 1.520e+06 3.476e+03 Flask 0.000e+00 0 0  
k\_beta arrhenius 8.600e+09 8.600e+03 Flask 0.000e+00 0 0  
kt\_comMCR constant 1.000e+06 0  
Reverse b-scission  
kad\_small constant 5.170e+06 0  
k\_ad constant 5.170e+06 0  
k\_beta\_trimer arrhenius 8.600e+09 8.600e+03 Flask 0.000e+00 0 0  
k\_beta\_half arrhenius 4.300e+10 8.600e+03 Flask 0.000e+00 0 0  
kp\_tert\_half arrhenius 7.600e+05 3.476e+03 Flask 0.000e+00 0 0  
dummies  
3 constant 3.000e+00 0  
2 constant 2.000e+00 0

Lowmol.Species 11  
alias start molm. density d(copol) heat cap. hc(copol) Feed Reactor type graph conversion  
X X 0.000e+00 1.0000e+02 D(1.00e+03) D(1.00e+00) HC(0.00e+00) HC(0.00e+00) 0.0000e+00 Flask - yes no  
BA Monomer 7.006e+00 1.2800e+02 D(1.00e+03) D(1.00e+00) HC(0.00e+00) HC(0.00e+00) 0.0000e+00 Flask - yes yes  
AIBN therm.\_Initiator 5.000e-03 1.6400e+02 D(1.00e+03) D(1.00e+00) HC(0.00e+00) HC(0.00e+00) 0.0000e+00 Flask - yes no  
LCB 0.000e+00 0.0000e+00 D(1.00e+00) D(1.00e+00) HC(0.00e+00) HC(0.00e+00) 0.0000e+00 Flask - no no  
SCB 0.000e+00 0.0000e+00 D(1.00e+00) D(1.00e+00) HC(0.00e+00) HC(0.00e+00) 0.0000e+00 Flask - no no

```

trimer_MMH trimer_MM 0.000e+00 3.8400e+02 D(1.00e+03) D(1.00e+00) HC(0.00e+00) HC(0.00e+00) 0.0000e+00 Flask
- no no
dimer_radical dimer_radical 0.000e+00 3.8400e+02 D(1.00e+03) D(1.00e+00) HC(0.00e+00) HC(0.00e+00) 0.0000e+00
Flask - no no
LCB_dash 0.000e+00 0.0000e+00 D(1.00e+03) D(1.00e+00) HC(0.00e+00) HC(0.00e+00) 0.0000e+00 Flask - no no
T 0.000e+00 5.0000e+01 D(1.00e+03) D(1.00e+00) HC(0.00e+00) HC(0.00e+00) 0.0000e+00 Flask - no no
CTA 1.000e-01 1.4629e+02 D(1.00e+03) D(1.00e+00) HC(0.00e+00) HC(0.00e+00) 0.0000e+00 Flask - yes no
dummy 0.000e+00 0.0000e+00 D(1.00e+03) D(1.00e+00) HC(0.00e+00) HC(0.00e+00) 0.0000e+00 Flask - no no

```

## Distributions 46

```

start molm. density reactor type chainlength graph weight log Mn,Mw Mz

```

```

MMH 0 1.280e+02 D(1.00e+03) Flask - no yes no no no no
MMX 0 1.280e+02 D(1.00e+03) Flask - no yes no no no no
HP 0 1.280e+02 D(1.00e+03) Flask - no no no no no no
XP 0 1.280e+02 D(1.00e+03) Flask - no no no no no no
TP 0 1.280e+02 D(1.00e+03) Flask - no no yes no no no
HMCRbb 0 1.280e+02 D(1.00e+03) Flask - no no no no no no
XMCRbb 0 1.280e+02 D(1.00e+03) Flask - no no no yes no no
TMCRbb 0 1.280e+02 D(1.00e+03) Flask - no no no no no no
HMCRH 0 1.280e+02 D(1.00e+03) Flask - no no no no no no
XMCRH 0 1.280e+02 D(1.00e+03) Flask - no no no no no no
XMCRX 0 1.280e+02 D(1.00e+03) Flask - no no no no no no
HPolymerH 0 1.280e+02 D(1.00e+03) Flask - no yes no no no no
XPolymerH 0 1.280e+02 D(1.00e+03) Flask - no yes no no no no
XPolymerX 0 1.280e+02 D(1.00e+03) Flask - no yes no no no no
XXP 0 1.280e+02 D(1.00e+03) Flask - no no no no no no
XXHPolymer 0 1.280e+02 D(1.00e+03) Flask - no no no no no no
XXXPolymer 0 1.280e+02 D(1.00e+03) Flask - no no no no no no
Q1HH 0 1.280e+02 D(1.00e+03) Flask - no no no no no no
Q2HH 0 1.280e+02 D(1.00e+03) Flask - no no no no no no
Q1XH 0 1.280e+02 D(1.00e+03) Flask - no no no no no no
Q2XH 0 1.280e+02 D(1.00e+03) Flask - no no no no no no
Q1XX 0 1.280e+02 D(1.00e+03) Flask - no no no no no no
Q2XX 0 1.280e+02 D(1.00e+03) Flask - no no no no no no
TPolymerH 0 1.280e+02 D(1.00e+03) Flask - no yes no no no no
TPolymerT 0 1.280e+02 D(1.00e+03) Flask - no yes no no no no
TPolymerX 0 1.280e+02 D(1.00e+03) Flask - no yes no no no no
TMCRX 0 1.280e+02 D(1.00e+03) Flask - no no no no no no
TMCRH 0 1.280e+02 D(1.00e+03) Flask - no no no no no no
TMCRT 0 1.280e+02 D(1.00e+03) Flask - no no no no no no
TTP 0 1.280e+02 D(1.00e+03) Flask - no no no no no no
TXP 0 1.280e+02 D(1.00e+03) Flask - no no no no no no
MMT 0 1.280e+02 D(1.00e+03) Flask - no no no no no no
XXTPolymer 0 1.280e+02 D(1.00e+03) Flask - no no no no no no
TTTPolymer 0 1.280e+02 D(1.00e+03) Flask - no no no no no no
TTHPolymer 0 1.280e+02 D(1.00e+03) Flask - no no no no no no
TTXPolymer 0 1.280e+02 D(1.00e+03) Flask - no no no no no no
TXHPolymer 0 1.280e+02 D(1.00e+03) Flask - no no no no no no
Q1TH 0 1.280e+02 D(1.00e+03) Flask - no no no no no no
Q2TH 0 1.280e+02 D(1.00e+03) Flask - no no no no no no
Q1TT 0 1.280e+02 D(1.00e+03) Flask - no no no no no no
Q2TT 0 1.280e+02 D(1.00e+03) Flask - no no no no no no
Q1XT 0 1.280e+02 D(1.00e+03) Flask - no no no no no no
Q2XT 0 1.280e+02 D(1.00e+03) Flask - no no no no no no
XTP 0 1.280e+02 D(1.00e+03) Flask - no no no no no no
dummy 0 0.000e+00 D(1.00e+03) Flask - no no no no no no
BA 0 0.000e+00 D(1.00e+03) Flask - no no no no no no

```

## Reactionsteps 209

```

AIBN ---> X + X , kd , Elementalreaction
X + BA ---> XP(1) , kini , Initiation(anion)
T + BA ---> TP(1) , kre_ini , Initiation(anion)
HP(s) + BA ---> HP(s+1) , kp , Propagation

```

$TP(s) + BA \rightarrow TP(s+1)$  ,  $k_p$  , Propagation  
 $XP(s) + BA \rightarrow XP(s+1)$  ,  $k_p$  , Propagation  
 $dimer\_radical + BA \rightarrow HP(3)$  ,  $k_p$  , Initiation(n-mer)  
 $HP(s) + HP(r) \rightarrow HPolymerH(s+r)$  ,  $k_{t\_com}$  , Combination  
 $HP(s) + HP(r) \rightarrow HPolymerH(s) + HPolymerH(r)$  ,  $k_{t\_dis}$  , Disproportion. (average\_termination)  
 $XP(s) + XP(r) \rightarrow XPolymerX(s+r)$  ,  $k_{t\_com}$  , Combination  
 $XP(s) + XP(r) \rightarrow XPolymerX(s) + XPolymerX(r)$  ,  $k_{t\_dis}$  , Disproportion. (average\_termination)  
 $XP(s) + HP(r) \rightarrow XPolymerH(s+r)$  ,  $k_{t\_com}$  , Combination(copolymer)  
 $XP(s) + HP(r) \rightarrow XPolymerH(s) + XPolymerH(r)$  ,  $k_{t\_dis}$  , Combination(copolymer)  
 $TP(s) + HP(r) \rightarrow TPolymerH(s+r)$  ,  $k_{t\_com}$  , Combination(copolymer)  
 $TP(s) + HP(r) \rightarrow TPolymerH(s) + TPolymerH(r)$  ,  $k_{t\_dis}$  , Combination(copolymer)  
 $TP(s) + TP(r) \rightarrow TPolymerT(s+r)$  ,  $k_{t\_com}$  , Combination(copolymer)  
 $TP(s) + TP(r) \rightarrow TPolymerT(s) + TPolymerT(r)$  ,  $k_{t\_dis}$  , Combination(copolymer)  
 $TP(s) + XP(r) \rightarrow TPolymerX(s+r)$  ,  $k_{t\_com}$  , Combination(copolymer)  
 $TP(s) + XP(r) \rightarrow TPolymerX(s) + TPolymerX(r)$  ,  $k_{t\_dis}$  , Combination(copolymer)  
 $TP(s) + CTA \rightarrow TPolymerH(s) + T$  ,  $k_{trans\_thiolSPR}$  , Change  
 $HP(s) + CTA \rightarrow HPolymerH(s) + T$  ,  $k_{trans\_thiolSPR}$  , Change  
 $XP(s) + CTA \rightarrow XPolymerH(s) + T$  ,  $k_{trans\_thiolSPR}$  , Change  
 $XMCRbb(s) + CTA \rightarrow XPolymerH(s) + T$  ,  $k_{trans\_thiolMCR}$  , Change  
 $TMCRbb(s) + CTA \rightarrow TPolymerH(s) + T$  ,  $k_{trans\_thiolMCR}$  , Change  
 $HMCRbb(s) + CTA \rightarrow HPolymerH(s) + T$  ,  $k_{trans\_thiolMCR}$  , Change  
 $HMCRH(s) + CTA \rightarrow HPolymerH(s) + T$  ,  $k_{trans\_thiolMCR}$  , Change  
 $XMCRH(s) + CTA \rightarrow XPolymerH(s) + T$  ,  $k_{trans\_thiolMCR}$  , Change  
 $XMCRX(s) + CTA \rightarrow XPolymerX(s) + T$  ,  $k_{trans\_thiolMCR}$  , Change  
 $TMCRX(s) + CTA \rightarrow TPolymerX(s) + T$  ,  $k_{trans\_thiolMCR}$  , Change  
 $TMCRH(s) + CTA \rightarrow TPolymerH(s) + T$  ,  $k_{trans\_thiolMCR}$  , Change  
 $TMCRT(s) + CTA \rightarrow TPolymerT(s) + T$  ,  $k_{trans\_thiolMCR}$  , Change  
 $XP(s) \rightarrow XMCRbb(s)$  ,  $k_{bb}$  , Change  
 $TP(s) \rightarrow TMCRbb(s)$  ,  $k_{bb}$  , Change  
 $HP(s) \rightarrow HMCRbb(s)$  ,  $k_{bb}$  , Change  
 $HP(s) \rightarrow HMCRH(s)$  ,  $k_{intra}$  , Change  
 $TP(s) \rightarrow TMCRH(s)$  ,  $k_{intra}$  , Change  
 $XP(s) \rightarrow XMCRH(s)$  ,  $k_{intra}$  , Change  
 $HP(s) + HPolymerH(r) \rightarrow HPolymerH(s) + HMCRH(r)$  ,  $k_{trans\_inter*r}$  , Transfer(LCB)  
 $HP(s) + XPolymerH(r) \rightarrow HPolymerH(s) + XMCRH(r)$  ,  $k_{trans\_inter*r}$  , Transfer(LCB)  
 $HP(s) + XPolymerX(r) \rightarrow HPolymerH(s) + XMCRX(r)$  ,  $k_{trans\_inter*r}$  , Transfer(LCB)  
 $HP(s) + TPolymerX(r) \rightarrow HPolymerH(s) + TMCRX(r)$  ,  $k_{trans\_inter*r}$  , Transfer(LCB)  
 $HP(s) + TPolymerH(r) \rightarrow HPolymerH(s) + TMCRH(r)$  ,  $k_{trans\_inter*r}$  , Transfer(LCB)  
 $HP(s) + TPolymerT(r) \rightarrow HPolymerH(s) + TMCRT(r)$  ,  $k_{trans\_inter*r}$  , Transfer(LCB)  
 $XP(s) + XPolymerX(r) \rightarrow XPolymerH(s) + XMCRX(r)$  ,  $k_{trans\_inter*r}$  , Transfer(LCB)  
 $XP(s) + XPolymerH(r) \rightarrow XPolymerH(s) + XMCRH(r)$  ,  $k_{trans\_inter*r}$  , Transfer(LCB)  
 $XP(s) + HPolymerH(r) \rightarrow XPolymerH(s) + HMCRH(r)$  ,  $k_{trans\_inter*r}$  , Transfer(LCB)  
 $XP(s) + TPolymerH(r) \rightarrow XPolymerH(s) + TMCRH(r)$  ,  $k_{trans\_inter*r}$  , Transfer(LCB)  
 $XP(s) + TPolymerT(r) \rightarrow XPolymerH(s) + TMCRT(r)$  ,  $k_{trans\_inter*r}$  , Transfer(LCB)  
 $XP(s) + TPolymerX(r) \rightarrow XPolymerH(s) + TMCRX(r)$  ,  $k_{trans\_inter*r}$  , Transfer(LCB)  
 $TP(s) + HPolymerH(r) \rightarrow TPolymerH(s) + HMCRH(r)$  ,  $k_{trans\_inter*r}$  , Transfer(LCB)  
 $TP(s) + XPolymerH(r) \rightarrow TPolymerH(s) + XMCRH(r)$  ,  $k_{trans\_inter*r}$  , Transfer(LCB)  
 $TP(s) + TPolymerH(r) \rightarrow TPolymerH(s) + TMCRH(r)$  ,  $k_{trans\_inter*r}$  , Transfer(LCB)  
 $TP(s) + TPolymerX(r) \rightarrow TPolymerH(s) + TMCRX(r)$  ,  $k_{trans\_inter*r}$  , Transfer(LCB)  
 $TP(s) + TPolymerT(r) \rightarrow TPolymerH(s) + TMCRT(r)$  ,  $k_{trans\_inter*r}$  , Transfer(LCB)  
 $TP(s) + XPolymerX(r) \rightarrow TPolymerH(s) + XMCRX(r)$  ,  $k_{trans\_inter*r}$  , Transfer(LCB)  
MCR\_propagation  
 $XMCRbb(s) + BA \rightarrow XP(s+1) + SCB$  ,  $k_{p\_tert}$  , Propagation(copolymer) (MCR\_propagation)  
 $HMCRbb(s) + BA \rightarrow HP(s+1) + SCB$  ,  $k_{p\_tert}$  , Propagation(copolymer)  
 $TMCRbb(s) + BA \rightarrow TP(s+1) + SCB$  ,  $k_{p\_tert}$  , Propagation(copolymer)  
 $HMCRH(s) + BA \rightarrow HP(s+1) + LCB$  ,  $k_{p\_tert}$  , Propagation(copolymer)  
 $XMCRH(s) + BA \rightarrow XP(s+1) + LCB$  ,  $k_{p\_tert}$  , Propagation(copolymer)  
 $TMCRH(s) + BA \rightarrow TP(s+1) + LCB$  ,  $k_{p\_tert}$  , Propagation(copolymer)  
 $XMCRX(s) + BA \rightarrow XXP(s+1) + LCB$  ,  $k_{p\_tert}$  , Propagation(copolymer)  
 $TMCRT(s) + BA \rightarrow TTP(s+1) + LCB$  ,  $k_{p\_tert}$  , Propagation(copolymer)  
 $TMCRX(s) + BA \rightarrow TXP(s+1) + LCB$  ,  $k_{p\_tert}$  , Propagation(copolymer)  
 $HMCRbb(s) + HP(r) \rightarrow HPolymerH(s+r) + SCB$  ,  $k_{t\_comMCR}$  , Combination(copolymer)  
 $HMCRbb(s) + HP(r) \rightarrow HPolymerH(s) + HPolymerH(r) + 2SCB$  ,  $k_{t\_dis}$  , Combination(copolymer)

HMCRbb(s) + XP(r) ----> XPolymerH(s+r) + SCB , kt\_comMCR , Combination(copolymer)  
 HMCRbb(s) + XP(r) ----> XPolymerH(s) + XPolymerH(r)+2SCB , kt\_dis , Combination(copolymer)  
 HMCRbb(s) + TP(r) ----> TPolymerH(s+r) + SCB , kt\_comMCR , Combination(copolymer)  
 HMCRbb(s) + TP(r) ----> TPolymerH(s) + TPolymerH(r)+2SCB , kt\_dis , Combination(copolymer)  
 XMCRbb(s) + HP(r) ----> XPolymerH(s+r) + SCB , kt\_comMCR , Combination(copolymer)  
 XMCRbb(s) + HP(r) ----> XPolymerH(s) + XPolymerH(r)+2SCB , kt\_dis , Combination(copolymer)  
 XMCRbb(s) + XP(r) ----> XPolymerX(s+r) + SCB , kt\_comMCR , Combination(copolymer)  
 XMCRbb(s) + XP(r) ----> XPolymerX(s) + XPolymerX(r)+2SCB , kt\_dis , Combination(copolymer)  
 XMCRbb(s) + TP(r) ----> TPolymerX(s+r) + SCB , kt\_comMCR , Combination(copolymer)  
 XMCRbb(s) + TP(r) ----> TPolymerX(s) + TPolymerX(r)+2SCB , kt\_dis , Combination(copolymer)  
 TMCRbb(s) + XP(r) ----> TPolymerX(s+r) + SCB , kt\_comMCR , Combination(copolymer)  
 TMCRbb(s) + XP(r) ----> TPolymerX(s) + TPolymerX(r)+2SCB , kt\_dis , Combination(copolymer)  
 TMCRbb(s) + HP(r) ----> TPolymerH(s+r) + SCB , kt\_comMCR , Combination(copolymer)  
 TMCRbb(s) + HP(r) ----> TPolymerH(s) + TPolymerH(r)+2SCB , kt\_dis , Combination(copolymer)  
 TMCRbb(s) + TP(r) ----> TPolymerT(s+r) + SCB , kt\_comMCR , Combination(copolymer)  
 TMCRbb(s) + TP(r) ----> TPolymerT(s) + TPolymerT(r)+2SCB , kt\_dis , Combination(copolymer)  
 HMCRRH(s) + HP(r) ----> HPolymerH(s+r) + LCB , kt\_comMCR , Combination(copolymer)  
 HMCRRH(s) + HP(r) ----> HPolymerH(s) + HPolymerH(r)+2LCB , kt\_dis , Combination(copolymer)  
 HMCRRH(s) + XP(r) ----> XPolymerH(s+r) + LCB , kt\_comMCR , Combination(copolymer)  
 HMCRRH(s) + XP(r) ----> XPolymerH(s) + XPolymerH(r)+2LCB , kt\_dis , Combination(copolymer)  
 HMCRRH(s) + TP(r) ----> TPolymerH(s+r) + LCB , kt\_comMCR , Combination(copolymer)  
 HMCRRH(s) + TP(r) ----> TPolymerH(s) + TPolymerH(r)+2LCB , kt\_dis , Combination(copolymer)  
 XMCRX(s) + XP(r) ----> XXXPolymer(s+r) + LCB , kt\_comMCR , Combination(copolymer)  
 XMCRX(s) + XP(r) ----> XXXPolymer(s) + XXXPolymer(r)+2LCB , kt\_dis , Combination(copolymer)  
 XMCRX(s) + HP(r) ----> XXHPolymer(s+r) + LCB , kt\_comMCR , Combination(copolymer)  
 XMCRX(s) + HP(r) ----> XXHPolymer(s) + XXHPolymer(r)+2LCB , kt\_dis , Combination(copolymer)  
 XMCRX(s) + TP(r) ----> XXTPolymer(s+r) + LCB , kt\_comMCR , Combination(copolymer)  
 XMCRX(s) + TP(r) ----> XXTPolymer(s) + XXTPolymer(r)+2LCB , kt\_dis , Combination(copolymer)  
 XMCRH(s) + HP(r) ----> XPolymerH(s+r) + LCB , kt\_comMCR , Combination(copolymer)  
 XMCRH(s) + HP(r) ----> XPolymerH(s) + XPolymerH(r)+2LCB , kt\_dis , Combination(copolymer)  
 XMCRH(s) + XP(r) ----> XPolymerX(s+r) + LCB , kt\_comMCR , Combination(copolymer)  
 XMCRH(s) + XP(r) ----> XPolymerX(s) + XPolymerX(r)+2LCB , kt\_dis , Combination(copolymer)  
 XMCRH(s) + TP(r) ----> TPolymerX(s+r) + LCB , kt\_comMCR , Combination(copolymer)  
 XMCRH(s) + TP(r) ----> TPolymerX(s) + TPolymerX(r)+2LCB , kt\_dis , Combination(copolymer)  
 TMCRH(s) + HP(r) ----> TPolymerH(s+r) + LCB , kt\_comMCR , Combination(copolymer)  
 TMCRH(s) + HP(r) ----> TPolymerH(s) + TPolymerH(r)+2LCB , kt\_dis , Combination(copolymer)  
 TMCRH(s) + XP(r) ----> TPolymerX(s+r) + LCB , kt\_comMCR , Combination(copolymer)  
 TMCRH(s) + XP(r) ----> TPolymerX(s) + TPolymerX(r)+2LCB , kt\_dis , Combination(copolymer)  
 TMCRH(s) + TP(r) ----> TPolymerT(s+r) + LCB , kt\_comMCR , Combination(copolymer)  
 TMCRH(s) + TP(r) ----> TPolymerT(s) + TPolymerT(r)+2LCB , kt\_dis , Combination(copolymer)  
 TMCRT(s) + TP(r) ----> TTPolymer(s+r) + LCB , kt\_comMCR , Combination(copolymer)  
 TMCRT(s) + TP(r) ----> TTPolymer(s) + TTPolymer(r)+2LCB , kt\_dis , Combination(copolymer)  
 TMCRT(s) + HP(r) ----> TTHPolymer(s+r) + LCB , kt\_comMCR , Combination(copolymer)  
 TMCRT(s) + HP(r) ----> TTHPolymer(s) + TTHPolymer(r)+2LCB , kt\_dis , Combination(copolymer)  
 TMCRT(s) + XP(r) ----> TTXPolymer(s+r) + LCB , kt\_comMCR , Combination(copolymer)  
 TMCRT(s) + XP(r) ----> TTXPolymer(s) + TTXPolymer(r)+2LCB , kt\_dis , Combination(copolymer)  
 TMCRX(s) + XP(r) ----> XXTPolymer(s+r) + LCB , kt\_comMCR , Combination(copolymer)  
 TMCRX(s) + XP(r) ----> XXTPolymer(s) + XXTPolymer(r)+2LCB , kt\_dis , Combination(copolymer)  
 TMCRX(s) + HP(r) ----> TXHPolymer(s+r) + LCB , kt\_comMCR , Combination(copolymer)  
 TMCRX(s) + HP(r) ----> TXHPolymer(s) + TXHPolymer(r)+2LCB , kt\_dis , Combination(copolymer)  
 TMCRX(s) + TP(r) ----> TTXPolymer(s+r) + LCB , kt\_comMCR , Combination(copolymer)  
 TMCRX(s) + TP(r) ----> TTXPolymer(s) + TTXPolymer(r)+2LCB , kt\_dis , Combination(copolymer)  
 HMCRbb(s) ----> MMH(s-2) + dimer\_radical , k\_beta , Degradation(n-mer)  
 XMCRbb(s) ----> MMX(s-2) + dimer\_radical , k\_beta , Degradation(n-mer)  
 TMCRbb(s) ----> MMT(s-2) + dimer\_radical , k\_beta , Degradation(n-mer)  
 HMCRbb(s) ----> HP(s-3) + trimer\_MMH , k\_beta\_trimer , Degradation(n-mer)  
 XMCRbb(s) ----> XP(s-3) + trimer\_MMH , k\_beta\_trimer , Degradation(n-mer)  
 TMCRbb(s) ----> TP(s-3) + trimer\_MMH , k\_beta\_trimer , Degradation(n-mer)  
 HMCRRH(s) ----> MMH(s-r) + HP(r) , k\_beta , Degradation(stat)  
 XMCRX(s) ----> MMX(s-r) + XP(r) , k\_beta , Degradation(stat)  
 TMCRT(s) ----> MMT(s-r) + TP(r) , k\_beta , Degradation(stat)  
 XMCRH(s) ----> MMX(s-r) + HP(r) , k\_beta\_half , Degradation(stat)  
 XMCRH(s) ----> MMH(s-r) + XP(r) , k\_beta\_half , Degradation(stat)

TMCRH(s) ---> MMT(s-r) + HP(r), k\_beta\_half, Degradation(stat)  
 TMCRH(s) ---> MMH(s-r) + TP(r), k\_beta\_half, Degradation(stat)  
 TMCRX(s) ---> MMT(s-r) + XP(r), k\_beta\_half, Degradation(stat)  
 TMCRX(s) ---> MMX(s-r) + TP(r), k\_beta\_half, Degradation(stat)  
 HP(s) + MMH(r) ---> Q1HH(s) + Q2HH(r), k\_ad, d-Termination  
 Q1HH(s) ---> MMH(s), k\_beta\_half, Change  
 Q1HH(s) ---> HP(s), k\_beta\_half, Change  
 Q2HH(s) ---> MMH(s), k\_beta\_half, Change  
 Q2HH(s) ---> HP(s), k\_beta\_half, Change  
 Q1HH(s) + HP(r) ---> HPolymerH(s+r) + LCB\_dash, kt\_comMCR, Combination(copolymer)  
 Q1HH(s) + HP(r) ---> HPolymerH(s) + HPolymerH(r)+2LCB\_dash, kt\_dis, Combination(copolymer)  
 Q1HH(s) + HP(r) ---> dummy(s) + HP(r), kt\_comMCR, d-Termination  
 Q2HH(s) + HP(r) ---> HPolymerH(s+r) + LCB\_dash, kt\_comMCR, Combination(copolymer)  
 Q2HH(s) + HP(r) ---> HPolymerH(s) + HPolymerH(r)+2LCB\_dash, kt\_dis, Combination(copolymer)  
 Q2HH(s) + HP(r) ---> dummy(s) + HP(r), kt\_comMCR, d-Termination  
 Q1HH(s) + TP(r) ---> TPolymerH(s+r) + LCB\_dash, kt\_comMCR, Combination(copolymer)  
 Q1HH(s) + TP(r) ---> TPolymerH(s) + TPolymerH(r)+2LCB\_dash, kt\_dis, Combination(copolymer)  
 Q1HH(s) + TP(r) ---> dummy(s) + TP(r), kt\_comMCR, d-Termination  
 Q2HH(s) + TP(r) ---> TPolymerH(s+r) + LCB\_dash, kt\_comMCR, Combination(copolymer)  
 Q2HH(s) + TP(r) ---> TPolymerH(s) + TPolymerH(r)+2LCB\_dash, kt\_dis, Combination(copolymer)  
 Q2HH(s) + TP(r) ---> dummy(s) + TP(r), kt\_comMCR, d-Termination  
 Q1HH(s) + BA ---> HP(s+1) + LCB\_dash, kp\_tert\_half, Propagation(copolymer)  
 Q1HH(s) + BA ---> dummy(s) + BA, kp\_tert\_half, Change  
 Q2HH(s) + BA ---> HP(s+1) + LCB\_dash, kp\_tert\_half, Propagation(copolymer)  
 Q2HH(s) + BA ---> dummy(s) + BA, kp\_tert\_half, Change  
 XP(s) + MMH(r) ---> Q1XH(s) + Q2XH(r), k\_ad, d-Termination  
 HP(s) + MMX(r) ---> Q1XH(s) + Q2XH(r), k\_ad, d-Termination  
 Q1XH(s) ---> MMX(s), k\_beta\_half, Change  
 Q1XH(s) ---> XP(s), k\_beta\_half, Change  
 Q2XH(s) ---> HP(s), k\_beta\_half, Change  
 Q2XH(s) ---> MMH(s), k\_beta\_half, Change  
 Q1XH(s) + HP(r) ---> XPolymerH(s+r) + LCB\_dash, kt\_comMCR, Combination(copolymer)  
 Q1XH(s) + HP(r) ---> XPolymerH(s) + XPolymerH(r)+2LCB\_dash, kt\_dis, Combination(copolymer)  
 Q1XH(s) + HP(r) ---> dummy(s) + HP(r), kt\_comMCR, d-Termination  
 Q2XH(s) + HP(r) ---> XPolymerH(s+r) + LCB\_dash, kt\_comMCR, Combination(copolymer)  
 Q2XH(s) + HP(r) ---> XPolymerH(s) + XPolymerH(r)+2LCB\_dash, kt\_dis, Combination(copolymer)  
 Q2XH(s) + HP(r) ---> dummy(s) + HP(r), kt\_comMCR, d-Termination  
 Q1XH(s) + TP(r) ---> TPolymerX(s+r) + LCB\_dash, kt\_comMCR, Combination(copolymer)  
 Q1XH(s) + TP(r) ---> TPolymerX(s) + TPolymerX(r)+2LCB\_dash, kt\_dis, Combination(copolymer)  
 Q1XH(s) + TP(r) ---> dummy(s) + TP(r), kt\_comMCR, d-Termination  
 Q2XH(s) + TP(r) ---> TPolymerX(s+r) + LCB\_dash, kt\_comMCR, Combination(copolymer)  
 Q2XH(s) + TP(r) ---> TPolymerX(s) + TPolymerX(r)+2LCB\_dash, kt\_dis, Combination(copolymer)  
 Q2XH(s) + TP(r) ---> dummy(s) + TP(r), kt\_comMCR, d-Termination  
 Q1XH(s) + BA ---> XP(s+1) + LCB\_dash, kp\_tert\_half, Propagation(copolymer)  
 Q1XH(s) + BA ---> dummy(s) + BA, kp\_tert\_half, Change  
 Q2XH(s) + BA ---> XP(s+1) + LCB\_dash, kp\_tert\_half, Propagation(copolymer)  
 Q2XH(s) + BA ---> dummy(s) + BA, kp\_tert\_half, Change  
 TP(s) + MMH(r) ---> Q1TH(s) + Q2TH(r), k\_ad, d-Termination  
 HP(s) + MMT(r) ---> Q1TH(s) + Q2TH(r), k\_ad, d-Termination  
 Q1TH(s) ---> MMT(s), k\_beta\_half, Change  
 Q1TH(s) ---> TP(s), k\_beta\_half, Change  
 Q2TH(s) ---> HP(s), k\_beta\_half, Change  
 Q2TH(s) ---> MMH(s), k\_beta\_half, Change  
 Q1TH(s) + HP(r) ---> TPolymerH(s+r) + LCB\_dash, kt\_comMCR, Combination(copolymer)  
 Q1TH(s) + HP(r) ---> TPolymerH(s) + TPolymerH(r)+2LCB\_dash, kt\_dis, Combination(copolymer)  
 Q1TH(s) + HP(r) ---> dummy(s) + HP(r), kt\_comMCR, d-Termination  
 Q2TH(s) + HP(r) ---> TPolymerH(s+r) + LCB\_dash, kt\_comMCR, Combination(copolymer)  
 Q2TH(s) + HP(r) ---> TPolymerH(s) + TPolymerH(r)+2LCB\_dash, kt\_dis, Combination(copolymer)  
 Q2TH(s) + HP(r) ---> dummy(s) + HP(r), kt\_comMCR, d-Termination  
 Q1TH(s) + TP(r) ---> TPolymerT(s+r) + LCB\_dash, kt\_comMCR, Combination(copolymer)  
 Q1TH(s) + TP(r) ---> TPolymerT(s) + TPolymerT(r)+2LCB\_dash, kt\_dis, Combination(copolymer)  
 Q1TH(s) + TP(r) ---> dummy(s) + TP(r), kt\_comMCR, d-Termination  
 Q2TH(s) + TP(r) ---> TPolymerT(s+r) + LCB\_dash, kt\_comMCR, Combination(copolymer)

Q2TH(s) + TP(r) ----> TPolymerT(s) + TPolymerT(r)+2LCB\_dash , kt\_dis , Combination(copolymer)  
 Q2TH(s) + TP(r) ----> dummy(s) + TP(r) , kt\_comMCR , d-Termination  
 Q1TH(s) + BA ----> TP(s+1) + LCB\_dash , kp\_tert\_half , Propagation(copolymer)  
 Q1TH(s) + BA ----> dummy(s) + BA , kp\_tert\_half , Change  
 Q2TH(s) + BA ----> TP(s+1) + LCB\_dash , kp\_tert\_half , Propagation(copolymer)  
 Q2TH(s) + BA ----> dummy(s) + BA , kp\_tert\_half , Change  
 XP(s) + MMX(r) ----> Q1XX(s) + Q2XX(r) , k\_ad , d-Termination  
 Q1XX(s) ----> MMX(s) , k\_beta\_half , Change  
 Q1XX(s) ----> XP(s) , k\_beta\_half , Change  
 Q2XX(s) ----> XP(s) , k\_beta\_half , Change  
 Q2XX(s) ----> MMX(s) , k\_beta\_half , Change  
 Q1XX(s) + HP(r) ----> XPolymerX(s+r) + LCB\_dash , kt\_comMCR , Combination(copolymer)  
 Q1XX(s) + HP(r) ----> XPolymerX(s) + XPolymerX(r)+2LCB\_dash , kt\_dis , Combination(copolymer)  
 Q1XX(s) + HP(r) ----> dummy(s) + HP(r) , kt\_comMCR , d-Termination  
 Q2XX(s) + HP(r) ----> XPolymerX(s+r) + LCB\_dash , kt\_comMCR , Combination(copolymer)  
 Q2XX(s) + HP(r) ----> XPolymerX(s) + XPolymerX(r)+2LCB\_dash , kt\_dis , Combination(copolymer)  
 Q2XX(s) + HP(r) ----> dummy(s) + HP(r) , kt\_comMCR , d-Termination  
 Q1XX(s) + TP(r) ----> XXTPolymer(s+r) + LCB\_dash , kt\_comMCR , Combination(copolymer)  
 Q1XX(s) + TP(r) ----> XXTPolymer(s) + XXTPolymer(r)+2LCB\_dash , kt\_dis , Combination(copolymer)  
 Q1XX(s) + TP(r) ----> dummy(s) + TP(r) , kt\_comMCR , d-Termination  
 Q2XX(s) + TP(r) ----> XXTPolymer(s+r) + LCB\_dash , kt\_comMCR , Combination(copolymer)  
 Q2XX(s) + TP(r) ----> XXTPolymer(s) + XXTPolymer(r)+2LCB\_dash , kt\_dis , Combination(copolymer)  
 Q2XX(s) + TP(r) ----> dummy(s) + TP(r) , kt\_comMCR , d-Termination  
 Q1XX(s) + BA ----> XXP(s+1) + LCB\_dash , kp\_tert\_half , Propagation(copolymer)  
 Q1XX(s) + BA ----> dummy(s) + BA , kp\_tert\_half , Change  
 Q2XX(s) + BA ----> XXP(s+1) + LCB\_dash , kp\_tert\_half , Propagation(copolymer)  
 Q2XX(s) + BA ----> dummy(s) + BA , kp\_tert\_half , Change  
 TP(s) + MMT(r) ----> Q1TT(s) + Q2TT(r) , k\_ad , d-Termination  
 Q1TT(s) ----> MMT(s) , k\_beta\_half , Change  
 Q1TT(s) ----> TP(s) , k\_beta\_half , Change  
 Q2TT(s) ----> TP(s) , k\_beta\_half , Change  
 Q2TT(s) ----> MMT(s) , k\_beta\_half , Change  
 Q1TT(s) + HP(r) ----> TPolymerT(s+r) + LCB\_dash , kt\_comMCR , Combination(copolymer)  
 Q1TT(s) + HP(r) ----> TPolymerT(s) + TPolymerT(r)+2LCB\_dash , kt\_dis , Combination(copolymer)  
 Q1TT(s) + HP(r) ----> dummy(s) + HP(r) , kt\_comMCR , d-Termination  
 Q2TT(s) + HP(r) ----> TPolymerT(s+r) + LCB\_dash , kt\_comMCR , Combination(copolymer)  
 Q2TT(s) + HP(r) ----> TPolymerT(s) + TPolymerT(r)+2LCB\_dash , kt\_dis , Combination(copolymer)  
 Q2TT(s) + HP(r) ----> dummy(s) + HP(r) , kt\_comMCR , d-Termination  
 Q1TT(s) + TP(r) ----> TTPolymer(s+r) + LCB\_dash , kt\_comMCR , Combination(copolymer)  
 Q1TT(s) + TP(r) ----> TTPolymer(s) + TTPolymer(r)+2LCB\_dash , kt\_dis , Combination(copolymer)  
 Q1TT(s) + TP(r) ----> dummy(s) + TP(r) , kt\_comMCR , d-Termination  
 Q2TT(s) + TP(r) ----> TTPolymer(s+r) + LCB\_dash , kt\_comMCR , Combination(copolymer)  
 Q2TT(s) + TP(r) ----> TTPolymer(s) + TTPolymer(r)+2LCB\_dash , kt\_dis , Combination(copolymer)  
 Q2TT(s) + TP(r) ----> dummy(s) + TP(r) , kt\_comMCR , d-Termination  
 Q1TT(s) + BA ----> TTP(s+1) + LCB\_dash , kp\_tert\_half , Propagation(copolymer)  
 Q1TT(s) + BA ----> dummy(s) + BA , kp\_tert\_half , Change  
 Q2TT(s) + BA ----> TTP(s+1) + LCB\_dash , kp\_tert\_half , Propagation(copolymer)  
 Q2TT(s) + BA(r) ----> dummy(s) + BA(r) , kp\_tert\_half , d-Termination  
 XP(s) + MMT(r) ----> Q1XT(s) + Q2XT(r) , k\_ad , d-Termination  
 TP(s) + MMX(r) ----> Q1XT(s) + Q2XT(r) , k\_ad , d-Termination  
 Q1XT(s) ----> MMT(s) , k\_beta\_half , Change  
 Q1XT(s) ----> TP(s) , k\_beta\_half , Change  
 Q2XT(s) ----> MMX(s) , k\_beta\_half , Change  
 Q2XT(s) ----> XP(s) , k\_beta\_half , Change  
 Q1XT(s) + HP(r) ----> TPolymerX(s+r) + LCB\_dash , kt\_comMCR , Combination(copolymer)  
 Q1XT(s) + HP(r) ----> TPolymerX(s) + TPolymerX(r)+2LCB\_dash , kt\_dis , Combination(copolymer)  
 Q1XT(s) + HP(r) ----> dummy(s) + HP(r) , kt\_comMCR , d-Termination  
 Q2XT(s) + HP(r) ----> TPolymerX(s+r) + LCB\_dash , kt\_comMCR , Combination(copolymer)  
 Q2XT(s) + HP(r) ----> TPolymerX(s) + TPolymerX(r)+2LCB\_dash , kt\_dis , Combination(copolymer)  
 Q2XT(s) + HP(r) ----> dummy(s) + HP(r) , kt\_comMCR , d-Termination  
 Q2XT(s) + TP(r) ----> TTXPolymer(s+r) + LCB\_dash , kt\_comMCR , Combination(copolymer)  
 Q2XT(s) + TP(r) ----> TTXPolymer(s) + TTXPolymer(r)+2LCB\_dash , kt\_dis , Combination(copolymer)  
 Q2XT(s) + TP(r) ----> dummy(s) + TP(r) , kt\_comMCR , d-Termination

Q1XT(s) + TP(r) ----> TTXPolymer(s+r) + LCB\_dash , kt\_comMCR , Combination(copolymer)  
Q1XT(s) + TP(r) ----> TTXPolymer(s) + TTXPolymer(r)+2LCB\_dash , kt\_dis , Combination(copolymer)  
Q1XT(s) + TP(r) ----> dummy(s) + TP(r) , kt\_comMCR , d-Termination  
Q1XT(s) + BA ----> XTP(s+1) + LCB\_dash , kp\_tert\_half , Propagation(copolymer)  
Q1XT(s) + BA ----> dummy(s) + BA , kp\_tert\_half , Change  
Q2XT(s) + BA ----> XTP(s+1) + LCB\_dash , kp\_tert\_half , Propagation(copolymer)  
Q2XT(s) + BA ----> dummy(s) + BA , kp\_tert\_half , Change  
HP(s) + trimer\_MMH ----> HMCRbb(s+2) , kad\_small , Propagation(n-mer)  
XP(s) + trimer\_MMH ----> XMCRbb(s+2) , kad\_small , Propagation(n-mer)  
TP(s) + trimer\_MMH ----> TMCRbb(s+2) , kad\_small , Propagation(n-mer)

File: Acrylate\_149.rsy  
Printed: 05/16/10, 22:14:52

## 9 List of Abbreviations

$\alpha$  – Mark-Houwink parameter

$\epsilon$  – molar absorptivity

A – frequency factor (pre/exponential factor in the Arrhenius equation)

ACHN – 1,1-azobis(cyclohexanecarbonitrile)

ATRP – atom transfer radical polymerization

b – path length of the cell

2-EHA – 2-ethyl hexyl acrylate

AIBN – 2,2'-azobis(isobutyronitrile)

*n*-BA – *n*-butyl acrylate

*t*-BA – *tert*-butyl acrylate

BenA – benzyl acrylate

*i*BoA – *iso*-bornyl acrylate

$C_{tr,i}$  – transfer constant to species *i*

CTA – chain transfer agent

CuAAC – copper catalyzed azide – alkyne cycloaddition

DA – dodecyl acrylate

DMPA – 2,2-dimethoxy-2-phenylacetophenone

$\overline{DP}_n$  – number average degree of polymerization

$E_A$  – activation energy (in the Arrhenius equation)

EA – ethyl acrylate

EEA – 1-ethoxyethyl acrylate

ESI – electrospray ionization

ESI-MS – electrospray ionization mass spectrometry

ESR – electron spin resonance

*f* – initiator efficiency

FAB – fast atom bombardment

FD – field desorption

FRP – free radical polymerization

GC – gas chromatography

*n*-HexA – *n*-hexyl acrylate

$I$  – intensity of transmitted radiation,

$I_0$  – intensity of incident radiation

$k_p$  – propagation rate coefficient

$k_t$  – termination rate coefficient

$k_{tr}$  – transfer rate coefficient

LC – liquid chromatography

[M] – monomer concentration

[M<sub>0</sub>] – initial monomer concentration

MA – methyl acrylate

MALDI-ToF-MS – matrix assisted laser desorption and ionization time-of-flight mass spectrometry

MCR – midchain radical

MHKS parameters– mark-houwink-kuhn-sakurada parameters

MM – macromonomer

$M_n$  – number average molecular weight

MMA – methyl methacrylate

MS – mass spectrometry

$M_w$  – weight average molecular weight

MWD – molecular weight distribution

$\eta$  – viscosity

NMP –nitroxide mediated polymerization

OctSH – 1-octanethiol

PCR group – Polymer Chemistry Research group

PDI – polydispersity index

PEG – poly(ethylene glycol)

PiBoA – poly(isobornyl acrylate)

PLP – pulsed laser polymerization

pMMA – poly(methyl methacrylate)

PREDICI<sup>®</sup> – Polyreactions Distributions by Countable System Integration

PS – polystyrene

RAFT – Reversible Addition-Fragmentation Transfer

$R_p$  – rate of polymerization

$R_{tr}$  – rate of transfer

$R_t$  – rate of termination

SEC – size exclusion chromatography

SNR – signal-to-noise ratio

TCP – thiol capped polymer

## 10 Curriculum Vitae

Date of Birth: 16 April 1984  
 Home Address: 19/60 Harbourne Road, Kingsford, Sydney, NSW 2032, Australia  
 Nationality: Australian

### Education

1998 - 2001 **Higher School Certificate**  
 Randwick Girls' High School, Randwick, NSW, Australia

2002 - 2006 **Bachelor of Engineering (Industrial Chemistry) Hons 1.**  
 University of New South Wales, Sydney, NSW, Australia  
 - *Recipient of a UNSW Co-Op Scholarship*

2006 - 2008 **Masters of Commerce (Business Strategy)**  
 University of New South Wales, Sydney, NSW, Australia

2007 - Current **PhD studies in Polymer Chemistry**  
 Under the supervision of Prof. Dr. Christopher Barner-Kowollik  
 University of New South Wales, Sydney, Australia  
 - *Recipient of an Australian Postgraduate Award scholarship*  
 Karlsruhe Institute of Technology, Karlsruhe, Germany

### Employment History

July 2008 -  
 Current **Institut für Technische Chemie und Polymerchemie**  
 Karlsruhe Institute of Technology, Karlsruhe, Germany  
 Scientific Co-Worker

March 2007 -  
 June 2008 **School of Chemical Sciences and Engineering**  
 Centre for Advanced Macromolecular Design  
 University of New South Wales, Sydney, NSW, Australia  
 Scientific Co-Worker

Jan 2007 -  
 June 2008 **School of Chemical Sciences and Engineering**  
 University of New South Wales, Sydney, NSW, Australia  
 Teaching Assistant

June 2005 -  
 December 2005 **BlueScope Steel Limited**  
 Old Port Road, Port Kembla, NSW, Australia  
 Coatings Research Chemist

December 2004 -  
 June 2005 **Memcor Australia Pty. Ltd. – A Siemens Business**  
 1 Memtec Parkway, South Windsor, NSW, Australia  
 Research & Development Chemist / Industrial Chemist

December 2003 -  
 February 2004 **Valspar Australia**  
 203 Power St, Glendenning, NSW, Australia  
 Production Support Chemist

December 2002 -  
 February 2003 **SydneyWater**  
 Malabar, NSW, Australia  
 Pilot Plant Engineer / Chemist

## 11 Publications

- [08] Reducing the Degree of Branching in Polyacrylates *via* Mid-Chain Radical Patching: A Quantitative Melt-State NMR Study  
Gaborieau, M.; Koo, S.P.S.; Castignolles, P.; Junkers, T.; Barner-Kowollik, C. *Macromolecules*, 2010, Submitted.
- [07] Determination of the Propagation Rate Coefficient of Acrylonitrile  
Junkers, T.; Koo, S.P.S.; Barner-Kowollik, C. *Polym. Chem.* 2010, DOI-10.1039/c0py00019a.
- [06] Limitations of Radical Thiol-ene Reactions for Polymer-Polymer Conjugation  
Koo, S.P.S.; Stamenović, M.M.; Prasath, R.A.; Inglis, A.J.; Du Prez, F.E.; Barner-Kowollik, C.; Van Camp, W.; Junkers, T. *J. Polym. Sci. Part A: Polym. Chem.* 2010, 48, 1699-1713.
- [05] Quantifying the Efficiency of Photo-Initiation Processes in Methyl Methacrylate Free Radical Polymerization *via* Electrospray Ionization Mass Spectrometry  
Günzler, F.; Wong, E. H.H.; Koo, S.P.S.; Junkers, T.; Barner-Kowollik, C. *Macromolecules* 2009, 42, 1488-1493.
- [04] Quantitative Product Spectrum Analysis of Poly(butyl acrylate) *via* Electrospray Ionization Mass Spectrometry  
Koo, S.P.S.; Junkers, T.; Barner-Kowollik, C. *Macromolecules* 2009, 42, 62–69.
- [03] Self-directed Formation of Uniform Unsaturated Macromolecules from Acrylate Monomers at High Temperatures  
Junkers, T.; Bennet, F.; Koo, S.P.S.; Barner-Kowollik, C. *J. Polym. Sci. Part A: Polym. Chem.* 2008, 46, 3433-3437.
- [02] Mapping Photolysis Product Radical Reactivities *via* Soft Ionization Mass Spectrometry in Acrylate, Methacrylate, and Itaconate Systems  
Szablan, Z.; Junkers, T.; Koo, S.P.S.; Lovestead, T.M.; Davis, T.P.; Stenzel, M.H.; Barner-Kowollik, C., *Macromolecules* 2007, 40, 6820-6833.
- [01] Mapping Poly(Butyl Acrylate) Product Distributions by Mass Spectrometry in a Wide Temperature Range: Suppression of Midchain Radical Side Reactions  
Junkers, T.; Koo, S.P.S.; Davis, T.P.; Stenzel, M.H.; Barner-Kowollik, C. *Macromolecules* 2007, 40, 8906-8912.

## 12 Conference Contributions

- [08] Limitations of Thermal Thiolene Chemistry for Polymer-Polymer Conjugation (poster presentation)  
Koo, S.P.S., Junkers, T., Barner-Kowollik, C., Binational Meeting on Controlled Radical Polymerization, Houffalize, Belgium, Sep. 2009.
- [07] Limitations of Thermal Thiol-ene Polymer-Polymer Conjugation (poster presentation)  
Koo, S.P.S., Junkers, T., Barner-Kowollik, C. *Frontiers in Polymer Science*, Mainz, Germany, May 2009.
- [06] Effiziente Zugänge zu komplexen Makromolekülen mittels lebender/kontrollierter radikalischer Polymerisation. Kontrolle, Kopplung und Charakterisierung (invited talk)  
Barner-Kowollik, C., Sinnwell, S., Junkers, T., Stenzel, M.H., Wong, E.H.H., Koo, S.P.S., Nebhani, L. *Makromolekulares Kolloquium*, Freiburg, Germany, Feb. 2009.
- [05] New Avenues to Complex Polymers: Synthesis and Characterization (invited talk)  
Barner-Kowollik, C., Sinnwell, S., Junkers, T., Stenzel, M.H., Wong, E.H.H., Koo, S.P.S., Nebhani, L. *Polymer Chemistry Conference*, Cancun, Mexico, Feb. 2009.
- [04] Exploring new avenues for the synthesis and characterization of well-defined polymeric materials (invited talk)  
Barner-Kowollik, C.; Sinnwell S.; Stenzel, M.H.; Junkers, T.; Inglis, A.; Nebhani, L.; Barner, L.; Hart-Smith, G.; Chaffey-Millar, H.; Koo, S.P.S.; Gründling, T.; Guilhaus, M.; Synatschke, C.; Wong, E.H.H., 30th Australasian Polymer Symposium, Melbourne, Australia, Dec. 2008.
- [03] Control and Utilization of Midchain Radicals in Acrylate Polymerization: From Kinetics to Polymer Synthesis (oral presentation)  
Junkers, T.; Koo, S.P.S.; Günzler, F.; Bennet, F.; Barner-Kowollik, C. *International Symposium on Microstructural Control in Radical Polymerization*, Clausthal, Germany, Oct. 2008.
- [02] Control and Utilization of Midchain Radical Side Reactions in Acrylate Polymerization (oral presentation)  
Junkers, T.; Koo, S.P.S.; Bennet, F.; Barner-Kowollik, C. *Polymer Synthesis 2008*, Cancun, Mexico, March 2008.
- [01] Extending the photolysis product radical reactivity map: A mass spectrometry study of photoinitiation processes in methyl acrylate and dimethyl itaconate free radical polymerization (poster presentation)  
Szablan, Z.; Koo, S.P.S.; Lovestead, T.; Junkers, T.; Davis, T.P.; Stenzel, M.H.; Barner-Kowollik, C. 29th Australasian Polymer Symposium, Hobart (Tasmania) – Australia, Feb. 2007.

---

*Begin at the beginning and go on until you come to the end; then stop. – Alice's Adventures in Wonderland (1865)*

## 13 Acknowledgments

I can no other answer make but thanks,  
And thanks, and ever thanks  
– *Twelfth Night, Or What You Will*

The successful completion of this, my *magnum opus*, was done in collaboration with many people, who implicitly and explicitly, with their time, words and gestures of encouragement, scientific and not so scientific ideas, good laughs, good food, and the occasional drink, have made this long journey that much more bearable. I am honored and grateful to have had your support over the years.

I would not have ended up in this mess were it not for Prof. Dr. Christopher Barner-Kowollik, with whom I have had the general pleasure of working with since 2006, but his dedicated support throughout the duration of this thesis has motivated me through many a scientific dark time. It is impossible to fault his commitment and enthusiasm to my projects, which at times were admittedly greater than my own. Prof. Dr. Thomas Junkers, apart from being a scientific mentor, has always made me see the lighter side of research, which was a much-needed alternate reality at times. Your coffee addiction is very scary by the way Thomas! Your bilateral support has endlessly facilitated working with the both of you – at any one time at least one of you would be inclined to see my perspective on things. I am not German enough to fully appreciate the term ‘Doctor Father’ but those would be the appropriate words to describe your combined roles in the making of this thesis. I am forever grateful for the scientific and social opportunities that you have made possible over the last few years. I also thank all those of you who have had scientific input into this thesis, notably the PCR group in Ghent, Dr. Patrice Castignolles, and Dr. Marianne Gaborieau, your work has been invaluable in the successful completion of this thesis.

I extend my gratitude to the *Bundesrepublik Deutschland*, of whom I have been a guest these past two years, and to the state of Baden-Württemberg, for paying my rent and all other costs and indulgences. Thanks to the KIT, for extending me an invitation to study in its nerdy halls. However I do not thank you for your tradition of kissing *Die Fridericiana* at graduation.

My colleagues in Sydney and in Karlsruhe have been an integral part in preserving my sanity, when they were not themselves accusing me of insanity. To all the people at Macroarc: Dominik, Anna, Andreas, Mathias and Mathias, Christina, Özcan, Nicolas, Michael, Thomas, David, James, Jördis, Anja, Herr Gerstel; your combined presence is essential in creating the group atmosphere we enjoy and the office would not be the same without you. Thanks in particular to Till, Leena, Edgar, Frankie, Chris Junior, Gene and Andrew for making it to Karlsruhe. Andrew, I have immensely enjoyed our discussions on the more esoteric words and grammar forms of the English language. Here are some more words to think about: misocapnist, adoxography, floccinaucinihilipilification, gambrinous, borborygmus, farctate, zenzizenzizencic. I have finally found the words to describe my afternoon hysterics: I am abderian, prone to cachinnation as an alternative to lalochezia! Till, I do not make up a lot of the words I use, just some of them, and none of them in this acknowledgment, and once and for all I am not an alcoholic. Thanks for the caffeine, sweets, hugs, good dress sense and nights out. You are a great manpanion! Leena, from whom stating the obvious is an eternal source of mirth for the rest of us (cf. “Ah ha” backwards is still “ah hA” – Mainz, 2009). Your impatience is also a force to be reckoned with, who could forget your on-stage outburst in Houffalize: “This is crap!” Your dedication to breaking the record for ‘Most hours spent in the office’ has meant that I have been rarely alone in the office, and your company was always very much appreciated. It’s nice to know someone else is freezing cold in winter in the office on the weekend. Very special thanks to Gabi, I have never seen anyone so efficient, you make things so much easier for everyone, and to Frau Schneider, you are always ready with a kind word, lots of empathy, and possess vital knowledge on the workings of the triple SEC.

My parents have been a source of perpetual support if not explicit encouragement, I suppose they read the other book on parenting that tells you to just assume your progeny can do anything and tell them as much. It seems to have paid off, I would not be where I am today without your confidence in me, and it has helped me strive to be the best that I can be. I hope to always live up to your expectations. Shane, you have always inspired me to be a good role model. I have learnt much from you too over the years and knowing you are just a phone call away to burst my bubble of sporadic self-pity was always motivation to snap myself out of it. Thank you also to Tatie, your interesting perspectives on all manner of

things are always refreshingly quirky and amusing. You are solely responsible for my love of words and I have no way of ever returning in kind what you have given me.

Many many thanks go to Joon, whose care packages meant I was still enjoying cup-a-soups and instant mac and cheese in Karlsruhe. Our weekly chats went a long way to buoy my spirits during the last two years. Thank you for your eternal patience. You have my deepest gratitude for your support. It's been hard but we got there.

To all my friends, you are too numerous to list here, but you know who you are. Over the years, I have turned to you many times for advice, inspiration, non-nerdy conversation, encouragement, laughs, strength, spiritual and physical nourishment, motivation, or just for a listening ear and you have never let me down. Thank you for being there for me.

Last but not least, thank you to the Hairy Hand of God, the Powers that Be, Lady Luck, the Flying Spaghetti Monster and as yet unidentified higher powers. I have enjoyed good health and good fortune, without which my accomplishments would have been much more difficult to achieve. Hat's off to you whomever you may be and may I always be in your good graces.

